frontiers | Research Topics

Advancing cancer therapy: innovative strategies targeting immune evasion and metabolic modulation

Edited by
Ana Luísa De Sousa-Coelho, Andrés Méndez Lucas, Nuno Miguel Nunes and Francesca Rapino

Coordinated by
Mónica Teotónio Fernandes

Published in
Frontiers in Immunology
Frontiers in Medicine
Frontiers in Oncology

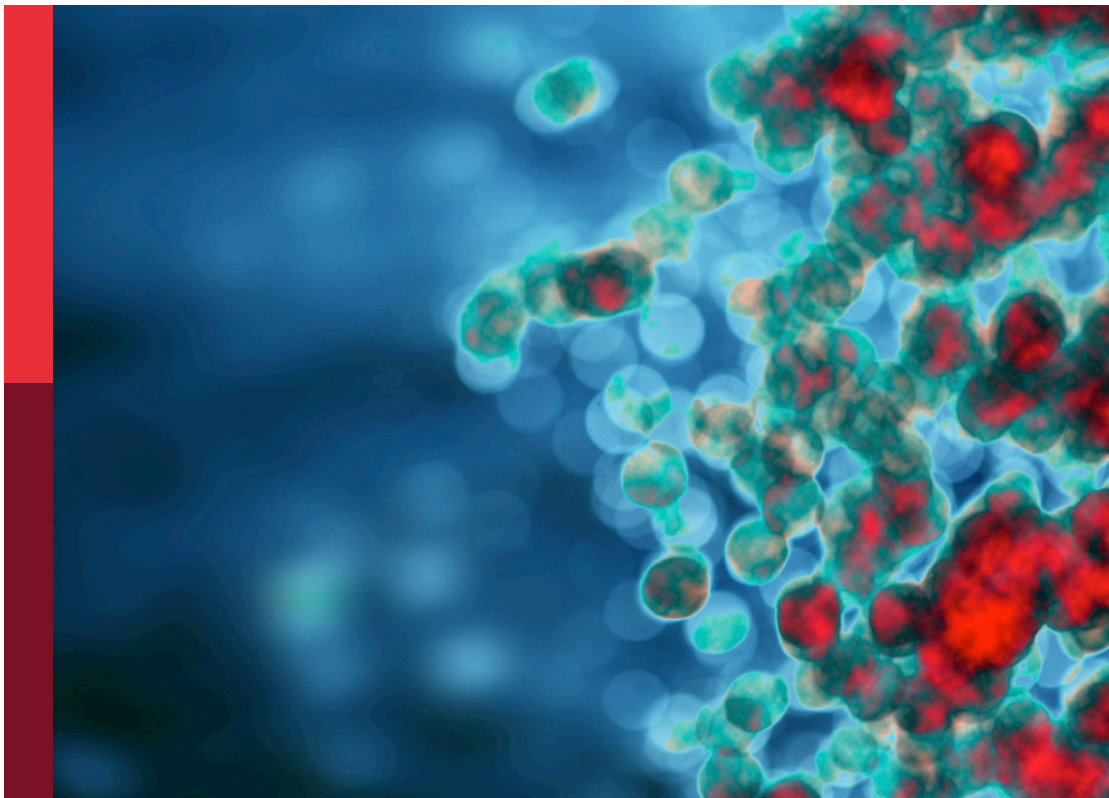

FRONTIERS EBOOK COPYRIGHT STATEMENT

The copyright in the text of individual articles in this ebook is the property of their respective authors or their respective institutions or funders. The copyright in graphics and images within each article may be subject to copyright of other parties. In both cases this is subject to a license granted to Frontiers.

The compilation of articles constituting this ebook is the property of Frontiers.

Each article within this ebook, and the ebook itself, are published under the most recent version of the Creative Commons CC-BY licence. The version current at the date of publication of this ebook is CC-BY 4.0. If the CC-BY licence is updated, the licence granted by Frontiers is automatically updated to the new version.

When exercising any right under the CC-BY licence, Frontiers must be attributed as the original publisher of the article or ebook, as applicable.

Authors have the responsibility of ensuring that any graphics or other materials which are the property of others may be included in the CC-BY licence, but this should be checked before relying on the CC-BY licence to reproduce those materials. Any copyright notices relating to those materials must be complied with.

Copyright and source acknowledgement notices may not be removed and must be displayed in any copy, derivative work or partial copy which includes the elements in question.

All copyright, and all rights therein, are protected by national and international copyright laws. The above represents a summary only. For further information please read Frontiers' Conditions for Website Use and Copyright Statement, and the applicable CC-BY licence.

ISSN 1664-8714
ISBN 978-2-8325-6845-3
DOI 10.3389/978-2-8325-6845-3

Generative AI statement
Any alternative text (Alt text) provided alongside figures in the articles in this ebook has been generated by Frontiers with the support of artificial intelligence and reasonable efforts have been made to ensure accuracy, including review by the authors wherever possible. If you identify any issues, please contact us.

About Frontiers

Frontiers is more than just an open access publisher of scholarly articles: it is a pioneering approach to the world of academia, radically improving the way scholarly research is managed. The grand vision of Frontiers is a world where all people have an equal opportunity to seek, share and generate knowledge. Frontiers provides immediate and permanent online open access to all its publications, but this alone is not enough to realize our grand goals.

Frontiers journal series

The Frontiers journal series is a multi-tier and interdisciplinary set of open-access, online journals, promising a paradigm shift from the current review, selection and dissemination processes in academic publishing. All Frontiers journals are driven by researchers for researchers; therefore, they constitute a service to the scholarly community. At the same time, the *Frontiers journal series* operates on a revolutionary invention, the tiered publishing system, initially addressing specific communities of scholars, and gradually climbing up to broader public understanding, thus serving the interests of the lay society, too.

Dedication to quality

Each Frontiers article is a landmark of the highest quality, thanks to genuinely collaborative interactions between authors and review editors, who include some of the world's best academicians. Research must be certified by peers before entering a stream of knowledge that may eventually reach the public - and shape society; therefore, Frontiers only applies the most rigorous and unbiased reviews. Frontiers revolutionizes research publishing by freely delivering the most outstanding research, evaluated with no bias from both the academic and social point of view. By applying the most advanced information technologies, Frontiers is catapulting scholarly publishing into a new generation.

What are Frontiers Research Topics?

Frontiers Research Topics are very popular trademarks of the *Frontiers journals series*: they are collections of at least ten articles, all centered on a particular subject. With their unique mix of varied contributions from Original Research to Review Articles, Frontiers Research Topics unify the most influential researchers, the latest key findings and historical advances in a hot research area.

Find out more on how to host your own Frontiers Research Topic or contribute to one as an author by contacting the Frontiers editorial office: frontiersin.org/about/contact

Advancing cancer therapy: innovative strategies targeting immune evasion and metabolic modulation

Topic editors
Ana Luísa De Sousa-Coelho — Algarve Biomedical Center Research Institute (ABC-RI), Portugal
Andrés Méndez Lucas — University of Barcelona, Spain
Nuno Miguel Nunes — University of Toronto, Canada
Francesca Rapino — University of Liège, Belgium

Topic coordinator
Mónica Teotónio Fernandes — University of Algarve, Portugal

Citation
De Sousa-Coelho, A. L., Méndez Lucas, A., Nunes, N. M., Rapino, F., Fernandes, M. T., eds. (2025). *Advancing cancer therapy: innovative strategies targeting immune evasion and metabolic modulation*. Lausanne: Frontiers Media SA.
doi: 10.3389/978-2-8325-6845-3

Table of contents

04 Editorial: Advancing cancer therapy: innovative strategies targeting immune evasion and metabolic modulation
Mónica Teotónio Fernandes, Ana Luísa De Sousa-Coelho and Andrés Méndez-Lucas

07 Tumor glucose metabolism and the T cell glycocalyx: implication for T cell function
Fabian Schuurmans, Kyra E. Wagemans, Gosse J. Adema and Lenneke A. M. Cornelissen

17 Clinical applications of STING agonists in cancer immunotherapy: current progress and future prospects
Bin Wang, Wanpeng Yu, Hongfei Jiang, Xiangwei Meng, Dongmei Tang and Dan Liu

27 Resveratrol contributes to NK cell-mediated breast cancer cytotoxicity by upregulating ULBP2 through miR-17-5p downmodulation and activation of MINK1/JNK/c-Jun signaling
Bisha Ding, Jie Li, Jia-Lin Yan, Chun-Yan Jiang, Ling-Bo Qian and Jie Pan

44 Single-cell sequencing and spatial transcriptomics reveal the evolution of glucose metabolism in hepatocellular carcinoma and identify G6PD as a potential therapeutic target
Deyang Xi, Yinshuang Yang, Jiayi Guo, Mengjiao Wang, Xuebing Yan and Chunyang Li

57 Predicting the immune therapy response of advanced non-small cell lung cancer based on primary tumor and lymph node radiomics features
Dong Xie, Jinna Yu, Cong He, Han Jiang, Yonggang Qiu, Linfeng Fu, Lingting Kong and Hongwei Xu

67 Pancreatic cancer subtyping - the keystone of precision treatment
Zeyang Fan, Yao Xiao, Yan Du, Yan Zhang and Wence Zhou

88 Metabolic reprogramming and therapeutic targeting in non-small cell lung cancer: emerging insights beyond the Warburg effect
Hong Cai, Feng Zhang, Fang Xu and Chunhui Yang

104 Prognostic effect of CD74 and development of a radiomic model for predicting CD74 expression in non-small cell lung cancer
Yancheng Wang, Zhen Gao, Meng Li, Zhen Feng and Hui Wang

117 Immunotherapy in advanced esophageal squamous cell cancer: earlier or later?
Shuang Wei, Zuoji Li, Tingting Liu, Guizhen Sun, Hongfu Sun and Wei Huang

frontiers | Frontiers in Medicine

TYPE Editorial
PUBLISHED 29 August 2025
DOI 10.3389/fmed.2025.1677300

Check for updates

OPEN ACCESS

EDITED AND REVIEWED BY
Alice Chen,
Consultant, Potomac, MD, United States

*CORRESPONDENCE
Mónica Teotónio Fernandes
✉ mafernandes@ualg.pt

RECEIVED 31 July 2025
ACCEPTED 06 August 2025
PUBLISHED 29 August 2025

CITATION
Fernandes MT, De Sousa-Coelho AL and Méndez-Lucas A (2025) Editorial: Advancing cancer therapy: innovative strategies targeting immune evasion and metabolic modulation. *Front. Med.* 12:1677300.
doi: 10.3389/fmed.2025.1677300

COPYRIGHT
© 2025 Fernandes, De Sousa-Coelho and Méndez-Lucas. This is an open-access article distributed under the terms of the Creative Commons Attribution License (CC BY). The use, distribution or reproduction in other forums is permitted, provided the original author(s) and the copyright owner(s) are credited and that the original publication in this journal is cited, in accordance with accepted academic practice. No use, distribution or reproduction is permitted which does not comply with these terms.

Editorial: Advancing cancer therapy: innovative strategies targeting immune evasion and metabolic modulation

Mónica Teotónio Fernandes[1,2]*, Ana Luísa De Sousa-Coelho[1,2] and Andrés Méndez-Lucas[3,4]

[1]Escola Superior de Saúde, Universidade do Algarve (ESSUAlg), Faro, Portugal, [2]Algarve Biomedical Center Research Institute (ABC-Ri), Universidade do Algarve (UAlg), Faro, Portugal, [3]Physiological Sciences Department, School of Medicine, University of Barcelona (UB), Barcelona, Spain, [4]Bellvitge Biomedical Research Institute (IDIBELL), L'Hospitalet de Llobregat, Spain

KEYWORDS

cancer therapy, biomarkers, immunotherapy, metabolism, therapy resistance, personalized medicine

Editorial on the Research Topic
Advancing cancer therapy: innovative strategies targeting immune evasion and metabolic modulation

Cancer remains one of the leading causes of death worldwide, with both incidence and mortality continuing to rise despite advances in diagnosis and treatment (1). While early-stage cancers often respond to conventional therapies, advanced and recurrent tumors frequently develop resistance, limiting long-term therapeutic efficacy (2).

Two fundamental hallmarks of cancer, immune evasion and metabolic reprogramming, enable tumors to thrive in hostile microenvironments (3, 4). Although immunotherapies have revolutionized cancer care, a significant proportion of patients either fail to respond or acquire resistance over time (5). In parallel, altered tumor metabolism is increasingly recognized as a promising therapeutic target, particularly for enhancing responses to immunotherapy (7).

This Research Topic highlights recent advances that move beyond traditional treatment. Collectively, the nine featured articles provide valuable insights into the interplay between immunity and metabolism in cancer, exploring strategies to overcome therapeutic resistance and improve clinical outcomes across diverse cancer types.

Several contributions in this Research Topic showcase innovative strategies in immuno-oncology, with a particular focus on integrating biomarkers, imaging techniques, and immune modulation to propel the development of personalized cancer therapies.

Wei et al. addressed a key clinical question in immuno-oncology: does the timing of immune checkpoint inhibitor (ICI) therapy influence outcomes in advanced esophageal squamous cell carcinoma? Their study revealed that, while early immunotherapy does not significantly improve overall survival, it does prolong progression-free survival, particularly in defined patient subgroups. These findings underscore the need to personalize not only the type of treatment but also its timing, especially in settings where biomarkers like PD-L1 are not routinely available (Wei et al.).

In the pursuit of biomarkers to predict immunotherapy response, a cornerstone of precision oncology, Wang Y. et al. explored the prognostic significance of CD74 expression in non-small cell lung cancer (NSCLC) and developed a radiomics-based machine learning model to predict CD74 levels from contrast-enhanced CT images. Their results demonstrate that high CD74 expression correlates with improved overall survival and enhanced antitumor immune activity. The radiomics models achieved strong predictive performance, offering a non-invasive method to stratify patients. This work positions CD74, a membrane glycoprotein involved in immune signaling, as both a prognostic biomarker and a potential therapeutic target in NSCLC, while showcasing the promise of AI-driven imaging biomarkers in precision oncology (Wang Y. et al.). Extending this theme, Xie et al. introduced another radiomics-based machine learning approach to predict response to neoadjuvant immunochemotherapy in advanced NSCLC. By analyzing pre-treatment CT scans, they developed a radiomic signature capable of distinguishing responders from non-responders. Together, these studies highlight radiomics as a non-invasive, scalable tool to guide patient selection and optimize immunotherapy outcomes (Xie et al.).

Focusing on immune evasion in breast cancer, Ding et al. examined how the natural compound resveratrol sensitizes breast cancer cells to natural killer (NK) cell-mediated cytotoxicity. Their work revealed that resveratrol downregulates miR-17-5p, leading to MINK1/JNK/c-Jun pathway activation and upregulation of the NKG2D ligand ULBP2. This enhanced NK cell recognition and killing of tumor cells both *in vitro* and *in vivo*, suggesting that dietary or pharmacologic interventions could potentiate innate immune clearance mechanisms (Ding et al.).

Finally, Wang B. et al. provide an insightful review of the cyclic GMP-AMP synthase-stimulator of interferon genes (cGAS-STING) pathway in the anti-tumor innate immune response and the use of STING agonists to overcome resistance to conventional therapies. The authors report mechanisms by which STING agonists have the potential to convert "cold" tumors, which lack immune cell infiltration, into "hot" tumors that are more responsive to immunotherapy, present a broad range of STING agonists categories, and discuss several challenges that must be addressed to fully realize the clinical potential of this approach (Wang B. et al.).

Among the selected contributions, other articles delve into cancer metabolism and emerging technologies that are shaping the future of personalized oncology.

The glycocalyx is a glycan-rich layer on the cell surface, with a distinct composition in tumor cells compared to healthy ones. On T cells, glycans regulate key functions and interact with glycan-binding proteins involved in tumor progression. Many immune receptors, such as PD-1, are glycosylated, affecting their stability, ligand binding, and recognition by therapeutic antibodies (6). These topics are discussed in Schuurmans et al., who reviewed the interplay between tumor glucose metabolism and T cell glycocalyx, which is essential for adequate T cell activation and may represent a relevant target to improve anti-tumor T cell biology.

The role of metabolic reprogramming in cancer progression and resistance to therapy in NSCLC was explored in a comprehensive review by Cai et al. After identifying NSCLC key metabolic vulnerabilities, the authors discuss how these can be exploited with drugs and/or compounds that target the glucose, mitochondrial, lipid, and amino acid metabolism pathways, which may be combined with immunotherapies (Cai et al.). The authors also highlight the use of single-cell and spatial metabolomics to identify metabolic subtypes, which could lead to more personalized treatments.

These emerging technologies were applied in an integrative original article, which analyzed single-cell sequencing and spatial transcriptomics data from hepatocellular carcinoma (HCC) sourced from databases (Xi et al.). Xi et al. used computational tools to map the expression of glucose metabolism-related genes and explored the spatial dynamics of glucose metabolism in HCC. From *in vitro* assays, G6PD, the rate-limiting enzyme of the pentose phosphate pathway, was identified to be involved in HCC progression, associated with glutathione metabolism and ROS production (Xi et al.).

Finally, a review by Fan et al. explores in depth the molecular subtyping of pancreatic cancer, integrating multiple layers of data encompassing gene mutations, genomics, transcriptomics, proteomics, metabolomics, and immunomics. They concluded that the integration of multi-omics approaches is critical for developing personalized treatment approaches and improving the clinical outcomes (Fan et al.).

This Research Topic showcases innovative research that collectively advances our understanding of how cancers escape immune detection and rewire metabolism to sustain growth. The nine featured studies offer mechanistic insights and propose translational strategies ranging from STING pathway activation to targeting metabolic vulnerabilities. We thank all the authors and reviewers for their valuable contributions and hope this Research Topic inspires continued efforts to bridge immunology, metabolism, and oncology for more effective and durable cancer therapies.

Author contributions

MF: Conceptualization, Supervision, Writing – original draft, Writing – review & editing. AD: Writing – original draft, Writing – review & editing. AM-L: Writing – original draft, Writing – review & editing.

Conflict of interest

The authors declare that the research was conducted in the absence of any commercial or financial relationships that could be construed as a potential conflict of interest.

Generative AI statement

The author(s) declare that no Gen AI was used in the creation of this manuscript.

Any alternative text (alt text) provided alongside figures in this article has been generated by Frontiers with the support of artificial intelligence and reasonable efforts have been made to ensure accuracy, including review by the authors wherever possible. If you identify any issues, please contact us.

Publisher's note

All claims expressed in this article are solely those of the authors and do not necessarily represent those of their affiliated organizations, or those of the publisher, the editors and the reviewers. Any product that may be evaluated in this article, or claim that may be made by its manufacturer, is not guaranteed or endorsed by the publisher.

References

1. Siegel RL, Kratzer TB, Giaquinto AN, Sung H, Jemal A. Cancer statistics, 2025. *CA Cancer J Clin*. (2025) 75:10–45. doi: 10.3322/caac.21871

2. Hanahan D, Weinberg RA. Hallmarks of cancer: the next generation. *Cell*. (2011) 144:646–74. doi: 10.1016/j.cell.2011.02.013

3. Pavlova NN, Thompson CB. The emerging hallmarks of cancer metabolism. *Cell Metab*. (2016) 23:27–47. doi: 10.1016/j.cmet.2015.12.006

4. Binnewies M, Roberts EW, Kersten K, Chan V, Fearon DF, Merad M, et al. Understanding the tumor immune microenvironment (TIME) for effective therapy. *Nat Med*. (2018) 24:541–50. doi: 10.1038/s41591-018-0014-x

5. Sharma P, Hu-Lieskovan S, Wargo JA, Ribas A. Primary, adaptive, and acquired resistance to cancer immunotherapy. *Cell*. (2017) 168:707–23. doi: 10.1016/j.cell.2017.01.017

6. De Bousser E, Meuris L, Callewaert N, Festjens N. Human T cell glycosylation and implications on immune therapy for cancer. *Hum Vaccin Immunother*. (2020) 16:2374–88. doi: 10.1080/21645515.2020.1730658

7. Ricci J-E. Tumor-induced metabolic immunosuppression: mechanisms and therapeutic targets. *Cell Rep*. (2025) 44:115206. doi: 10.1016/j.celrep.2024.115206

frontiers | Frontiers in Immunology

TYPE Review
PUBLISHED 31 May 2024
DOI 10.3389/fimmu.2024.1409238

Check for updates

OPEN ACCESS

EDITED BY
Dainius Characiejus,
Vilnius University, Lithuania

REVIEWED BY
Jörg Wischhusen,
University Hospital Würzburg, Germany
Jackwee Lim,
Singapore Immunology Network (A*STAR),
Singapore

*CORRESPONDENCE
Lenneke A. M. Cornelissen
Lenneke.Cornelissen@radboudumc.nl

RECEIVED 29 March 2024
ACCEPTED 21 May 2024
PUBLISHED 31 May 2024

CITATION
Schuurmans F, Wagemans KE, Adema GJ and Cornelissen LAM (2024) Tumor glucose metabolism and the T cell glycocalyx: implication for T cell function.
Front. Immunol. 15:1409238.
doi: 10.3389/fimmu.2024.1409238

COPYRIGHT
© 2024 Schuurmans, Wagemans, Adema and Cornelissen. This is an open-access article distributed under the terms of the Creative Commons Attribution License (CC BY). The use, distribution or reproduction in other forums is permitted, provided the original author(s) and the copyright owner(s) are credited and that the original publication in this journal is cited, in accordance with accepted academic practice. No use, distribution or reproduction is permitted which does not comply with these terms.

Tumor glucose metabolism and the T cell glycocalyx: implication for T cell function

Fabian Schuurmans, Kyra E. Wagemans, Gosse J. Adema and Lenneke A. M. Cornelissen*

Radiotherapy and OncoImmunology Laboratory, Department of Radiation Oncology, Radboud University Medical Center, Nijmegen, Netherlands

The T cell is an immune cell subset highly effective in eliminating cancer cells. Cancer immunotherapy empowers T cells and occupies a solid position in cancer treatment. The response rate, however, remains relatively low (<30%). The efficacy of immunotherapy is highly dependent on T cell infiltration into the tumor microenvironment (TME) and the ability of these infiltrated T cells to sustain their function within the TME. A better understanding of the inhibitory impact of the TME on T cells is crucial to improve cancer immunotherapy. Tumor cells are well described for their switch into aerobic glycolysis (Warburg effect), resulting in high glucose consumption and a metabolically distinct TME. Conversely, glycosylation, a predominant posttranslational modification of proteins, also relies on glucose molecules. Proper glycosylation of T cell receptors influences the immunological synapse between T cells and tumor cells, thereby affecting T cell effector functions including their cytolytic and cytostatic activities. This review delves into the complex interplay between tumor glucose metabolism and the glycocalyx of T cells, shedding light on how the TME can induce alterations in the T cell glycocalyx, which can subsequently influence the T cell's ability to target and eliminate tumor cells.

KEYWORDS

tumor microenvironment, metabolism, T cell glycocalyx, glycobiology, tumor immunity

1 Immunotherapy to reinvigorate T cell effector functions

The T cell is an immune cell subset highly effective in eliminating cancer cells. Upon priming by professional antigen presenting cells that present tumor (neo-)antigens, T cells become activated and can recognize cancer cells. T cell activation induces rapid T cell proliferation leading to the expansion of a population of T cells specifically targeting the cancer cell (1). The resulting effector T cells can directly kill cancer cells by releasing cytotoxic molecules such as perforin and granzymes, which induce programmed cell death

through a multi-hit mechanism (2). Additionally, T cells can induce apoptosis in cancer cells through interactions involving death receptors and ligands, such as Fas ligands (FasL) binding to Fas receptor on the surface of cancer cells (3). Furthermore, T cells can release cytokines such as interferon-gamma (IFNy) and tumor necrosis factor-alpha (TNFα), which have anti-tumor effects by inducing permanent growth arrest, leading to their elimination and promotion of inflammation (4).

Cancer cells evolve, however, mechanisms to evade T cell-mediated killing. Immune checkpoints, both stimulatory and inhibitory receptors, control and co-determine the functional outcome of T cell effector responses (5, 6). Immune checkpoint receptor/ligand pairs are present on a diverse set of cells where they regulate the initiation and course of the immune response, which otherwise can cause tissue damage or the development of autoimmunity. Immune checkpoint therapy aims to release the break and harness the body's immune system to enhance its ability to recognize and destroy cancer cells. The most targeted immune checkpoints in the onco-immunology field are PD-1, PD-L1 and CTLA-4. Monoclonal antibodies blocking these checkpoints interfere with T cell feedback loops and empowers T cells to eliminate cancer cells. Immune checkpoint therapy has shown significant clinical benefit for subgroups of patients with different malignancies (7–11), however, the overall response rate remains below 30% (12).

Next to immune checkpoint therapy, CAR T cell therapy constitutes another form of immunotherapy within the field of oncology. CAR T cell therapy involves genetically modifying a patient's T cell to express chimeric antigen receptors (CARs) that target specific antigens on cancer cells including glycosylated antigens (13–15). Such ex-vivo engineered CAR T cells are then infused back into the patient, where they can target and kill cancer cells expressing the corresponding antigen. CAR T cells therapy has shown remarkable success especially in hematologic malignancies (16). Despite is advancements, there are still many challenges and questions to address regarding CAR T cell therapies. Factors such as CAR T cell exhaustions and antigen escape contribute to treatment resistance and the occurrence of adverse events highlight the importance of monitoring and managing treatment-related complications (17). As an example, hyperglycosylation of the CAR T cell antigen CD19 directly inhibits CAR T cell effector functions, leading to less T cell cytotoxicity (18). In solid tumors, CAR T cell therapy has shown limited clinical efficacy due to factors such as inadequate tumor infiltration and an immunosuppressive tumor microenvironment (19).

T cell cytotoxicity requires multi-hit delivery to induce cell death and in the absence of suppressive signaling, T cells are capable to engage and eliminate multiple cancer cells successively (serial killing). Hence the efficacy of cancer immunotherapy is not solely dictated by T cell infiltration but also by the ability of the (CAR) T cells to sustain their functions within the TME. Obtaining more insights into the inhibitory impact of the TME on T cells is indispensable to improve immunotherapy. A century ago, Otto Heinrich Warburg noted a distinct contrast between the TME and non-malignant tissues in terms of metabolism. Tumor cells exhibit altered glucose metabolism, leading to high glucose consumption, which results in lactate production and acidification of the TME, commonly known as the Warburg effect (20, 21).

2 Tumor metabolism

Tumor cells exhibit a heightened need for energy to sustain their uncontrolled proliferation and to ensure survival. The Warburg effect involves preferential use of glucose for aerobic glycolysis even in the presence of oxygen. In non-cancerous context, the Warburg effect is exploited by rapidly proliferating cells. In tumor cells, the Warburg effect is a well-known metabolic alteration to support their high proliferation rate (Figure 1). This metabolic adaptation provides the tumor cells with energy, albeit less efficiently in terms of ATP production than oxidative phosphorylation (20). Tumor cells do favor aerobic glycolysis as it allows for quick energy production, and it provides intermediates that can be used for the biosynthesis of nucleotides, amino acids and lipids, the building blocks for the synthesis of cellular components. Moreover, the increased demand for Nicotinamide adenine dinucleotide (NAD^+) relative to ATP has been found to drive aerobic glycolysis (22). NAD^+ and its reduced forms (NADH, $NADP^+$ and NADPH) are essential redox metabolites in numerous metabolic processes, acting as hybrid-accepting and donating co-enzymes. The heightened glucose consumption by tumor cells results in a competition for glucose between immune cells and tumor cells and metabolically restricts infiltrating T cells. Together facilitating tumor growth and progression (23). Moreover, aerobic glycolysis culminates in the production of lactate, leading to heightened lactate concentration in the TME when glycolysis is increased. Lactate has been identified as an alternative energy source for tumor cells, as exogenous lactate can serve as a substrate for the tricarboxylic acid (TCA) cycle to fuel cancer cells growth (24, 25). At the same time, lactate causes extracellular acidification, which can facilitate tumor progression by suppressing immune response and promoting tumor invasion (26).

In addition to glucose, tumor cells can utilize glutamine as an alternative energy source. Similarly, the altered glutamine metabolism leads to a reduction in the availability of this essential nutrient for immune cells. The competition for glutamine can impair the function of immune cells, impacting their ability to mount an effective anti-tumor immune response (27). Moreover, tumor cells can switch to lipid metabolism as an alternative source of energy and building materials. Lipid metabolic reprogramming not only supports tumor development, it also modifies the TME by affecting the recruitment, function and survival of infiltrating immune cells (28). Fatty acids are involved in membrane proliferation (29) and can be secreted by the tumor cell to influence the functioning of immune cells (30).

Collectively, the TME displays metabolic abnormalities in comparison to healthy tissue. Research has demonstrated that competition for energy and nutrients hampers immunity. In addition, tumor metabolites affect the efficacy of immune cells, exerting a direct immunosuppressive effect on immune cells (31).

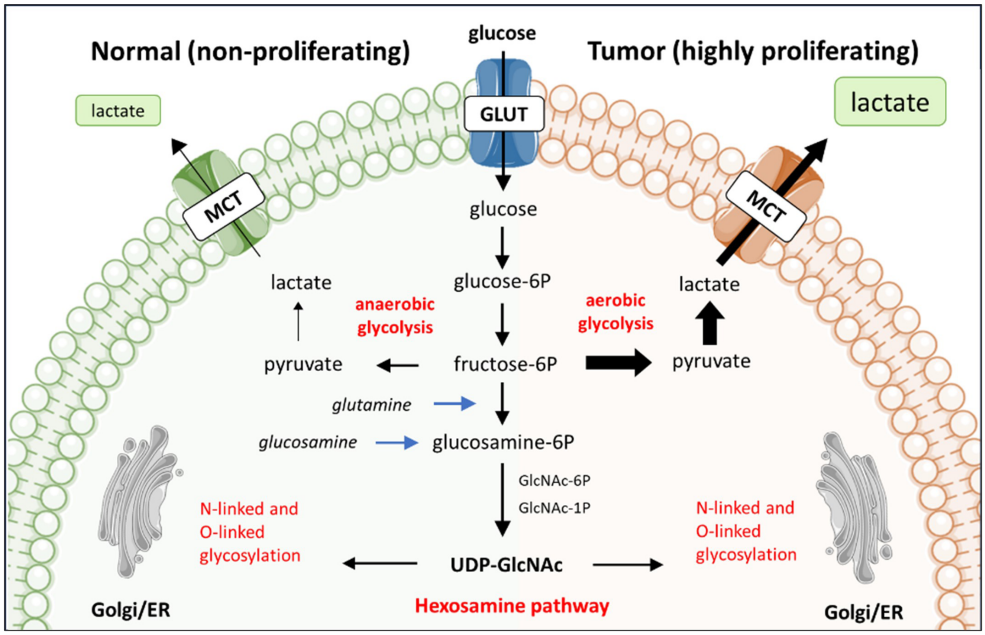

FIGURE 1
The preferential use of aerobic glycolysis by tumor cells and its relationship with glycosylation. The reliance of tumor cells on aerobic glycolysis, rather than oxidative phosphorylation, leads to heightened lactate production from glucose metabolism. This preference for aerobic glycolysis is associated with the hexosamine biosynthesis pathway (HBP), which shares the initial steps of glucose metabolism. The HBP is pivotal in protein and lipid glycosylation, thereby establish a significant interconnection between glycosylation and glucose metabolism.

The scope of this review is on tumor glucose metabolism and its impact on local T cell glycosylation and function.

3 The glucose metabolism pathway and glycosylation biosynthesis are intertwined

Tumor cells utilize high amounts of glucose and glutamine via aerobic glycolysis. These glucose and glutamine molecules, however, are also consumed by the metabolic hexosamine biosynthesis pathway (HBP) in the cytoplasm of the cell. The HBP converts glucose or glutamine to UPD-*N*-acetylglucosamine (UPD-GlcNAc) via a six-step pathway that shares the first two steps with glycolysis (Figure 1). UDP-GlcNAc is one of the essential intermediates for glycosylation, hence HBP plays a significant role in regulating glycosylation. For instance, low levels of glucose have been observed to reduce the availability of glycosylation precursors in expression systems such as CHO cells. Consequently leading to more non-glycosylated proteins produced by these CHO cells (32). In contrast, supplementation of glucose to primary murine T cell cultures changed the glycosylation profile of the T cells with functional consequences. Specifically, the attachment of β1,6-GlcNAc-branched *N*-glycans to cell surface glycoproteins negatively regulated T cell receptor clustering and signaling at the immune synapse (33), an essential interface between cells needed for proper activation of naïve T cell as well as the ability of effector T cells to kill tumor cells.

Glycosylation is the process of covalently attaching monosaccharides to other monosaccharides, proteins, and lipids, creating a wide repertoire of cellular glycans, collectively referred to as the glycome. There are ten monosaccharide building blocks, which can be modified via phosphorylation, sulfation or acetylation. Unlike DNA/RNA transcription, glycosylation is a non-template driven process and regulated via a wide variety of enzymes (34). The product of HBP, UDP-GlcNAc, serves as a substrate of *O*-GlcNAc transferases (OGT). OGT catalyzes the attachment of a GlcNAc through an *O*-glycosidic linkage to a serine (Ser) or threonine (Thr) residues on intracellular proteins. A delicate on/off competition mechanism between O-GlcNAcylation and phosphorylation takes place on either the same or adjacent Ser/Thr residues. This on/off mechanism regulates the interactions, stability, subcellular localization, and enzymatic activity of shared target proteins involved in essential biological processes (35). Unlike extracellular glycosylation, *O*-GlcNAc is not elongated with monosaccharides to generate more complex glycan structures. In addition to *O*-GlcNAcylation, UDP-GlcNAc serves as a crucial precursor for the biosynthesis of monosaccharides such as UDP-GalNAc and CMP-Neu5Ac that are often utilized in *N*-linked and *O*-linked glycosylation processes (36). Once located at the cell membrane, extracellular glycosylation can be further modified by soluble glycan modifying enzymes including glycosidases and sulfatases (37). It has been described that extrinsic sialyltransferases and glycan substrates, supplied among others by platelets, can modify glycan structures present on cell membranes (38–40). Moreover, monocyte differentiation results in up-regulation of neuraminidase 1 (Neu1)

that activates phagocytoses in macrophages and dendritic cells via desialylation of surface receptors (41, 42).

As glycans coat the surface of cells, this posttranslational modification is important in the development of all living organisms (43). The tree-like layer composed of glycans on the outer cell membrane is known as the glycocalyx. The specific biochemical composition of the glycocalyx is unique for each cell type (44). Glycans highly impact protein functions and are consequently involved in numerous biological processes including cell adhesion, signal transduction, receptor retention and endocytosis of molecules. In the context of cancer, glycans are implicated in cell invasion, regulation of vascular permeability, immune modulation, and cancer metastasis (45). Given the immunosuppressive impact of tumor metabolites, it is plausible that the interconnected metabolic and glycosylation biosynthesis pathways may contribute to these cancer phenomena. This remains, however, still a largely unexplored research area.

4 The tumor glycocalyx

Tumor cells are well described to have a different glycocalyx composition when compared to their healthy counterparts (46, 47). This aberrant tumor glycosylation profile has been related to the acquisition of hallmarks of cancer (48) and consequently, associated with patient outcomes. For instance, Jiang et al. (49) demonstrate that the expression of aberrant O-glycans, including the Tn antigen, in colorectal cancer is linked to tumor metastatic potential and poor prognosis. More recently, Sun et al. (50) identified a glycosylation signature for predicting the progression and immunotherapeutic response of prostate cancer, emphasizing the role of glycosylation in disease advancement and treatment outcomes.

The aberrant glycosylation profile of tumor cells is affected by various factors, including alterations in glycosyltransferase expression levels and changes in the availability of glycan substrates within the TME (51). Changes in cellular metabolic status can contribute to changes in the availability of glycan substrates, particularly through modulation of the HBP (52). Hyperglycemia, for instance, has been associated with exacerbating colon cancer malignancy through the HBP, indicating a direct relationship between glucose metabolism, HBP, and tumor progression (53, 54). Moreover, hypoxia, a common feature of the TME, has been associated with alterations in glycosylation patterns in cancer cells. Hypoxia-driven changes in glycosylation can impact cell migration and invasion, contribution to tumor aggressiveness (55).

The aberrant glycosylation profile of tumors cells impacts the interaction of tumor cells with the immune system within the TME (56–59). As an example, the aberrant O-linked glycosylation of MUC1 in carcinomas can alter the interaction of MUC1 with glycan binding receptors, consequently affecting the tumor-immune interplay (60). How alterations in tumor glycosylation affects tumor immunity, has comprehensively reviewed by others and is not the scope of this review (61–64).

Besides tumor-immune interactions, the tumor glycocalyx has also been described to be involved in the regulation of tumor cell proliferation. A cytostatic effect on tumor cells refers to the inhibition of cell proliferation without inducing cell death. This effect is crucial in cancer treatment as it aims to halt the growth and spread of tumors. Several reports propose that tumor glycoproteins may play a role in the outcome of cytostatic effects on tumor cells. The P-glycoprotein (P-gp) is a glycosylated transmembrane protein that acts as a multidrug transporter and reported to play a crucial role in multidrug resistance in cancer cells by actively removing cytostatic drugs, including chemotherapy, from tumor cells (65, 66). Whether glycosylation does impact the functionality of P-gp, has not been explored. CD44, a cell surface adhesive glycoprotein, plays a crucial role in tumorigenes. An increasing amount of literature indicates CD44, and especially the CD44v isoforms, as a marker for cancer stem cells. CD44 regulates cancer stemness, including self-renewal and metastasis (67). Hou et al. demonstrated that *N*-glycosylation of CD44 enhances its stability, consequently promoting tumor cell proliferation (68). Beyond transmembrane glycoproteins, intracellular *O*-GlcNAcylation has been linked to tumor proliferation by modulating cellular pathways (47). Inhibition of *O*-GlcNAcylation leads to accumulation of bladder cancer cells in G0/G1 phase (69). Consequently, targeting *O*-GlcNAcylation has been proposed to overcome cancer resistance to therapies including cytostatic drugs (70).

Certain subsets of T cells, particularly the regulatory T cells, as well as cancer cells are known to be able to produce transforming growth factor beta (TGFβ). TGFβ is a cytokine that plays a complex role in cancer progression. In certain contexts, TGFβ generates a population of cancer cells that reside in the G0/G1 phase with high motility and metastatic potential (71, 72). Additionally, TGFβ can induce dormancy in cancer cells, underscoring its role in maintaining quiescence in cancer cells (73). In the context of tumor dormancy, changes in TGFβ glycosylation could potentially affect its ability to induce cell cycle arrest or promote a quiescent state in cancer cells. Glycosylation alterations may influence the interaction of TGFβ with its receptors and downstream effectors, leading to differential effect on cell proliferation and dormancy (74). For instance, Sun et al. (75) demonstrates that glycosylation of TGFβ receptor II is indispensable for proper TGFβ signaling, which further promotes cell cycle arrest-like traits in breast cancer. These studies illustrate the cytostatic mechanism by which the immune system can affect cancer cells and highlight the crucial role of glycosylation alterations this process.

5 The T cell glycocalyx

Like the tumor cell, the T cell membrane is also covered with glycan structures. The T cell glycocalyx co-regulates key pathophysiological steps within T cell biology including T cell development, activation and proliferation (76–79). Different kinds of protein glycosylation including *O*-GlcNAcylation, fucosylation and sialylation have been described to be involved in the different stages of T cell development, from homing of T cell precursors to the thymus, to selection and maturation of single positive $CD4^+$ and $CD8^+$ T cells (34). The conserved Notch signaling pathway plays a

major role in the initial commitment to the T cell lineage within the thymus. Early thymocyte progenitors develop in the thymus from their double negative ($CD4^-$ and $CD8^-$) state into T cells via the Notch pathway (80). The glycosylation profile of Notch receptors has been shown to control Notch-dependent intracellular signal transduction, stressing the relevance of glycosylation for T cell development (81). For instance, *N*-acetylglucosaminyltransferases modify Notch receptors and loss of these glycosyltransferases leads to reduced binding of Notch to Delta-like ligands, altering the frequencies of T cell subsets in the thymus (82). Mannose-restricted thymocyte glycans were found to impair key developmental checkpoints such as normal lineage choice, Treg cell generation and T cell receptor (TCR) β-selection (83). Moreover, during thymic development the reactivity of the TCR reactivity is tightly regulated and influenced by its glycosylation pattern. De-sialylation was found to enhance the sensitivity of mature T cells to low-affinity TCR ligands or self-ligands (84). Similarly, the binding ability of CD8 to MHC class I is decreased by enhanced T cell sialylation upon T cell maturation during T cell development (85). This underscores the significance of the T cell glycosylation machinery during thymic development.

The process of T cell activation typically involves three main signals. First, the TCR recognizes a specific antigen presented by antigen-presenting cells (APC) in the context of MHC molecules. Secondly, co-stimulatory molecules, such as CD28 on T cells and CD80/86 on APCs reinforces T cell activation. The third signal is obtained from cytokines released by the APC and surrounding cells that influences the differentiation, proliferation, and effector functions of the activated T cell. T cell activation leads to exceptionally high rate of growth and proliferation. Activated T cells rapidly upregulate their glucose uptake and glycolysis to fuel the energetic and biosynthetic demands for rapid clonal expansion (86). This includes generation of glycan-donor substrates required for glycan biosynthesis that is needed for proper T cell function (87). Moreover, TCR signaling induced by anti-CD3/CD28 monoclonal antibodies on T cells co-regulates mRNA expression of multiple *N*-glycan processing enzymes including MGAT5 and Golgi α-mannosidase enzymes, to promote *N*-glycan branching and formation of mature glycans (88). Involvement of glycosylation in T cell activation and sustaining their effector functions is mainly by *N*-glycosylation of the TCR, CD25 and co-stimulatory and -inhibitory receptors (34, 81, 89). Glycans can play a stabilizing role in complexes formed at the immunological synapse (34). For instance, a deficiency in β1,6 *N*-acetylglucosaminyltransferase V (MGAT5) enhances TCR clustering, resulting in a lower T cell activation (76). MGAT5 initiates GlcNAc β1,6 *N*-glycan branching (90). A deficiency in *N*-glycan branching results in lower presence of *N*-acetylglucosamine, the ligand for galectins. Galectins are known to modulate T cell proliferation and apoptosis (91) by regulating TCR clustering and recruitment to the site of antigen presentation. By removing galectin ligands, the threshold for T cell activation is lowered. The absence of MgatV has then also been associated with increased susceptibility for autoimmune disease (76). Opposingly, when inhibiting *N*-glycosylation by point mutations in *N*-glycosylation sites of CD28, CD28 showed an increased binding to CD80, leading to enhanced CD28 signaling activity (92). Collectively, *N*-glycosylation is profoundly involved in T cell activation and its impact is significantly determined by inhibiting the whole *N*-glycosylation machinery versus inhibition of *N*-glycosylation on specified T cell glycoproteins.

Besides T cell biology, the glycans on the T cell surface serve as signals for glycan binding proteins (GBPs). GBPs are widely express among a diverse set of immune cells, thereby regulating the immune response. The three main types of GBPs are galectins, Sialic acid-binding immunoglobulin-type lectins (Siglecs) and C-type lectins (93). The GBPs and their immune regulatory roles are highly diverse and complex (43, 93, 94). For example, Galectin-1 is pro-tumorigenic and proangiogenic in tumor progression. Tumor secreted Galectin-1 has immunosuppressive effects and serves as an important marker in diagnosis, prognosis, and treatment of cancer (34, 95, 96). Moreover, Galectin-1 was found to negatively influence the proliferation of $CD8^+$ T cells and therefore affect antitumor immunity (97). One of the targets of Galectin-1 is the CD45 receptor on T cells. CD43 and CD45 are highly abundant glycoproteins on the T cell surface and are decorated with *O*- and *N*-glycans, regulating their function and binding. For instance, sialylation of CD45 was shown to inhibit Galectin-1-induced clustering, an initial step in Galectin-1 mediated cell death (98). This indicates that CD45 glycosylation can control T cell susceptibility to cell death (99).

Collectively, glycans serve as regulators of T cell biology, exerting significant influence on the immunological synapse, including interactions between T cells and tumor cells. Therefore, the T cell glycocalyx represents as a target to improve anti-tumor T cell immunity.

6 The influence of the TME on T cell functions via the T cell glycocalyx

The efficacy of T cells in inducing cancer cell arrest and elimination relies heavily on their ability to sustain functional within the TME. The TME can, however, induce T cell exhaustion and senescence, leading to altered differentiation and hypofunctional status of T cells (100, 101). Persistent antigen presentation in the TME can be associated with the induction of T cell dysfunctions, resulting in an exhausted state (101). Exhausted T cells typically exhibit heightened expression of inhibitory receptors, reduced effector cytokine production, and impaired cytolytic activity. Besides prolonged exposure to antigen, metabolites present in the TME can also influence T cell function. Elevated lactate levels, for instance, have been shown to suppress the anti-tumor activity of T cells by increasing the accumulation of H^+ ions and maintaining a low pH environment (102, 103). In general, the functional outcome of T cells is co-determined by the activation of stimulatory and inhibitory receptors on T cells. The majority of these immune receptors are glycosylated (89, 104). The glycosylation pattern can influence the receptor's stability, ligand binding affinity (105, 106), and recognition by therapeutic monoclonal antibodies, thus affecting their anti-tumor efficacy (107, 108). Moreover, the glycosylation machinery of a cell is dynamic and reflects the functional state of a cell. As an example, T cells present in PBMCs isolated at time of SARS-Cov-2 diagnoses

(within 72h of positive PCR SARS-Cov-2 test) displayed an altered glycosylation profile when compared to healthy controls (109). A metabolic altered TME could similarly cause alterations in the T cell glycocalyx with possibly functional consequences.

Recent studies report on how *N*-glycosylation can directly interfere with T cell function within the TME. Malignant ascites fluid obtained from ovarian cancer patients, inhibited glucose uptake by $CD4^+$ T cells and resulted in *N*-linked glycosylation defects. The loss of fully *N*-glycosylated proteins suppressed mitochondrial activity and IFNγ production by the $CD4^+$ T cells. Restoration of *N*-linked glycosylation enhanced mitochondrial respiration again in $CD4^+$ T cells exposed to malignant ovarian ascites (110). In addition to $CD4^+$ T cells, Kim et al. (111) demonstrated that deficient *N*-glycosylation impairs IFNγ mediated effector function also in tumor-infiltrating $CD8^+$ T cells, impacting the anti-tumor immune response. Mechanistically, tumor infiltrating and exhausted $CD8^+$ T cells downregulate the oligosaccharyltransferase (OST) complex. The OST complex catalyzes the attachment of precursor *N*-glycans to nascent target proteins in the endoplasmic reticulum (ER). OST complex is therefore indispensable for the *N*-glycosylation pathway. Interestingly, restoration of the OST complex complemented *N*-glycosylation that restored the IFNγ production and alleviated $CD8^+$ T cell exhaustion, consequently resulting in reduced tumor growth in preclinical models (111).

T cell proliferation and activation is dependent on the competitive binding of CTLA-4 or CD28 on the T cell to the CD80/86 ligand on an APC. When CTLA-4 binds CD80/86 instead of CD28, T cell proliferation is inhibited (112). Increased CTLA-4 glycan branching retains CTLA-4 on the cell surface, suppressing T cell activation (88). Upon activation, T cell upregulate PD-1. Upon binding of PD-1 to its ligand, PD-L1, the glycolysis metabolism is attenuated, limiting the energy supply, and impeding the differentiation into effector T cells (113). This binding also induces protumor genic rapamycin (mTOR) signaling, reactive oxygen species (ROS) production and mitochondrial respiration (114). These processes all exert negative effects on T cell activity and cytotoxicity. Immune checkpoint proteins including CTLA-4 and PD-1 are glycosylated, which can be crucial for their function (89). PD-1 contains four *N*-glycosylation sites that are critical for maintaining PD-1 membrane expression (105). Inhibition of core fucosylation enhanced the ubiquitination of PD-1, leading to PD-1 degradation by the proteasome (115). Also, glycosylation of PD-1 impacts the binding to its ligand PD-L1 (105). Similarly, recognition of PD-1 by the anti-PD-1 blocking antibody Camrelizumab used for the treatment of relapsed or refractory classical Hodgkin lymphoma (116) is affected by PD-1 glycosylation (108). Whether changes in glycosylation of immune checkpoints occur within the tumor microenvironment has, however, not extensively been researched. First studies show that elevated glycosylation on tumor cells results in overexpression of PD-L1, therefore increasing its immunosuppressive activity (106, 117). However, whether the TME can affect PD-1 glycosylation remains largely unstudied.

Glyco-metabolism changes could possibly also indirectly impact T cell function by affecting glycans on extracellular matrix (ECM)

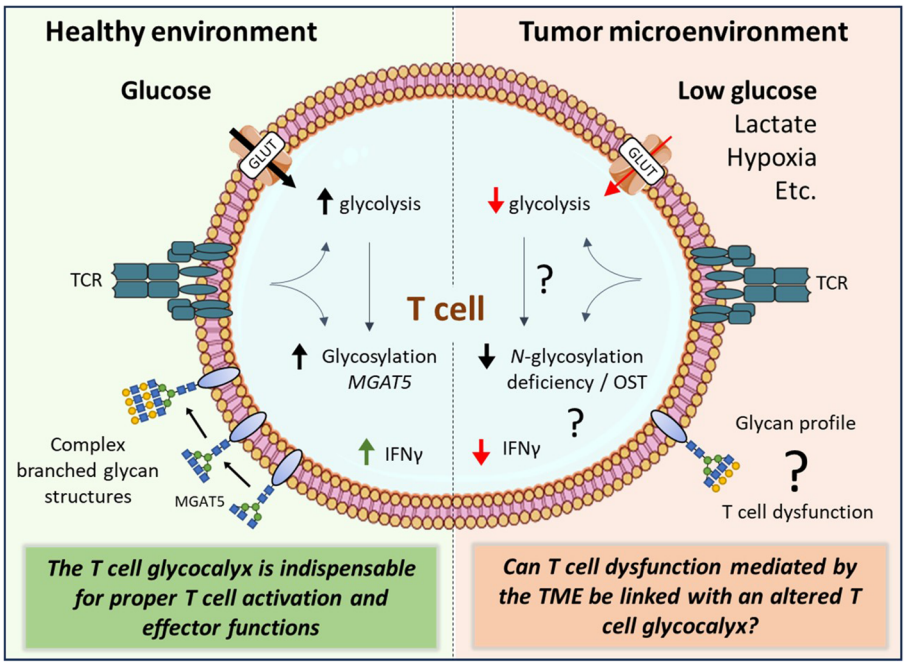

FIGURE 2
The complex interplay between the tumor microenvironment and the T cell glycocalyx. Activated T cells rapidly increase their glucose uptake to fuel their energetic demands. The tumor microenvironment (TME), however, is deprived from nutrients including glucose. The TME can induce T cell exhaustion and senescence. Although glycolysis and glycan biosynthesis pathways are highly interconnected, it remains unknown how TME factors affect T cell effector functions through changes in glycan biosynthesis of T cells. glucose transporter (GLUT), β1,6 N-acetylglucosaminyltransferase V (MGAT5), oligosaccharyltransferase (OST), interferon gamma (IFNγ), T cell receptor (TCR).

components in the TME and hence binding of secreted factors such as immunomodulatory cytokines and chemokines. IL-2, TGFβ and IFNγ are for instance known to bind the ECM glycosaminoglycans such as heparin sulfate and this binding modulates the biological activity of these cytokines (118–120).

In summary, the T cell glycocalyx is indispensable for proper T cell activation and effector functions (Figure 2). Glycan biosynthesis requires glucose molecules, yet the levels of glucose in the TME are significantly lower compared to those in non-malignant tissue. To gain a deeper understanding of how the TME impacts T cell biology, future research should encompass the influence of the TME on the T cell glycocalyx, potentially leading to T cell dysfunction (see '?', Figure 2).

7 Conclusion & Future perspectives

The onco-immunology field has witnessed significant advancements, in part driven by immunotherapies such as immune checkpoint and CAR T cell therapy. Although immunotherapies have demonstrated clinical success, T cell infiltration alone does not determine efficacy. Tumor cells exhibit altered metabolism, notably the Warburg effect, impacting glucose consumption and lactate production, thereby fostering a metabolically restricted TME. This influences the competition for glucose and other nutrients between tumor and immune cells. Most of the proteins expressed on T cells require glycosylation to function properly. The competition for glucose might have a direct effect on the glycosylation profile of T cell proteins and consequently affecting T cell effector functions. The key question that now arises is: How exactly does the TME influence the T cell glycocalyx and can this be linked with T cell functioning? There is evidence that T cells are exhausted inside the TME because of glucose-restriction, hypoxia, and elevated lactate levels, but can this be linked with an altered glycosylation machinery within the T cell?

Collectively, understanding the intricate connection between tumor glucose metabolism, the T cell glycocalyx and T cell biology will provide new insights for advancing immune checkpoint and adoptive (CAR) T cell immunotherapy. Targeting these interconnected pathways may provide new avenues for enhancing therapeutic efficacy and overcoming challenges in the rapidly evolving landscape of onco-immunology.

Author contributions

FS: Writing – original draft, Writing – review & editing. KW: Writing – original draft. GA: Conceptualization, Funding acquisition, Supervision, Writing – review & editing. LC: Conceptualization, Funding acquisition, Supervision, Writing – original draft, Writing – review & editing.

Funding

The author(s) declare financial support was received for the research, authorship, and/or publication of this article. This work was supported by grants from the Dutch Cancer Society awarded to LC and GA (KWF 15326), and GA, Kim C.M. Santegoets, and Pieter Wesseling (KWF 11266).

Acknowledgments

The authors would like to express their appreciation to everyone involved in drafting and preparing the manuscript as well as the Dutch Cancer Society for their support.

Conflict of interest

The authors declare that the research was conducted in the absence of any commercial or financial relationships that could be construed as a potential conflict of interest.

Publisher's note

All claims expressed in this article are solely those of the authors and do not necessarily represent those of their affiliated organizations, or those of the publisher, the editors and the reviewers. Any product that may be evaluated in this article, or claim that may be made by its manufacturer, is not guaranteed or endorsed by the publisher.

References

1. Farber DL. Form and function for T cells in health and disease. *Nat Rev Immunol.* (2020) 20:83–4. doi: 10.1038/s41577-019-0267-8

2. Weigelin B, den Boer AT, Wagena E, Broen K, Dolstra H, de Boer RJ, et al. Cytotoxic T cells are able to efficiently eliminate cancer cells by additive cytotoxicity. *Nat Commun.* (2021) 12(1):5217. doi: 10.1038/s41467–021-25282–3

3. Lowin B, Hahne M, Mattmann C, Tschopp J. Cytolytic T-cell cytotoxicity is mediated through perforin and Fas lytic pathways. *Nat.* (1994) 370:650–2. doi: 10.1038/370650a0

4. Braumüller H, Wieder T, Brenner E, Aßmann S, Hahn M, Alkhaled M, et al. T-helper-1-cell cytokines drive cancer into senescence. *Nature.* (2013) 494:361–5. doi: 10.1038/nature11824

5. Qin S, Xu L, Yi M, Yu S, Wu K, Luo S. Novel immune checkpoint targets: Moving beyond PD-1 and CTLA-4. *Mol Cancer.* (2019) 18:1–14. doi: 10.1186/s12943-019-1091-2

6. Guo Z, Zhang R, Yang AG, Zheng G. Diversity of immune checkpoints in cancer immunotherapy. *Front Immunol.* (2023) 14:1–15. doi: 10.3389/fimmu.2023.1121285

7. Chamoto K, Hatae R, Honjo T. Current issues and perspectives in PD-1 blockade cancer immunotherapy. *Int J Clin Oncol.* (1234) 25:790–800. doi: 10.1007/s10147-019-01588-7

8. Topalian SL, Hodi FS, Brahmer JR, Gettinger SN, Smith DC, McDermott DF, et al. Safety, activity, and immune correlates of anti-PD-1 antibody in cancer. *N Engl J Med.* (2012) 366:2443–54. doi: 10.1056/NEJMoa1200690

9. Brahmer JR, Drake CG, Wollner I, Powderly JD, Picus J, Sharfman WH, et al. Phase I study of single-agent anti-programmed death-1 (MDX-1106) in refractory solid tumors: Safety, clinical activity, pharmacodynamics, and immunologic correlates. *J Clin Oncol.* (2010) 28:3167–75. doi: 10.1200/JCO.2009.26.7609

10. Formenti SC, Rudqvist NP, Golden E, Cooper B, Wennerberg E, Lhuillier C, et al. Radiotherapy induces responses of lung cancer to CTLA-4 blockade. *Nat Med.* (2018) 24(12):1845–51. doi: 10.1038/s41591-018-0232-2

11. Ott PA, Hodi FS, Robert C. CTLA-4 and PD-1/PD-L1 blockade: new immunotherapeutic modalities with durable clinical benefit in melanoma patients. *Clin Cancer Res*. (2013) 19:5300–9. doi: 10.1158/1078-0432.CCR-13-0143

12. Srinivasa BJ, Prakash Lalkota B, Sapkota S, Sarathy V, Bayas N, Naik R. Clinical profile and results in cancers treated with nivolumab: A single centre study. *Open J Immunol*. (2018) 08:107–11. doi: 10.4236/oji.2018.84007

13. Steentoft C, Migliorini D, King TR, Mandel U, June CH, Posey AD. Glycan-directed CAR-T cells. *Glycobiology*. (2018) 28:656–69. doi: 10.1093/glycob/cwy008

14. Miliotou AN, Papadopoulou LC. CAR T-cell therapy: A new era in cancer immunotherapy. *Curr Pharm Biotechnol*. (2018) 19:5–18. doi: 10.2174/1389201019666180418095526

15. Sterner RC, Sterner RM. CAR-T cell therapy: current limitations and potential strategies. *Blood Cancer J*. (2021) 11. doi: 10.1038/s41408–021-00459–7

16. Savoldo B, Grover N, Dotti G. CAR T cells for hematological Malignancies. *J Clin Invest*. (2024) 134. doi: 10.1172/JCI177160

17. Zhang Y, Xu Y, Dang X, Zhu Z, Qian W, Liang A, et al. Challenges and optimal strategies of CAR T therapy for hematological Malignancies. *Chin Med J (Engl)*. (2023) 136:269–79. doi: 10.1097/CM9.0000000000002476

18. Heard A, Landmann JH, Hansen AR, Papadopolou A, Hsu YS, Selli ME, et al. Antigen glycosylation regulates efficacy of CAR T cells targeting CD19. *Nat Commun*. (2022) 13. doi: 10.1038/s41467-022-31035-7

19. Wu S, Ji F, Xu B, Wu F. Delivering CAR-T cells into solid tumors via hydrogels. *MedComm – Oncol*. (2023) 2(2). doi: 10.1002/mog2.40

20. Courtnay R, Ngo DC, Malik N, Ververis K, Tortorella SM, Karagiannis TC. Cancer metabolism and the Warburg effect: the role of HIF-1 and PI3K. *Mol Biol Rep*. (2015) 42:841–51. doi: 10.1007/s11033-015-3858-x

21. Lin X, Xiao Z, Chen T, Liang SH, Guo H. Glucose metabolism on tumor plasticity, diagnosis, and treatment. *Front Oncol*. (2020) 10:1–10. doi: 10.3389/fonc.2020.00317

22. Luengo A, Li Z, Gui DY, Spranger S, Matheson NJ, Vander MG, et al. Increased demand for NAD + relative to ATP drives aerobic glycolysis ll Increased demand for NAD + relative to ATP drives aerobic glycolysis. *Mol Cell*. (2021) 81:691–707. doi: 10.1016/j.molcel.2020.12.012

23. Chang CH, Qiu J, O'Sullivan D, Buck MD, Noguchi T, Curtis JD, et al. Metabolic competition in the tumor microenvironment is a driver of cancer progression. *Cell*. (2015) 162:1229–41. doi: 10.1016/j.cell.2015.08.016

24. Doherty JR, Cleveland JL. Targeting lactate metabolism for cancer therapeutics. *J Clin Invest*. (2013) 123:3685–92. doi: 10.1172/JCI69741

25. Montal ED, Bhalla K, Dewi RE, Ruiz CF, Haley JA, Ropell AE, et al. Inhibition of phosphoenolpyruvate carboxykinase blocks lactate utilization and impairs tumor growth in colorectal cancer. *Cancer Metab*. (2019) 7:1–14. doi: 10.1186/s40170–019-0199–6

26. de la Cruz-López KG, Castro-Muñoz LJ, Reyes-Hernández DO, García-Carrancá A, Manzo-Merino J. Lactate in the regulation of tumor microenvironment and therapeutic approaches. *Front Oncol*. (2019) 9. doi: 10.3389/fonc.2019.01143

27. Ma G, Zhang Z, Li P, Zhang Z, Zeng M, Liang Z, et al. Reprogramming of glutamine metabolism and its impact on immune response in the tumor microenvironment. *Cell Commun Signal*. (2022) 20:1–15. doi: 10.1186/s12964–022-00909–0

28. Yang K, Wang X, Song C, He Z, Wang R, Xu Y, et al. The role of lipid metabolic reprogramming in tumor microenvironment. *Theranostics*. (2023) 13:1774–808. doi: 10.7150/thno.82920

29. Cao T, Dong J, Huang J, Tang Z, Shen H. Identification of fatty acid signature to predict prognosis and guide clinical therapy in patients with ovarian cancer. *Front Oncol*. (2022) 12:979565. doi: 10.3389/fonc.2022.979565

30. Fu Y, Zou T, Shen X, Nelson PJ, Li J, Wu C, et al. Lipid metabolism in cancer progression and therapeutic strategies. *MedComm*. (2021) 2:27–59. doi: 10.1002/mco2.27

31. Buck MD, Sowell RT, Kaech SM, Pearce EL. Leading edge review metabolic instruction of immunity. *Cell*. (2017) 169(4):570–86. doi: 10.1016/j.cell.2017.04.004

32. Villacrés C, Tayi VS, Lattová E, Perreault H, Butler M. Low glucose depletes glycan precursors, reduces site occupancy and galactosylation of a monoclonal antibody in CHO cell culture. *Biotechnol J*. (2015) 10:1051–66. doi: 10.1002/biot.201400662

33. Grigorian A, Lee SU, Tian W, Chen IJ, Gao G, Mendelsohn R, et al. Control of T cell-mediated autoimmunity by metabolite flux to N-glycan biosynthesis. *J Biol Chem*. (2007) 282:20027–35. doi: 10.1074/jbc.M701890200

34. De Bousser E, Meuris L, Callewaert N, Festjens N. Human T cell glycosylation and implications on immune therapy for cancer. *Hum Vaccines Immunother*. (2020) 16 (10):2374–88. doi: 10.1080/21645515.2020.1730658

35. van der Laarse SAM, Leney AC, Heck AJR. Crosstalk between phosphorylation and O-GlcNAcylation: friend or foe. *FEBS J*. (2018) 285:3152–67. doi: 10.1111/febs.14491

36. Varki A, Cummings RD, Esko JD, Stanley P, Hart GW, Aebi M, et al. editors. *Essentials of Glycobiology [Internet]. 4th edition*. Cold Spring Harbor (NY): Cold Spring Harbor Laboratory Press. (2022). doi: 10.1101/978162182421

37. Parker RB, Kohler JJ. Regulation of intracellular signaling by extracellular glycan remodeling. *ACS Chem Biol*. (2010) 5:35. doi: 10.1021/cb9002514

38. Lee-Sundlov MM, Ashline DJ, Hanneman AJ, Grozovsky R, Reinhold VN, Hoffmeister KM, et al. Circulating blood and platelets supply glycosyltransferases that enableextrinsic extracellular glycosylation. *Glycobiology*. (2017) 27:188. doi: 10.1093/glycob/cww108

39. Manhardt CT, Punch PR, Dougher CWL, Lau JTY. Extrinsic sialylation is dynamically regulated by systemic triggers in vivo. *J Biol Chem*. (2017) 292:13514. doi: 10.1074/jbc.C117.795138

40. Lee MM, Nasirikenari M, Manhardt CT, Ashline DJ, Hanneman AJ, Reinhold VN, et al. Platelets support extracellular sialylation by supplying the sugar donor substrate. *J Biol Chem*. (2014) 289:8742–8. doi: 10.1074/jbc.C113.546713

41. Seyrantepe V, Iannello A, Liang F, Kanshin E, Jayanth P, Samarani S, et al. Regulation of phagocytosis in macrophages by neuraminidase 1. *J Biol Chem*. (2010) 285(1):206–15. doi: 10.1016/j.ymgme.2008.11.128

42. Liang F, Seyrantepe V, Landry K, Ahmad R, Ahmad A, Stamatos NM, et al. Monocyte differentiation up-regulates the expression of the lysosomal sialidase, Neu1, and triggers its targeting to the plasma membrane via major histocompatibility complex class II-positive compartments. *J Biol Chem*. (2006) 281:27526–38. doi: 10.1074/jbc.M605633200

43. Ohtsubo K, Marth JD. Glycosylation in cellular mechanisms of health and disease. *Cell*. (2006) 126:855–67. doi: 10.1016/j.cell.2006.08.019

44. Reitsma S, Slaaf DW, Vink H, van Zandvoort MAMJ, oude Egbrink MGA. The endothelial glycocalyx: composition, functions, and visualization

45. Cheng WK, Oon CE. How glycosylation aids tumor angiogenesis: An updated review. *BioMed Pharmacother*. (2018) 103:1246–52. doi: 10.1016/j.biopha.2018.04.119

46. Brown Chandler K E, Costello C, Rahimi N. Glycosylation in the tumor microenvironment: implications for tumor angiogenesis and metastasis. *Cells*. (2019) 8:544. doi: 10.3390/cells8060544

47. Stowell SR, Ju T, Cummings RD. Protein glycosylation in cancer. *Annu Rev Pathol Mech Dis*. (2015) 10:473–510. doi: 10.1146/annurev-pathol-012414-040438

48. Munkley J, Elliott DJ, Munkley J, Elliott DJ. Hallmarks of glycosylation in cancer. *Oncotarget*. (2016) 7:35478–89. doi: 10.18632/oncotarget.v7i23

49. Jiang Y, Liu Z, Xu F, Dong X, Cheng Y, Hu Y, et al. Aberrant O-glycosylation contributes to tumorigenesis in human colorectal cancer. *J Cell Mol Med*. (2018) 22 (10):4875–85. doi: 10.1111/jcmm.13752

50. Sun K, Feng Z, Fan C, Min X, Zhang P, Xia L. A glycosylation signature for predicting the progression and immunotherapeutic response of prostate cancer. *J Gene Med*. (2023) 25(6):e3489. doi: 10.1002/jgm.3489

51. Hoessli DC, Micheau O, Todeschini AR, Vasconcelos-Dos-Santos A, Oliveira IA, Lucena MC, et al. Biosynthetic machinery involved in aberrant glycosylation: promising targets for developing of drugs against cancer. *Front Oncol*. (2015) 5:138. doi: 10.3389/fonc.2015.00138

52. Lucena MC, Carvalho-Cruz P, Donadio JL, Oliveira IA, De Queiroz RM, Marinho-Carvalho MM, et al. Epithelial mesenchymal transition induces aberrant glycosylation through hexosamine biosynthetic pathway activation. *J Biol Chem*. (2016) 291:12917–29. doi: 10.1074/jbc.M116.729236

53. Vasconcelos-dos-Santos A, Loponte H, Mantuano N, Oliveira I, de Paula I, Teixeira L, et al. Hyperglycemia exacerbates colon cancer Malignancy through hexosamine biosynthetic pathway. *Oncogenesis*. (2017) 6:306. doi: 10.1038/oncsis.2017.2

54. Tibullo D, Giallongo C, Romano A, Vicario N, Barbato A, Puglisi F, et al. Mitochondrial functions, energy metabolism and protein glycosylation are interconnected processes mediating resistance to bortezomib in multiple myeloma cells. *Biomolecules*. (2020) 10:696. doi: 10.3390/biom10050696

55. Arriagada C, Silva P, Torres VA. Role of glycosylation in hypoxia-driven cell migration and invasion. *Cell Adh Migr*. (2019) 13(1):13–22. doi: 10.1080/19336918.2018.1491234

56. Cornelissen LAM, Blanas A, Zaal A, van der Horst JC, Kruijssen LJW, O'Toole T, et al. Tn antigen expression contributes to an immune suppressive microenvironment and drives tumor growth in colorectal cancer. *Front Oncol*. (2020) 10:1–15. doi: 10.3389/fonc.2020.01622

57. Büll C, Boltje TJ, Balneger N, Weischer SM, Wassink M, Van Gemst JJ, et al. Sialic acid blockade suppresses tumor growth by enhancing t-cell-mediated tumor immunity. *Cancer Res*. (2018) 78:3574–88. doi: 10.1158/0008-5472.CAN-17-3376

58. R E, B K, B K, EL RJ, K L, B SCM, et al. Sialic acids in pancreatic cancer cells drive tumour-associated macrophage differentiation via the Siglec receptors Siglec-7 and Siglec-9. *Nat Commun*. (2021) 12(1):1270. doi: 10.1038/s41467-021-21550-4

59. Dusoswa SA, Verhoeff J, Abels E, Méndez-Huergo SP, Croci DO, Kuijper LH, et al. Glioblastomas exploit truncated O-linked glycans for local and distant immune modulation via the macrophage galactose-type lectin. *Proc Natl Acad Sci U.S.A*. (2020) 117:3693–703. doi: 10.1073/pnas.1907921117

60. Beatson R, Tajadura-Ortega V, Achkova D, Picco G, Tsourouktsoglou TD, Klausing S, et al. The mucin MUC1 modulates the tumor immunological microenvironment through engagement of the lectin Siglec-9. *Nat Immunol*. (2016) 17:1273–81. doi: 10.1038/ni.3552

61. van Houtum EJH, Büll C, Cornelissen LAM, Adema GJ. Siglec signaling in the tumor microenvironment. *Front Immunol*. (2021) 12. doi: 10.3389/fimmu.2021.790317

62. van de Wall S, Santegoets KCM, van Houtum EJH, Büll C, Adema GJ. Sialoglycans and siglecs can shape the tumor immune microenvironment. *Trends Immunol*. (2020) 41(4):274–85. doi: 10.1016/j.it.2020.02.001

63. Rodríguez E, Schetters STT, van Kooyk Y. The tumour glyco-code as a novel immune checkpoint for immunotherapy. *Nat Rev Immunol*. (2018) 18(3):204–11. doi: 10.1038/nri.2018.3

64. Mantuano NR, Natoli M, Zippelius A, Läubli H. Tumor-associated carbohydrates and immunomodulatory lectins as targets for cancer immunotherapy. *J Immunother Cancer*. (2020) 8:e001222. doi: 10.1136/jitc-2020-001222

65. Ahmed Juvale II, Abdul Hamid AA, Abd Halim KB, Che Has AT. P-glycoprotein: new insights into structure, physiological function, regulation and alterations in disease. *Heliyon*. (2022) 8:e09777. doi: 10.1016/j.heliyon.2022.e09777

66. Lin JH, Yamazaki M. Clinical relevance of P-glycoprotein in drug therapy. *Drug Metab Rev*. (2003) 35:417–54. doi: 10.1081/DMR-120026871

67. Wang L, Zuo X, Xie K, Wei D. The role of CD44 and cancer stem cells. *Methods Mol Biol*. (2018) 1692:31–42. doi: 10.1007/978–1-4939–7401-6_3

68. Hou H, Ge C, Sun H, Li H, Li J, Tian H. Tunicamycin inhibits cell proliferation and migration in hepatocellular carcinoma through suppression of CD44s and the ERK1/2 pathway. *Cancer Sci*. (2018) 109:1088–100. doi: 10.1111/cas.13518

69. Wang L, Chen S, Zhang Z, Zhang J, Mao S, Zheng J, et al. Suppressed OGT expression inhibits cell proliferation while inducing cell apoptosis in bladder cancer. *BMC Cancer*. (2018) 18:1–12. doi: 10.1186/s12885-018-5033-y

70. Very N, El Yazidi-Belkoura I. Targeting O-GlcNAcylation to overcome resistance to anti-cancer therapies. *Front Oncol*. (2022) 12:960312. doi: 10.3389/fonc.2022.960312

71. Takahashi K, Podyma-Inoue KA, Saito M, Sakakitani S, Sugauchi A, Iida K, et al. TGF-β generates a population of cancer cells residing in G1 phase with high motility and metastatic potential via KRTAP2–3. *Cell Rep*. (2022) 40:111411. doi: 10.1016/j.celrep.2022.111411

72. Majumdar A, Curley SA, Wu X, Brown P, Hwang JP, Shetty K, et al. Hepatic stem cells and transforming growth factor β in hepatocellular carcinoma. *Nat Rev Gastroenterol Hepatol*. (2012) 9(9):530–8. doi: 10.1038/nrgastro.2012.114

73. Ikushima H, Miyazono K. TGFβ signalling: a complex web in cancer progression. *Nat Rev Cancer*. (2010) 10:415–24. doi: 10.1038/nrc2853

74. Zhang J, ten Dijke P, Wuhrer M, Zhang T. Role of glycosylation in TGF-β signaling and epithelial-to-mesenchymal transition in cancer. *Protein Cell*. (2021) 12:89–106. doi: 10.1007/s13238–020-00741–7

75. Sun X, He Z, Guo L, Wang C, Lin C, Ye L, et al. ALG3 contributes to stemness and radioresistance through regulating glycosylation of TGF-β receptor II in breast cancer. *J Exp Clin Cancer Res*. (2021) 40:1–26. doi: 10.1186/s13046-021-01932-8

76. Demetriou M, Granovsky M, Quaggin S, Dennis JW. Negative regulation of T-cell activation and autoimmunity by Mgat5 N-glycosylation. *Nat*. (2001) 409:733–9. doi: 10.1038/35055582

77. Swamy M, Pathak S, Grzes KM, Damerow S, Sinclair LV, Van Aalten DMF, et al. Glucose and glutamine fuel protein O-GlcNAcylation to control T cell self-renewal and Malignancy. *Nat Immunol*. (2016) 17:712–20. doi: 10.1038/ni.3439

78. Rossi FMV, Corbel SY, Merzaban JS, Carlow DA, Gossens K, Duenas J, et al. Recruitment of adult thymic progenitors is regulated by P-selectin and its ligand PSGL-1. *Nat Immunol*. (2005) 6:626–34. doi: 10.1038/ni1203

79. Merzaban JS, Richer MJ, Van Kooyk Y, Pereira MS, Alves I, Vicente M, et al. Glycans as key checkpoints of T cell activity and function. *Front Immunol*. (2018) 9:2754. doi: 10.3389/fimmu.2018.02754

80. Sun L, Su Y, Jiao A, Wang X, Zhang B. T cells in health and disease. *Signal Transduct Target Ther*. (2023) 8(1):235. doi: 10.1038/s41392-023-01471-y

81. Pereira MS, Alves I, Vicente M, Campar A, Silva MC, Padrão NA, et al. Glycans as key checkpoints of T cell activity and function. *Front Immunol Front Media S.A*. (2018) 9. doi: 10.3389/fimmu.2018.02754

82. Song Y, Kumar V, Wei H-X, Qiu J, Stanley P. Lunatic, manic, and radical fringe each promote T and B cell development. *J Immunol*. (2016) 196:232–43. doi: 10.4049/jimmunol.1402421

83. Vicente MM, Alves I, Fernandes Â, Dias AM, Santos-Pereira B, Pérez-Anton E, et al. Mannosylated glycans impair normal T-cell development by reprogramming commitment and repertoire diversity. *Cell Mol Immunol*. (2023) 20:955–68. doi: 10.1038/s41423-023-01052-7

84. Starr TK, Daniels MA, Lucido MM, Jameson SC, Hogquist KA. Thymocyte sensitivity and supramolecular activation cluster formation are developmentally regulated: A partial role for sialylation. *J Immunol*. (2003) 171:4512–20. doi: 10.4049/jimmunol.171.9.4512

85. Daniels MA, Devine L, Miller JD, Moser JM, Lukacher AE, Altman JD, et al. CD8 binding to MHC class I molecules is influenced by T cell maturation and glycosylation. *Immunity*. (2001) 15:1051–61. doi: 10.1016/S1074-7613(01)00252-7

86. Gerriets VA, Rathmell JC. Metabolic pathways in T cell fate and function. *Trends Immunol*. (2012) 33:168–73. doi: 10.1016/j.it.2012.01.010

87. Wellen KE, Thompson CB. A two-way street: Reciprocal regulation of metabolism and signalling. *Nat Rev Mol Cell Biol*. (2012) 13:270–6. doi: 10.1038/nrm3305

88. Chen HL, Li CF, Grigorian A, Tian W, Demetriou M. T cell receptor signaling co-regulates multiple golgi genes to enhance N-glycan branching ×◆. *J Biol Chem*. (2009) 284:32454–61. doi: 10.1074/jbc.M109.023630

89. Sun R, Kim AMJ, Lim SO. Glycosylation of immune receptors in cancer. *Cells*. (2021) 10(5):1100. doi: 10.3390/cells10051100

90. Cummingst RD, Trowbridge& IS, Kornfeldt S. A mouse lymphoma cell line resistant to the leukoagglutinating lectin from Phaseolus vulgaris is deficient in UDP-GlcNAc: alpha-D-mannoside beta 1,6 N-acetylglucosaminyltransferase. *J Biol Chem*. (1982) 257:13421–7. doi: 10.1016/S0021-9258(18)33465-3

91. Perillo NL, Pace KE, Seilhamer JJ, Baum LG. Apoptosis of T cells mediated by galectin-1. *Nat*. (1995) 378:736–9. doi: 10.1038/378736a0

92. Ma SL, Zhu WX, Guo QL, Liu YC, Xu MQ. CD28 T cell costimulatory receptor function is negatively regulated by N-linked carbohydrates. *Biochem Biophys Res Commun*. (2004) 317:60–7. doi: 10.1016/j.bbrc.2004.03.012

93. Pinho SS, Alves I, Gaifem J, Rabinovich GA. Immune regulatory networks coordinated by glycans and glycan-binding proteins in autoimmunity and infection. *Cell Mol Immunol*. (2023) 20(10):1101–13. doi: 10.1038/s41423–023-01074–1

94. Crocker PR, Paulson JC, Varki A. Siglecs and their roles in the immune system. *Nat Rev Immunol*. (2007) 7:255–66. doi: 10.1038/nri2056

95. Cagnoni AJ, Giribaldi ML, Blidner AG, Cutine AM, Gatto SG, Morales RM, et al. Galectin-1 fosters an immunosuppressive microenvironment in colorectal cancer by reprogramming CD8+ regulatory T cells. *Proc Natl Acad Sci U.S.A*. (2021) 118: e2102950118. doi: 10.1073/pnas.2102950118

96. Rabinovich GA. Galectin-1 as a potential cancer target. *Br J Cancer*. (2005) 92:1188–92. doi: 10.1038/sj.bjc.6602493

97. Clemente T, Vieira NJ, Cerliani JP, Adrain C, Luthi A, Dominguez MR, et al. Proteomic and functional analysis identifies galectin-1 as a novel regulatory component of the cytotoxic granule machinery. *Cell Death Dis*. (2017) 8:1–10. doi: 10.1038/cddis.2017.506

98. Amano M, Galvan M, He J, Baum LG. The ST6Gal I sialyltransferase selectively modifies N-glycans on CD45 to negatively regulate galectin-1-induced CD45 clustering, phosphatase modulation, and T cell death. *J Biol Chem*. (2003) 278:7469–75. doi: 10.1074/jbc.M209595200

99. Earl LA, Baum LG. CD45 glycosylation controls T-cell life and death. *Immunol Cell Biol*. (2008) 86:608–15. doi: 10.1038/icb.2008.46

100. Jiang Y, Li Y, Zhu B. T-cell exhaustion in the tumor microenvironment. *Cell Death Dis*. (2015) 6(6):e1792. doi: 10.1038/cddis.2015.162

101. Zhao Y, Shao Q, Peng G. Exhaustion and senescence: two crucial dysfunctional states of T cells in the tumor microenvironment. *Cell Mol Immunol*. (2020) 17:27–35. doi: 10.1038/s41423–019-0344–8

102. Elia I, Rowe JH, Johnson S, Joshi S, Notarangelo G, Kurmi K, et al. Tumor cells dictate anti-tumor immune responses by altering pyruvate utilization and succinate signaling in CD8+ T cells. *Cell Metab*. (2022) 34:1137–50.e6. doi: 10.1016/j.cmet.2022.06.008

103. Wang ZH, Peng WB, Zhang P, Yang XP, Zhou Q. Lactate in the tumour microenvironment: From immune modulation to therapy. *EBioMedicine*. (2021) 73:103627. doi: 10.1016/j.ebiom.2021.103627

104. Xiao L, Guan X, Xiang M, Wang Q, Long Q, Yue C, et al. B7 family protein glycosylation: Promising novel targets in tumor treatment. *Front Immunol*. (2022) 13. doi: 10.3389/fimmu.2022.1088560

105. Sun L, Li C-W, Chung EM, Yang R, Kim Y-S, Park AH, et al. Targeting glycosylated PD-1 induces potent antitumor immunity. *Cancer Res*. (2020) 80:2298–310. doi: 10.1158/0008-5472.CAN-19-3133

106. Li CW, Lim SO, Xia W, Lee HH, Chan LC, Kuo CW, et al. Glycosylation and stabilization of programmed death ligand-1 suppresses T-cell activity. *Nat Commun*. (2016) 7:12632. doi: 10.1038/ncomms12632

107. Lee H-H, Wang Y-N, Xia W, Chen C-H, Rau K-M, Ye L, et al. Removal of N-linked glycosylation enhances PD-L1 detection and predicts anti-PD-1/PD-L1 therapeutic efficacy. *Cancer Cell*. (2019) 36(2):168–78.e4. doi: 10.1016/j.ccell.2019.06.008

108. Liu K, Tan S, Jin W, Guan J, Wang Q, Sun H, et al. N-glycosylation of PD-1 promotes binding of camrelizumab. *EMBO Rep*. (2020) 21(12):e51444. doi: 10.15252/embr.202051444

109. Alves I, Vicente MM, Gaifem J, Fernandes Â, Dias AM, Rodrigues CS, et al. SARS-CoV-2 infection drives a glycan switch of peripheral T cells at diagnosis. *J Immunol*. (2021) 207:1591–8. doi: 10.4049/jimmunol.2100131

110. Song M, Sandoval TA, Chae CS, Chopra S, Tan C, Rutkowski MR, et al. IRE1α–XBP1 controls T cell function in ovarian cancer by regulating mitochondrial activity. *Nat*. (2018) 562:423–8. doi: 10.1038/s41586-018-0597-x

111. Kim S, Min H, Nah J, Jeong J, Park K, Kim W, et al. Defective N-glycosylation in tumor-infiltrating CD8+ T cells impairs IFN-γ-mediated effector function. *Immunol Cell Biol*. (2023) 101:610–24. doi: 10.1111/imcb.12647

112. Alegre ML, Frauwirth KA. Thompson CB. T-cell regulation by CD28 and CTLA-4. *Nat Rev Immunol*. (2001) 1:220–8. doi: 10.1038/35105024

113. Patsoukis N, Bardhan K, Chatterjee P, Sari D, Liu B, Bell LN, et al. ARTICLE PD-1 alters T-cell metabolic reprogramming by inhibiting glycolysis and promoting

lipolysis and fatty acid oxidation. *Nat Commun*. (2015) 6:6692. doi: 10.1038/ncomms7692

114. Martins C, Rasbach E, Heppt MV, Singh P, Kulcsar Z, Holzgruber J, et al. Tumor cell–intrinsic PD-1 promotes Merkel cell carcinoma growth by activating downstream mTOR-mitochondrial ROS signaling. *Sci Adv*. (2024) 10:1–16. doi: 10.1126/sciadv.adi2012

115. Zhang N, Li M, Xu X, Zhang Y, Liu Y, Zhao M, et al. Loss of core fucosylation enhances the anticancer activity of cytotoxic T lymphocytes by increasing PD-1 degradation. *Eur J Immunol*. (2020) 50:1820–33. doi: 10.1002/eji.202048543

116. Markham A, Keam SJ. Camrelizumab: first global approval. *Drugs*. (2019) 79:1355–61. doi: 10.1007/s40265–019-01167–0

117. Kim B, Sun R, Oh W, Kim AMJ, Schwarz JR, Lim SO. Saccharide analog, 2-deoxy-d-glucose enhances 4–1BB-mediated antitumor immunity via PD-L1 deglycosylation. *Mol Carcinog*. (2020) 59:691–700. doi: 10.1002/mc.23170

118. Miller JD, Clabaugh SE, Smith DR, Stevens RB, Wrenshall LE. Interleukin-2 is present in human blood vessels and released in biologically active form by heparanase. *Immunol Cell Biol*. (2012) 90:159. doi: 10.1038/icb.2011.45

119. McCaffrey TA, Falcone DJ, Du B. Transforming growth factor-β1 is a heparin-binding protein: Identification of putative heparin-binding regions and isolation of heparins with varying affinity for TGF-β1. *J Cell Physiol*. (1992) 152:430–40. doi: 10.1002/jcp.1041520226

120. Kemna J, Gout E, Daniau L, Lao J, Weißert K, Ammann S, et al. IFNγ binding to extracellular matrix prevents fatal systemic toxicity. *Nat Immunol*. (2023) 24:414–22. doi: 10.1038/s41590-023-01420-5

frontiers | Frontiers in Immunology

TYPE Mini Review
PUBLISHED 02 October 2024
DOI 10.3389/fimmu.2024.1485546

Check for updates

OPEN ACCESS

EDITED BY
Ana Luísa De Sousa-Coelho,
Algarve Biomedical Center Research Institute (ABC-RI), Portugal

REVIEWED BY
Joshi Ramanjulu,
GlaxoSmithKline, United States
Xiang Zhou,
Wuhan University of Science and Technology, China

*CORRESPONDENCE
Xiangwei Meng
mxwzbszxyy@163.com
Dongmei Tang
dongmeiiou@163.com
Dan Liu
940980418@qq.com

†These authors have contributed equally to this work

RECEIVED 24 August 2024
ACCEPTED 16 September 2024
PUBLISHED 02 October 2024

CITATION
Wang B, Yu W, Jiang H, Meng X, Tang D and Liu D (2024) Clinical applications of STING agonists in cancer immunotherapy: current progress and future prospects.
Front. Immunol. 15:1485546.
doi: 10.3389/fimmu.2024.1485546

COPYRIGHT
© 2024 Wang, Yu, Jiang, Meng, Tang and Liu. This is an open-access article distributed under the terms of the Creative Commons Attribution License (CC BY). The use, distribution or reproduction in other forums is permitted, provided the original author(s) and the copyright owner(s) are credited and that the original publication in this journal is cited, in accordance with accepted academic practice. No use, distribution or reproduction is permitted which does not comply with these terms.

Clinical applications of STING agonists in cancer immunotherapy: current progress and future prospects

Bin Wang[1†], Wanpeng Yu[1†], Hongfei Jiang[1,2], Xiangwei Meng[3*], Dongmei Tang[1,4*] and Dan Liu[2*]

[1]The Affiliated Hospital of Qingdao University, Qingdao University, Qingdao, China, [2]Medical Education Department, Guangdong Provincial People's Hospital, Zhuhai Hospital (Jinwan Central Hospital of Zhuhai), Zhuhai, China, [3]Department of Drug Clinical Trials, Zibo Central Hospital, Zibo, China, [4]Department of Anesthesia, Affiliated Hospital of Qingdao University, Qingdao, China

The STING (Stimulator of Interferon Genes) pathway is pivotal in activating innate immunity, making it a promising target for cancer immunotherapy. STING agonists have shown potential in enhancing immune responses, particularly in tumors resistant to traditional therapies. This scholarly review examines the diverse categories of STING agonists, encompassing CDN analogues, non-CDN chemotypes, CDN-infused exosomes, engineered bacterial vectors, and hybrid structures of small molecules-nucleic acids. We highlight their mechanisms, clinical trial progress, and therapeutic outcomes. While these agents offer significant promise, challenges such as toxicity, tumor heterogeneity, and delivery methods remain obstacles to their broader clinical use. Ongoing research and innovation are essential to overcoming these hurdles. STING agonists could play a transformative role in cancer treatment, particularly for patients with hard-to-treat malignancies, by harnessing the body's immune system to target and eliminate cancer cells.

KEYWORDS

STING agonists, cancer immunotherapy, innate immunity, cGAS-STING pathway, tumor microenvironment

1 Introduction

The cyclic GMP-AMP synthase-stimulator of interferon genes (cGAS-STING) pathway is a critical component of the innate immune system, playing a pivotal role in the detection of cytosolic DNA and the subsequent activation of an immune response (1–5). This pathway is evolutionarily conserved and acts as a crucial defense mechanism against pathogens, as well as a mediator of autoimmune responses (6–8). Upon detection of cytosolic DNA, typically from viral or bacterial pathogens, the cGAS enzyme synthesizes cyclic GMP-AMP (cGAMP),

a second messenger that directly activates the STING receptor located on the endoplasmic reticulum membrane (9–11). Once activated, STING initiates a cascade of signaling events leading to the production of type I interferons (IFNs) and NF-kB driven pro-inflammatory cytokines, such as TNF-α and IL-6, which are essential for mounting an effective immune response (12).

In the context of cancer, the STING pathway has garnered significant attention due to its ability to induce a potent anti-tumor immune response (13). Tumor cells often harbor aberrant DNA that can activate the cGAS-STING pathway, thereby promoting the production of cytokines and chemokines that recruit and activate immune cells within the tumor microenvironment (14–16). This immunostimulatory effect of STING has positioned it as a promising target for cancer immunotherapy. STING agonists, which are molecules designed to activate the STING pathway, have shown potential in enhancing the immune system's ability to recognize and destroy tumor cells (17–20). These agonists work by mimicking the natural ligands of STING, thereby amplifying the immune response against tumors.

Given the critical role of STING in immune surveillance and its emerging relevance in cancer therapy, STING agonists have been the subject of intense research (21). Several STING agonists have entered clinical trials, with many showing promising results in enhancing the efficacy of existing immunotherapies, such as immune checkpoint inhibitors (22). These developments highlight the potential of STING agonists to overcome resistance to conventional therapies and to improve outcomes in patients with various types of cancer.

The objective of this review is to provide a comprehensive overview of the current progress in the clinical application of STING agonists in cancer immunotherapy. This review will explore the mechanisms by which STING agonists enhance anti-tumor immunity, summarize the various types of STING agonists currently in clinical development, and discuss the clinical outcomes observed in trials to date. Through this review, we aim to highlight the therapeutic potential of STING agonists in cancer immunotherapy and to discuss their future prospects as a cornerstone of cancer treatment. As research continues to evolve, it is anticipated that STING agonists will play an increasingly important role in the development of novel cancer therapies, offering new hope for patients with difficult-to-treat malignancies.

2 Mechanism of STING activation

The STING (Stimulator of Interferon Genes) pathway is a central player in the innate immune system, responsible for detecting cytosolic DNA from various sources, such as viruses, bacteria, and even damaged host cells (23). This pathway initiates a potent immune response that is critical for antiviral defense and has emerging importance in cancer therapy.

2.1 Detection and activation

The STING pathway begins with the recognition of cytosolic DNA by the cGAS (cyclic GMP-AMP synthase) enzyme. Upon detecting double-stranded DNA in the cytosol, cGAS catalyzes the synthesis of cyclic GMP-AMP (cGAMP), a cyclic dinucleotide that serves as a secondary messenger (Figure 1). cGAMP then binds directly to the STING protein located on the membrane of the endoplasmic reticulum (ER). This binding triggers a conformational change in STING, leading to its activation (24, 25).

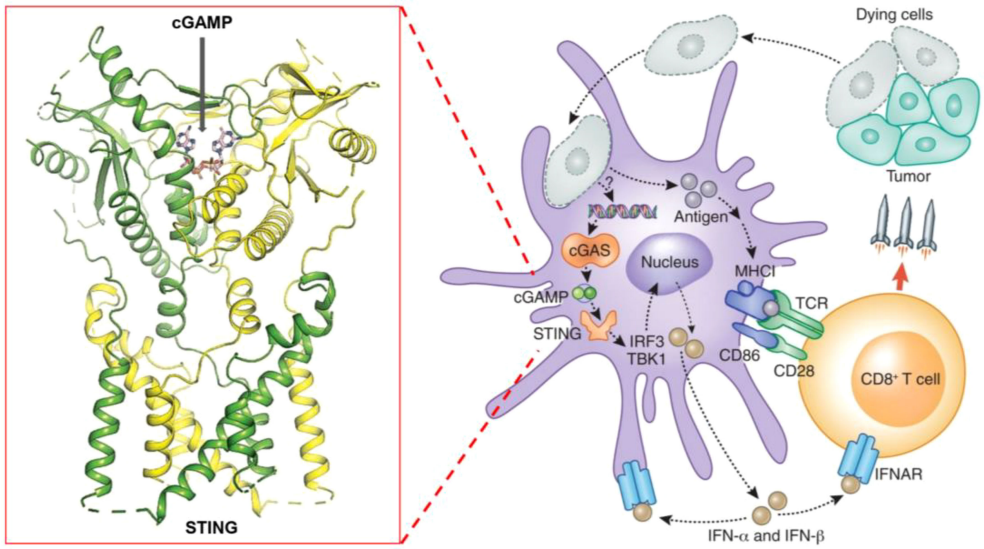

FIGURE 1
Schematic representation of the STING pathway and its role in cancer immunotherapy, highlighting key steps of activation, downstream signaling, and therapeutic targets.

2.2 Downstream signaling

Activated STING translocates from the ER to the Golgi apparatus, where it recruits and activates TBK1 (TANK-binding kinase 1) (26). TBK1, in turn, phosphorylates the transcription factor IRF3 (Interferon Regulatory Factor 3) (27). Phosphorylated IRF3 dimerizes and translocates to the nucleus, where it induces the expression of type I interferons and other pro-inflammatory cytokines. These cytokines play a crucial role in recruiting and activating various immune cells, such as dendritic cells, natural killer cells, and T cells, within the tumor microenvironment.

2.3 Immune response and tumor suppression

The production of type I interferons and cytokines triggers a robust immune response, enhancing the body's ability to recognize and eliminate tumor cells (28). Additionally, the activation of STING can lead to the upregulation of immune checkpoint molecules, making tumors more susceptible to immunotherapies like checkpoint inhibitors.

Figure 1 schematically represents these key steps in the STING pathway, highlighting the crucial role of cGAMP in STING activation, the subsequent signaling cascade, and the production of immune mediators. By understanding these mechanisms, researchers have developed STING agonists that mimic natural ligands like cGAMP, aiming to harness this pathway for cancer immunotherapy.

3 Categories of STING agonists

In this section, we explore the diverse categories of STING agonists currently in development for cancer immunotherapy. These agonists can be broadly classified into several types based on their molecular structure and mechanism of action: cyclic dinucleotide (CDN) analogs, which mimic natural cyclic dinucleotides to directly activate STING; non-CDN STING agonists, which trigger STING activation through alternative mechanisms; CDN-loaded exosomes, which use vesicles to deliver STING agonists more efficiently; engineered bacteria vectors that produce STING-activating molecules in situ; small molecule–nucleic acid hybrids that combine stability with specificity; and some undisclosed types whose structures or mechanisms are not fully revealed. Each category represents a unique approach to harnessing the STING pathway, offering different advantages and challenges in clinical application.

3.1 CDN analogs

CDN analogs are synthetic molecules that mimic the natural cyclic dinucleotides (such as cGAMP) involved in activating the STING pathway (29, 30). These analogs directly bind to the STING receptor, initiating a cascade of immune responses crucial for anti-tumor activity (31). CDN analogs have shown significant promise in early clinical trials, particularly in combination with immune checkpoint inhibitors.

3.1.1 MK-1454

MK-1454 is a CDN analog developed by Merck, currently in Phase I/II clinical trials (ClinicalTrials.gov-NCT03010176). It is being evaluated for its efficacy in treating solid tumors and lymphomas. In early studies, MK-1454 has been administered intratumorally, and when combined with the anti-PD-1 antibody pembrolizumab, it has demonstrated a favorable safety profile and potential efficacy. Preliminary results indicate that MK-1454 can induce strong immune responses, enhancing the effectiveness of pembrolizumab in shrinking tumors. This drug specifically targets the STING pathway by binding to the STING receptor, leading to the activation of type I interferons and other pro-inflammatory cytokines, which play a crucial role in anti-tumor immunity. Moreover, the localized administration helps to minimize systemic side effects while maximizing immune activation within the tumor microenvironment. The clinical outcomes from these trials suggest that MK-1454 may overcome resistance to PD-1 blockade in some patients (32, 33).

3.1.2 ADU-S100 (MIW815)

ADU-S100, also known as MIW815, is another CDN analog that has been the focus of several clinical studies (ClinicalTrials.gov-NCT02675439, NCT03172936, NCT03937141). Developed by Aduro Biotech and Novartis, ADU-S100 has been evaluated in combination with spartalizumab, an anti-PD-1 therapy. In Phase I/II trials, ADU-S100 is administered intratumorally in patients with solid tumors and lymphomas. The results have shown that ADU-S100, when used in conjunction with spartalizumab, can significantly enhance immune responses, leading to tumor regression in some cases. The combination therapy has been particularly effective in generating a localized immune response, which may help control tumor growth and spread (34, 35).

3.1.3 BMS-986301

BMS-986301 is a CDN analog developed by Bristol-Myers Squibb, currently in Phase I clinical trials for advanced cancers (ClinicalTrials.gov-NCT03956680, NCT03843359). Although detailed clinical data is still emerging, early findings suggest that BMS-986301 has the potential to activate the STING pathway effectively, leading to enhanced anti-tumor immunity. The ongoing trials aim to determine the safety and optimal dosing of BMS-986301, as well as its efficacy in combination with other immunotherapies, such as nivolumab (anti-PD-1) and ipilimumab (anti-CTLA-4) (36).

3.1.4 BI-1387446

BI-1387446 is a CDN analog in development by Boehringer Ingelheim, also in Phase I trials (ClinicalTrials.gov-NCT04147234). This STING agonist is being studied for its use in advanced cancers, and early data indicates that it might be administered in

combination with Ezabenlimab, an anti-PD-L1 therapy. While specific clinical outcomes have not yet been fully disclosed, the trials focus on evaluating the safety, tolerability, and preliminary efficacy of BI-1387446 in inducing an immune response against tumors (37).

3.1.5 TAK-676

TAK-676 is a CDN analog being developed by Takeda Oncology, currently in Phase I/II clinical trials (ClinicalTrials.gov-NCT04420884, NCT04879849). This STING agonist is administered intravenously, either alone or in combination with pembrolizumab, in patients with advanced solid tumors and lymphomas. Preliminary results from these trials indicate that TAK-676 is well-tolerated and may potentiate the effects of pembrolizumab, particularly in tumors that are otherwise resistant to immune checkpoint blockade. Ongoing studies are focused on determining the optimal dosing and combination strategies to maximize the therapeutic benefits of TAK-676 (38–40).

3.2 Non-CDN chemotypes

Non-CDN STING agonists represent a diverse group of molecules that activate the STING pathway through mechanisms distinct from those of cyclic dinucleotides (CDNs). These agonists often have unique chemical structures that allow them to bind and activate STING in different ways, offering alternative therapeutic strategies for cancer treatment. Below are some of the key non-CDN STING agonists currently in clinical development.

3.2.1 SNX281

SNX281 is a non-CDN STING agonist developed by Silicon Therapeutics, now part of Roivant Sciences. It is currently in Phase I clinical trials for advanced solid tumors (ClinicalTrials.gov-NCT04609579). Unlike CDNs, SNX281 is a small molecule that activates STING without mimicking the natural dinucleotides. The clinical trials are evaluating the safety, tolerability, and preliminary efficacy of SNX281 both as a monotherapy and in combination with pembrolizumab, an anti-PD-1 antibody. Early data suggest that SNX281 can enhance anti-tumor immunity, potentially overcoming resistance to checkpoint inhibitors in some cancers. SNX281's mechanism involves activating STING, which leads to the production of type I interferons and pro-inflammatory cytokines, ultimately stimulating the infiltration of immune cells into the tumor microenvironment. This process could help convert 'cold' tumors into 'hot' tumors, making them more responsive to immunotherapy (41).

3.2.2 HG-381

HG-381 is a non-CDN STING agonist developed by HitGen, currently in Phase I clinical trials (ClinicalTrials.gov-NCT04998422). This small molecule is being tested for its ability to treat advanced solid tumors. While specific clinical data is still emerging, HG-381 has shown potential in preclinical models to induce a strong immune response by activating STING, leading to the production of type I interferons and other cytokines that can suppress tumor growth. The ongoing clinical trials aim to determine the safety, optimal dosing, and preliminary efficacy of HG-381 in cancer patients (42).

3.2.3 GSK3745417

GSK3745417 is a non-CDN STING agonist developed by GlaxoSmithKline, currently in Phase I clinical trials (ClinicalTrials.gov-NCT03843359). This agonist is being evaluated for its efficacy in treating advanced solid tumors. GSK3745417 works by directly binding to and activating the STING receptor, leading to the production of interferons and other immune-modulatory cytokines. The ongoing trials are focused on assessing the safety, tolerability, and early signs of efficacy, both as a monotherapy and potentially in combination with other immunotherapies. Early data suggest that GSK3745417 has a manageable safety profile, with potential for inducing anti-tumor immune responses (43).

3.2.4 E-7766

E-7766 is a non-CDN STING agonist developed by Eisai, currently in Phase I clinical trials (ClinicalTrials.gov-NCT04144140). This drug is being tested in patients with advanced solid tumors and lymphomas. E-7766 is designed to activate the STING pathway, thereby stimulating the immune system to attack cancer cells. Early clinical studies are assessing the safety, tolerability, and preliminary efficacy of E-7766. The initial data indicate that E-7766 can induce immune activation with a tolerable safety profile, although further studies are needed to determine its therapeutic potential in combination with other cancer treatments (44, 45).

3.3 CDN-infused exosomes

CDN-loaded exosome STING agonists represent an innovative approach to cancer immunotherapy, combining the potency of cyclic dinucleotide (CDN) STING agonists with the targeted delivery capabilities of exosomes. Exosomes are small, naturally occurring vesicles that can be engineered to carry therapeutic molecules, such as CDNs, directly to specific cells, including immune cells within the tumor microenvironment. This method enhances the effectiveness of STING activation while potentially reducing systemic toxicity.

exoSTING is a prime example of a CDN-loaded exosome STING agonist, developed by Codiak BioSciences. This therapy is designed to enhance the delivery and activation of the STING pathway within tumors, leveraging the natural properties of exosomes to improve the targeting and uptake of CDNs by immune cells. exoSTING is currently being evaluated in Phase I/II clinical trials for advanced solid tumors (ClinicalTrials.gov-NCT04592484). The drug is administered intratumorally, with the aim of directly stimulating the STING pathway within the tumor microenvironment. The exosome-based delivery system allows for a localized and potent activation of STING, leading to

robust immune responses characterized by increased infiltration of T cells and other immune effectors into the tumor. The ongoing clinical trials are focused on further characterizing the safety and efficacy of exoSTING, as well as exploring its potential in combination with other immunotherapies, such as checkpoint inhibitors. The preliminary results are promising, suggesting that exoSTING could become a valuable addition to the arsenal of STING-based cancer therapies, particularly for tumors that are resistant to conventional treatments. In addition, the ability of exoSTING to focus its activity within the tumor microenvironment while minimizing systemic exposure may reduce the risk of side effects, making it an attractive option for enhancing the therapeutic index of STING agonists (46).

3.4 Engineered bacteria vectors

Engineered bacteria vectors represent a novel and innovative approach to cancer immunotherapy, where genetically modified bacteria are used to deliver therapeutic agents directly to the tumor microenvironment. These bacteria are designed to produce and release STING agonists within the tumor, thereby activating the STING pathway in situ. This method leverages the natural ability of bacteria to colonize tumors, providing a targeted and sustained activation of the immune system against cancer cells.

SYNB1891 is a leading example of an engineered bacteria vector designed to activate the STING pathway. Developed by Synlogic, SYNB1891 is a live, engineered strain of the probiotic bacterium of Escherichia coli Nissle 1917, which has been modified to produce cyclic di-GMP, a potent STING agonist. This STING agonist is released directly within the tumor microenvironment, where it can trigger an immune response by activating the STING pathway in local immune cells.

SYNB1891 is currently in Phase I clinical trials for patients with advanced solid tumors (ClinicalTrials.gov-NCT04167137). The drug is administered intratumorally, allowing the bacteria to colonize the tumor and produce the STING agonist directly where it is needed. The Phase I trials are primarily focused on evaluating the safety and tolerability of SYNB1891, as well as its ability to induce an immune response. The intratumoral administration of SYNB1891 has led to localized immune activation, characterized by increased production of type I interferons and other pro-inflammatory cytokines within the tumor. These immune responses are associated with enhanced infiltration of T cells into the tumor, suggesting that SYNB1891 may help convert "cold" tumors, which are typically resistant to immunotherapy, into "hot" tumors that are more responsive to immune-based treatments. Furthermore, the use of engineered bacteria allows for sustained release of STING agonists within the tumor microenvironment, offering prolonged immune activation without the need for repeated systemic dosing (47).

In addition to its use as a monotherapy, SYNB1891 is also being evaluated in combination with immune checkpoint inhibitors, such as atezolizumab (anti-PD-L1). The rationale for this combination is that the STING-mediated immune activation induced by SYNB1891 could enhance the effectiveness of checkpoint inhibitors, particularly in tumors that have previously shown resistance to such therapies. The ongoing clinical trials aim to further characterize the immune responses induced by SYNB1891 and to assess its potential as a component of combination therapies for cancer. The preliminary results are promising, indicating that engineered bacteria vectors like SYNB1891 could offer a new and effective approach to cancer immunotherapy (48).

3.5 Hybrid structures of small molecules-nucleic acids

Small molecule–nucleic acid hybrids represent an emerging class of STING agonists designed to combine the stability and pharmacokinetic properties of small molecules with the specificity and functionality of nucleic acids. These hybrids aim to enhance the activation of the STING pathway while improving drug delivery and minimizing off-target effects. This innovative approach seeks to harness the advantages of both molecular types to create more effective and targeted cancer therapies.

SB 11285 is a leading example of a small molecule–nucleic acid hybrid STING agonist, developed by Spring Bank Pharmaceuticals. SB 11285 is designed to activate the STING pathway more effectively than traditional small molecules by leveraging its hybrid structure, which combines a potent small molecule with a nucleic acid component. By combining the stability of a small molecule with the specificity of a nucleic acid, SB 11285 aims to overcome the limitations of conventional STING agonists, ensuring better pharmacokinetic properties and more targeted immune activation. SB 11285 is currently in Phase I/II clinical trials for patients with solid tumors and hematologic malignancies (ClinicalTrials.gov-NCT04096638). The ongoing trials are also exploring SB 11285 in combination with immune checkpoint inhibitors, such as atezolizumab (anti-PD-L1). The rationale behind this combination is that SB 11285's activation of the STING pathway could enhance the effectiveness of checkpoint inhibitors by increasing the immune system's ability to recognize and attack tumor cells. Early results suggest that the combination therapy may improve outcomes in patients with tumors that are otherwise resistant to checkpoint inhibitors alone. The trials aim to further assess the efficacy of SB 11285, particularly its ability to induce durable responses and improve survival outcomes in cancer patients. As a small molecule–nucleic acid hybrid, SB 11285 represents a promising new approach in the development of STING-based therapies, potentially offering enhanced efficacy and safety over traditional STING agonists (49, 50).

3.6 Undisclosed type

The "Undisclosed Type" category includes STING agonists whose precise molecular mechanisms or structures have not been fully disclosed to the public. These agonists are often in early stages of development, with companies keeping details confidential for

strategic reasons. Despite the lack of detailed structural information, these agents are advancing through clinical trials and show potential in activating the STING pathway for cancer immunotherapy.

3.6.1 MK-2118

MK-2118 is a STING agonist developed by Merck, currently in Phase I clinical trials (ClinicalTrials.gov-NCT03249792). While the exact molecular structure of MK-2118 has not been publicly revealed, it is known that the drug is being tested in patients with solid tumors, particularly in combination with pembrolizumab, an anti-PD-1 antibody. Early clinical data suggest that MK-2118 has a favorable safety profile and can enhance the anti-tumor effects of pembrolizumab. MK-2118 is administered intratumorally, ensuring that the STING agonist is delivered directly to the tumor microenvironment, which helps maximize immune activation locally while reducing potential systemic side effects. Furthermore, its ability to activate the STING pathway may help improve the immune system's recognition of tumors that are resistant to conventional immunotherapies. The combination therapy aims to stimulate a stronger immune response against tumors that are resistant to checkpoint inhibitors alone (51).

3.6.2 XMT-2056

XMT-2056 is another STING agonist with an undisclosed mechanism, developed by Mersana Therapeutics. XMT-2056 is currently in Phase I clinical trials, focusing on patients with advanced solid tumors (ClinicalTrials.gov-NCT05514717). This drug is administered intravenously and is designed to target tumors with a high degree of precision. Although detailed clinical data are still pending, XMT-2056 is being investigated both as a monotherapy and in combination with other cancer treatments, including immune checkpoint inhibitors. The goal of these studies is to assess the drug's safety, tolerability, and preliminary efficacy in inducing an anti-tumor immune response.

The secrecy surrounding these agents adds an element of intrigue, as the exact mechanisms by which they activate the STING pathway remain speculative. However, the ongoing clinical trials are crucial in determining their potential efficacy and safety profiles. The early-stage results for both MK-2118 and XMT-2056 are promising, suggesting that these undisclosed-type STING agonists could become significant players in the field of cancer immunotherapy (52, 53).

While the STING agonists discussed in this review encompass a diverse range of structures—spanning CDN analogs, small molecule agonists, nucleic acid hybrids, and engineered bacterial vectors—these compounds share several key functional characteristics. Most notably, they all target the STING pathway by engaging the STING protein to initiate immune signaling. CDN analogs, such as MK-1454 and exoSTING, closely mimic natural cyclic dinucleotides, binding to the same pocket on the STING protein that recognizes endogenous STING activators. Non-CDN agonists, including SNX281 and SB 11285, achieve similar activation through alternative molecular scaffolds, ensuring they can engage STING without mimicking the natural ligands. Despite these structural differences, the shared objective of these agonists is to stimulate type I interferon production and activate pro-inflammatory cytokines, leading to enhanced immune infiltration into the tumor microenvironment. By modulating the immune response in this way, STING agonists can convert 'cold' tumors into 'hot' tumors, making them more susceptible to immunotherapies.

To comprehensively showcase the current research progress of STING agonists in cancer immunotherapy, we have summarized the STING agonists at various stages of clinical development (Table 1). These agonists encompass a variety of chemical types, including cyclic dinucleotide (CDN) analogs, non-CDN chemotypes, CDN-loaded exosomes, and engineered bacterial vectors. Detailed information on each agonist's developing company, clinical trial phase, administration methods, and whether they are used in combination with other immunotherapies is provided. Through this table, readers can gain a clear understanding of the current research hotspots and clinical advancements of STING agonists.

4 Challenges and limitations

While STING agonists represent a promising avenue for cancer immunotherapy, several challenges and limitations must be addressed to fully realize their potential. These challenges span from biological complexities to clinical application hurdles, each requiring careful consideration in the development and deployment of STING-based therapies.

Managing the toxicity of STING agonists is a significant challenge. Activation of the STING pathway can lead to the excessive production of pro-inflammatory cytokines, including type I interferons (e.g., IFN-α, IFN-β) and non-type I interferons such as IFN-γ, causing severe side effects like fever, chills, and cytokine release syndrome (CRS). The risk is higher with systemic administration, making it crucial to optimize dosing strategies and develop more selective STING activators to minimize off-target effects (54). Tumor heterogeneity and response variability present major challenges for STING agonists. Tumors differ in genetic makeup and immune environment, leading to inconsistent responses. "Cold" tumors with low immune cell infiltration may not respond well due to insufficient STING ligands or necessary immune cells. Identifying predictive biomarkers is essential to select patients who will benefit most from STING-based therapies (55). Effective delivery and targeting of STING agonists remain challenging. Intratumoral injections, while effective, are not feasible for all tumors, and systemic delivery risks widespread immune activation and toxicity (56, 57). Experimental methods like nanoparticles, exosomes, and engineered bacteria are being explored to improve targeting and minimize systemic exposure, but further research is needed to confirm their efficacy and safety (58, 59).

Resistance to STING agonists is a significant concern in cancer therapy. Tumors may downregulate STING expression, mutate pathway components, or alter the microenvironment to evade immune responses. Understanding these mechanisms is crucial for developing combination therapies, such as pairing STING

10.3389/fimmu.2024.1485546

TABLE 1 Summary of STING agonists currently in clinical trials, including their chemical structures, target phases, indications, combination therapies, and clinical outcomes.

Drug Name	Chemical Structure	Target Phase	Indication	Combination Therapies	Clinical Outcome
MK-1454	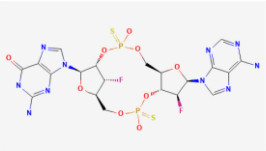	Phase I/II	Solid Tumors, Lymphomas	Pembrolizumab (anti-PD-1)	Early results show safety and potential efficacy
ADU-S100 (MIW815)	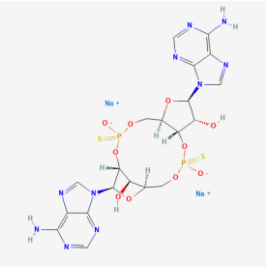	Phase I/II	Solid Tumors, Lymphomas	Spartalizumab (anti-PD-1)	Encouraging immune response in combination with PD-1 blockade
TAK-676	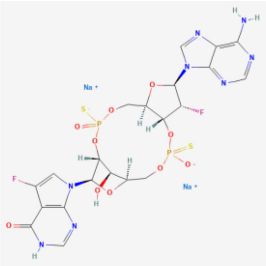	Phase I/II	Advanced Solid Tumors, Lymphomas	± Pembrolizumab (anti-PD-1)	Ongoing, early data pending
BI-1387446	The structure has not been made public, it belongs to the CDN small molecule agonist class	Phase I	Advanced Cancers	± Ezabenlimab (anti-PD-L1)	Ongoing, early data pending
BMS-986301	The structure has not been made public, it belongs to the CDN small molecule agonist class	Phase I	Advanced Cancers	None currently reported	Ongoing, early data pending
E7766	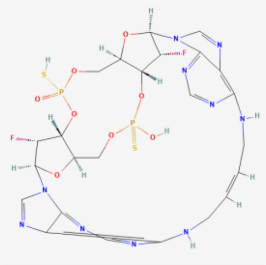	Phase I	Advanced Solid Tumors, Lymphomas	None currently reported	Ongoing, early data pending
SNX281	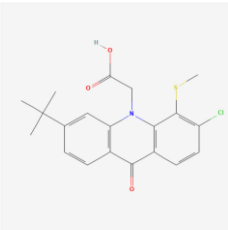	Phase I	Advanced Solid Tumors	None currently reported	Ongoing, early data pending
HG-381	The structure has not been made public, it belongs to the non-CDN small molecule agonist class	Phase I	Advanced Solid Tumors	Monotherapy	Early-stage, shows potential
GSK3745417	The structure has not been made public, it belongs to the non-CDN small molecule agonist class	Phase I	Advanced Solid Tumors	None currently reported	Ongoing, early data pending

(Continued)

10.3389/fimmu.2024.1485546

TABLE 1 Continued

Drug Name	Chemical Structure	Target Phase	Indication	Combination Therapies	Clinical Outcome
exoSTING	The structure has not been made public, it belongs to the CDN-loaded exosome class	Phase I/II	Advanced Solid Tumors	Monotherapy	Completed, shows promising results
SYNB1891	The structure has not been made public, it belongs to the engineered bacteria vector class	Phase I	Advanced Solid Tumors	± Atezolizumab	Completed, data pending
SB 11285	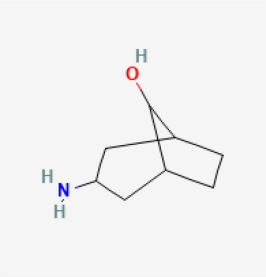	Phase I/II	Solid Tumors, Hematologic Malignancies	Potential future combination with checkpoint inhibitors	Early-stage results showing promise in safety and immunogenicity
MK-2118	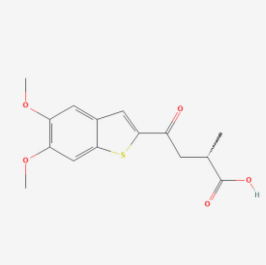	Phase I	Solid Tumors	± Pembrolizumab	Completed, shows potential
XMT-2056	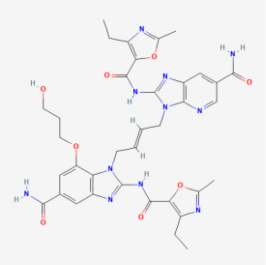	Phase I	Advanced Solid Tumors	Monotherapy	Ongoing, early data pending

agonists with checkpoint inhibitors or chemotherapies, to enhance efficacy and prevent resistance (60). Finally, Regulatory and manufacturing challenges are significant for STING agonists, especially those with novel mechanisms or delivery systems. Rigorous testing is needed to meet regulatory standards, and the complexity of therapies involving engineered bacteria or exosomes complicates manufacturing, scalability, and quality control. Ensuring consistent production and stability is crucial for successful clinical translation (3, 61, 62).

In some types of cancers, the STING pathway may be deficient due to genetic mutations, epigenetic silencing, or functional suppression within the tumor microenvironment (63). Repairing the STING pathway in these cases is a significant challenge, but several strategies are under investigation. Gene therapy approaches, such as using CRISPR or viral vectors, could be employed to repair mutations in the STING gene or other components of the pathway, restoring STING functionality. Alternatively, combination therapies that pair STING agonists with immune checkpoint inhibitors or DNA damage response inhibitors may enhance immune activation even in tumors with partial STING deficiency. Epigenetic therapies, which reverse silencing of STING-related genes, are also being explored to restore STING pathway signaling. While these approaches hold promise, further clinical studies are needed to determine their viability and effectiveness in repairing STING pathway deficiencies (64).

5 Conclusion

STING agonists have emerged as a promising class of agents in cancer immunotherapy, capable of initiating a robust immune response through the activation of the STING pathway. These agents have demonstrated potential in early-phase clinical trials, particularly when combined with immune checkpoint inhibitors, offering hope for treating tumors that are resistant to conventional therapies. The ability of STING agonists have the potential to convert 'cold' tumors, which lack immune cell infiltration, into 'hot' tumors that are more responsive to immunotherapy by promoting the production of chemokines such as CCL5, CXCL9, and CXCL10, which recruit immune cells like T cells and NK cells

to the tumor microenvironment, highlights their transformative potential in cancer treatment.

However, several challenges must be addressed to fully realize the clinical potential of STING agonists. Managing the toxicity associated with systemic immune activation, ensuring effective delivery to tumor sites, and overcoming tumor heterogeneity and resistance mechanisms are critical hurdles. Additionally, the development and manufacturing of STING agonists, especially those involving novel delivery systems like nanoparticles and engineered bacteria, pose significant regulatory and quality control challenges.

Despite these obstacles, the future of STING agonists in cancer therapy remains bright. Continued research into optimizing delivery methods, identifying predictive biomarkers, and developing combination therapies will be key to overcoming current limitations. As our understanding of the STING pathway deepens, these agents could become integral components of cancer treatment, offering new hope to patients with difficult-to-treat malignancies. The next few years will be crucial in determining whether STING agonists can transition from experimental therapies to widely accepted clinical options, potentially revolutionizing the landscape of cancer immunotherapy.

Author contributions

BW: Writing – original draft. WY: Writing – original draft. HJ: Writing – original draft, Writing – review & editing. XM: Writing – original draft, Writing – review & editing. DT: Writing – original draft, Writing – review & editing. DL: Writing – original draft, Writing – review & editing.

Funding

The author(s) declare financial support was received for the research, authorship, and/or publication of this article. This study was supported by Natural Science Foundation of Shandong Province (No. ZR2022QH388) and The Affiliated Hospital of Qingdao University Clinical Medicine+X Research Project (QDFYQN202102038).

Conflict of interest

The authors declare that the research was conducted in the absence of any commercial or financial relationships that could be construed as a potential conflict of interest.

Publisher's note

All claims expressed in this article are solely those of the authors and do not necessarily represent those of their affiliated organizations, or those of the publisher, the editors and the reviewers. Any product that may be evaluated in this article, or claim that may be made by its manufacturer, is not guaranteed or endorsed by the publisher.

References

1. Samson N, Ablasser A. The cGAS–STING pathway and cancer. *Nat Cancer*. (2022) 3:1452–63. doi: 10.1038/s43018-022-00468-w

2. Decout A, Katz JD, Venkatraman S, Ablasser A. The cGAS–STING pathway as a therapeutic target in inflammatory diseases. *Nat Rev Immunol*. (2021) 21:548–69. doi: 10.1038/s41577-021-00524-z

3. Liang J-L, Jin X-K, Deng X-C, Huang Q-X, Zhang S-M, Chen W-H, et al. Targeting activation of cGAS-STING signaling pathway by engineered biomaterials for enhancing cancer immunotherapy. *Mater Today*. (2024).

4. Schmid M, Fischer P, Engl M, Widder J, Kerschbaum-Gruber S, Slade D. The interplay between autophagy and cGAS-STING signaling and its implications for cancer. *Front Immunol*. (2024) 15:1356369. doi: 10.3389/fimmu.2024.1356369

5. Lu Q, Chen Y, Li J, Zhu F, Zheng Z. Crosstalk between cGAS-STING pathway and autophagy in cancer immunity. *Front Immunol*. (2023) 14:1139595. doi: 10.3389/fimmu.2023.1139595

6. Jin X, Wang W, Zhao X, Jiang W, Shao Q, Chen Z, et al. The battle between the innate immune cGAS-STING signaling pathway and human herpesvirus infection. *Front Immunol*. (2023) 14:1235590. doi: 10.3389/fimmu.2023.1235590

7. Zhao J, Xiao R, Zeng R, He E, Zhang A. Small molecules targeting cGAS-STING pathway for autoimmune disease. *Eur J Med Chem*. (2022) 238:114480. doi: 10.1016/j.ejmech.2022.114480

8. Hu Y, Chen B, Yang F, Su Y, Yang D, Yao Y, et al. Emerging role of the cGAS-STING signaling pathway in autoimmune diseases: Biologic function, mechanisms and clinical prospection. *Autoimmun Rev*. (2022) 21:103155. doi: 10.1016/j.autrev.2022.103155

9. Xie W, Patel DJ. Structure-based mechanisms of 2′3′-cGAMP intercellular transport in the cGAS–STING immune pathway. *Trends Immunol*. (2023) 44:450–67. doi: 10.1016/j.it.2023.04.006

10. Eaglesham JB, Pan Y, Kupper TS, Kranzusch PJ. Viral and metazoan poxins are cGAMP-specific nucleases that restrict cGAS–STING signalling. *Nature*. (2019) 566:259–63. doi: 10.1038/s41586-019-0928-6

11. Blest HTW, Chauveau L. cGAMP the travelling messenger. *Front Immunol*. (2023) 14:1150705. doi: 10.3389/fimmu.2023.1150705

12. Liu K, Zhao X, Guo M, Zhu J, Li D, Ding J, et al. Microcystin-leucine arginine (MC-LR) induces mouse ovarian inflammation by promoting granulosa cells to produce inflammatory cytokine via activation of cGAS-STING signaling. *Toxicol Lett*. (2022) 358:6–16. doi: 10.1016/j.toxlet.2022.01.003

13. Xagoraris I, Stathopoulou K, Xyderou P, Palma M, Drakos E, Vassilakopoulos TP, et al. Modulation of the CGAS-sting anti-tumor immune response pathway in an NF-KB-dependent or -independent manner as a potential therapeutic target in classical hodgkin lymphoma (cHL). *Blood*. (2022) 140:3579–80. doi: 10.1182/blood-2022-164497

14. Zierhut C. Potential cGAS-STING pathway functions in DNA damage responses, DNA replication and DNA repair. *DNA Repair*. (2024) 133:103608. doi: 10.1016/j.dnarep.2023.103608

15. An J, Zhang C-P, Qiu H-Y, Zhang H-X, Chen Q-B, Zhang Y-M, et al. Enhancement of the viability of T cells electroporated with DNA via osmotic dampening of the DNA-sensing cGAS–STING pathway. *Nat Biomed Eng*. (2024) 8:149–64.

16. Chen Q, Sun L, Chen ZJ. Regulation and function of the cGAS–STING pathway of cytosolic DNA sensing. *Nat Immunol*. (2016) 17:1142–9. doi: 10.1038/ni.3558

17. Wang J, Meng F, Yeo Y. Delivery of STING agonists for cancer immunotherapy. *Curr Opin Biotechnol*. (2024) 87:103105. doi: 10.1016/j.copbio.2024.103105

18. Chen S, Peng A, Chen M, Zhan M. Nanomedicines targeting activation of STING to reshape tumor immune microenvironment and enhance immunotherapeutic efficacy. *Front Oncol*. (2023) 12:1093240. doi: 10.3389/fonc.2022.1093240

19. Ramanjulu JM, Pesiridis GS, Yang J, Concha N, Singhaus R, Zhang S-Y, et al. Design of amidobenzimidazole STING receptor agonists with systemic activity. *Nature*. (2018) 564:439–43.

20. Cherney EC, Zhang L, Lo J, Huynh T, Wei D, Ahuja V, et al. Discovery of non-nucleotide small-molecule STING agonists via chemotype hybridization. *J Med Chem*. (2022) 65:3518–38. doi: 10.1021/acs.jmedchem.1c01986

21. Huang C, Shao N, Huang Y, Chen J, Wang D, Hu G, et al. Overcoming challenges in the delivery of STING agonists for cancer immunotherapy: A comprehensive review of strategies and future perspectives. *Mater Today Bio*. (2023) 23:100839. doi: 10.1016/j.mtbio.2023.100839

22. Jiang M, Chen P, Wang L, Li W, Chen B, Liu Y, et al. cGAS-STING, an important pathway in cancer immunotherapy. *J Hematol Oncol*. (2020) 13:81. doi: 10.1186/s13045-020-00916-z

23. Lim S, Jung HR, Lee H, Chu Y, Kim H, Kim E, et al. Microtubule-destabilizing agents enhance STING-mediated innate immune response via biased mechanism in human monocyte cells. *Biomed Pharmacother*. (2023) 169:115883. doi: 10.1016/j.biopha.2023.115883

24. Wu J, Sun L, Chen X, Du F, Shi H, Chen C, et al. Cyclic GMP-AMP is an endogenous second messenger in innate immune signaling by cytosolic DNA. *Science*. (2013) 339:826–30. doi: 10.1126/science.1229963

25. Zhong B, Yang Y, Li S, Wang Y-Y, Li Y, Diao F, et al. The adaptor protein MITA links virus-sensing receptors to IRF3 transcription factor activation. *Immunity*. (2008) 29:538–50. doi: 10.1016/j.immuni.2008.09.003

26. Ishii KJ, Kawagoe T, Koyama S, Matsui K, Kumar H, Kawai T, et al. TANK-binding kinase-1 delineates innate and adaptive immune responses to DNA vaccines. *Nature*. (2008) 451:725–9. doi: 10.1038/nature06537

27. Tanaka Y, Chen ZJ. STING specifies IRF3 phosphorylation by TBK1 in the cytosolic DNA signaling pathway. *Sci Signaling*. (2012) 5:ra20–0. doi: 10.1126/scisignal.2002521

28. Watson RO, Bell SL, MacDuff DA, Kimmey JM, Diner EJ, Olivas J, et al. The Cytosolic Sensor cGAS Detects Mycobacterium tuberculosis DNA to Induce Type I Interferons and Activate Autophagy. *Cell Host Microbe*. (2015) 17:811–9. doi: 10.1016/j.chom.2015.05.004

29. Jenal U, Reinders A, Lori C. Cyclic di-GMP: second messenger extraordinaire. *Nat Rev Microbiol*. (2017) 15:271–84. doi: 10.1038/nrmicro.2016.190

30. Ma J, Xu H, Hou K, Cao Y, Xie D, Yan J, et al. Design and synthesis of cyclic dinucleotide analogues containing triazolyl C–Nucleosides. *J Organic Chem*. (2024) 89:11089–836. doi: 10.1021/acs.joc.4c01055

31. Magand J, Roy V, Meudal H, Rose S, Quesniaux V, Chalupska D, et al. Synthesis of novel 3',3'-cyclic dinucleotide analogues targeting STING protein. *Asian J Organic Chem*. (2023) 12:76–86. doi: 10.1002/ajoc.202200597

32. Harrington KJ, Brody J, Ingham M, Strauss J, Cemerski S, Wang M, et al. LBA15 - Preliminary results of the first-in-human (FIH) study of MK-1454, an agonist of stimulator of interferon genes (STING), as monotherapy or in combination with pembrolizumab (pembro) in patients with advanced solid tumors or lymphomas. *Ann Oncol*. (2018) 29:viii712. doi: 10.1093/annonc/mdy424.015

33. Gogoi H, Mansouri S, Jin L. The age of cyclic dinucleotide vaccine adjuvants. *Vaccines*. (2020), 453.

34. Meric-Bernstam F, Sandhu SK, Hamid O, Spreafico A, Kasper S, Dummer R, et al. Phase Ib study of MIW815 (ADU-S100) in combination with spartalizumab (PDR001) in patients (pts) with advanced/metastatic solid tumors or lymphomas. *J Clin Oncol*. (2019) 37:2507–7. doi: 10.1200/jco.2019.37.15_suppl.2507

35. Meric-Bernstam F, Sweis RF, Hodi FS, Messersmith WA, Andtbacka RHI, Ingham M, et al. Phase I dose-escalation trial of MIW815 (ADU-S100), an intratumoral STING agonist, in patients with advanced/metastatic solid tumors or lymphomas. *Clin Cancer Res*. (2022) 28:677–88. doi: 10.1158/1078-0432.ccr-21-1963

36. Li K, Wang J, Espinoza B, Xiong Y, Niu N, Wang J, et al. Abstract 6736: Overcome the challenge for intratumoral injection of STING agonist for pancreatic cancer by systemic administration. *Cancer Res*. (2024) 84:6736–6. doi: 10.1158/1538-7445.am2024-6736

37. Harrington K, Parkes E, Weiss J, Ingham M, Cervantes A, Calvo E, et al. Abstract CT217: Phase I, first-in-human trial evaluating BI 1387446 (STING agonist) alone and in combination with ezabenlimab (BI 754091; anti-PD-1) in solid tumors. *Cancer Res*. (2021) 81:CT217–7. doi: 10.1158/1538-7445.am2021-ct217

38. Appleman VA, Berger AJ, Roberts ER, Maldonado-Lopez AE, Ganno ML, Christensen CI, et al. Abstract 3448: The IV STING agonist, TAK-676, enhances immune-mediated anti-tumor activity of radiation in syngeneic mouse models. *Cancer Res*. (2022) 82:3448–8. doi: 10.1158/1538-7445.am2022-3448

39. Cooper BT, Chmura SJ, Luke JJ, Shiao SL, Basho RK, Iams WT, et al. TAK-676 in combination with pembrolizumab after radiation therapy in patients (pts) with advanced non–small cell lung cancer (NSCLC), triple-negative breast cancer (TNBC), or squamous-cell carcinoma of the head and neck (SCCHN): Phase 1 study design. *J Clin Oncol*. (2022) 40:TPS2698–TPS2698. doi: 10.1200/jco.2022.40.16_suppl.tps2698

40. Carideo Cunniff E, Sato Y, Mai D, Appleman VA, Iwasaki S, Kolev V, et al. TAK-676: A novel stimulator of interferon genes (STING) agonist promoting durable IFN-dependent antitumor immunity in preclinical studies. *Cancer Res Commun*. (2022) 2:489–502. doi: 10.1158/2767-9764.crc-21-0161

41. Wang J, Falchook G, Nabhan S, Kulkarni M, Sandy P, Dosunmu O, et al. 495 Trial of SNX281, a systemically delivered small molecule STING agonist, in solid tumors and lymphomas. *J ImmunoTher Cancer*. (2021) 9:A527–7.

42. Fan Y, Feng R, Zhang X, Wang Z-L, Xiong F, Zhang S, et al. Encoding and display technologies for combinatorial libraries in drug discovery: The coming of age from biology to therapy. *Acta Pharm Sin B*. (2024) 14:3362–84. doi: 10.1016/j.apsb.2024.04.006

43. Montesinos P, Al-Ali H, Alonso-Dominguez JM, Jentzsch M, Jongen-Lavrencic M, Martelli MP, et al. Abstract CT124: A first-in-clinic phase 1 study of GSK3745417 STING agonist in relapsed/refractory acute myeloid leukemia and high-risk myelodysplastic syndrome. *Cancer Res*. (2023) 83:CT124–4. doi: 10.1158/1538-7445.am2023-ct124

44. Kim D-S, Endo A, Fang FG, Huang K-C, Bao X, . Choi H-w, et al. E7766, a macrocycle-bridged stimulator of interferon genes (STING) agonist with potent pan-genotypic activity. *ChemMedChem*. (2021) 16:1741–4. doi: 10.1002/cmdc.202100068

45. Endo A, Kim D-S, Huang K-C, Hao M-H, Mathieu S, Choi H-w, et al. Abstract 4456: Discovery of E7766: A representative of a novel class of macrocycle-bridged STING agonists (MBSAs) with superior potency and pan-genotypic activity. *Cancer Res*. (2019) 79:4456–6. doi: 10.1158/1538-7445.am2019-4456

46. Jang SC, Economides KD, Moniz RJ, Sia CL, Lewis N, McCoy C, et al. ExoSTING, an extracellular vesicle loaded with STING agonists, promotes tumor immune surveillance. *Commun Biol*. (2021) 4:497. doi: 10.1038/s42003-021-02004-5

47. Leventhal DS, Sokolovska A, Li N, Plescia C, Kolodziej SA, Gallant CW, et al. Immunotherapy with engineered bacteria by targeting the STING pathway for anti-tumor immunity. *Nat Commun*. (2020) 11:2739. doi: 10.1038/s41467-020-16602-0

48. Janku F, Luke JJ, Brennan A, Riese R, Varterasian M, Armstrong MB, et al. Abstract CT110: Intratumoral injection of SYNB1891, a synthetic biotic designed to activate the innate immune system, demonstrates target engagement in humans including intratumoral STING activation. *Cancer Res*. (2021) 81:CT110–0. doi: 10.1158/1538-7445.am2021-ct110

49. Challa SV, Zhou S, Sheri A, Padmanabhan S, Meher G, Gimi R, et al. Preclinical studies of SB 11285, a novel STING agonist for immuno-oncology. *J Clin Oncol*. (2017) 35:e14616–6. doi: 10.1200/jco.2017.35.15_suppl.e14616

50. Challa S, Ramachandran B, Vijayakrishnan L, Weitzel D, Zhou S, Iyer K. Abstract B96: Pharmacodynamic studies of SB 11285, a systemically bioavailable STING agonist in orthotopic tumor models. *Cancer Immunol Res*. (2020) 8:B96–6. doi: 10.1158/2326-6074.tumimm18-b96

51. Lyons TW, Thaisrivongs DA, Kuhl N, Chung CK, Angeles A, Steinhuebel D, et al. The first GMP synthesis of MK-2118, a small molecule agonist for stimulator of interferon genes. *Organic Process Res Dev*. (2024) 28:2309–16. doi: 10.1021/acs.oprd.4c00102

52. Duvall JR, Bukhalid RA, Cetinbas NM, Catcott KC, Lancaster K, Bentley KW, et al. Abstract 3503: XMT-2056, a HER2-targeted Immunosynthen STING-agonist antibody-drug conjugate, binds a novel epitope of HER2 and shows increased anti-tumor activity in combination with trastuzumab and pertuzumab. *Cancer Res*. (2022) 82:3503–3. doi: 10.1158/1538-7445.am2022-3503

53. Soomer-James J, Damelin M, Malli N. Abstract 4423: XMT-2056, a HER2-targeted STING agonist antibody-drug conjugate, exhibits ADCC function that synergizes with STING pathway activation and contributes to anti-tumor responses. *Cancer Res*. (2023) 83:4423–3. doi: 10.1158/1538-7445.am2023-4423

54. Li T, Chen ZJ. The cGAS–cGAMP–STING pathway connects DNA damage to inflammation, senescence, and cancer. *J Exp Med*. (2018) 215:1287–99. doi: 10.1084/jem.20180139

55. Bakhoum SF, Ngo B, Laughney AM, Cavallo J-A, Murphy CJ, Ly P, et al. Chromosomal instability drives metastasis through a cytosolic DNA response. *Nature*. (2018) 553:467–72. doi: 10.1038/nature25432

56. Zhao H, Yu J, Zhang R, Chen P, Jiang H, Yu W. Doxorubicin prodrug-based nanomedicines for the treatment of cancer. *Eur J Med Chem*. (2023) 258:115612. doi: 10.1016/j.ejmech.2023.115612

57. Jiang H, Gong Q, Zhang R, Yuan H. Tetrazine-based metal-organic frameworks. *Coordination Chem Rev*. (2024) 499:215501. doi: 10.1016/j.ccr.2023.215501

58. Zhang J, Wang S, Zhang D, He X, Wang X, Han H, et al. Nanoparticle-based drug delivery systems to enhance cancer immunotherapy in solid tumors. *Front Immunol*. (2023) 14:1230893. doi: 10.3389/fimmu.2023.1230893

59. Zhang R, Zhao X, Jia A, Wang C, Jiang H. Hyaluronic acid-based prodrug nanomedicines for enhanced tumor targeting and therapy: A review. *Int J Biol Macromol*. (2023) 249:125993. doi: 10.1016/j.ijbiomac.2023.125993

60. Vanpouille-Box C, Alard A, Aryankalayil MJ, Sarfraz Y, Diamond JM, Schneider RJ, et al. DNA exonuclease Trex1 regulates radiotherapy-induced tumour immunogenicity. *Nat Commun*. (2017) 8:15618. doi: 10.1038/ncomms15618

61. Wu X, Feng N, Wang C, Jiang H, Guo Z. Small molecule inhibitors as adjuvants in cancer immunotherapy: enhancing efficacy and overcoming resistance. *Front Immunol*. (2024) 15:1444452. doi: 10.3389/fimmu.2024.1444452

62. Jiang H, Chen W, Wang J, Zhang R. Selective N-terminal modification of peptides and proteins: Recent progresses and applications. *Chin Chem Lett*. (2022) 33:80–8. doi: 10.1016/j.cclet.2021.06.011

63. Bian X, Jiang H, Meng Y, Li YP, Fang J, Lu Z. Regulation of gene expression by glycolytic and gluconeogenic enzymes. *Trends Cell Biol*. (2022) 32:786–99. doi: 10.1016/j.tcb.2022.02.003

64. Zhang R, Yu J, Guo Z, Jiang H, Wang C. Camptothecin-based prodrug nanomedicines for cancer therapy. *Nanoscale*. (2023) 15:17658–97. doi: 10.1039/d3nr04147f

frontiers | Frontiers in Immunology

TYPE Original Research
PUBLISHED 03 February 2025
DOI 10.3389/fimmu.2025.1515605

Check for updates

OPEN ACCESS

EDITED BY
Ana Luísa De Sousa-Coelho,
Algarve Biomedical Center Research Institute (ABC-RI), Portugal

REVIEWED BY
Mónica Teotónio Fernandes,
University of Algarve, Portugal
Shreyas Gaikwad,
Texas Tech University Health Sciences Center, United States

*CORRESPONDENCE
Jie Pan
jiepan@hmc.edu.cn
Ling-Bo Qian
bioqian@163.com

RECEIVED 23 October 2024
ACCEPTED 14 January 2025
PUBLISHED 03 February 2025

CITATION
Ding B, Li J, Yan J-L, Jiang C-Y, Qian L-B and Pan J (2025) Resveratrol contributes to NK cell-mediated breast cancer cytotoxicity by upregulating ULBP2 through miR-17-5p downmodulation and activation of MINK1/JNK/c-Jun signaling.
Front. Immunol. 16:1515605.
doi: 10.3389/fimmu.2025.1515605

COPYRIGHT
© 2025 Ding, Li, Yan, Jiang, Qian and Pan. This is an open-access article distributed under the terms of the Creative Commons Attribution License (CC BY). The use, distribution or reproduction in other forums is permitted, provided the original author(s) and the copyright owner(s) are credited and that the original publication in this journal is cited, in accordance with accepted academic practice. No use, distribution or reproduction is permitted which does not comply with these terms.

Resveratrol contributes to NK cell-mediated breast cancer cytotoxicity by upregulating ULBP2 through miR-17-5p downmodulation and activation of MINK1/JNK/c-Jun signaling

Bisha Ding[1], Jie Li[2], Jia-Lin Yan[2], Chun-Yan Jiang[2], Ling-Bo Qian[2]* and Jie Pan[2]*

[1]Cancer Center, Department of Medical Oncology, Zhejiang Provincial People's Hospital, Affiliated People's Hospital, Hangzhou Medical College, Hangzhou, Zhejiang, China, [2]School of Basic Medical Sciences and Forensic Medicine, Hangzhou Medical College, Hangzhou, Zhejiang, China

Backgrounds: Natural killer (NK) cell mediated cytotoxicity is a crucial form of anti-cancer immune response. Natural killer group 2 member D (NKG2D) is a prominent activating receptor of NK cell. UL16-binding protein 2 (ULBP2), always expressed or elevated on cancer cells, functions as a key NKG2D ligand. ULBP2-NKG2D ligation initiates NK cell activation and subsequent targeted elimination of cancer cells. Enhanced expression of ULBP2 on cancer cells leads to more efficient elimination of these cells by NK cells. Resveratrol (RES) is known for its multiple health benefits, while current understanding of its role in regulating cancer immunogenicity remains limited. This study aims to investigate how RES affects the expression of ULBP2 and the sensitivity of breast cancer (BC) cells to NK cell cytotoxicity, along with the underlying mechanisms.

Methods: The effects of RES on ULBP2 expression were detected with qRT-PCR, western blot, flow cytometry analysis and immunohistochemistry. The effects of RES on sensitivity of BC cells to NK cell cytotoxicity were evaluated *in vitro* and *in vivo*. The target gene of miR-17-5p were predicted with different algorithms from five databases and further confirmed with dual-luciferase reporter assay. Overexpression and knockdown experiments of miR-17-5p and MINK1 were conducted to investigate their roles in regulating ULBP2 expression and subsequent JNK/c-Jun activation. The JNK inhibitor sp600125 was utilized to elucidate the specific role of JNK in modulating ULBP2 expression.

Results: RES increased ULBP2 expression on BC cells, thereby augmenting their vulnerability to NK cell-mediated cytotoxicity both *in vitro* and *in vivo*. RES administration led to a reduction in cellular miR-17-5p level. MiR-17-5p negatively regulated ULBP2 expression. Specifically, miR-17-5p directly targeted MINK1, leading to its suppression. MINK1 played a role in facilitating the activation of JNK and its downstream effector, c-Jun. Furthermore, treatment with sp600125, a JNK inhibitor, resulted in the suppression of ULBP2 expression.

Conclusions:: RES potentiates ULBP2-mediated immune eradication of BC cells by NK cells through the downregulation of miR-17-5p and concurrent activation of the MINK1/JNK/c-Jun cascade. This finding identifies RES as a potentially effective therapeutic agent for inhibiting BC progression and optimizing NK cell-based cancer immunotherapy.

KEYWORDS

NK cell, ULBP2, cytotoxicity, MINK1, JNK, resveratrol, breast cancer

1 Introduction

Resveratrol (RES), a naturally occurring polyphenol compound, is present in over 70 widely distributed dietary and medical plants species such as peanuts, grapes, berries and white hellebore (1). In recent decades, RES has garnered significant attention for its wide array of well-documented health benefits, including antioxidant, anti-aging, anti-inflammatory, and anticancer properties (2). The potential of RES as an anticancer agent is well-established through an extensive array of preclinical studies (3–5). Breast cancer, one of the most prevalent cancers among women globally, can potentially be prevented through RES by mechanisms that include inhibiting cell proliferation, inducing cell cycle arrest and apoptosis, reducing inflammatory responses, suppressing angiogenesis, and facilitating epigenetic modifications (6–8). Of particular interest, RES has demonstrated its ability to strengthen the immune system, thereby enhancing antitumor immunity. This is achieved through several mechanisms such as attenuating resistance in cancer stem cells, inhibiting the production of immunosuppressive cytokines, and alleviating immunosuppression within the tumor microenvironment (9, 10). However, the mechanism underlying cancer immunomodulation by RES remains fragmentary and deserves more studies.

Natural killer group 2 member D ligands (NKG2DLs) are important targets in cancer immunomodulation. They consist of eight surface glycoproteins, namely MICA and MICB (major histocompatibility complex class I chain-related proteins A and B), and ULBP1-6 (UL16-binding proteins 1-6) (11). NKG2DLs are the specific ligands of natural killer group 2 member D (NKG2D) receptor, a key activating receptor prominently featured on natural killer (NK) cells (12). NKG2DLs, typically either undetectable or low expressed on healthy cells, can be induced in the progression of cellular malignant transformation (11). The ligation of NKG2DL and NKG2D leads to NK cell activation, subsequently enabling the killing of cancer cells. This process is a pivotal mechanism of immunosurveillance and immune clearance. In breast cancer, the upregulation of NKG2DLs was shown to be associate with cancer suppression (13–15).

NKG2D initiates cytotoxicity against cancer cells that display NKG2DLs on their surface. However, malignantly transformed cells often reduce or downregulate the expression of surface NKG2DLs to evade the immune clearance. Cancer cells manipulate the expression of these ligands at both transcriptional and post-transcriptional levels. Several transcription factors, including krüppel-like factor 4 (KLF4), nuclear factor kappa-B (NF-κB) and c-Myc, are documented to function in NKG2DL transcription (16–18). The growth and metastasis of breast cancer in mice were enhanced by the downregulation of NKG2DL expression, with glycogen synthase kinase-3β (GSK-3β) contributing to these processes (14). Our earlier investigation has demonstrated that the downregulation of MICA/B and ULBP2 by some NKG2D ligand-targeting microRNAs (miRNAs) resulted in a diminished NK cell-mediated cytotoxic response against breast cancer cells (15). And shedding or internalization is also involved in the reduction of the surface ligands (19). Given the significant role that NKG2DLs play in tumoricidal activity, they have attracted considerable interest as promising candidates for designing innovative cancer preventive and immunotherapeutic strategies. Pharmacological interventions, such as metformin, decitabine, and valproic acid, have been shown to effectively increase NKG2DL levels, thereby enhancing the immune clearance of cancer cells (15, 20, 21).

Herein, RES was found to effectively upregulate the expression of ULBP2, a pivotal component of NKG2DLs, thereby augmenting the cytolytic activity of NK cells against breast cancer cells both *in*

Abbreviations: BC, Breast cancer; DMSO, Dimethyl sulfoxide; ERK, Extracellular signal regulated kinase; GSK-3β, Glycogen synthase kinase-3β; IHC, Immunohistochemistry; JNK, C-Jun N-terminal kinase; KEGG, Kyoto encyclopedia of genes and genomes; KLF4, Krüppel-like factor 4; LDH, Lactate dehydrogenase; MAP4K6, Mitogen-activated protein kinase kinase kinase kinase 6; MAPK, Mitogen-activated protein kinase; MICA, Major histocompatibility complex class I chain-related proteins A; MICB, Major histocompatibility complex class I chain-related proteins B; MINK1, Misshapen like kinase 1; NC, Negative control; NF-κB, Nuclear factor kappa-B; NK, Natural killer; NKG2D, Natural killer group 2 member D; NKG2DL, Natural killer group 2 member D ligand; PBS, Phosphate-buffered saline; qRT-PCR, Quantitative reverse transcription-polymerase chain reaction; RES, Resveratrol; TCGA, The cancer genome atlas; TPM, Transcripts Per Million; ULBP1-6, UL16-binding proteins 1-6; ULBP2, UL16-binding protein 2.

vitro and *in vivo*. Mechanistically, RES suppressed the oncogenic miR-17-5p, which directly targets misshapen like kinase 1 (MINK1). MINK1 activates ULBP2 through its downstream JNK/c-Jun signaling cascade. A high surface expression level of ULBP2 significantly facilitates the recognition and subsequent elimination of breast cancer cells by NK cells.

2 Materials and methods

2.1 Cell culture and reagents

The cell lines (MDA-MB-231, BCap37, MCF7, MDA-MB-468 and HeLa) were obtained from the Cell Bank of the Chinese Academy of Sciences (Shanghai, China). MDA-MB-231 and MDA-MB-468 are triple-negative breast cancer cell lines, whereas BCap37 and MCF7 are estrogen receptor-positive breast cancer cell lines. MDA-MB-231, MDA-MB-468 and HeLa cells were maintained in Dulbecco's modified Eagle's medium (DMEM, Gibco, Life technologies, Carlsbad, CA, USA). BCap37and MCF-7 cells were cultured in Roswell Park Memorial Institute 1640 medium (Gibco, USA). The media were supplemented with 10% fetal bovine serum (Gibco, USA) and 1% streptomycin/penicillin antibiotics, and the cultures were incubated at 37°C under a 5% CO_2 atmosphere. RES (Selleck Chemicals, Houston, TX, USA) was solubilized in dimethyl sulfoxide (DMSO) to yield a 109.5 mmol/L stock solution, which was then stored at -20°C. The cells were exposed to various concentrations of RES (6.25, 12.5, or 25 µmol/L) for a duration of 48 hours.

2.2 Plasmids and cell transfection

The overexpression plasmid of MINK1(pcDNA3.1-MINK1), pcDNA3.1 control and siRNAs of MINK1 (si-MINK1-1, si-MINK1-2), SQSTM1 (si-SQSTM1-1, si-SQSTM1-2), CDKN1A (si-CDKN1A-1, si-CDKN1A-2) were obtained from Repbio (Hangzhou, China). The mimic, inhibitor and negative controls (NC) of miR-17-5p were bought from Ribobio (Guangzhou, China). The siRNA sequences were listed in Table 1. The aforementioned siRNA, plasmids and miRNA mimics/inhibitors were introduced into their respective target cells using Lipofectamine 3000, following the previously described transfection protocol (22).

TABLE 1 Sequence of siRNA.

siRNA	Sequence
si-MINK1-1	GGAACAAGAUUCUGCACAA
si-MINK1-2	GAAAGAGGAGACAGAAUAU
si-SQSTM1-1	CUUCCGAAUCUACAUUAAA
si-SQSTM1-2	GAAUCUACAUUAAAGAGAA
si-CDKN1A-1	AGUUUGUGUGUCUUAAUUA
si-CDKN1A-2	GCUUAGUGUACUUGGAGUA

2.3 RNA extraction and quantitative reverse transcription-polymerase chain reaction

Total RNA was isolated from cells using RNAiso Plus (TaKaRa, Kusatsu, Japan) and then subjected to reverse transcription into complementary DNA (cDNA) utilizing the PrimeScriptTM RT Reagent Kit (#RR037A, TaKaRa). For conventional RNA RT-PCR, random hexamer primers were employed, whereas specific primers (Ribobio) were utilized for miRNA RT-PCR. The expressions of ULBP2, MINK1, CDKN1A and SQSTM1 were quantified using qRT-PCR with GAPDH as internal control. The sequences of specific primers were provided in Table 2. Expression level of miR-17-5p was quantified using a BulgeLoop miRNA qRT-PCR primer set (Ribobio), with U6 serving as an endogenous reference for normalization. The qRT-PCR assays were carried out on a LightCycler 480II system (Roche Diagnostics, Basel, Switzerland), employing the SYBR Premix EX Tag Kit (#RR420A, TaKaRa). Relative expression levels of both miRNA and RNA were determined using the $2^{-\Delta Ct}$ method, following normalization to a reference control.

2.4 Western blot

The cells subjected to pretreatment were lysed in radioimmunoprecipitation assay buffer for total protein extraction. The protein concentrations were subsequently measured with a bicinchoninic acid (BCA) protein assay kit (Beyotime Biotec, China). Equivalent quantities of denatured protein samples (40 µg) were subjected to separation via 4%–20% SDS-polyacrylamide gel electrophoresis and then transferred onto polyvinylidene fluoride membranes. Following a 1-hour blocking step at room temperature with 5% skim milk (Yili, Hohhot, China) in tris-buffered saline containing 0.1% Tween-20, the membranes were incubated with the specific primary antibodies detailed in

TABLE 2 Primers for quantitative RT-PCR.

Primer	Sequence
MINK1	FP: GGAGGACTGTATCGCCTATATCT RP: GTCTCGATGGATCACCTTGTG
CDKN1A	FP: TGTCCGTCAGAACCCATGC RP: AAAGTCGAAGTTCCATCGCTC
SQSTM1	FP: GCACCCCAATGTGATCTGC RP: CGCTACACAAGTCGTAGTCTGG
ULBP2	FP: CAGAGCAACTGCGTGACATT RP: GGCCACAACCTTGTCATTCT
ULBP5	FP: ACAGGATGGCTTGAGGACTTCTTG RP: TGATGAGGAGGCAGCAAAGGATG
ULBP6	FP: GCTTCATCCTCCCTGGCATCTG RP: GGCTGCTGGACATACACCGTAG
GAPDH	FP: CTGGGCTACACTGAGCACC RP: AAGTGGTCGTTGAGGGCAATG
U6	FP: CTCGCTTCGGCAGCACATA RP: AACGCTTCACGAATTTGCG

Table 3 at 4°C overnight. GAPDH served as an internal control for normalization purposes. The membranes were subsequently incubated with an optimally diluted solution of the corresponding secondary antibodies conjugated to horseradish peroxidase for a duration of 2 hours at room temperature. Finally, the immunoreactive bands were visualized utilizing an enhanced chemiluminescence detection system (Thermo Scientific, Darmstadt, Germany).

2.5 Flow cytometry analysis

After pretreatment, the cells were rinsed with phosphate-buffered saline (PBS) and then incubated with the antibodies specified in Table 3 for 25 minutes at 4°C in the dark. The flow cytometry assays were conducted using a BD FACSCalibur flow cytometer (BD Biosciences, San Jose, California, USA), with data acquisition and interpretation carried out utilizing the CellQuest software. The cells were gated based on their higher forward scatter and lower side scatter; characteristics typically indicative of live cells. No additional specific protocols were implemented to explicitly exclude dead cells. The mean fluorescence intensity (MFI) change (denoted as ΔMFI) was determined using the following formula: ΔMFI= (MFIwith specific mAb−MFIwith isotype control) ÷MFIwith isotype control. To further facilitate comparison between the ΔMFI observed for a specific experimental treatment and that of a control treatment, the relative MFI (rMFI) was computed as follows: rMFI=ΔMFIspecific treatment/ΔMFIcontrol treatment×100% (23).

2.6 Dual-luciferase reporter assay

The wild-type (WT) and mutant (MUT) 3′-UTR sequences of *ULBP2* were individually cloned into the pmirGLO vector (Repbio). HEK-293 T cells were cultured into 96-well plates. After 24 hours, the cells were co-transfected with 100 ng of either wild-type or mutant reporter plasmids, along with 100 nmol of miR-17-5p mimics or NC, for a duration of 6 hours. Forty-eight hours later, the Firefly/Renilla luciferase activities were quantified using the Dual Luciferase Reporter Assay Kit as described in the manufacturer's instructions (Promega, Madison, WI, USA).

TABLE 3 Antibodies for western blot and flow cytometry analysis.

Antibodies	Application	Source	Identifier
GAPDH	WB	abcam	ab181602
ULBP-2	WB	abcam	ab275023
MINK1	WB	Proteintech	13137-1-AP
JNK	WB	abcam	ab179461
Phospho-JNK	WB	CST	4668
c-Jun	WB	abcam	ab40766
Phospho-c-Jun	WB	abcam	ab32385
Anti-human ULBP2/5/6 PE	Flow Cyt	R&D systems	FAB1298P
Mouse IgG2A PE-conjugated Antibody	Flow Cyt	R&D systems	IC003P

2.7 NK cell cytotoxicity assay *in vitro*

MDA-MB-231 cells were subjected to treatment with either 12.5 μM or 25 μM RES for a duration of 48 hours and subsequently seeded into a round-bottom 96-well plate. Before the cytotoxicity assay, the NK-92MI cell line was exposed to either PBS or anti-NKG2D antibody (50 mg/mL, Novus Biologicals, Littleton, CO, USA) for a period of 1 hour. Next, the effector NK-92MI cells were added to the respective wells at varying effector-to-target cell ratios of 10:1, 5:1, and 2.5:1. Following co-incubation at 37°C under an atmosphere containing 5% CO_2 for a period of 4 hours, the supernatant was collected and subjected to analysis utilizing the CytoTox 96 NonRadioactive Cytotoxicity Kit (Promega). According to the protocols provided in the instruction manual for the Kit, damaged cells release intracellular lactate dehydrogenase (LDH), so the level of LDH is proportional to the number of the damaged cells. The LDH release is quantified by measuring the absorbance at 490 nm. The cytotoxic potential of the effector cells towards the target cells was quantified using the following formula: Cytotoxicity (%) = (LDH Release $_{\text{Experimental}}$ - LDH Release $_{\text{Effector spontaneous}}$ - LDH Release $_{\text{Target spontaneous}}$)/(LDH Release $_{\text{Target maximum}}$ - LDH Release $_{\text{Target spontaneous}}$) ×100. The spontaneous LDH release from effector cells and target cells was assessed to mitigate any potential influence of LDH spontaneously released by NK cells and breast cancer cells on the experimental outcomes. The difference "LDH Release $_{\text{Target maximum}}$ - LDH Release $_{\text{Target spontaneous}}$" corresponds to the LDH release resulting from 100% lysis of all breast cancer cells, indicating the amount of LDH released when all breast cancer cells are completely damaged or killed.

2.8 Acute lung clearance assay

C57BL/6 male mice, aged 8 to 9 weeks, were allocated into three distinct groups and intraperitoneally administered one of the following treatments: anti-NK1.1 antibodies (dose: 300 μg per mouse, Clone PK136, 108759, Biolegend, San Diego, CA, USA), anti-mouse NKG2D monoclonal antibodies (dose: 300 μg per mouse, Clone 191004, MAB1547, Novus Biologicals), or IgG isotype control (dose: 300 μg per mouse, Clone 20116, MAB004, Novus Biologicals). Twenty-four hours later, the pretreated MDA-MB-231 cells were labeled with CFSE (Invitrogen). HeLa cells, which served as an internal control due to their relative insensitivity to killing by mouse NK cells, were labeled with PKH26 (Invitrogen). A suspension of the labeled cells (5×10^6 cells of each population) was prepared by mixing them in 1 mL of PBS. Subsequently, 0.4 mL of this cell mixture was intravenously injected into the tail vein of each mouse. Five hours later, the lungs were excised and processed to generate single-cell suspensions suitable for flow cytometric analysis. The ratio of the tested target MDA-MB-231 cells to the control HeLa

cells within these lung suspensions was then calculated. All animal experiments were conducted in strict compliance with the ethical guidelines set forth by the Ethics Committee for the Use of Experimental Animals in Hangzhou Medical College and adhered to the principles outlined in the Guide for the Care and Use of Laboratory Animals published by the US NIH (the 8th Edition, NRC 2011).

2.9 Immunohistochemistry in a xenograft model

MDA-MB-231 cells were subcutaneously inoculated into the right hind flanks of female BALB/c (nu/nu) immunodeficient mice. Once the tumors attained an approximate volume of 40 mm^3, the mice were randomly allocated into three distinct groups. RES was dissolved in a vehicle solution composed of DMSO, polyethylene glycol 400, and distilled deionized water at a ratio of 1:1:3. The RES solution was administered intraperitoneally at daily dosages of either 25 mg/kg or 100 mg/kg for a continuous four-week period. The control group received an equivalent volume of the vehicle alone. At last, the mice were euthanized. The tumors were promptly fixed in 4% paraformaldehyde obtained from Sinopharm Chemical Reagent Co. (Shanghai, China), followed by tissue processing and sectioning. Paraffin-embedded sections of the xenograft tumor tissues, with a thickness of 4 μm, were prepared and utilized for immunohistochemical (IHC) staining. The slides were subjected to IHC using an anti-ULBP2 antibody (MA5-29636, Invitrogen, Carlsbad, CA, USA). Staining was visualized under an Olympus optical microscope.

2.10 Bioinformatic analysis

The target genes of miR-17-5p were computationally predicted using distinct algorithms from five databases: miRanda(http://www.microrna.org/microrna/home.do), TargetScan(http://www.targetscan.org), miRmap(https://mirmap.ezlab.org), PITA (http://genie.weizmann.ac.il/pubs/mir07/mir07_data.html) and picTar(https://pictar.mdc-berlin.de). The results of Kyoto Encyclopedia of Genes and Genomes (KEGG) pathway enrichment analysis for the shared predicted target genes were visualized utilizing the R package clusterProfiler from the Bioconductor project. Statistical significance was set at an adjusted p-value threshold of <0.05. mRNA and miRNA expression data for breast cancer samples (N=1104; Subtype: Luminal A 43.03%, Luminal B 19.11%, Triple negative 16.49%, Her2(+) 8.24%, NA 13.13%; Sex: Female 98.82%, Male 1.18%) were obtained from The Cancer Genome Atlas (TCGA) database (https://cancergenome.nih.gov/). Patient characteristics of breast cancer samples were shown in Supplementary Figure 1. According to the information provided by TCGA, mRNA and miRNA expressions were measured using IIIumina HiSeq 2000 Sequencing. Differential expression and correlation analyses were performed using the R package edgeR.

2.11 Statistical analysis

Statistical tests were performed and analyzed using Microsoft Excel and GraphPad Prism 9.0 software (San Diego, CA, USA). All data from a minimum of three independent experiments were expressed as mean ± standard deviation (SD). In the statistical analysis comparing two groups, the Shapiro-Wilk test was first used to assess the normality of the data. For non-normally distributed data, the non-parametric Mann-Whitney U test was employed to compare the two groups. For normally distributed data, an F test was conducted to compare variances between the groups. When both normality and equal variances were confirmed, an unpaired two-tailed Student's t-test was used to determine statistical significance. If the variances were found to be unequal, the Welch's t-test (t-test with Welch's correction) was applied instead. A p-value threshold of <0.05 was adopted to denote statistical significance, represented graphically as* for $p<0.05$, ** for $p<0.01$, and *** for $p<0.001$.

3 Results

3.1 Resveratrol upregulates the expression of ULBP2 in breast cancer

To investigate the effect of RES on NKG2DL expression in breast cancer, four distinct cell lines—MDA-MB-231, Bcap37, MCF7, and MDA-MB-468—were exposed to RES at concentrations of 6.25 μM, 12.5 μM, or 25 μM, as well as to a vehicle control, for a period of 48 hours. Our flow cytometric analysis demonstrated a dose-dependent increase in the MFI due to an antibody specific for ULBP2, ULBP5, and ULBP6 in cells treated with RES. This suggests that the expression of one or more of these ligands was upregulated in response to RES treatment (Figures 1A–E). To precisely determine which ligands are modulated by RES, we quantified mRNA expression levels in RES-treated and control cells using qRT-PCR with primers specific to each ULBP. Among all the *ULBP* genes analyzed, it was revealed that ULBP2 exhibited a consistent, pronounced, and dose-dependent increase in mRNA expression following RES treatment (Figures 1F–I). Moreover, the results from western blot assays demonstrated that exposure to RES led to a significant elevation in ULBP2 protein levels in both the MDA-MB-231 and MCF7 cell lines (Figures 1J, K). This finding corroborates the observed increase in ULBP2 mRNA expression, indicating that RES increases ULBP2 expression at both the transcriptional and translational levels in these cell lines.

ULBP2 is always undetectable or low-expressed on healthy cells, while it can be induced at the onset of malignant transformation. To assess the differential expression of ULBP2 between normal and neoplastic breast tissues, we conducted an analysis of data obtained from TCGA. Our findings revealed that the mean value of ULBP2 expression was significantly elevated in breast cancer specimens (n=1104) compared to a cohort of adjacent normal breast tissue samples (n=113) (Figure 1L).

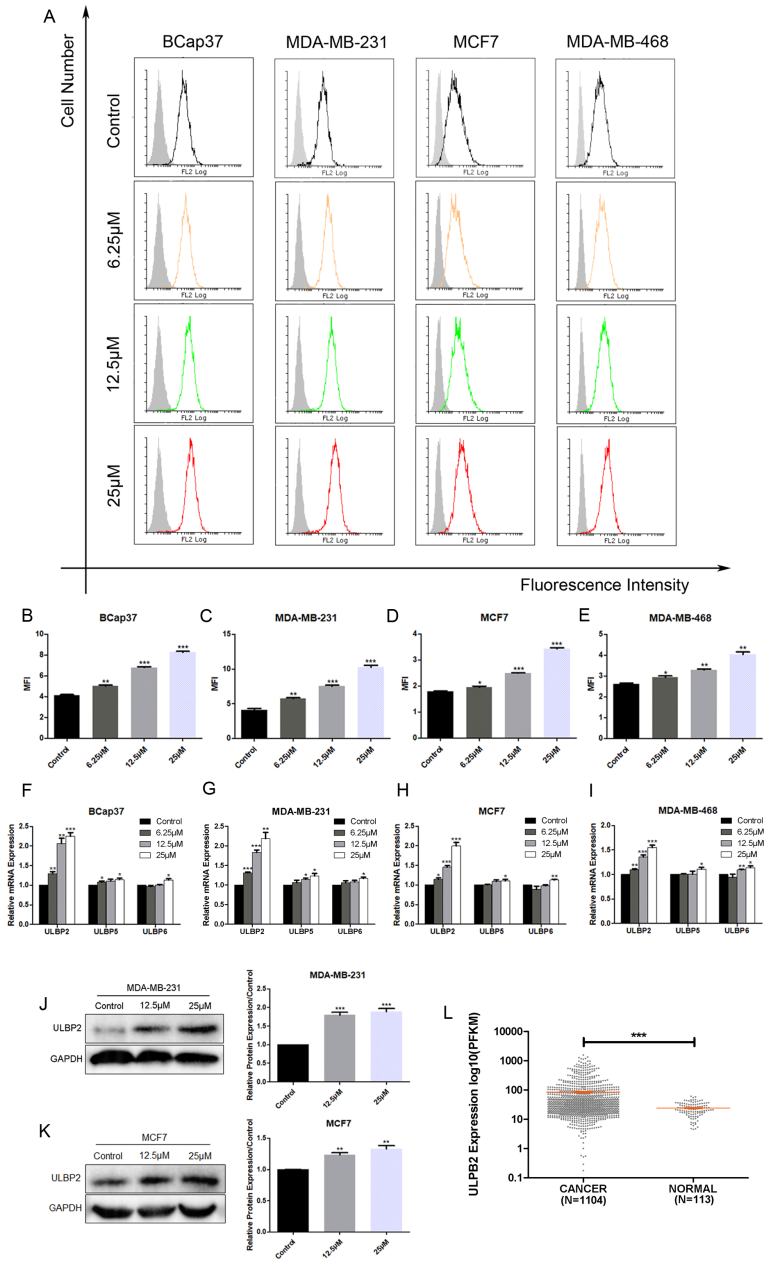

FIGURE 1
Resveratrol (RES) upregulates the expression of ULBP2 in breast cancer cells. Breast cancer cell lines (BCap37, MDA-MB-231, MCF-7 and MDA-MB-468) were treated with various concentrations of RES or control for 48 hours. **(A-E)** The surface protein levels of ULBP2/5/6 on BCap37, MDA-MB-231, MCF-7 and MDA-MB-468 cells were detected by flow cytometry. **(A)** are the depicted representative results from **(B-E)**. **(F-I)** The mRNA expression levels of ULBP2, ULBP5 and ULBP6 were detected in RES pretreated BCap37, MDA-MB-231, MCF-7 and MDA-MB-468 cells by qRT-PCR, with GAPDH as a reference. **(J, K)** The expression of ULBP2 protein was determined in RES pretreated MDA-MB-231and MCF-7 cells by Western blot (left) and the blots were further quantified with ImageJ (right). GAPDH was used as a loading control. **(L)** The differential expression of ULBP2 between breast cancer samples (n=1104) and adjacent normal breast tissue samples (n=113) from The Cancer Genome Atlas dataset was analyzed using Welch's t-test. The unpaired two-tailed Student's t-test was used to determine statistical significance in **(B-K)**, *$p<0.05$, **$p<0.01$, ***$p<0.001$ versus Control.

3.2 MiR-17-5p which is suppressed in RES treated breast cancer cells inhibits ULBP2 expression

To elucidate the molecular mechanism underlying ULBP2 regulation by RES, level of miR-17-5p was determined in RES treated breast cancer cells. When MDA-MB-231 and MCF7 cells were exposed to RES at concentrations of either 12.5 μM or 25 μM for 48 hours, a dose-dependent decrease in miR-17-5p levels was observed (Figures 2A, B), which substantiated the suppressive influence of RES on miR-17-5p expression.

To determine the regulatory role of miR-17-5p on ULBP2 expression, we transiently transfected MDA-MB-231 and MCF7 cells with either a miR-17-5p mimic, a miR-17-5p inhibitor, or a

negative control (NC) oligonucleotide. With flow cytometry assays, the surface ULBP2/5/6 proteins were shown to be increased on miR-17-5p inhibitor-transfected MDA-MB-231 cells, while decreased on mimic-transfected cells. A similar pattern of observation was noted in MCF7 cells as well (Figure 2C–E). Western blot analysis revealed that the protein level of ULBP2 was consistently downregulated upon transfection with miR-17-5p mimics, while correspondingly upregulated following miR-17-5p inhibitor transfection in both MDA-MB-231 and MCF7 cell lines (Figures 2F, G). Thus, these observations indicate that RES suppresses the expression of miR-17-5p, and miR-17-5p negatively regulates the expression of ULBP2 in breast cancer.

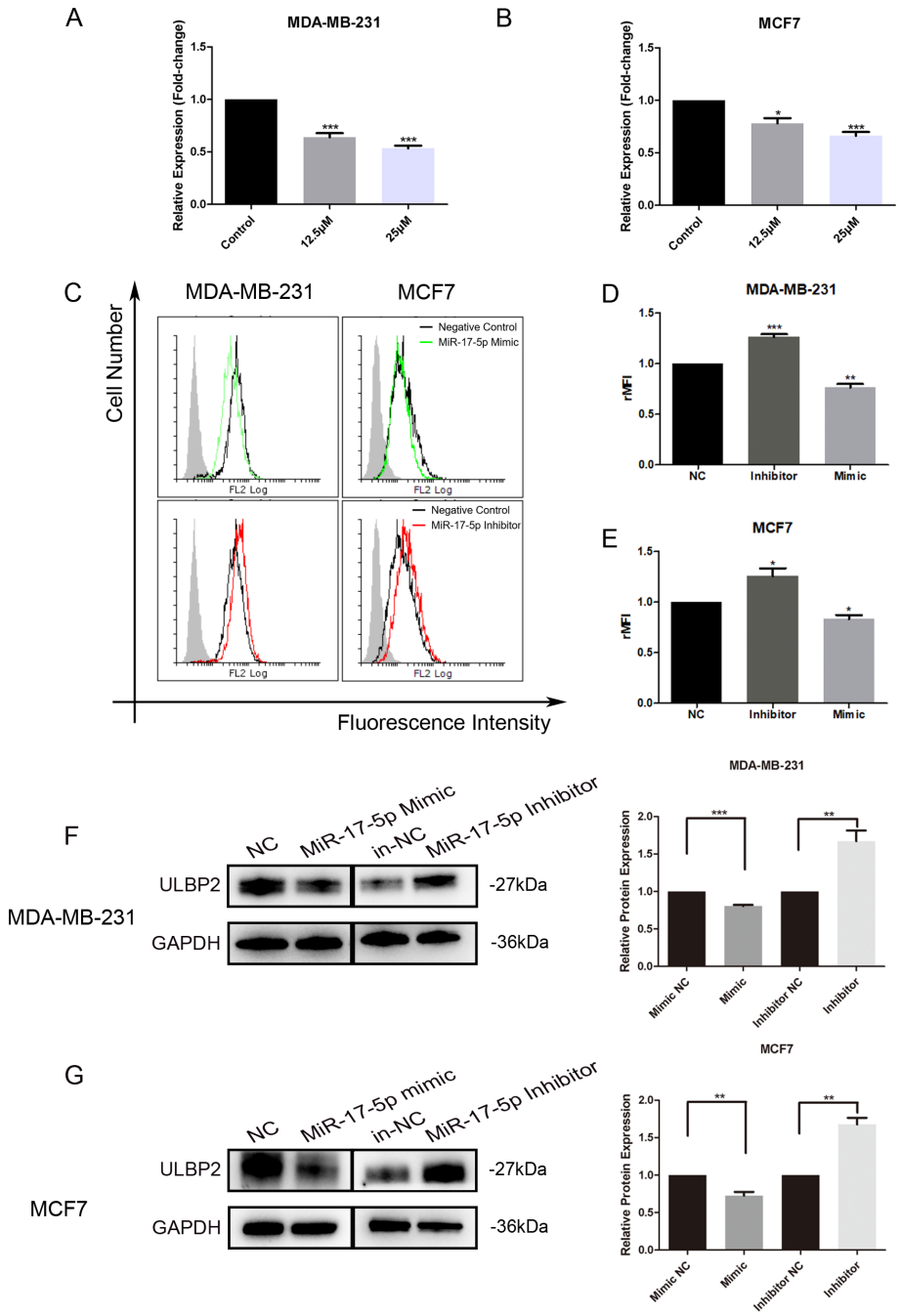

FIGURE 2
MiR-17-5p which is suppressed in RES treated breast cancer cells inhibits ULBP2 expression. **(A, B)** The breast cancer cells were treated with RES or control medium for 48 hours. The level of miR-17-5p was assessed with qRT-PCR, with U6 as a reference. **(C-G)** The breast cancer cells were transfected with miR-17-5p mimic, inhibitor or negative control (NC), respectively. **(C-E)** The expression of ULBP2/5/6 was determined by flow cytometry. **(C)** are depicted representative results from **(D, E)**. **(F, G)** The level of ULBP2 protein was detected by Western blot (left) and the blots were further quantified with ImageJ (right). GAPDH was used as a loading control. The unpaired two-tailed Student's t-test was used to determine statistical significance. *$p<0.05$, **$p<0.01$, ***$p<0.001$ versus Control or NC.

3.3 *MINK1* is predicted as the target gene of miR-17-5p in ULBP2 regulation

Despite evidence suggesting that miR-17-5p can suppress ULBP2 expression, bioinformatics analysis indicates that ULBP2 is not a direct target of miR-17-5p. This implies the existence of a more intricate and indirect regulatory mechanism governing ULBP2 expression by miR-17-5p. To elucidate the connection between miR-17-5p and ULBP2, we initially identified 428 commonly predicted target genes of miR-17-5p across five online databases: PITA, miRmap, miRanda, picTar, and TargetScan (Figure 3A). For better understanding the biological features of these genes, we performed KEGG pathway enrichment analysis. The results, presented in Figure 3B, revealed that these genes are predominantly associated with several key pathways. Among these pathways, three are particularly relevant to breast cancer and ULBP2 regulation: mammary gland, invasive breast cancer, and cellular responses to stress. As shown in the Venn diagram, three genes (*CDKN1A, MINK1* and *SQSTM1*) were overlapped in the three pathways (Figure 3C). Then, differential expression analysis of the three predicted genes were performed between breast cancer (BC) tissues and adjacent normal breast tissues using data from TCGA. The analysis revealed differential expression patterns of the three predicted genes between BC tissues and adjacent normal breast tissues. CDKN1A and MINK1 were both downregulated in BC, with median TPM (Transcripts Per Million) values decreasing from 5925.963 in normal tissue to 4547.018 in BC tissue for CDKN1A, and from 5896.905 in normal tissue to 4666.032 in BC tissue for MINK1. Conversely, SQSTM1 exhibited an opposite expression pattern, with its median TPM value increasing from 11834.51 in normal tissue to 14738.95 in BC tissue (Figures 3D–F). This indicates that CDKN1A and MINK1 are downregulated in breast cancer relative to normal tissue, while SQSTM1 shows upregulation in the same comparison. MDA-MB-231 cells were transfected with miR-17-5p mimics or inhibitors, after which the expression levels of the three genes were assessed using qRT-PCR. As shown in Figures 3G–H, the expression levels of these genes were found to be inversely correlated with miR-17-5p levels.

To explore the roles the three predicted genes played in ULBP2 regulation, their corresponding siRNAs were constructed and respectively transfected into breast cancer cells. Knockdown of CDKN1A, MINK1 or SQSTM1 in MDA-MB-231 cells led to reduced expression of ULBP2 (Figure 3I). For MCF7 cells, ULBP2 expression was downregulated in the MINK1 siRNA-transfected group but upregulated in the CDKN1A and SQSTM1 siRNA-transfected groups. This pattern of ULBP2 expression modulation was not consistent with that observed in MDA-MB-231 cells (Figure 3J). The findings demonstrate that the regulation of ULBP2 expression by CDKN1A and SQSTM1 may be cell-specific. In both MDA-MB-231 and MCF7 cells, MINK1 knockdown resulted in the inhibition of ULBP2 expression, leading to its selection for further study. Si-MINK1-2, exhibiting superior efficacy in ULBP2 inhibition compared to si-MINK1-1, was hence chosen for further investigations.

3.4 MiR-17-5p downregulates ULBP2 expression by directly binding to 3′-UTR of *MINK1*

Further analyses and studies were conducted to more comprehensively elucidate the regulation of MINK1 by miR-17-5p. An inverse correlation between endogenous miR-17-5p and MINK1 was demonstrated in breast cancer specimens using StarBase analysis (https://starbase.sysu.edu.cn/), suggesting a potential role for miR-17-5p in modulating MINK1 expression in breast cancer patients (Figure 4A). To validate the direct binding of miR-17-5p to 3′-UTRs of *MINK1*, a dual-luciferase reporter assay was conducted. The assay showed that miR-17-5p significantly suppressed the luciferase activity of constructs harboring the wild-type *MINK1* 3′-UTR, whereas transfection with miR-17-5p mimic did not produce any appreciable alteration in the luciferase activity of reporters containing mutated *MINK1* 3′-UTR sequences (Figures 4B, C). These findings confirm that miR-17-5p suppresses MINK1 expression by directly binding to its 3′-UTR. Overexpression of miR-17-5p caused a marked downregulation of MINK1 protein levels in MDA-MB-231 cells, whereas suppression of miR-17-5p led to a significant upregulation of MINK1 protein levels (Figure 4D).

To investigate the effect of MINK1 on ULBP2, we first constructed siRNA (si-MINK1) for MINK1 knockdown and an overexpression vector (pcDNA3.1-MINK1) for MINK1 upregulation. The efficiencies of these constructs were confirmed by Western blot analysis (Figure 4E). Then, MDA-MB-231 cells were co-transfected with si-MINK1, pcDNA3.1-MINK1, miR-17-5p mimics, inhibitors or respective controls. As shown in Figure 4F, si-MINK1 abrogated the increase in ULBP2 expression induced by miR-17-5p inhibitors, whereas pcDNA3.1-MINK1 plasmids effectively counteracted the suppressive impact of miR-17-5p mimics on ULBP2. Taken together, the results indicate the key role MINK1 plays within the pathway through which miR-17-5p downregulates ULBP2.

3.5 JNK/c-Jun is involved in ULBP2 regulation mediated by the miR-17-5p/MINK1 axis

MINK1, also known as MAP4K6 (Mitogen-activated protein kinase kinase kinase kinase 6), is a serine/threonine kinase that functions as a mitogen-activated protein kinase (MAPK) kinase within the MAPK signaling cascade. Notably, c-Jun N-terminal kinase (JNK) is a prototypical member of the MAPK family. Herein, we explored the involvement of JNK and its downstream target, c-Jun, within the regulation of ULBP2. Western blot analysis demonstrated a significant reduction in the expression levels of phosphorylated JNK (p-JNK, at Thr183/Tyr185) and phosphorylated c-Jun (p-c-Jun, at Ser63) in breast cancer cells that overexpressed miR-17-5p. Conversely, cells transfected with miR-17-5p inhibitors exhibited a notable increase in the levels of these phosphorylated proteins (Figure 5A). Knockdown of MINK1 resulted in decreased expression of p-JNK and p-c-Jun, whereas

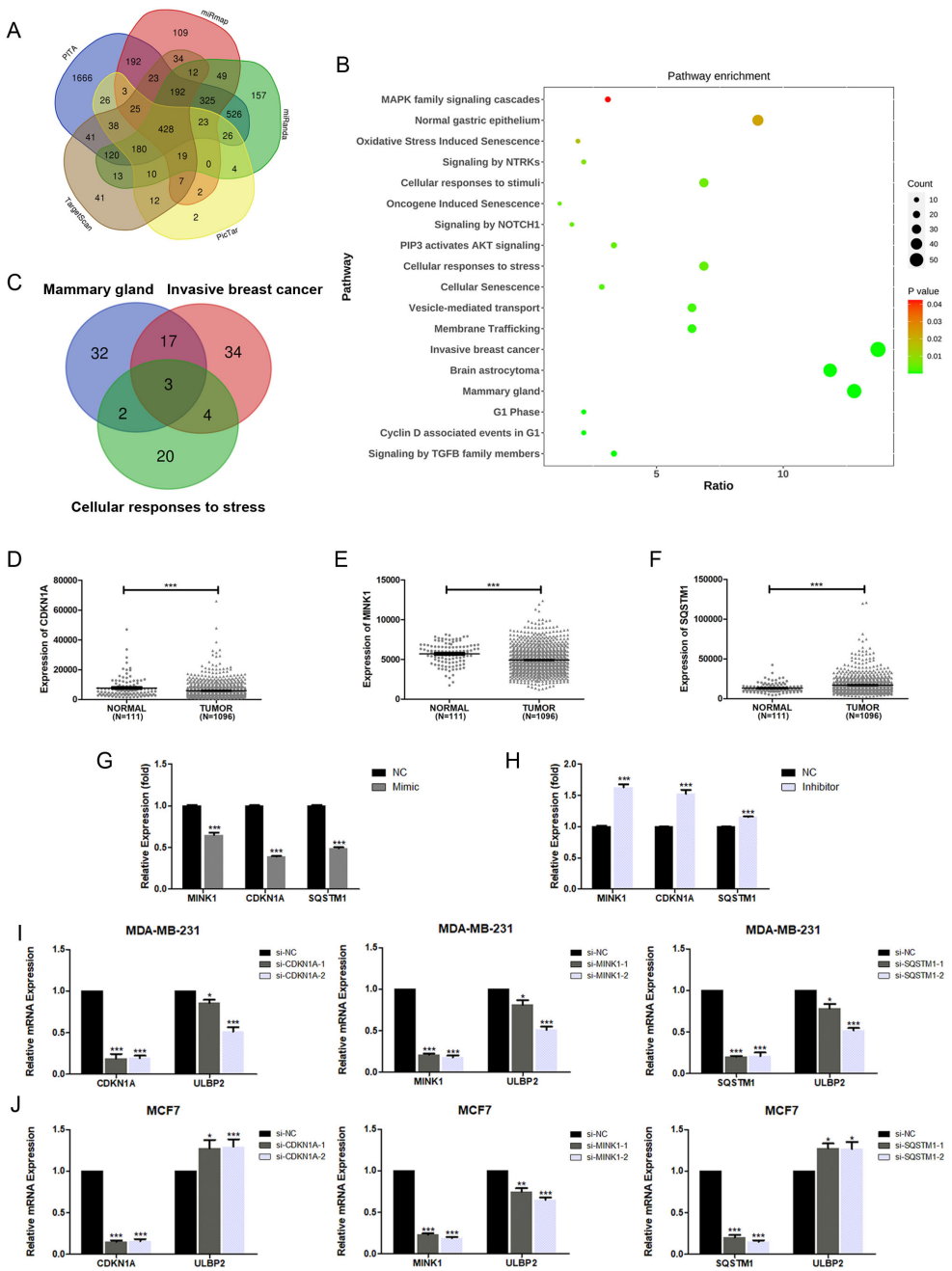

FIGURE 3
The target gene screening of miR-17-5p in ULBP2 regulation. **(A)** 428 genes were predicted as direct targets for miR-17-5p using PITA, miRmap, miRanda, picTar and TargetScan database. **(B)** The enrichment analysis of KEGG pathways was performed in the 428 genes. **(C)** Three genes (*CDKN1A, MINK1* and *SQSTM1*) were overlapped among the three relevant pathways (Mammary gland, Invasive breast cancer and Cellular responses to stress). **(D-F)** The levels of CDKN1A, MINK1 and SQSTM1 were analyzed in breast cancer (n=1096) and adjacent normal breast tissue (n=111) cohorts from The Cancer Genome Atlas. Statistical significance was determined by the non-parametric Mann-Whitney U test. **(G, H)** The mRNA expressions of CDKN1A, MINK1 and SQSTM1 were detected using qRT-PCR in MDA-MB-231 cells transfected with miR-17-5p mimic, inhibitor or negative control (NC), with GAPDH as a reference. **(I, J)** The mRNA expression of ULBP2 was determined by qRT-PCR in CDKN1A, MINK1 or SQSTM1 knocked-down breast cancer cells, with GAPDH as a reference. The unpaired two-tailed Student's t-test was used to determine statistical significance in **(G-J)**. *p<0.05, **p<0.01, ***p<0.001 versus NC or si-NC.

overexpression of MINK1 led to increased levels of these phosphorylated proteins (Figure 5B). Furthermore, treatment with sp600125, a specific JNK inhibitor, potentiated the suppressive influence of miR-17-5p on ULBP2 expression (Figure 5C). Altogether, the data demonstrate that the JNK/c-Jun pathway contributes to the promotion of ULBP2 expression in breast cancer cells and, to a certain extent, is involved in the mechanism by which miR-17-5p modulates ULBP2.

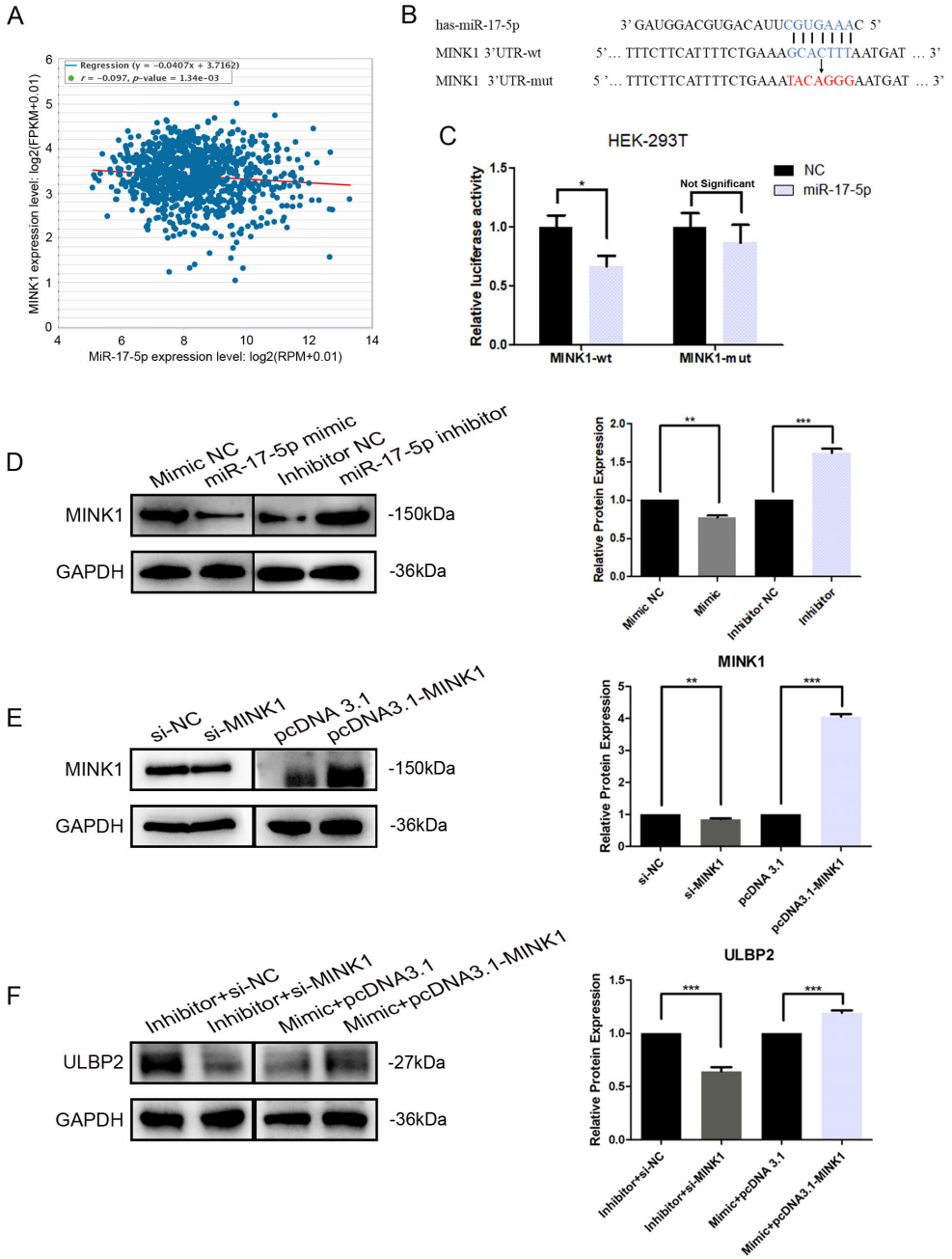

FIGURE 4
MINK1 is the target gene of miR-17-5p and promotes ULBP2 expression. **(A)** The correlation between miR-17-5p and MINK1 in 1085 breast tissue samples from TCGA. Linear regression analysis was used to assess the relationship between miR-17-5p and MINK1 expression. **(B)** Schematic representation of predicted miR-17-5p binding sites in the 3'-UTR of *MINK1* and 3'-UTR mutated alignment. **(C)** The dual luciferase assays were performed in HEK-293 T cells. **(D)** MDA-MB-231 cells were transfected with 50 nM of miR-17-5p inhibitor, mimic or negative control (NC) for 24 hours. The MINK1 protein levels were detected by western blot. **(E)** The efficiency of MINK1 knockdown and overexpression was confirmed by western blot. **(F)** The effects of MINKI on ULBP2 expression were assessed using western blot in miR-17-5p exogenously expressed or suppressed MDA-MB-231 cells. **(D-F)** GAPDH was used as a reference in western blot assays and the blots were further quantified with ImageJ (right). The unpaired two-tailed Student's t-test was used to determine statistical significance. *$p<0.05$, **$p<0.01$, ***$p<0.001$.

3.6 Resveratrol treatment increases the sensitivity of breast cancer cells to NK cell-mediated lysis both *in vitro* and *in vivo*

To assess the effects of RES on the susceptibility of breast cancer cells to clearance by NK cells, MDA-MB-231 cells were exposed to different concentrations of RES for 48 hours. Results from *in vitro* NK cytotoxicity assays at different effector-to-target ratios demonstrated that the lysis of MDA-MB-231 cells by NK cells increased with the concentration of RES pre-treated on the target cells (Figure 6A). However, when the NK cells were preconditioned by incubation with an anti-NKG2D blocking antibody, RES

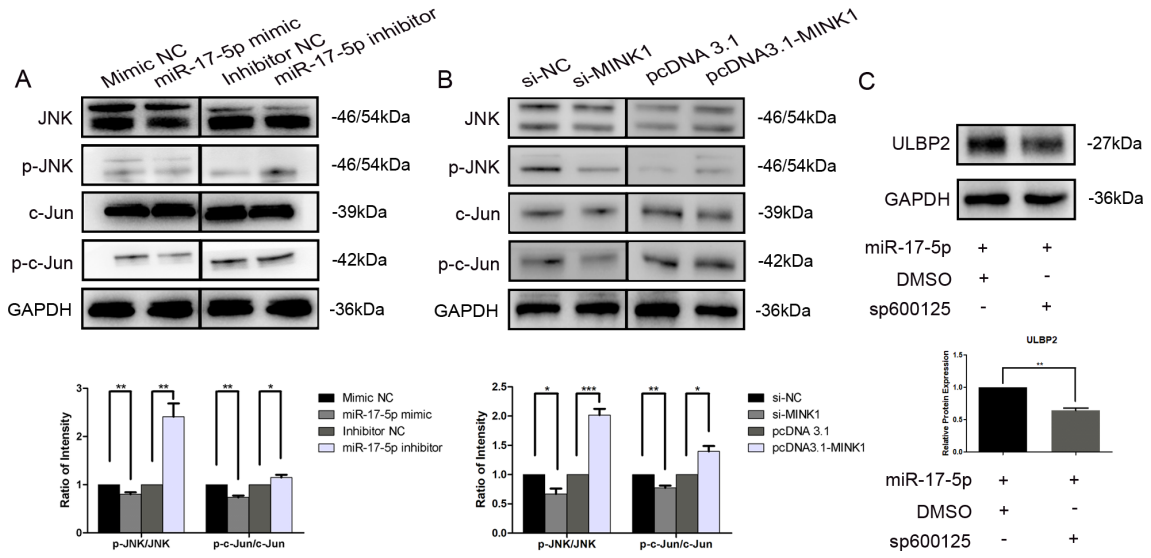

FIGURE 5
JNK/c-Jun is involved in ULBP2 regulation mediated by the miR-17-5p/MINK1 axis. **(A)** MDA-MB-231 cells were transfected with miR-17-5p inhibitors, mimics or the corresponding controls (NC) for 24 hours. The levels of JNK, p-JNK, c-Jun and p-c-Jun were detected by western blot. **(B)** The expressions of JNK, p-JNK, c-Jun and p-c-Jun were determined in MINK1 knocked-down or overexpressed MDA-MB-231 cells by western blot. **(C)** MDA-MB-231 cells exogenously expressing miR-17-5p were treated with 10 μM of sp600125, a JNK inhibitor, or dimethyl sulfoxide (DMSO, as a vehicle control) for 24 hours. Subsequently, ULBP2 expression was evaluated by Western blot. GAPDH was used as a reference. All the blots were quantified with ImageJ. The unpaired two-tailed Student's t-test was used to determine statistical significance. *$p<0.05$, **$p<0.01$, ***$p<0.001$.

exposure induced increase in cancer cell lysis by NK cell would be effectively abolished (Figure 6B). This observation points to the critical role of NKG2D receptor recognition and activation in the process.

As illustrated in Figure 6C, the *in vivo* cytotoxicity experiments were performed in C57BL/6 mice with HeLa cells as internal control. The survival rate of MDA-MB-231 cells, as determined by the ratio of CFSE-positive cells to PKH26-positive cells, inversely correlated with the concentration of RES used in treatment (Figures 6D, E). The anti-NKG2D or anti-NK1.1 antibodies were intraperitoneally injected into mice in the respective groups to block NKG2D receptors or deplete NK cells. In mice pretreated with anti-NKG2D antibodies, the stimulatory effect of RES on the clearance of breast cancer cells by NK cells was abolished (Figure 6F). This finding implies that the process is mediated by NKG2D. And similar observations were made in the anti-NK1.1 group, suggesting that NK cells are the primary effectors responsible for the clearance (Figure 6G).

Moreover, we investigated the influence of miR-17-5p on tumor cell eradication within an *in vivo* context. MDA-MB-231 cells transfected with miR-17-5p mimics exhibited reduced susceptibility to lysis by immune effector cells. As a result, a lower proportion of cancer cells were eliminated, leading to a higher number of CFSE-labeled cells in the single cell suspension compared to the control group. In contrast, the group transfected with miR-17-5p inhibitors exhibited a lower number of CFSE-labeled cells, indicative of increased elimination of cancer cells. Importantly, all these differences between the groups were completely abolished in mice pretreated with anti-NKG2D and antiNK1.1 antibodies (Figures 6H–J).

These results confirm that RES enhances the vulnerability of breast cancer cells to NK cell-mediated cytotoxicity, whereas miR-17-5p functions as a negative regulator of this sensitivity.

3.7 Resveratrol increases the level of ULBP2 in xenograft tumors and meanwhile suppresses tumor growth

To further investigate the *in vivo* effects of RES on breast cancer growth and ULBP2 expression, female BALB/c (nu/nu) mice were subjected to subcutaneous implantation of MDA-MB-231 cells to establish xenograft tumors. Thereafter, RES was administered intraperitoneally at doses of 0, 25, or 100 mg/kg per day. At the conclusion of a 28-day treatment period, the mice were euthanized, and their tumors were excised and weighed. A marked, dose-dependent reduction in both tumor volume and weight was observed in the RES-treated groups compared to the control group (Figures 7A–C). Moreover, IHC and western blot analyses confirmed RES promoted ULBP2 expression in xenograft tumors, consistent with the findings obtained from breast cancer cell lines *in vitro* (Figures 7D, E). The data indicate that RES upregulates ULBP2 expression in breast cancer cells and concurrently suppresses tumor growth in an *in vivo* setting.

4 Discussion

The study of natural compounds as disease preventive agents or alternatives to synthetic molecules for therapeutic use has become

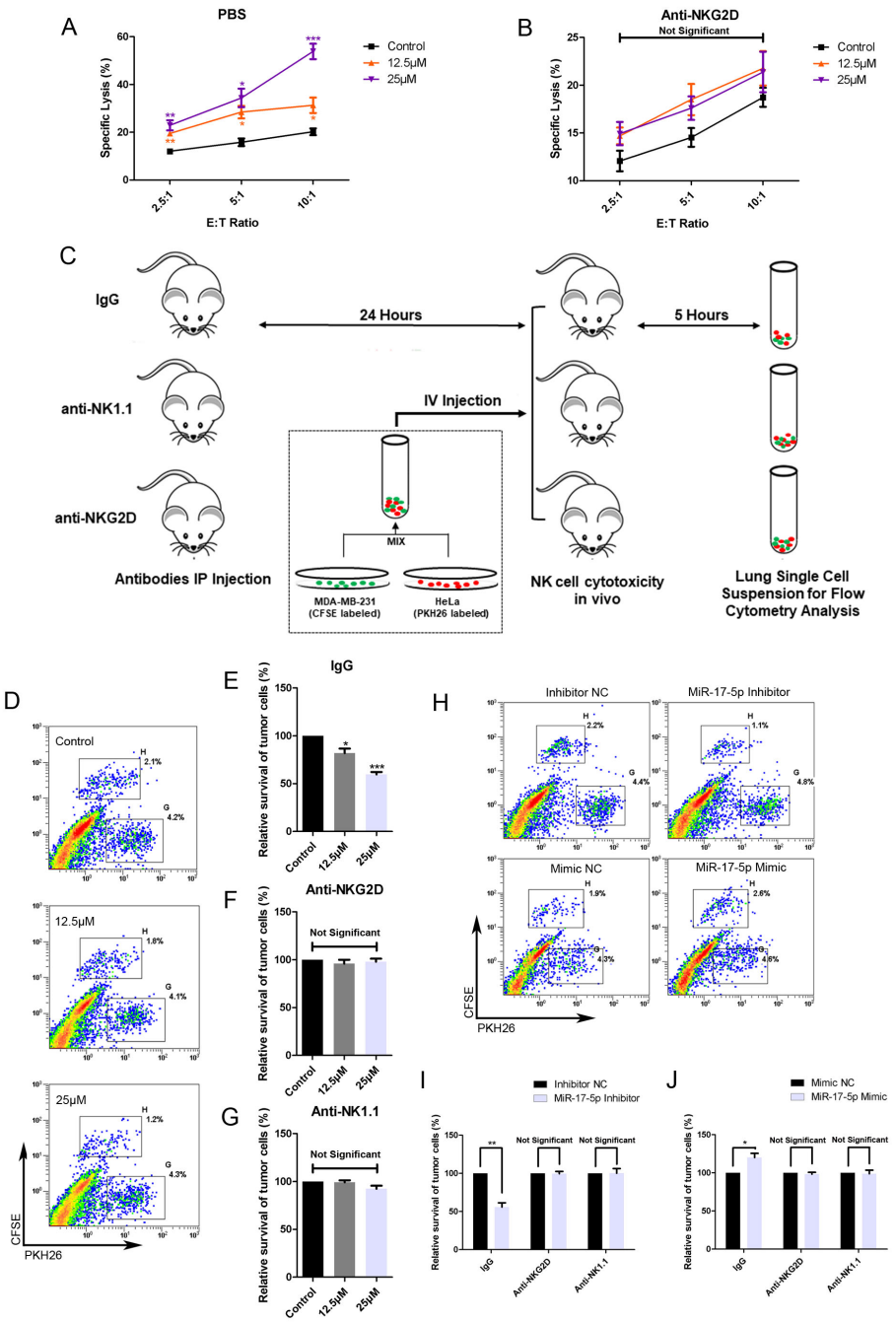

FIGURE 6
RES contributes to NK mediated cytolysis against breast cancer cells *in vitro* and *in vivo*. **(A, B)** MDA-MB-231 cells were exposed to different concentrations of RES for 48 hours. The NK cell line NK-92MI cells were pretreated with phosphate buffered saline (PBS) **(A)** or anti-NKG2D antibodies **(B)** for 1 hour before the cytotoxicity assay. Cytotoxicity assays were performed with NK-92MI cells as effector cells at different effector-to-target ratios. **(C)** Schematic representation of the *in vivo* experimental procedures. Male C57BL/6 mice were intraperitoneally (IP) injected with 300 μg per mouse of IgG, anti-NKG2D antibody, or anti-NK1.1 antibody. 24 hours later, the mice received an intravenous (IV) injection of a mixture containing [2×10^6] MDA-MB-231 cells and [2×10^6] HeLa cells. After 5 hours, the mice were sacrificed, and their lungs were excised and processed to generate single-cell suspensions. **(D-G)** MDA-MB-231 cells were pretreated with different concentrations of RES for 48 hours. Flow cytometry assays were used to analyze the ratios of MDA-MB-231 cells to HeLa cells in lung single-cell suspensions. **(D)** depicts representative results from IgG pretreated groups. **(H-J)** MDA-MB-231 cells were transfected with 50 nM of miR-17-5p mimic, inhibitor or negative control (NC), respectively. Flow cytometry assays were used to analyze the ratios of MDA-MB-231 cells to HeLa cells in lung single-cell suspensions. **(H)** depicts representative results from IgG pretreated groups. Statistical significance was determined by the unpaired two-tailed Student's t-test. *$p<0.05$, **$p<0.01$, ***$p<0.001$ versus Control.

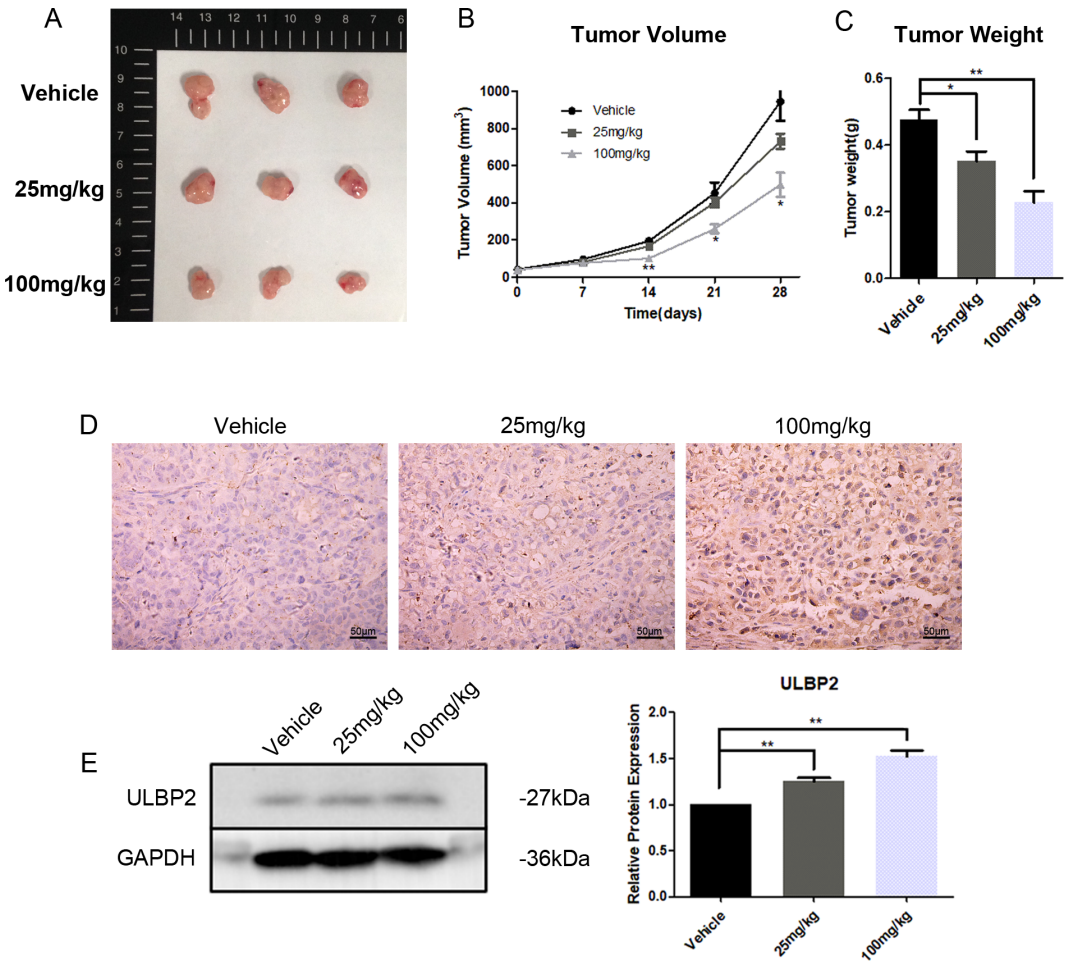

FIGURE 7
RES suppresses tumor growth and increases ULBP2 expression in xenograft tumors. MDA-MB-231 cells were subcutaneously implanted into female BALB/c (nu/nu) mice. RES or vehicle control was administrated intraperitoneally every day for 28 days. **(A)** The mice were sacrificed for xenograft tumor tissues. **(B)** Tumor volumes were measured every 7 days. **(C)** Tumor weights were measured at the endpoint of the experiment. **(D)** Representative images from immunohistochemistry assay for ULBP2 expression (magnification ×400). **(E)** Levels of ULBP2 protein were examined by western blot with GAPDH as a reference and the blots were quantified with ImageJ. Statistical significance was determined by the unpaired two-tailed Student's t-test. *$p<0.05$, **$p<0.01$ versus Vehicle.

an important subject of interest in recent decades. RES, one of the most representative compounds, has gained the focus of a variety of researches in chemistry and medicine (24). RES exhibits excellent tolerability in both experimental animals and humans. No obvious adverse effects were observed in dogs administered RES orally at a dose of 600 mg/kg/day for 90 days (25). In a subset of healthy volunteers administered oral RES at a high dose of 2000 mg twice daily, only mild-to-moderate gastrointestinal disturbances were reported (26). RES performs multiple health-promoting activities, including anticancer. Breast cancer, the most prevalent malignancy among females globally, threatens human health seriously and imposes a heavy burden on patients, their families and society (27, 28). A growing body of research increasingly substantiates RES's potential in breast cancer prophylaxis and therapy. This includes mechanisms such as the inhibition of angiogenesis, suppression of cell migration and metastasis, induction of cell cycle arrest and apoptosis, as well as modulation of epigenetic processes (7, 29–31). Consistently, the present study revealed that administering RES to mice at doses of either 25 mg/kg/day or 100 mg/kg/day for a 28-day period was well-tolerated and effectively inhibited cancer growth.

Considering the critical role that ULBP2 plays in facilitating cancer cell elimination by NK cells and the immune-modulatory effects exerted by RES, the current research aimed to elucidate the impact of RES on ULBP2 expression and the underlying molecular mechanisms involved. RES was demonstrated to augment ULBP2 expression in four breast cancer cell lines. It heightened the susceptibility of MDA-MB-231 cells to NK cell-mediated cytotoxicity *in vitro*. However, the increased susceptibility was diminished when cytolysis was performed with NK cells whose NKG2D receptors were blocked, suggesting that NKG2D plays a crucial role in this process. Furthermore, *in vivo* experiments demonstrated that RES dose-dependently enhanced the killing of intravenously injected MDA-MB-231 cells in C57BL/6 mice. This effect was eliminated in mice pre-treated with anti-NKG2D and anti-NK1.1 antibodies, suggesting that the *in vivo* cytotoxicity

against MDA-MB-231 cells was primarily executed by NKG2D-activated NK cells. These results point to the potential that RES may serve as an enhancer of ULBP2-mediated cancer cell clearance by NK cells. Subsequently, the mechanism by which RES upregulates the expression of ULBP2 was intensively investigated.

MiR-17-5p is upregulated in various types of cancer and is known for its oncogenic properties (32, 33). It drives cancer initiation, progression, and metastasis by promoting cancer cell motility, proliferation, invasiveness, angiogenesis and chemoresistance (34–37). Accordantly, findings from our previous research indicated that miR-17-5p plays a pivotal role in promoting the epithelial-mesenchymal transition, thereby enhancing the migratory and invasive capabilities of breast cancer cells (22). In the current study, the exposure to RES led to a dose-dependent reduction in miR-17-5p levels in breast cancer cells. MiR-17-5p has been documented to suppress the expression of MICA and MICB, two other important NKG2DLs, in hepatocellular and colorectal cancers (38, 39). However, the potential regulatory role of miR-17-5p in modulating ULBP2 expression has not yet been reported. Herein, miR-17-5p was demonstrated to suppress ULBP2 expression in breast cancer line MDA-MB-231 and MCF7 cells. And its effect on the susceptibility of MDA-MB-231 cells to NK cell-mediated cytolysis was evaluated in mouse model. MDA-MB-231 cells transfected with miR-17-5p mimics exhibited reduced susceptibility to lysis by murine NK cells, while the cells transfected with miR-17-5p inhibitors showed higher sensitivity to NK cell killing *in vivo*. However, these changes in susceptibility induced by miR-17-5p upregulation or downregulation were abolished in mice pretreated with anti-NKG2D and anti-NK1.1 antibodies. Anti-NKG2D antibodies block NKG2D receptors, while anti-NK1.1 antibodies deplete NK cells. These findings suggest that both NK cells and their activating receptor NKG2D play a critical role in mediating cytotoxicity against breast cancer cells in mice. Additionally, the regulatory role of miR-17-5p in modulating ULBP2 expression, a ligand for NKG2D, was confirmed. This further indicates that miR-17-5p influences the recognition and killing of breast cancer cells by NK cells through its effect on ULBP2 expression.

But bioinformatic analysis did not identify any predicted miR-17-5p binding sites within the 3′-UTR of *ULBP2*, indicating that *ULBP2* was not a direct target gene of miR-17-5p. Consequently, we focused on screening potential target genes of miR-17-5p in the context of ULBP2 regulation. Our efforts led to the prediction that *MINK1* is the most probable target gene. An inverse correlation between MINK1 expression and miR-17-5p levels was observed across 1085 breast cancer specimens in the TCGA dataset. Cellular MINK1 levels were diminished upon transfection with miR-17-5p mimics and augmented following treatment with miR-17-5p inhibitors, respectively. using a dual-luciferase reporter assay, we demonstrated that miR-17-5p inhibited MINK1 expression by directly interacting with its 3′-UTR, thereby validating their direct targeting relationship. The exogenous expression of MINK1 effectively counteracted the decrease in ULBP2 protein levels induced by miR-17-5p overexpression, thus demonstrating the positive regulatory role of MINK1 on ULBP2 expression.

MINK1, an integral member of the mammalian Ste20-like serine/threonine kinase family, functions as a MAPK kinase in regulating diverse cellular processes such as senescence, motility, and chemoresistance (40–42). The MAPK pathway is a well characterized signaling pathway which controls a multitude of fundamental cellular processes, including inflammation, differentiation, apoptosis, proliferation, and others (43). But its role in NKG2DL regulation has not yet been well defined. Extracellular signal regulated kinase (ERK), a component of MAPK signaling cascade, was verified to promote ULBP2 expression in breast cancer in our previous research, which indicated the involvement of MAPK signaling in NKG2DL regulation (15). The JNK/c-Jun pathway is one of the classical

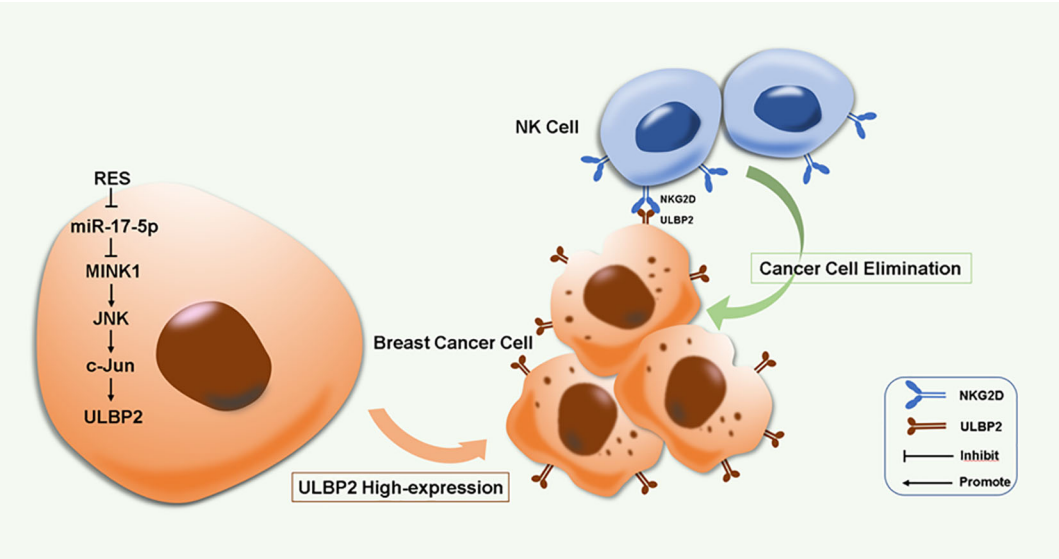

FIGURE 8
A proposed model for RES induced immune elimination of breast cancer cells by NK cells via miR-17-5p/MINK1/JNK/c-Jun/ULBP2 cascade.

MAPK pathways (44). In this work, the activation of JNK and its downstream effector molecule c-Jun was attenuated in breast cancer cells overexpressing miR-17-5p or subjected to MINK1 knockdown, whereas miR-17-5p downregulation or MINK1 upregulation led to opposing outcomes. Moreover, the JNK inhibitor sp600125 potentiated the suppressive effect of miR-17-5p on ULBP2 expression. These findings confirmed the involvement of JNK/c-Jun MAPK signaling cascade in ULBP2 regulation. It is reasonable to ask how the JNK/c-Jun pathway contributes to ULBP2 expression. C-Jun, a well-characterized transcription factor primarily activated by the JNK pathway, plays a crucial role in multiple biological processes by binding to specific DNA sequences to initiate transcriptional activity (45, 46). Due to this, ULBP2 expression might be regulated by c-Jun directly or indirectly. However, this possibility requires further exploration. Moreover, RES exhibited suppression of xenograft tumor growth in mice. Although the underlying mechanisms warrant further exploration, it is speculated that the downregulation of miR-17-5p, given its oncogenic properties, may contribute, at least in part, to the inhibitory effect of RES on breast cancer growth in murine models.

Considering the established capacity of RES to enhance NK cell-mediated cytotoxicity against breast cancer cells, further preclinical investigations are warranted to evaluate the administration route, optimal dosage, and treatment duration to maximize therapeutic efficacy while minimizing potential toxicity. Whether RES impacts ULBP2 expression in normal cells warrants further investigation. Additionally, methods to improve the bioavailability of RES should be developed. Moreover, integrating RES with conventional breast cancer treatment regimens deserves further exploration to leverage potential synergistic benefits.

5 Conclusion

RES induces ULBP2 expression and consequently enhances breast cancer cell elimination by NK cells through the suppression of miR-17-5p and activation of the MINK1/JNK/c-Jun cascade. This represents a novel biological mechanism in ULBP2 regulation (Figure 8). Our work suggests that RES has the potential to be an effective therapeutic agent for inhibiting breast cancer progression and enhancing NK cell-based cancer immunotherapy.

Data availability statement

The raw data supporting the conclusions of this article will be made available by the authors, without undue reservation.

Ethics statement

The animal study was approved by the Ethics Committee for the Use of Experimental Animals in Hangzhou Medical College. The study was conducted in accordance with the local legislation and institutional requirements.

Author contributions

BD: Formal analysis, Funding acquisition, Investigation, Methodology, Project administration, Visualization, Writing – original draft, Writing – review & editing. JL: Investigation, Methodology, Validation, Writing – original draft. J-LY: Investigation, Methodology, Validation, Writing – original draft. C-YJ: Investigation, Methodology, Validation, Writing – original draft. L-BQ: Conceptualization, Formal analysis, Funding acquisition, Supervision, Writing – review & editing. JP: Conceptualization, Data curation, Formal analysis, Funding acquisition, Investigation, Supervision, Writing – original draft, Writing – review & editing.

Funding

The author(s) declare financial support was received for the research, authorship, and/or publication of this article. This research was supported by Zhejiang Provincial Natural Science Foundation of China (ZCLTGD24H1001, LTGY24H150006); Department of Education of Zhejiang Province (Y202351847); Basic Scientific Research Funding of Hangzhou Medical College (KYZD202202); State Scholarship Fund of China (202308330429) and National Natural Science Foundation of China (82303417).

Conflict of interest

The authors declare that the research was conducted in the absence of any commercial or financial relationships that could be construed as a potential conflict of interest.

Generative AI statement

The author(s) declare that no Generative AI was used in the creation of this manuscript.

Publisher's note

All claims expressed in this article are solely those of the authors and do not necessarily represent those of their affiliated organizations, or those of the publisher, the editors and the reviewers. Any product that may be evaluated in this article, or claim that may be made by its manufacturer, is not guaranteed or endorsed by the publisher.

Supplementary material

The Supplementary Material for this article can be found online at: https://www.frontiersin.org/articles/10.3389/fimmu.2025.1515605/full#supplementary-material

References

1. Brockmueller A, Sajeev A, Koklesova L, Samuel SM, Kubatka P, Büsselberg D, et al. Resveratrol as sensitizer in colorectal cancer plasticity. *Cancer metastasis Rev*. (2023) 43:55-85. doi: 10.1007/s10555-023-10126-x

2. Breuss JM, Atanasov AG, Uhrin P. Resveratrol and its effects on the vascular system. *Int J Mol Sci*. (2019) 20:1523. doi: 10.3390/ijms20071523

3. Brockmueller A, Buhrmann C, Shayan P, Shakibaei M. Resveratrol induces apoptosis by modulating the reciprocal crosstalk between p53 and Sirt-1 in the CRC tumor microenvironment. *Front Immunol*. (2023) 14:1225530. doi: 10.3389/fimmu.2023.1225530

4. Hankittichai P, Thaklaewphan P, Wikan N, Ruttanapattanakul J, Potikanond S, Smith DR, et al. Resveratrol Enhances Cytotoxic Effects of Cisplatin by Inducing Cell Cycle Arrest and Apoptosis in Ovarian Adenocarcinoma SKOV-3 Cells through Activating the p38 MAPK and Suppressing AKT. *Pharm (Basel Switzerland)*. (2023) 16:755. doi: 10.3390/ph16050755

5. Song B, Wang W, Tang X, Goh RMW, Thuya WL, Ho PCL, et al. Inhibitory potential of resveratrol in cancer metastasis: from biology to therapy. *Cancers*. (2023) 15:2758. doi: 10.3390/cancers15102758

6. Selvakumar P, Badgeley A, Murphy P, Anwar H, Sharma U, Lawrence K, et al. Flavonoids and other polyphenols act as epigenetic modifiers in breast cancer. *Nutrients*. (2020) 12:761. doi: 10.3390/nu12030761

7. Sun Y, Zhou QM, Lu YY, Zhang H, Chen QL, Zhao M, et al. Resveratrol inhibits the migration and metastasis of MDA-MB-231 human breast cancer by reversing TGF-beta1-induced epithelial-mesenchymal transition. *Molecules*. (2019) 24:1131. doi: 10.3390/molecules24061131

8. Kowsari H, Davoodvandi A, Dashti F, Mirazimi SMA, Bahabadi ZR, Aschner M, et al. Resveratrol in cancer treatment with a focus on breast cancer. *Curr Mol Pharmacol*. (2023) 16:346–61. doi: 10.2174/1874467215666220616145216

9. Chen L, Musa AE. Boosting immune system against cancer by resveratrol. *Phytotherapy research: PTR*. (2021) 35:5514–26. doi: 10.1002/ptr.7189

10. Delmas D, Hermetet F, Aires V. PD-1/PD-L1 checkpoints and resveratrol: A controversial new way for a therapeutic strategy. *Cancers*. (2021) 13:4509. doi: 10.3390/cancers13184509

11. Schmiedel D, Mandelboim O. NKG2D ligands-critical targets for cancer immune escape and therapy. *Front Immunol*. (2018) 9:2040. doi: 10.3389/fimmu.2018.02040

12. Campos-Silva C, Kramer MK, Valés-Gómez M. NKG2D-ligands: Putting everything under the same umbrella can be misleading. *Hla*. (2018) 91:489–500. doi: 10.1111/tan.13246

13. Yang C, Qian C, Zheng W, Dong G, Zhang S, Wang F, et al. Ginsenoside Rh2 enhances immune surveillance of natural killer (NK) cells via inhibition of ERp5 in breast cancer. *Phytomedicine: Int J phytotherapy phytopharmacology*. (2024) 123:155180. doi: 10.1016/j.phymed.2023.155180

14. Jin F, Wu Z, Hu X, Zhang J, Gao Z, Han X, et al. The PI3K/Akt/GSK-3β/ROS/eIF2B pathway promotes breast cancer growth and metastasis via suppression of NK cell cytotoxicity and tumor cell susceptibility. *Cancer Biol Med*. (2019) 16:38–54. doi: 10.20892/j.issn.2095-3941.2018.0253

15. Shen J, Pan J, Du C, Si W, Yao M, Xu L, et al. Silencing NKG2D ligand-targeting miRNAs enhances natural killer cell-mediated cytotoxicity in breast cancer. *Cell Death Dis*. (2017) 8:e2740. doi: 10.1038/cddis.2017.158

16. Wu HY, Li KX, Pan WY, Guo MQ, Qiu DZ, He YJ, et al. Venetoclax enhances NK cell killing sensitivity of AML cells through the NKG2D/NKG2DL activation pathway. *Int immunopharmacology*. (2022) 104:108497. doi: 10.1016/j.intimp.2021.108497

17. Zhao P, Sun X, Li H, Liu Y, Cui Y, Tian L, et al. c-myc targets HDAC3 to suppress NKG2DL expression and innate immune response in N-type SCLC through histone deacetylation. *Cancers*. (2022) 14:457. doi: 10.3390/cancers14030457

18. Alkhayer R, Ponath V, Frech M, Adhikary T, Graumann J, Neubauer A, et al. KLF4-mediated upregulation of the NKG2D ligand MICA in acute myeloid leukemia: a novel therapeutic target identified by enChIP. *Cell communication signaling: CCS*. (2023) 21:94. doi: 10.1186/s12964-023-01118-z

19. Ullrich E, Koch J, Cerwenka A, Steinle A. New prospects on the NKG2D/NKG2DL system for oncology. *Oncoimmunology*. (2013) 2:e26097. doi: 10.4161/onci.26097

20. Allende-Vega N, Marco Brualla J, Falvo P, Alexia C, Constantinides M, de Maudave AF, et al. Metformin sensitizes leukemic cells to cytotoxic lymphocytes by increasing expression of intercellular adhesion molecule-1 (ICAM-1). *Sci Rep*. (2022) 12:1341. doi: 10.1038/s41598-022-05470-x

21. Vasu S, He S, Cheney C, Gopalakrishnan B, Mani R, Lozanski G, et al. Decitabine enhances anti-CD33 monoclonal antibody BI 836858-mediated natural killer ADCC against AML blasts. *Blood*. (2016) 127:2879–89. doi: 10.1182/blood-2015-11-680546

22. Bao C, Liu T, Qian L, Xiao C, Zhou X, Ai H, et al. Shikonin inhibits migration and invasion of triple-negative breast cancer cells by suppressing epithelial-mesenchymal transition via miR-17-5p/PTEN/Akt pathway. *J Cancer*. (2021) 12:76–88. doi: 10.7150/jca.47553

23. Boissel N, Rea D, Tieng V, Dulphy N, Brun M, Cayuela JM, et al. BCR/ABL oncogene directly controls MHC class I chain-related molecule A expression in chronic myelogenous leukemia. *J Immunol (Baltimore Md: 1950)*. (2006) 176:5108–16. doi: 10.4049/jimmunol.176.8.5108

24. Duta-Bratu CG, Nitulescu GM, Mihai DP, Olaru OT. Resveratrol and other natural oligomeric stilbenoid compounds and their therapeutic applications. *Plants (Basel Switzerland)*. (2023) 12:2935. doi: 10.3390/plants12162935

25. Johnson WD, Morrissey RL, Usborne AL, Kapetanovic I, Crowell JA, Muzzio M, et al. Subchronic oral toxicity and cardiovascular safety pharmacology studies of resveratrol, a naturally occurring polyphenol with cancer preventive activity. *Food Chem Toxicol*. (2011) 49:3319–27. doi: 10.1016/j.fct.2011.08.023

26. la Porte C, Voduc N, Zhang G, Seguin I, Tardiff D, Singhal N, et al. Steady-State pharmacokinetics and tolerability of trans-resveratrol 2000 mg twice daily with food, quercetin and alcohol (ethanol) in healthy human subjects. *Clin Pharmacokinet*. (2010) 49:449–54. doi: 10.2165/11531820-000000000-00000

27. Siegel RL, Miller KD, Wagle NS, Jemal A. Cancer statistics, 2023. *CA: Cancer J Clin*. (2023) 73:17–48. doi: 10.3322/caac.21763

28. Xia C, Dong X, Li H, Cao M, Sun D, He S, et al. Cancer statistics in China and United States, 2022: profiles, trends, and determinants. *Chin Med J*. (2022) 135:584–90. doi: 10.1097/cm9.0000000000002108

29. Liang ZJ, Wan Y, Zhu DD, Wang MX, Jiang HM, Huang DL, et al. Resveratrol mediates the apoptosis of triple negative breast cancer cells by reducing POLD1 expression. *Front Oncol*. (2021) 11:569295. doi: 10.3389/fonc.2021.569295

30. Izquierdo-Torres E, Hernandez-Oliveras A, Meneses-Morales I, Rodriguez G, Fuentes-Garcia G, Zarain-Herzberg A. Resveratrol up-regulates ATP2A3 gene expression in breast cancer cell lines through epigenetic mechanisms. *Int J Biochem Cell Biol*. (2019) 113:37–47. doi: 10.1016/j.biocel.2019.05.020

31. Farghadani R, Naidu R. The anticancer mechanism of action of selected polyphenols in triple-negative breast cancer (TNBC). *Biomedicine pharmacotherapy = Biomedecine pharmacotherapie*. (2023) 165:115170. doi: 10.1016/j.biopha.2023.115170

32. Pidíková P, Herichová I. miRNA clusters with up-regulated expression in colorectal cancer. *Cancers*. (2021) 13:2979. doi: 10.3390/cancers13122979

33. Moi L, Braaten T, Al-Shibli K, Lund E, Busund LR. Differential expression of the miR-17-92 cluster and miR-17 family in breast cancer according to tumor type; results from the Norwegian Women and Cancer (NOWAC) study. *J Trans Med*. (2019) 17:334. doi: 10.1186/s12967-019-2086-x

34. Sun K, Chen L, Li Y, Huang B, Yan Q, Wu C, et al. METTL14-dependent maturation of pri-miR-17 regulates mitochondrial homeostasis and induces chemoresistance in colorectal cancer. *Cell Death Dis*. (2023) 14:148. doi: 10.1038/s41419-023-05670-x

35. Zhang Y, Wang S, Lai Q, Fang Y, Wu C, Liu Y, et al. Cancer-associated fibroblasts-derived exosomal miR-17-5p promotes colorectal cancer aggressive phenotype by initiating a RUNX3/MYC/TGF-β1 positive feedback loop. *Cancer Lett*. (2020) 491:22–35. doi: 10.1016/j.canlet.2020.07.023

36. Kim TW, Lee YS, Yun NH, Shin CH, Hong HK, Kim HH, et al. MicroRNA-17-5p regulates EMT by targeting vimentin in colorectal cancer. *Br J cancer*. (2020) 123:1123–30. doi: 10.1038/s41416-020-0940-5

37. Song J, Liu Y, Wang T, Li B, Zhang S. MiR-17-5p promotes cellular proliferation and invasiveness by targeting RUNX3 in gastric cancer. *Biomedicine pharmacotherapy = Biomedecine pharmacotherapie*. (2020) 128:110246. doi: 10.1016/j.biopha.2020.110246

38. Wu J, Zhang XJ, Shi KQ, Chen YP, Ren YF, Song YJ, et al. Hepatitis B surface antigen inhibits MICA and MICB expression via induction of cellular miRNAs in hepatocellular carcinoma cells. *Carcinogenesis*. (2014) 35:155–63. doi: 10.1093/carcin/bgt268

39. Qian M, Geng J, Luo K, Huang Z, Zhang Q, Zhang JA, et al. BCL11B regulates MICA/B-mediated immune response by acting as a competitive endogenous RNA. *Oncogene*. (2020) 39:1514–26. doi: 10.1038/s41388-019-1083-0

40. Mohanty S, Mohapatra P, Shriwas O, Ansari SA, Priyadarshini M, Priyadarsini S, et al. CRISPR-based kinome-screening revealed MINK1 as a druggable player to rewire 5FU-resistance in OSCC through AKT/MDM2/p53 axis. *Oncogene*. (2022) 41:4929–40. doi: 10.1038/s41388-022-02475-8

41. Nicke B, Bastien J, Khanna SJ, Warne PH, Cowling V, Cook SJ, et al. Involvement of MINK, a Ste20 family kinase, in Ras oncogene-induced growth arrest in human ovarian surface epithelial cells. *Mol Cell*. (2005) 20:673–85. doi: 10.1016/j.molcel.2005.10.038

42. Chuang HC, Wang X, Tan TH. MAP4K family kinases in immunity and inflammation. *Adv Immunol*. (2016) 129:277–314. doi: 10.1016/bs.ai.2015.09.006

43. Burgermeister E. Mitogen-activated protein kinase and exploratory nuclear receptor crosstalk in cancer immunotherapy. *Int J Mol Sci*. (2023) 24:14546. doi: 10.3390/ijms241914546

44. Hammouda MB, Ford AE, Liu Y, Zhang JY. The JNK signaling pathway in inflammatory skin disorders and cancer. *Cells*. (2020) 9:857. doi: 10.3390/cells9040857

45. Fan F, Podar K. The role of AP-1 transcription factors in plasma cell biology and multiple myeloma pathophysiology. *Cancers*. (2021) 13:2326. doi: 10.3390/cancers13102326

46. Hasanpourghadi M, Pandurangan AK, Mustafa MR. Modulation of oncogenic transcription factors by bioactive natural products in breast cancer. *Pharmacol Res*. (2018) 128:376–88. doi: 10.1016/j.phrs.2017.09.009

frontiers | Frontiers in Oncology

TYPE Original Research
PUBLISHED 25 March 2025
DOI 10.3389/fonc.2025.1553722

Check for updates

OPEN ACCESS

EDITED BY
Ana Luísa De Sousa-Coelho,
Algarve Biomedical Center Research Institute (ABC-RI), Portugal

REVIEWED BY
Leandro José de Assis,
University of Plymouth, United Kingdom
Krishna Singh,
Johns Hopkins University, United States

*CORRESPONDENCE
Chunyang Li
13775989791@126.com

†These authors have contributed equally to this work

RECEIVED 31 December 2024
ACCEPTED 04 March 2025
PUBLISHED 25 March 2025

CITATION
Xi D, Yang Y, Guo J, Wang M, Yan X and Li C (2025) Single-cell sequencing and spatial transcriptomics reveal the evolution of glucose metabolism in hepatocellular carcinoma and identify G6PD as a potential therapeutic target. *Front. Oncol.* 15:1553722.
doi: 10.3389/fonc.2025.1553722

COPYRIGHT
© 2025 Xi, Yang, Guo, Wang, Yan and Li. This is an open-access article distributed under the terms of the Creative Commons Attribution License (CC BY). The use, distribution or reproduction in other forums is permitted, provided the original author(s) and the copyright owner(s) are credited and that the original publication in this journal is cited, in accordance with accepted academic practice. No use, distribution or reproduction is permitted which does not comply with these terms.

Single-cell sequencing and spatial transcriptomics reveal the evolution of glucose metabolism in hepatocellular carcinoma and identify G6PD as a potential therapeutic target

Deyang Xi[1,2†], Yinshuang Yang[1†], Jiayi Guo[1,2], Mengjiao Wang[1,2], Xuebing Yan[2] and Chunyang Li*[,2]

[1]Graduate School, Xuzhou Medical University, Xuzhou, Jiangsu, China, [2]Department of Infectious Diseases, The Affiliated Hospital of Xuzhou Medical University, Xuzhou, Jiangsu, China

Background: Glucose metabolism reprogramming provides significant insights into the development and progression of malignant tumors. This study aims to explore the temporal-spatial evolution of the glucose metabolism in HCC using single-cell sequencing and spatial transcriptomics (ST), and validates G6PD as a potential therapeutic target for HCC.

Methods: We collected single-cell sequencing data from 7 HCC and adjacent non-cancerous tissues from the GSE149614 database, and ST data from 4 HCC tissues from the HRA000437 database. Pseudotime analysis was performed on the single-cell data, while ST data was used to analyze spatial metabolic activity. High-throughput sequencing and experiments, including wound healing, CCK-8, and transwell assays, were conducted to validate the role and regulatory mechanisms of G6PD in HCC.

Results: Our study identified a progressive upregulation of PPP-related genes during tumorigenesis. ST analysis revealed elevated PPP metabolic scores in the central and intermediate tumor regions compared to the peripheral zones. High-throughput sequencing and experimental validation further suggested that

G6PD-mediated regulation of HCC cell proliferation, migration, and invasion is likely associated with glutathione metabolism and ROS production. Finally, Cox regression analysis cofirmed G6PD as an independent prognostic factor for overall survival in HCC patients.

Conclusion: Our study provides novel insights into the changes in glucose metabolism in HCC from both temporal and spatial perspectives. We experimentally demonstrated that G6PD regulates proliferation, migration, and invasion in HCC and propose G6PD as a prognostic marker and therapeutic metabolic target for the HCC.

KEYWORDS

hepatocellular carcinoma, metabolic reprogramming, carbohydrate metabolism, prognostic biomarker, bioinformatics

Introduction

Hepatocellular carcinoma (HCC) is the most prevalent malignant liver tumor, ranking as the sixth most common cancer and the third leading cause of cancer-related mortality worldwide (1, 2). Over the past few decades, the incidence of HCC has risen, particularly in the Asia-Pacific region and parts of Africa, where there is a high prevalence of hepatitis B and C viruses (3). With improved living standards, liver cancers arising from metabolic liver diseases are also on the rise (4). HCC is highly aggressive, and most patients are diagnosed at an advanced stage with a poor prognosis (5). Although targeted therapies have extended survival times to some extent, their high cost and severe side effects limit their widespread clinical use (6).

Cancer cells adapt their energy metabolism to optimize the rapid consumption and utilization of glucose to support their rapid proliferation and growth needs (7–9). This metabolic mode, known as the Warburg effect, entails a preference for glycolysis over oxidative phosphorylation even in the presence of adequate oxygen, thereby efficiently generating energy to promote tumor growth and survival (10, 11). Through metabolic reprogramming, cancer cells can rapidly synthesize intermediates such as nucleic acids, lipids, and proteins to continually support their proliferation and spread (12). Hence, targeting glucose metabolism—including glycolysis, the pentose phosphate pathway (PPP), and the TCA cycle—is considered an attractive approach to cancer therapy (13).

Reprogramming of glucose metabolism provides a better understanding of the onset and progression of malignancies, further clarifying the complexities of cancer (14, 15). This study aims to explore the evolution of glucose metabolism in HCC through detailed analysis using single-cell RNA sequencing (scRNA-seq) and spatial transcriptomics (ST) and to ascertain the role of G6PD in the malignant transformation of HCC, thereby providing suitable metabolic targets for drug development.

Materials and methods

Single-cell sequencing data acquisition and processing

We retrieved data from the GEO database, specifically dataset GSE149614, which included cancer and adjacent non-tumor tissues from 10 HCC patients. Patients 1 and 2, who only had cancer tissue samples without corresponding adjacent non-tumor tissues, were excluded from the analysis. We utilized the R packages “Seurat” and “SingleR” to analyze the scRNA-seq data (16, 17). Mitochondrial gene expression levels are typically associated with cellular health. When the proportion of mitochondrial genes exceeds 10%, it often indicates that the cell is under stress or undergoing apoptosis (18–20). To ensure the inclusion of high-quality cellular data, cells with gene counts outside the 2% to 98% percentile range and those with mitochondrial gene content exceeding 10% were excluded. Anomalies in patient 7’s cancer tissue, which only contained 489 cells, suggested clinical sample issues, leading to their exclusion. Ultimately, data from 7 cancer tissues and their corresponding adjacent non-tumor tissues were included. We normalized the scRNA-seq data using the “NormalizeData” function in the Seurat R package. The normalized data were then converted into Seurat objects, and the top 5000 variable genes were identified using the “FindVariableFeatures” function. Dimensionality reduction of the scRNA-seq data was performed using the “RunPCA” function for principal component analysis (PCA). To mitigate batch effects between samples, we applied the “harmony” R package. Cell clustering was accomplished using the “FindNeighbors” and “FindClusters” functions with a resolution parameter of 0.5, followed by visualization of the results using the t-SNE method. Cell type annotation was refined using the “SingleR” R package, which predicts cell types based on their correlation with a reference database, continuously eliminating the least correlated types (21).

Pseudotime analysis

We employed the "Monocle2" R package to infer the developmental trajectory of our target cells through gene conversion into reverse graph embedding and dimensionality reduction techniques, arranging cells in a pseudotime sequence (22). To explore the evolutionary differentiation of glucose metabolism in HCC, we extracted a hepatocyte subgroup from all cells and conducted trajectory analysis using "Monocle2." The "DDTree" method was used for dimensionality reduction of these cells. Cell ordering was performed using the "orderCells" function. The results were visually analyzed using the "plot_cell_trajectory" function to understand the dynamic changes in cellular states across the developmental continuum (23, 24).

Acquisition and processing of spatial transcriptomics data

The ST data were sourced from the HRA000437 database (25). During the quality control phase, we eliminated genes expressed in fewer than 5 spots, spots with fewer than 300 detected features, and spots where mitochondrial gene content exceeded 10%. Normalization was performed using the SCTransform method with default parameters in the Seurat R package. Dimensionality reduction and clustering of the data were achieved using the RunPCA, FindNeighbors, FindClusters, and RunUMAP functions in Seurat.

Spatial data visualization was conducted using the "SpatialDimPlot" function, with the center of the tumor serving as the center for spatial plotting of transcriptomics cells. First, we calculated the distance of each cell from the tumor center using the formula (Distance = $\sqrt{(x - x_{center})^2 + (y - y_{center})^2}$), Subsequently, we divided the spatial domain into three regions using tertiles to ensure that each region contained approximately one-third of the cells:

- First region (Central Core): Includes cells from the minimum distance up to the first tertile.
- Second region (Intermediate zones): Spans from the first to the second tertile.
- Third region (Out Periphery): Ranges from the second tertile to the maximum distance.

For quantifying metabolic activity at a single-cell resolution, we employed the "scMetabolism" R package, applying it to measure the metabolic activities across all hepatocytes (26).

Cell transfection

HepG2 and Hep3B cells were cultured in Dulbecco's Modified Eagle's Medium (Gibco, USA) supplemented with 10% fetal bovine serum (Gibco, USA) and 1x penicillin/streptomycin (Biyuntian, China). All cultures were maintained at 37°C in a 5% CO_2 incubator (Thermo Fisher Scientific, USA). Gene knockdown of G6PD was achieved using small interfering RNA (siRNA), specifically si-G6PD#1 and si-G6PD#2. The mRNA levels of G6PD were quantified relative to β-Actin mRNA levels using RT-qPCR and Western Blot (WB) to assess transfection efficiency. For the WB analysis, the membrane strips were initially trimmed and subsequently individually hybridized with antibodies, with four markers retained on each membrane. The full WB image is a composite created after antibody hybridization. Relative gene expression levels were calculated using the 2^-ΔΔCt method. All primers were supplied by Sangon Biotech (Sangon Biotech, China), with sequences listed in Supplementary Table 1. This study was reviewed and approved by the Ethics Committee of the Affiliated Hospital of Xuzhou Medical University (No: XYFY2024-KL283-01).

CCK-8 Assay, wound healing assay, and transwell assay

CCK-8 Assay: 1×10^3 cells were cultured in each well of a 96-well plate. A 1% CCK-8 solution (Meilunbio, China) was added to each well, and the cells were incubated at 37°C in a 5% CO2 incubator for 1 hour to assess cell proliferation. Absorbance at OD450 was measured daily from day 1 to day 7 using a microplate reader (Synergy H1, USA).

Wound healing assay: Cells were cultured in 6-well plates until 95% confluence. A sterile 200 μl plastic pipette tip was used to scratch a straight line in each well. The wells were gently washed twice with PBS to remove unattached cells and debris. Cell migration was observed at 0h and 48h. Images of the scratch wounds were taken at 0 hours and 48 hours using Image J software, and the cell migration rate was calculated (Migration rate= (Width at 48h−Width at 0h)/Width at 48h).

Transwell assay: Treated cells (2×10^5) were seeded into the upper chamber of a 24-well plate and incubated for 48 hours. To assess cell migration and invasion capabilities, the upper surface of the insert was either left uncoated or pre-coated with matrix gel solution (LYNJUNE, China). After removing cells from the surface, the remaining cells on the bottom were fixed with 4% paraformaldehyde and stained with 0.1% crystal violet (VICMED, China).

G6PD knockdown HepG2 Cell Line construction and RNA sequencing

Cells were seeded in 24-well plates for gene knockdown experiments. Using Lipofectamine 2000, recombinant lentivirus particles were transfected into 293T cells to produce lentivirus. The plasmids contained G6PD-specific shRNA (5'-GCCGTGTACACCAAGATGA-3'). HepG2 cells were transfected with lentiviral particles and selected with puromycin to generate

stable cell lines. Total RNA was isolated and purified using TRIzol, and RNA libraries were sequenced on the Illumina NovaseqTM 6000 platform (LC Bio Technology CO., Ltd., Hangzhou, China) according to standard procedures. Differential analysis was performed using DESeq2, and GSEA enrichment analysis was conducted using the "clusterProfiler" R package (27).

NADP/NADPH measurement and ROS detection

NADP/NADPH measurement: NADP/NADPH levels were measured using the BIOSS (AK302) kit. Cells were collected into centrifuge tubes and treated with alkaline/acidic extraction solution. After centrifugation, the supernatant was collected, and absorbance was measured at OD570 nm using a microplate reader (Synergy H1, USA).

ROS Detection: DCFH-DA (Beyotime, China) was diluted in serum-free medium at a 1:1000 ratio to achieve a final concentration of 10 μM. After removing the culture medium from the cells, they were washed with PBS, and then 1.5 mL of the diluted DCFH-DA was added to each well. The cells were incubated at 37°C in a 5% CO2 incubator for 20 minutes. After the incubation, cells were washed three times with serum-free medium, fixed with paraformaldehyde, and the fluorescence intensity was measured using a flow cytometer (FACScanto II*, USA) with an excitation at 488 nm and emission at 525 nm. Analysis was performed using FlowJo software.

Pan-cancer analyses of differential G6PD expression and survival analysis

We collected G6PD mRNA levels and clinical information from tumor and normal tissues across 33 cancer types available in the TCGA database. Differential expression of the gene was analyzed using the 'ggplot2' R package. Bar charts were utilized to display the expression level differences across various cancers.

For survival analysis, univariate Cox regression was conducted using the "survival" and "forestplot" R packages to evaluate the prognostic relevance of G6PD expression with respect to overall survival (OS), disease-specific survival (DSS), progression-free interval (PFI), and disease-free interval (DFI) across different cancer types. Additionally, clinical and transcriptomic data were collected for 319 HCC patients from the TCGA database, 229 HCC patients from the ICGC database, and 177 HCC patients from the GSE14520 database. Both univariate and multivariate Cox regression analyses were performed to identify independent risk factors affecting overall survival in HCC patients.

Statistical analysis

All statistical analyses were conducted using R version 4.3.1. For continuous data, comparisons between two groups were made using either the independent samples t-test or the Mann-Whitney U test. Univariate and multivariate Cox regression analyses were performed using the "survival" R package to identify independent risk factors. The threshold for defining statistical significance was set at $P<0.05$ (*$P < 0.05$, **$P < 0.01$, ***$P < 0.001$; ns: not significant).

Results

Single-cell atlas and intercellular communication analysis

To comprehensively identify the cellular composition and structure of HCC and adjacent non-tumor tissues, we conducted single-cell sequencing analysis on samples from 7 HCC patients. After stringent quality control measures to exclude low-quality cells, a total of 49,324 cells from these tissues for in-depth analysis. Using t-distributed stochastic neighbor embedding (t-SNE) clustering, we organized these cells into 22 distinct clusters (Figure 1A). Cell types within the single-cell atlas were annotated using "SingleR" R package, categorizing the cells into 9 types (Figure 1B) including smooth muscle cells (ACTA2, TAGLN, RGS5), B cells (CD79A, MS4A1, IGHD), dendritic cells (HLA-DPB1, CLEC9A, CD83), NK cells (NKG7, GNLY, GZMB), T cells (CD3D, CD2, CD3E), monocytes (S100A8, AREG, FCN1), hepatocytes (ALB, TTR, TF), endothelial cells (CLEC4G, ENG, PECAM1), and macrophages (CD68, CD163, CD14) (Supplementary Figure 1A). The expression of marker genes in the single-cell map was also displayed (Supplementary Figure 1B). Supplementary Figures 2A, B shows the cellular composition of both HCC and adjacent non-tumor cells from the 7 cases. We noted a higher proportion of macrophages and a reduced proportion of T cells and NK cells in the tumor tissue compared to the adjacent non-tumor tissue.

Pseudotime analysis reveals the evolution of glucose metabolism in HCC

To better explore the evolution of glucose metabolism in hepatocytes, we constructed a pseudotime cell trajectory for 11 clusters of hepatocytes (Figure 1C) and mapped a bifurcated trajectory representing the development from non-malignant to malignant cells (Figure 1D). Cluster 6 (C6), almost exclusively derived from adjacent non-tumor tissue, was identified at the lower right of the trajectory, serving as the initial state's starting point. This trajectory then bifurcated into two distinct cell fates. Through our pseudotime analysis, we identified three different transformation patterns, colored red (gene expression progressively increasing), blue (gene expression progressively decreasing), and pink (gene expression initially increasing then decreasing) (Supplementary Figure 2C).

Enrichment analysis of the biological processes associated with these transformation patterns revealed that the red module was primarily associated with major metabolic processes, including carbohydrate metabolism, fatty acid metabolism, and amino acid metabolism. The blue module was mainly related to immune

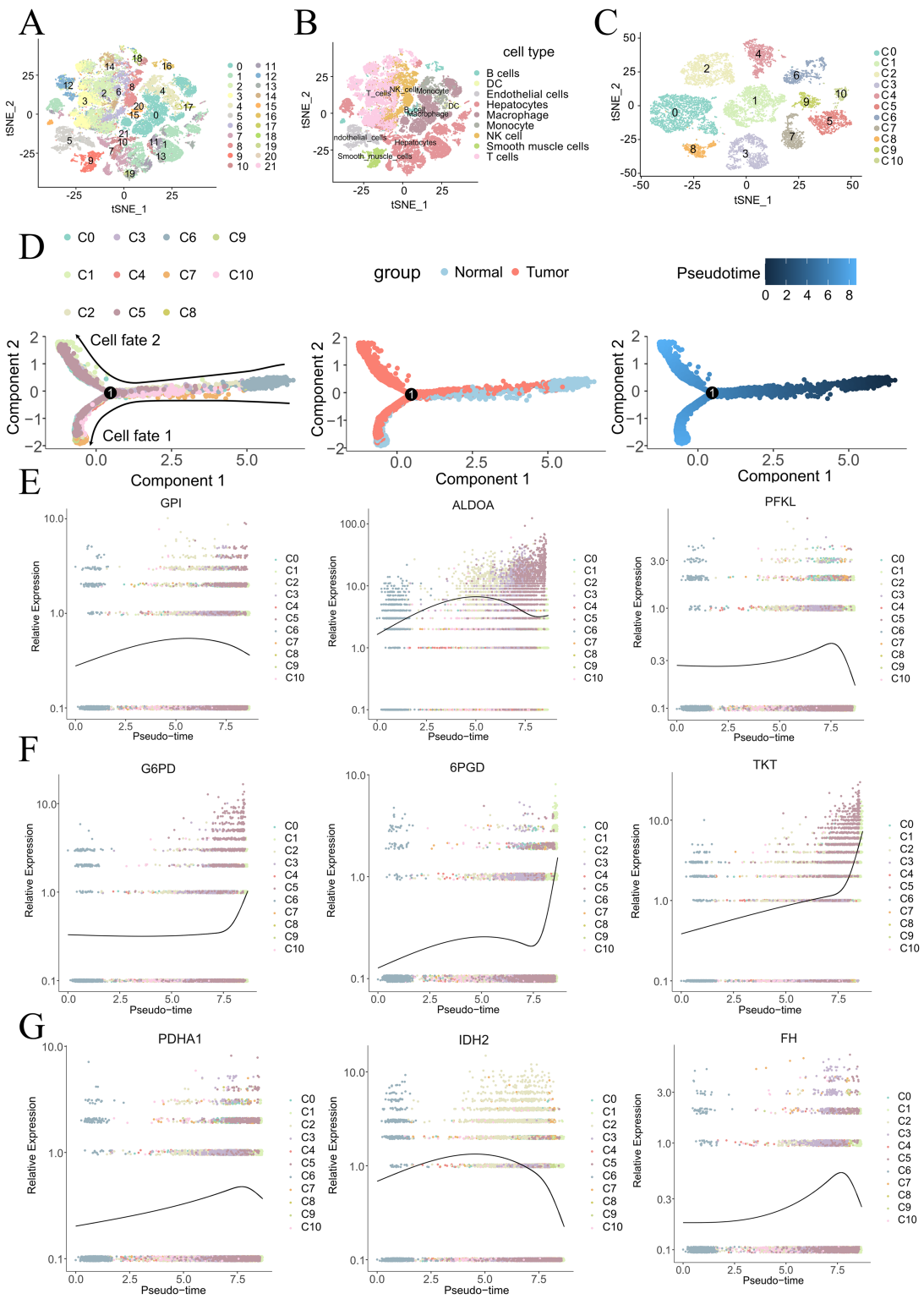

FIGURE 1
Cell atlas and pseudotime analysis of cancerous and adjacent non-tumor tissues in HCC. t-SNE plots depicting 22 cell populations **(A)** and 9 annotated cell types **(B)** from 7 HCC tissues and paired adjacent non-tumor tissues. **(C)** t-SNE plot of 11 re-clustered hepatocyte populations. Pseudotime analysis **(D)** reveals dynamic expression patterns of glycolysis-related genes **(E)**, PPP-related genes **(F)**, and TCA cycle-related genes **(G)**.

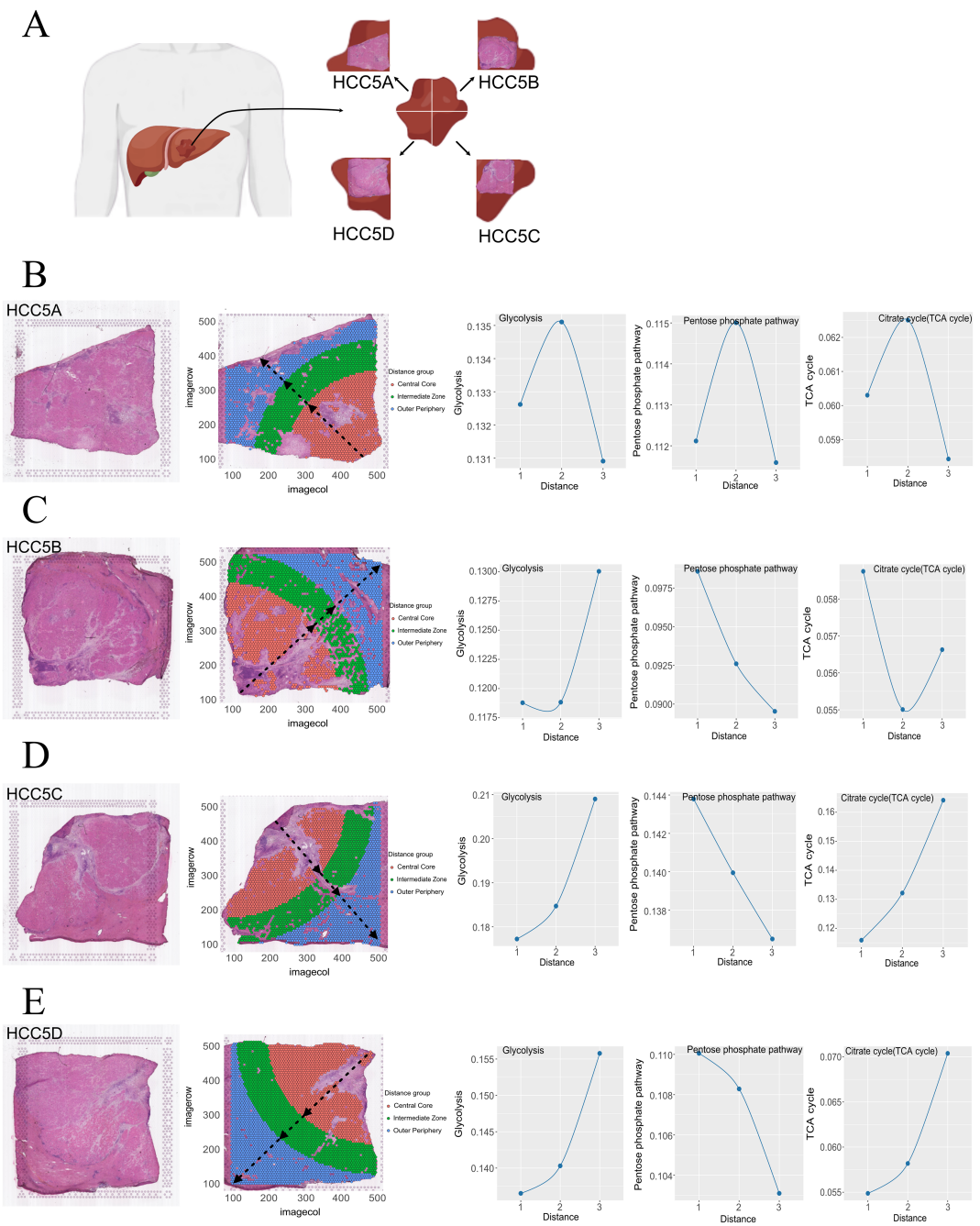

FIGURE 2
HCC section division diagram **(A)**. Spatial partitioning and glucose metabolism evolution in four cases of HCC **(B–E)**.

responses and cell differentiation, while the pink module was associated with protein folding, refolding, and modification.

Mapping glucose metabolism-related genes onto the cell trajectory, we observed trends in the developmental process of the malignancy. Glycolysis-related genes (GPI, ALDOA, PFKL) (Figure 1E) and TCA cycle-related genes (PDHA1, IDH2, FH) (Figure 1F) both showed trends of initially increasing and then decreasing. In contrast, genes related to thePPP (G6PD, 6PGD, TKT) (Figure 1G) exhibited a consistently increasing trend throughout the development of the tumor (28).

Spatial evolution of glucose metabolism in the HCC Microenvironment

Spatial transcriptomics preserves transcriptional data within a spatial context, facilitating the analysis of metabolic pathway activities in localized regions (29). Prior to this study, the spatial dynamics of glucose metabolism within HCC had not been explored. We collected a complete series of tumor sections from HCC patients (HCC5) listed in HRA000437, dividing them into four parts (Figure 2A). After removing stromal cells, the sections were further

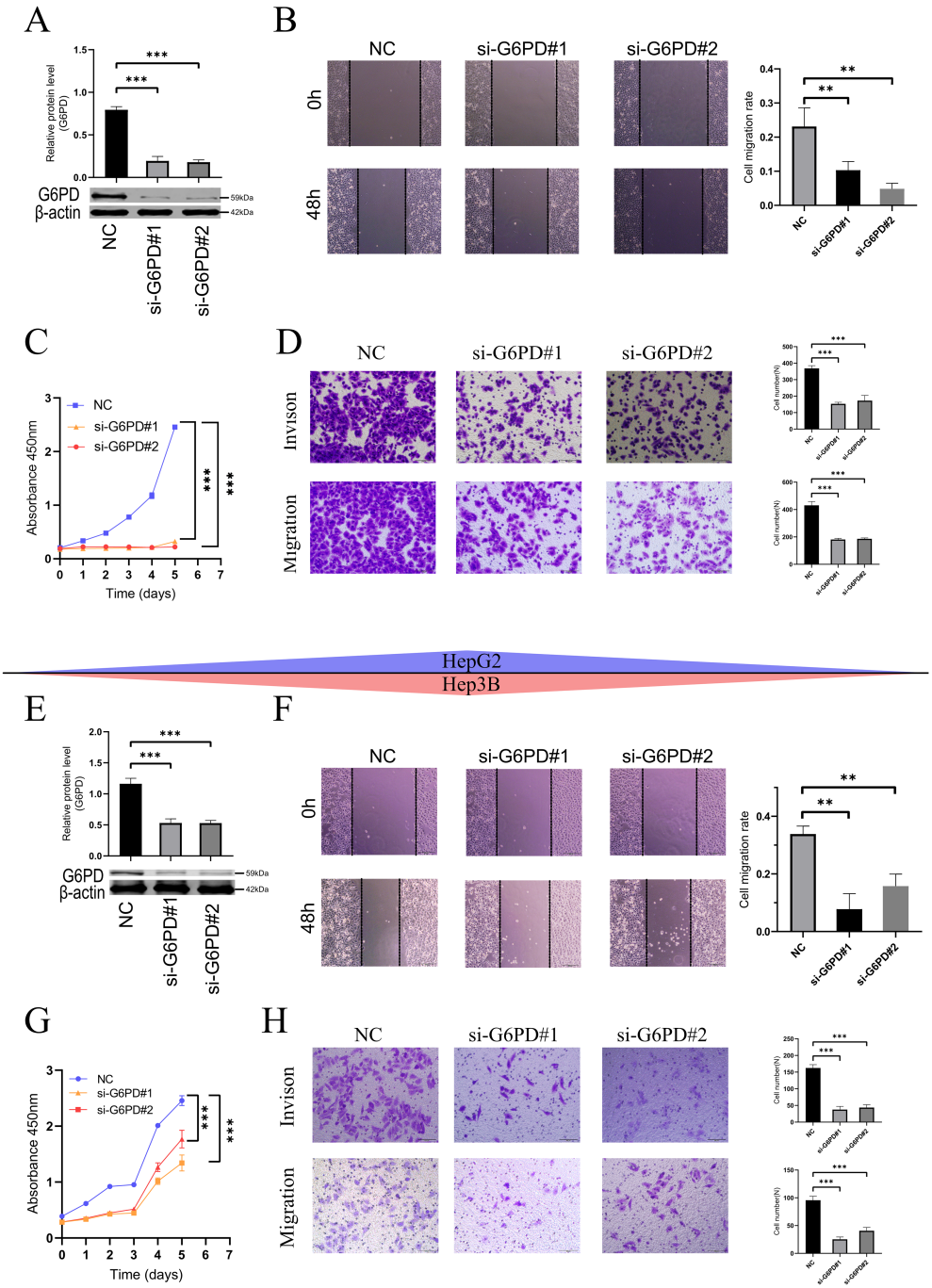

FIGURE 3
Downregulation of G6PD inhibits proliferation, migration, and invasion in HCC cells (HepG2 and Hep3B). **(A, E)** Western blot (Please refer to Supplementary Figure 3b for the detailed WB images) verify the efficiency of G6PD knockdown. **(B, F)** Wound healing assays demonstrate reduced migration rates in HCC cells with lowered G6PD expression. **(C, G)** CCK8 assays indicate that downregulating G6PD inhibits cell proliferation. **(D, H)**. Transwell assays show reduced migration and invasion of HCC cells following G6PD knockdown. (*P < 0.05, **P < 0.01, ***P < 0.001; ns: not significant).

divided into three regions using the tertile method: the central core, intermediate zones, and outer periphery.

Using the scMetabolism tool, we assigned metabolic scores to each cell. For HCC5A (Figure 2B), we observed an initial increase followed by a subsequent decrease in the metabolic activity of glycolysis, the PPP, and the TCA cycle from the central core to the outer periphery. In HCC5B (Figure 2C), glycolysis and TCA cycle metabolic scores showed a trend of initially decreasing and then increasing towards the out periphery, while the PPP activity consistently decreased. For HCC5C and For HCC5C and HCC5D (Figures 2D, E), both glycolysis and TCA cycle activities exhibited an increasing trend, whereas PPP activity consistently decreased from the central core to the outer periphery.

Knockdown of G6PD inhibits proliferation, migration, and invasion in HCC cells

Glucose-6-phosphate dehydrogenase (G6PD) acts as the rate-limiting enzyme in the PPP and plays a crucial role in the development and progression of cancer (30–32). Our study revealed that liver cancer cells (HepG2 and Hep3B) exhibit high endogenous expression of G6PD. Therefore, we constructed G6PD-knockdown HepG2 cells (Figure 3A) and Hep3B cells (Figure 3E, Supplementary Figure 3a).

Wound healing assays (Figures 3B, F) revealed that, following G6PD downregulation, both HepG2 and Hep3B cells exhibited slower migration rates. Consistent with these findings, CCK8 assays (Figures 3C, G) demonstrated that G6PD knockdown significantly inhibited the proliferation of HepG2 and Hep3B HCC cells. Similarly, in Transwell assays (Figures 3D, H), cells with reduced G6PD expression also displayed weaker migration and invasion capabilities.

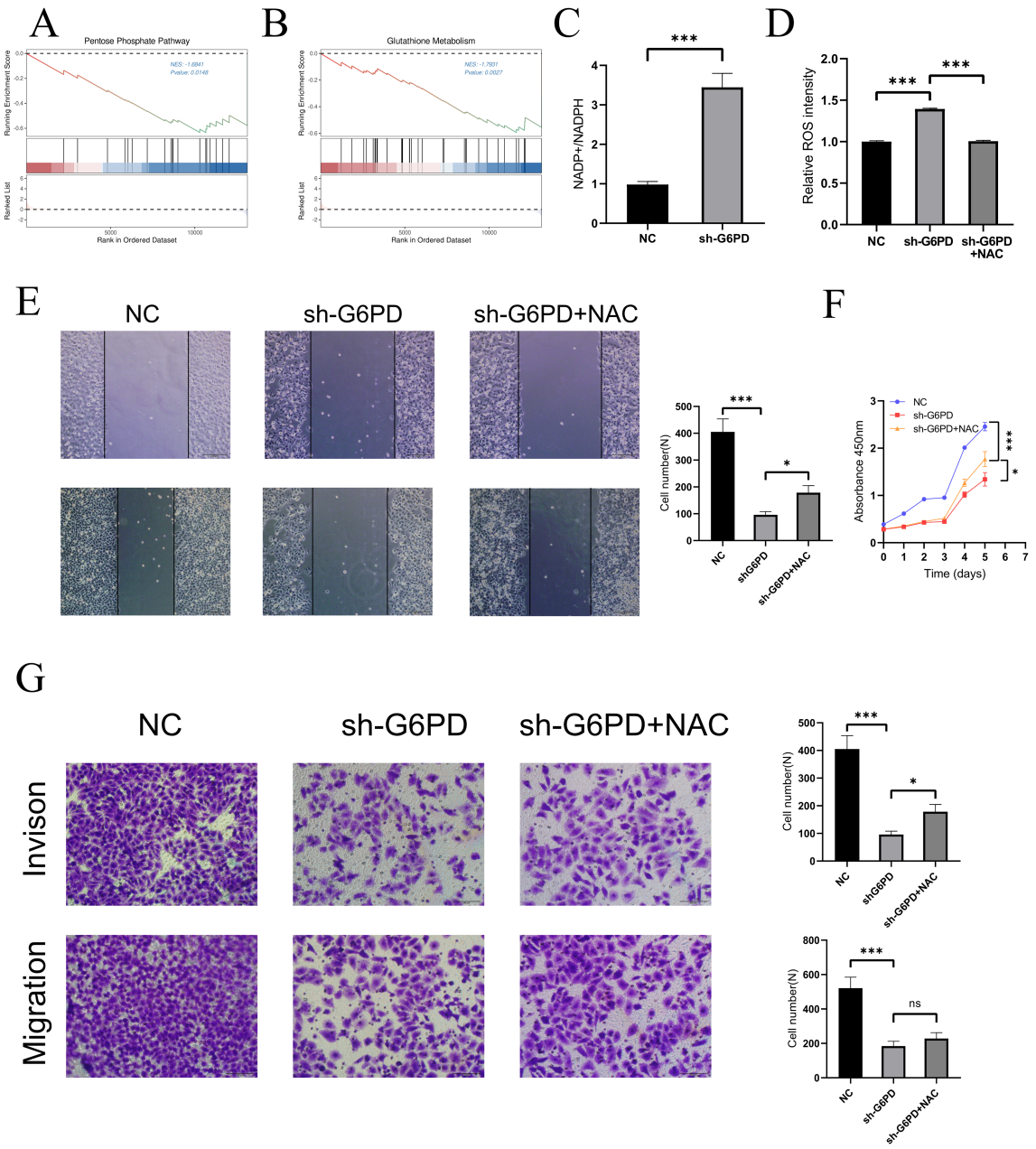

FIGURE 4
Potential mechanisms by which G6PD promotes proliferation and differentiation in HCC cells. **(A, B)** GSEA enrichment analysis revealed the possible mechanism of G6PD regulation of HCC. **(C)** Downregulation of G6PD leads to increased NADP+/NADPH levels within the HCC cells. **(D)** Downregulation of G6PD leads to increased ROS levels in HCC cells, which could be reversed after NAC treatment. Wound healing assays **(E)**, CCK8 assay **(F)** and transwell assay **(G)** confirmed that ROS can partially regulate the proliferation, migration and invasion of hepatocellular carcinoma. (*P < 0.05, **P < 0.01, ***P < 0.001; ns: not significant).

Potential mechanisms by which G6PD promotes malignant progression in HCC

To preliminarily explore the possible mechanisms by which G6PD promotes hepatocellular carcinoma (HCC) cell proliferation and differentiation, transcriptomic sequencing was performed on the constructed shG6PD HepG2 cells. Notably, GSEA enrichment analysis revealed differential metabolism of the pentose phosphate pathway between the two groups (Figure 4A). Additionally, significant differences were observed in glutathione metabolism (Figure 4B). We measured NADP+/NADPH levels between the two groups and found that the NADP+/NADPH ratio was higher in the shG6PD group compared to the NC group (Figure 4C). As NADPH serves as a reducing equivalent and regulates cellular

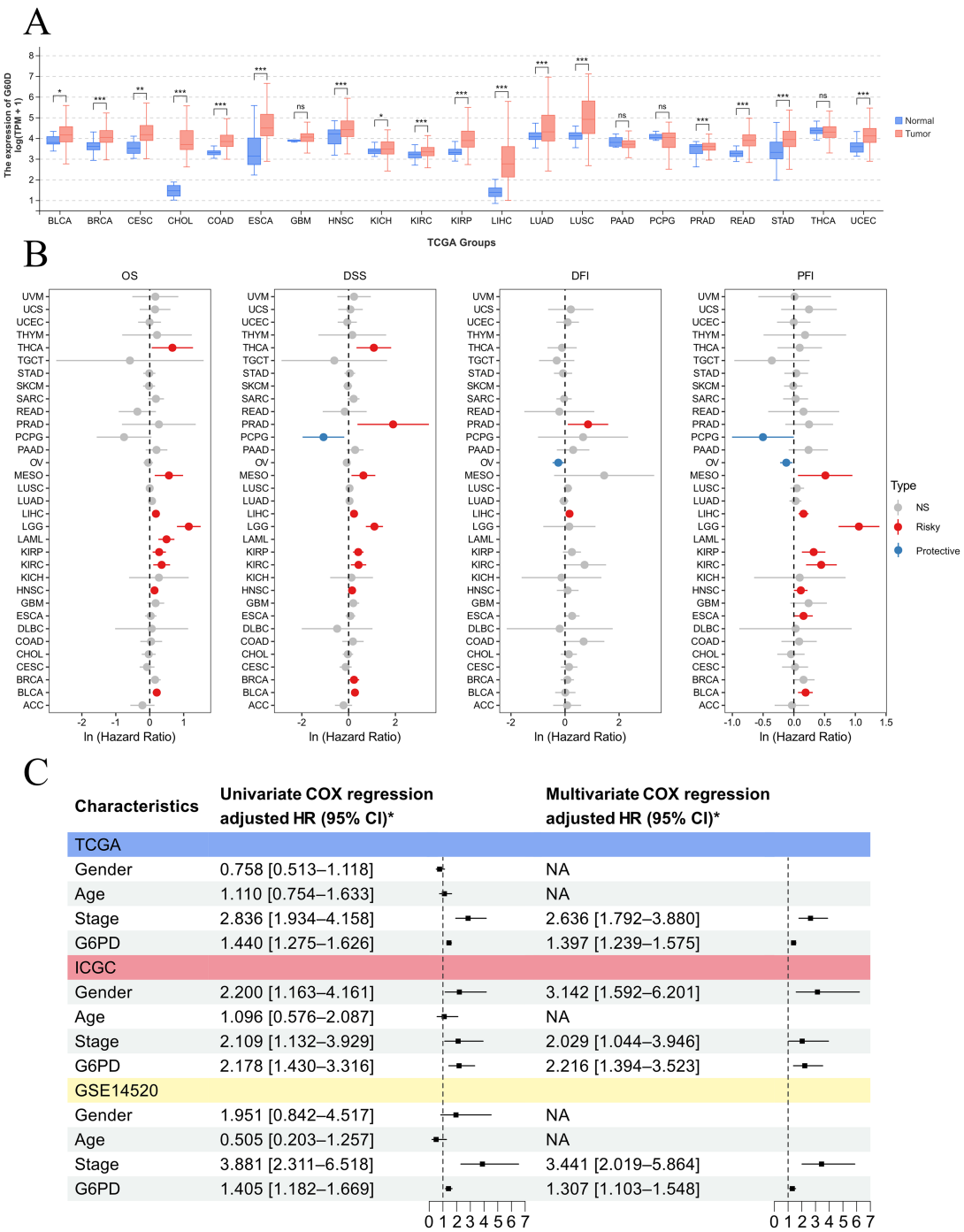

FIGURE 5
Pan-cancer analysis demonstrating that G6PD is a prognostic biomarker across various cancers. **(A)** Differences in G6PD expression between different tumors and adjacent non-tumor tissues. **(B)** Prognostic analysis of G6PD across various cancers. **(C)** Univariate and multivariate Cox regression analyses reveal that G6PD is an independent risk factor for overall survival in HCC.

reactive oxygen species (ROS) stability, we next measured ROS levels and found that downregulation of G6PD led to an increase in ROS in HCC cells (Figure 4D). This increase was normalized after treatment with N-acetylcysteine (NAC,1mM). To further investigate whether ROS affects HepG2 cell proliferation, migration, and invasion, we performed wound healing assays (Figure 4E), which showed slower migration in the shG6PD cells, and migration was restored following NAC treatment. CCK-8 assays (Figure 4F) indicated that shG6PD inhibited HepG2 cell proliferation, which could be partially reversed by NAC treatment. Consistent with the wound healing results, Transwell assays (Figure 4G) showed that shG6PD cells had impaired migration and invasion abilities, and these abilities were partially restored after NAC treatment.

High expression of G6PD correlated with poor prognosis in HCC patients

To explore the specific expression of G6PD in cancer and its clinical implications, we analyzed the differences in G6PD expression levels between tumor tissues and adjacent normal tissues using data from the TCGA database. Our results (Figure 5A) demonstrated that G6PD expression is significantly elevated in multiple cancers, including BLCA, BRCA, CHOL, COAD, ESCA, HNSC, KICH, KIRP, LIHC, LUAD, LUSC, READ, STAD, and UCEC. The abbreviations and full names of tumors can be found in Supplementary Table 2.

Subsequently, we utilized univariate Cox regression analysis to clarify the relationship between G6PD levels and patient prognosis in the TCGA cohort (Figure 5B). We found that G6PD expression is correlated with prognosis across several cancers, identifying G6PD as a risk factor for overall survival (OS), disease-specific survival (DSS), progression-free interval (PFI), and disease-free interval (DFI) in HCC patients. To further validate the correlation between G6PD expression and prognosis in HCC patients, we collected transcriptomic and clinical data from liver cancer patients across three major databases: TCGA, ICGC, and GEO. Through both univariate and multivariate Cox regression analysis, we established that G6PD is an independent risk factor affecting the overall survival (OS) of HCC patients (Figure 5C).

In summary, our study suggests that the rate-limiting enzyme of the PPP, G6PD, regulates NADPH production, which in turn modulates glutathione metabolism and ROS generation. This ultimately promotes tumor cell proliferation, migration, and invasion (Figure 6).

Discussion

In this study, through scRNA-seq and ST, we unveiled the dynamic evolution of glucose metabolism in HCC. We described changes in glycolysis, the PPP, and the TCA cycle from both temporal and spatial perspectives. Temporally, we observed an initial increase followed by a decrease in glycolysis and TCA cycle-related genes, whereas PPP-related genes consistently increased. Spatially, from the core to the periphery, the metabolic activity of glycolysis shows a gradual increase, while the activity of the PPP gradually decreases. The metabolic changes observed in HCC5A are inconsistent with those in the other samples; we suspect this is because HCC5A is composed almost entirely of HCC cells from the core region, with little to no representation of HCC cells from the tumor periphery. Additionally, we confirmed through cellular experiments that G6PD, a key enzyme in the PPP, can regulate the proliferation, migration, and invasion of HCC cells and preliminarily analyzed potential mechanisms by which G6PD facilitates malignant progression in HCC.

Metabolic reprogramming in cancer cells allows for the adjustment of intracellular metabolic pathways and the

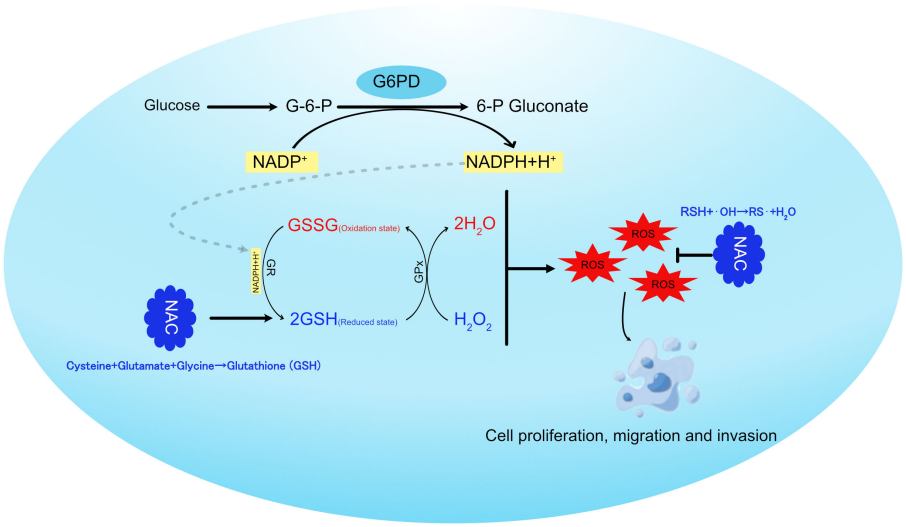

FIGURE 6
Schematic representation of G6PD regulating glutathione metabolism in hepatocellular carcinoma cells.

distribution of metabolic products, thereby modulating cell function and physiological states (33, 34). The growth and proliferation of cancer cells demand substantial energy and resources (35). Reprogramming glucose metabolism helps adjust glucose turnover within cells, enabling more efficient energy production and synthesis of necessary macromolecules, thereby supporting malignant proliferation and differentiation (36–39). Our findings suggest that enhanced glycolysis in tumor cells presents an initial rise followed by a decline, possibly due to several factors: 1. Fast ATP production by glycolysis, which compensates for the inhibited mitochondrial oxidative phosphorylation due to local hypoxia or other factors (40). 2. Intermediate metabolic product accumulation from glycolysis, such as pyruvate, which can be used for lipid synthesis (41). 3. Acidification of the microenvironment by lactate produced through glycolysis, facilitating tumor invasion and immune evasion (42, 43). In the late stages of tumor development, the decline in glycolysis-related gene expression could be linked to extreme environmental stresses (like severe hypoxia or ischemia) or a reduced metabolic state akin to dormancy due to internal or external pressures. We observed a similar phenomenon at the spatial level, where the glycolytic metabolic activity in the tumor core region was less vigorous than in the tumor periphery. This may also be related to the extreme stress environment and the internal and external pressures that lead to tumor cell dormancy.

In clinical research, inhibition of G6PD has emerged as a promising strategy for cancer therapy (44). G6PD is a pivotal enzyme in the glycolytic pathway, primarily producing NADPH via the pentose phosphate pathway (PPP), which is crucial for maintaining cellular redox balance and influencing cellular processes such as growth, differentiation, and apoptosis (45). The upregulation of G6PD is not only associated with the enhanced proliferation, migration, and invasion of tumor cells but also promotes epithelial-mesenchymal transition (EMT) and metastasis through the modulation of cellular redox status (46). Furthermore, G6PD is closely linked to chemotherapy resistance in various cancers, as it aids tumor cells in counteracting oxidative stress and DNA damage induced by chemotherapeutic agents (47). Several small-molecule G6PD inhibitors, such as 6-aminohexose (6-AN) and dehydroepiandrosterone (DHEA), have demonstrated potential to suppress tumor growth (48–50). In experimental settings, DHEA has been shown to enhance the sensitivity of certain tumor cells to conventional chemotherapeutic agents like paclitaxel and doxorubicin, and even to counteract chemotherapy resistance in tumors (50, 51). However, inhibition of G6PD not only impacts tumor cell metabolism but may also have detrimental effects on normal cells. G6PD inhibition results in decreased NADPH levels, thereby weakening the cellular antioxidant capacity and increasing oxidative stress and DNA damage. This effect could lead to damage in normal cells, with particularly pronounced effects on organs such as the liver and bone marrow (52). Currently, there is no consensus regarding the optimal timing and administration methods for G6PD inhibitors in clinical settings. Given the multifaceted role of G6PD in tumor cells, we propose that simple G6PD inhibition may be insufficient to fully suppress tumor growth. However, combining G6PD inhibitors with chemotherapeutic agents could offer a novel treatment strategy for cancer patients. Presently, the administration of G6PD inhibitors has certain drawbacks. For instance, 6-AN and DHEA are typically administered orally; however, their significant side effects and limited targeting capabilities significantly hinder their broad clinical application (53). With the advancement of nanomaterials, strategies involving local delivery or encapsulation of G6PD inhibitors in nanoparticles may allow for targeted delivery to tumor cells, minimizing systemic side effects while enhancing therapeutic efficacy (54). In conclusion, G6PD, as a critical metabolic regulator, is emerging as a novel target for cancer therapy. While clinical research is still in its early stages, the therapeutic opportunities and challenges it presents warrant further exploration.

In our study, the metabolic activity of the PPP consistently increased over time and was more pronounced in the core and intermediate areas of tumors. The PPP, alongside glycolysis, generates ribose-5-phosphate and NADPH, which can reduce excessive ROS in cells, maintaining internal cellular balance and normal growth conditions (55). However, when this balance is disrupted, ROS can promote tumor development by increasing genetic instability, but post-tumor establishment, it can limit cancer cell survival and growth (56, 57). G6PD is the rate-limiting enzyme in the PPP. Studies have shown that PBX3 binds to the G6PD promoter, stimulating the PPP in colorectal cancer and increasing the production of nucleotides and NADPH, thereby promoting the biosynthesis of nucleic acids and lipids while reducing oxidative stress (58). Consistent with our findings, knocking down G6PD significantly inhibited proliferation, migration, and invasion of HepG2 and Hep3B cells, likely linked to the production of ribose-5-phosphate and NADPH (59). NADPH provides the reducing equivalents necessary to convert oxidized glutathione (GSSG) back to its reduced form (GSH), thereby maintaining cellular antioxidant capacity. In turn, GSH plays a crucial role in mitigating the excessive accumulation of ROS (60). Additionally, Min Li et al., through transcriptomic analysis, demonstrated that Aldob directly binds to G6PD and inhibits its activity, thereby suppressing the PPP and exerting a novel tumor-suppressive role in HCC (61). Therefore, G6PD inhibition represents a viable strategy for cancer treatment.

In conclusion, our integrated scRNA-seq and ST analysis revealed the metabolic evolution of glycolysis, PPP, and TCA cycle in HCC cells, confirming G6PD's regulatory role on tumor aggressiveness and its potential as a prognostic marker and therapeutic target in HCC. Nonetheless, our study has inherent limitations: single-cell and spatial transcriptomic data were not from the same patient samples; and while bioinformatics analysis and experimental validations were employed, more extensive experimental validations are needed to corroborate these findings. Although our study utilized two liver cancer cell lines for validation, it still cannot replicate the heterogeneity of liver cancer. Further experimental validation using primary cell cultures is needed. Finally, our study also lacks further *in vivo* exploration, particularly animal studies. Future work will focus on recruiting a

larger cohort of HCC patients and conducting animal studies to overcome these limitations and employ diverse methods to rigorously analyze glucose metabolism alterations in HCC.

Data availability statement

The original contributions presented in the study are included in the article/Supplementary Material. The TCGA dataset was downloaded from the GDC portal (https://portal.gdc.cancer.gov/); The GSE14520 and GSE149614 datasets were downloaded from the GEO database (https://www.ncbi.nlm.nih.gov/geo/query/acc.cgi?acc=GSE14520 and https://www.ncbi.nlm.nih.gov/geo/query/acc.cgi?acc=GSE149614); HRA000437 reported in this article can be acquired from the Genome Sequence Archive (GSA-Human: HRA000437) and is publicly accessible at https://ngdc.cncb.ac.cn/gsa-human/browse/HRA000437. Further inquiries can be directed to the corresponding author(s).

Ethics statement

Ethical approval was not required for the studies on humans in accordance with the local legislation and institutional requirements because only commercially available established cell lines were used.

Author contributions

DX: Conceptualization, Formal Analysis, Methodology, Project administration, Validation, Visualization, Writing – original draft, Writing – review & editing. YY: Data curation, Investigation, Software, Validation, Writing – review & editing. JG: Conceptualization, Methodology, Validation, Writing – original draft. MW: Data curation, Formal Analysis, Validation, Writing – original draft. XY: Funding acquisition, Project administration, Supervision, Writing – review & editing. CL: Investigation, Project administration, Supervision, Visualization, Writing – original draft, Writing – review & editing.

Funding

The author(s) declare that financial support was received for the research and/or publication of this article. This research was funded by Prevention and Treatment of Major Infectious Diseases Such as AIDS and Viral Hepatitis (2018ZX10302206-003-010) and Postgraduate Research Innovation Program of Jiangsu Province (KYCX24_3067).

Conflict of interest

The authors declare that the research was conducted in the absence of any commercial or financial relationships that could be construed as a potential conflict of interest.

Generative AI statement

The author(s) declare that no Generative AI was used in the creation of this manuscript.

Publisher's note

All claims expressed in this article are solely those of the authors and do not necessarily represent those of their affiliated organizations, or those of the publisher, the editors and the reviewers. Any product that may be evaluated in this article, or claim that may be made by its manufacturer, is not guaranteed or endorsed by the publisher.

Supplementary material

The Supplementary Material for this article can be found online at: https://www.frontiersin.org/articles/10.3389/fonc.2025.1553722/full#supplementary-material

References

1. Vogel A, Meyer T, Sapisochin G, Salem R, Saborowski A. Hepatocellular carcinoma. *Lancet*. (2022) 400:1345–62. doi: 10.1016/S0140-6736(22)01200-4

2. Kotsari M, Dimopoulou V, Koskinas J, Armakolas A. Immune system and hepatocellular carcinoma (HCC): new insights into HCC progression. *Int J Mol Sci*. (2023) 24:11471. doi: 10.3390/ijms241411471

3. Kulik L, El-Serag HB. Epidemiology and management of hepatocellular carcinoma. *Gastroenterology*. (2019) 156:477–491.e1. doi: 10.1053/j.gastro.2018.08.065

4. Powell E, Wong VW, Rinella M. Non-alcoholic fatty liver disease. *Lancet*. (2021) 397:2212–24. doi: 10.1016/S0140-6736(20)32511-3

5. Torimura T, Iwamoto H. Treatment and the prognosis of hepatocellular carcinoma in Asia. *Liver Int*. (2022) 42:2042–54. doi: 10.1111/liv.15130

6. Anwanwan D, Singh SK, Singh S, Saikam V, Singh R. Challenges in liver cancer and possible treatment approaches. *Biochim Biophys Acta Rev Cancer*. (2020) 1873:188314. doi: 10.1016/j.bbcan.2019.188314

7. Li Z, Zhang H. Reprogramming of glucose, fatty acid and amino acid metabolism for cancer progression. *Cell Mol Life Sci*. (2016) 73:377–92. doi: 10.1007/s00018-015-2070-4

8. Abdel-Wahab AF, Mahmoud W, Al-Harizy RM. Targeting glucose metabolism to suppress cancer progression: prospective of anti-glycolytic cancer therapy. *Pharmacol Res*. (2019) 150:104511. doi: 10.1016/j.phrs.2019.104511

9. Pavlova NN, Zhu J, Thompson CB. The hallmarks of cancer metabolism: Still emerging. *Cell Metab*. (2022) 34:355–77. doi: 10.1016/j.cmet.2022.01.007

10. Dang CV, Hamaker M, Sun P, Le A, Gao P. Therapeutic targeting of cancer cell metabolism. *J Mol Med (Berl)*. (2011) 89:205–12. doi: 10.1007/s00109-011-0730-x

11. Wang Y, Patti GJ. The Warburg effect: a signature of mitochondrial overload. *Trends Cell Biol*. (2023) 33:1014–20. doi: 10.1016/j.tcb.2023.03.013

12. Faubert B, Solmonson A, DeBerardinis RJ. Metabolic reprogramming and cancer progression. *Science*. (2020) 368:eaaw5473. doi: 10.1126/science.aaw5473

13. Luengo A, Gui DY, Vander Heiden MG. Targeting metabolism for cancer therapy. *Cell Chem Biol*. (2017) 24:1161–80. doi: 10.1016/j.chembiol.2017.08.028

14. Halma MTJ, Tuszynski JA, Marik PE. Cancer metabolism as a therapeutic target and review of interventions. *Nutrients*. (2023) 15:4245. doi: 10.3390/nu15194245

15. Qiu L, Yang Q, Zhao W, Xing Y, Li P, Zhou X, et al. Dysfunction of the energy sensor NFE2L1 triggers uncontrollable AMPK signaling and glucose metabolism reprogramming. *Cell Death Dis*. (2022) 13:501. doi: 10.1038/s41419-022-04917-3

16. Stuart T, Butler A, Hoffman P, Hafemeister C, Papalexi E, Mauck WM 3rd, et al. Comprehensive integration of single-cell data. *Cell*. (2019) 177:1888–1902.e21. doi: 10.1016/j.cell.2019.05.031

17. Aran D, Looney AP, Liu L, Wu E, Fong V, Hsu A, et al. Reference-based analysis of lung single-cell sequencing reveals a transitional profibrotic macrophage. *Nat Immunol*. (2019) 20:163–72. doi: 10.1038/s41590-018-0276-y

18. Zhu H, Chen J, Liu K, Gao L, Wu H, Ma L, et al. Human PBMC scRNA-seq-based aging clocks reveal ribosome to inflammation balance as a single-cell aging hallmark and super longevity. *Sci Adv*. (2023) 9:q7599. doi: 10.1126/sciadv.abq7599

19. Ren X, Wen W, Fan X, Hou W, Su B, Cai P, et al. COVID-19 immune features revealed by a large-scale single-cell transcriptome atlas. *Cell*. (2021) 184:1895–913. doi: 10.1016/j.cell.2021.01.053

20. Zhou Y, Yang D, Yang Q, Lv X, Huang W, Zhou Z, et al. Single-cell RNA landscape of intratumoral heterogeneity and immunosuppressive microenvironment in advanced osteosarcoma. *Nat Commun*. (2020) 11:6322. doi: 10.1038/s41467-020-20059-6

21. Jin S, Guerrero-Juarez CF, Zhang L, Chang I, Ramos R, Kuan CH, et al. Inference and analysis of cell-cell communication using CellChat. *Nat Commun*. (2021) 12:1088. doi: 10.1038/s41467-021-21246-9

22. Trapnell C, Cacchiarelli D, Grimsby J, Pokharel P, Li S, Morse M, et al. The dynamics and regulators of cell fate decisions are revealed by pseudotemporal ordering of single cells. *Nat Biotechnol*. (2014) 32:381–6. doi: 10.1038/nbt.2859

23. Pös O, Radvanszky J, Buglyó G, Pös Z, Rusnakova D, Nagy B, et al. DNA copy number variation: Main characteristics, evolutionary significance, and pathological aspects. *BioMed J*. (2021) 44:548–59. doi: 10.1016/j.bj.2021.02.003

24. Patel AP, Tirosh I, Trombetta JJ, Shalek AK, Gillespie SM, Wakimoto H, et al. Single-cell RNA-seq highlights intratumoral heterogeneity in primary glioblastoma. *Science*. (2014) 344:1396–401. doi: 10.1126/science.1254257

25. Wu R, Guo W, Qiu X, Wang S, Sui C, Lian Q, et al. Comprehensive analysis of spatial architecture in primary liver cancer. *Sci Adv*. (2021) 7:eabg3750. doi: 10.1126/sciadv.abg3750

26. Wu Y, Yang S, Ma J, Chen Z, Song G, Rao D, et al. Spatiotemporal immune landscape of colorectal cancer liver metastasis at single-cell level. *Cancer Discovery*. (2022) 12:134–53. doi: 10.1158/2159-8290.CD-21-0316

27. Yu G, Wang LG, Han Y, He QY. clusterProfiler: an R package for comparing biological themes among gene clusters. *OMICS*. (2012) 16:284–7. doi: 10.1089/omi.2011.0118

28. Du D, Liu C, Qin M, Zhang X, Xi T, Yuan S, et al. Metabolic dysregulation and emerging therapeutical targets for hepatocellular carcinoma. *Acta Pharm Sin B*. (2022) 12:558–80. doi: 10.1016/j.apsb.2021.09.019

29. Yu Q, Jiang M, Wu L. Spatial transcriptomics technology in cancer research. *Front Oncol*. (2022) 12:1019111. doi: 10.3389/fonc.2022.1019111

30. Liu B, Fu X, Du Y, Feng Z, Chen R, Liu X, et al. Pan-cancer analysis of G6PD carcinogenesis in human tumors. *Carcinogenesis*. (2023) 44:525–34. doi: 10.1093/carcin/bgad043

31. Zeng T, Li B, Shu X, Pang J, Wang H, Cai X, et al. Pan-cancer analysis reveals that G6PD is a prognostic biomarker and therapeutic target for a variety of cancers. *Front Oncol*. (2023) 13:1183474. doi: 10.3389/fonc.2023.1183474

32. Li M, He X, Guo W, Yu H, Zhang S, Wang N, et al. Aldolase B suppresses hepatocellular carcinogenesis by inhibiting G6PD and pentose phosphate pathways. *Nat Cancer*. (2020) 1:735–47. doi: 10.1038/s43018-020-0086-7

33. Xia L, Oyang L, Lin J, Tan S, Han Y, Wu N, et al. The cancer metabolic reprogramming and immune response. *Mol Cancer*. (2021) 20:28. doi: 10.1186/s12943-021-01316-8

34. Biswas SK. Metabolic reprogramming of immune cells in cancer progression. *Immunity*. (2015) 43:435–49. doi: 10.1016/j.immuni.2015.09.001

35. Counihan JL, Grossman EA, Nomura DK. Cancer metabolism: current understanding and therapies. *Chem Rev*. (2018) 118:6893–923. doi: 10.1021/acs.chemrev.7b00775

36. Paul S, Ghosh S, Kumar S. Tumor glycolysis, an essential sweet tooth of tumor cells. *Semin Cancer Biol*. (2022) 86:1216–30. doi: 10.1016/j.semcancer.2022.09.007

37. Zhou R, Ni W, Qin C, Zhou Y, Li Y, Huo J, et al. A functional loop between YTH domain family protein YTHDF3 mediated m^6A modification and phosphofructokinase PFKL in glycolysis of hepatocellular carcinoma. *J Exp Clin Cancer Res*. (2022) 41:334. doi: 10.1186/s13046-022-02538-4

38. Yang W, Xia Y, Hawke D, Li X, Liang J, Xing D, et al. PKM2 phosphorylates histone H3 and promotes gene transcription and tumorigenesis. *Cell*. (2014) 158:1210. doi: 10.1016/j.cell.2014.08.003

39. Pan L, Feng F, Wu J, Fan S, Han J, Wang S, et al. Demethylzeylasteral targets lactate by inhibiting histone lactylation to suppress the tumorigenicity of liver cancer stem cells. *Pharmacol Res*. (2022) 181:106270. doi: 10.1016/j.phrs.2022.106270

40. Chelakkot C, Chelakkot VS, Shin Y, Song K. Modulating glycolysis to improve cancer therapy. *Int J Mol Sci*. (2023) 24:2606. doi: 10.3390/ijms24032606

41. Ganapathy-Kanniappan S, Geschwind JF. Tumor glycolysis as a target for cancer therapy: progress and prospects. *Mol Cancer*. (2013) 12:152. doi: 10.1186/1476-4598-12-152

42. Rabinowitz JD, Enerbäck S. Lactate: the ugly duckling of energy metabolism. *Nat Metab*. (2020) 2:566–71. doi: 10.1038/s42255-020-0243-4

43. Zhao Y, Li M, Yao X, Fei Y, Lin Z, Li Z, et al. HCAR1/MCT1 regulates tumor ferroptosis through the lactate-mediated AMPK-SCD1 activity and its therapeutic implications. *Cell Rep*. (2020) 33:108487. doi: 10.1016/j.celrep.2020.108487

44. Li R, Wang W, Yang Y, Gu C. Exploring the role of glucose–6–phosphate dehydrogenase in cancer (Review). *Oncol Rep*. (2020) 44:2325–36. doi: 10.3892/or.2020.7803

45. Ahamed A, Hosea R, Wu S, Kasim V. The emerging roles of the metabolic regulator G6PD in human cancers. *Int J Mol Sci*. (2023) 24:17238. doi: 10.3390/ijms242417238

46. Lu F, Fang D, Li S, Zhong Z, Jiang X, Qi Q, et al. Thioredoxin 1 supports colorectal cancer cell survival and promotes migration and invasion under glucose deprivation through interaction with G6PD. *Int J Biol Sci*. (2022) 18:5539–53. doi: 10.7150/ijbs.71809

47. Li Y, Tang S, Shi X, Lv J, Wu X, Zhang Y, et al. Metabolic classification suggests the GLUT1/ALDOB/G6PD axis as a therapeutic target in chemotherapy-resistant pancreatic cancer. *Cell Rep Med*. (2023) 4:101162. doi: 10.1016/j.xcrm.2023.101162

48. Li Y, Zheng F, Zhang Y, Lin Z, Yang J, Han X, et al. Targeting glucose-6-phosphate dehydrogenase by 6-AN induces ROS-mediated autophagic cell death in breast cancer. *FEBS J*. (2023) 290:763–79. doi: 10.1111/febs.16614

49. Luo M, Fu A, Wu R, Wei N, Song K, Lim S, et al. High expression of G6PD increases doxorubicin resistance in triple negative breast cancer cells by maintaining GSH level. *Int J Biol Sci*. (2022) 18:1120–33. doi: 10.7150/ijbs.65555

50. Chen X, Xu Z, Zhu Z, Chen A, Fu G, Wang Y, et al. Modulation of G6PD affects bladder cancer via ROS accumulation and the AKT pathway *in vitro*. *Int J Oncol*. (2018) 53:1703–12. doi: 10.3892/ijo.2018.4501

51. Lou SJ, Li XH, Zhou XL, Fang DM, Gao F. Palladium-catalyzed synthesis and anticancer activity of paclitaxel-dehydroepiandrosterone hybrids. *ACS Omega*. (2020) 5:5589–600. doi: 10.1021/acsomega.0c00558

52. Song J, Sun H, Zhang S, Shan C. The multiple roles of glucose-6-phosphate dehydrogenase in tumorigenesis and cancer chemoresistance. *Life (Basel)*. (2022) 12:271. doi: 10.3390/life12020271

53. Li M, Dong Y, Wang Z, Zhao Y, Dai Y, Zhang B. Engineering hypoxia-responsive 6-aminonicotinamide prodrugs for on-demand NADPH depletion and redox manipulation. *J Mater Chem B*. (2024) 12:8067–75. doi: 10.1039/d4tb01338g

54. El MS, Garbayo E, Amundarain A, Pascual-Gil S, Carrasco-León A, Prosper F, et al. Lipid nanoparticles for siRNA delivery in cancer treatment. *J Control Release*. (2023) 361:130–46. doi: 10.1016/j.jconrel.2023.07.054

55. TeSlaa T, Ralser M, Fan J, Rabinowitz JD. The pentose phosphate pathway in health and disease. *Nat Metab*. (2023) 5:1275–89. doi: 10.1038/s42255-023-00863-2

56. Wang Y, Qi H, Liu Y, Duan C, Liu X, Xia T, et al. The double-edged roles of ROS in cancer prevention and therapy. *Theranostics*. (2021) 11:4839–57. doi: 10.7150/thno.56747

57. Wang W, Dong X, Liu Y, Ni B, Sai N, You L, et al. Itraconazole exerts anti-liver cancer potential through the Wnt, PI3K/AKT/mTOR, and ROS pathways. *BioMed Pharmacother*. (2020) 131:110661. doi: 10.1016/j.biopha.2020.110661

58. Luo X, Wei M, Li W, Zhao H, Kasim V, Wu S. PBX3 promotes pentose phosphate pathway and colorectal cancer progression by enhancing G6PD expression. *Int J Biol Sci*. (2023) 19:4525–38. doi: 10.7150/ijbs.86279

59. Roy K, Wu Y, Meitzler JL, Juhasz A, Liu H, Jiang G, et al. NADPH oxidases and cancer. *Clin Sci (Lond)*. (2015) 128:863–75. doi: 10.1042/CS20140542

60. Lu M, Lu L, Dong Q, Yu G, Chen J, Qin L, et al. Elevated G6PD expression contributes to migration and invasion of hepatocellular carcinoma cells by inducing epithelial-mesenchymal transition. *Acta Biochim Biophys Sin (Shanghai)*. (2018) 50:370–80. doi: 10.1093/abbs/gmy009

61. Li M, He X, Guo W, Yu H, Zhang S, Wang N, et al. Aldolase B suppresses hepatocellular carcinogenesis by inhibiting G6PD and pentose phosphate pathways. *Nat Cancer*. (2020) 1:735–47. doi: 10.1038/s43018-020-0086-7

frontiers | Frontiers in Medicine

TYPE Original Research
PUBLISHED 03 April 2025
DOI 10.3389/fmed.2025.1541376

Check for updates

OPEN ACCESS

EDITED BY
Alberto Traverso,
San Raffaele Hospital (IRCCS), Italy

REVIEWED BY
Fariba Tohidinezhad,
Maastricht University Medical Centre,
Netherlands
Donato Tiano,
Vita-Salute San Raffaele University, Italy

*CORRESPONDENCE
Dong Xie
✉ dongalex915@163.com

RECEIVED 07 December 2024
ACCEPTED 20 March 2025
PUBLISHED 03 April 2025

CITATION
Xie D, Yu J, He C, Jiang H, Qiu Y, Fu L, Kong L and Xu H (2025) Predicting the immune therapy response of advanced non-small cell lung cancer based on primary tumor and lymph node radiomics features. *Front. Med.* 12:1541376.
doi: 10.3389/fmed.2025.1541376

COPYRIGHT
© 2025 Xie, Yu, He, Jiang, Qiu, Fu, Kong and Xu. This is an open-access article distributed under the terms of the Creative Commons Attribution License (CC BY). The use, distribution or reproduction in other forums is permitted, provided the original author(s) and the copyright owner(s) are credited and that the original publication in this journal is cited, in accordance with accepted academic practice. No use, distribution or reproduction is permitted which does not comply with these terms.

Predicting the immune therapy response of advanced non-small cell lung cancer based on primary tumor and lymph node radiomics features

Dong Xie[1]*, Jinna Yu[1], Cong He[1], Han Jiang[2], Yonggang Qiu[1], Linfeng Fu[1], Lingting Kong[1] and Hongwei Xu[1]

[1]Department of Radiology, Shaoxing Second Hospital Medical Community General Hospital, Shaoxing, China, [2]Department of Medical Oncology, Shaoxing Second Hospital Medical Community General Hospital, Shaoxing, China

Objective: To identify imaging biomarkers of primary tumors and lymph nodes in patients with stage III–IV non-small cell lung cancer (NSCLC) and assess their predictive ability for treatment response (response vs. non-response) to immune checkpoint inhibitors (ICIs) after 6 months.

Methods: Retrospective analysis of 83 NSCLC patients treated with ICIs. Quantitative imaging features of the maximum primary lung tumors and lymph nodes on contrast-enhanced CT imaging were extracted at baseline (time point 0, TP0) and after 2–3 cycles of immunotherapy (time point 1, TP1). Delta-radiomics features (delta-RFs) were defined as the net changes in radiomics features (RFs) between TP0 and TP1. Interobserver interclass coefficient (ICC) and Pearson correlation analyses were applied for feature selection, and logistic regression (LR) was used to build a model for predicting treatment response.

Results: Four and five important delta-RFs were selected to construct the nodal and tumor models, respectively. Δ Tumor diameter was used for constructing the clinical prediction model. The predictive efficacy of the nodal model for the treatment response status was higher than that of the tumor and clinical models. In the training set, the AUC values for the three models were 0.96 (95% CI = 0.90–1.00), 0.86 (95% CI = 0.76–0.95), and 0.82 (95% CI = 0.71–0.93), respectively. In the validation set, the AUC values were 0.94 (95% CI = 0.85–1.00), 0.77 (95% CI = 0.56–0.98), and 0.74 (95% CI = 0.48–1.00), respectively.

Conclusion: The nodal model based on delta-RFs performed well in distinguishing responders from non-responders and could identify patients more likely to benefit from immunotherapy. Finally, the nodal model exhibited a higher classification performance than the tumor model.

KEYWORDS

non-small cell lung cancer, lymph nodes, radiomics, delta, immunity, prediction model

1 Introduction

Non-small cell lung cancer (NSCLC) accounts for 85% of all lung cancers and is the leading cause of cancer-related deaths worldwide (1). Despite recent advancements in lung cancer treatment, the 5-year survival rate of patients with lung cancer remains disappointing at only 15% (2). In recent years, immune checkpoint inhibitors (ICIs) have improved the treatment outcomes of patients with advanced NSCLC without targetable mutations. However, according to published evidence (3), the increase in progression-free survival (PFS) and/or overall survival (OS) is still limited to a small percentage of patients (15–30%). Although the expression of the tumor cell PD-L1 has been widely used as a biomarker for selecting patients for immune therapy (2, 4), the relationship between PD-L1 expression and the efficacy of ICIs treatment remains uncertain.

Radiomics is an emerging field in medical imaging, which can quantify medical imaging data and translate qualitative clinical problems into quantitative ones, thus providing a more objective approach to solving clinical problems (5). Recent studies (6) have shown that non-invasive diagnostic images can describe the phenotype of lung tumors, and their use could be feasible to predict the survival stratification of patients with advanced NSCLC under different treatment methods. In these noninvasive imaging-based prediction or classification models, a radiomics method based on CT images has been developed and applied to establish prognosis prediction models, evaluate the effectiveness and necessity of different treatment methods, and predict early clinical outcomes. More specifically, traditional radiomics methods use baseline medical images for evaluation or prediction and ignore changes in tumors during treatment or follow-up. Alternatively, delta radiomics utilize changes in radiomic features (RFs) during or after treatment to guide clinical decision-making and may be more suitable for evaluating tumor responses to treatment (7, 8).

In locally advanced NSCLC, tumors tend to spread from the primary site to lymph nodes. Pretreatment lymph node staging is closely associated with disease progression and poor prognosis (9). As such, involved lymph nodes may have unique phenotypic characteristics related to the biological processes that affect disease spread, and thus, treatment response. In this study, we hypothesized that the presence of more invasive cancer cells in the metastatic mediastinal/paratracheal lymph nodes may determine prognosis and provide additional valuable information regarding the primary tumors of patients with NSCLC. To prove this, we analyzed the delta-radiomic features (delta-RFs) of the primary tumor and metastatic lymph nodes based on contrast-enhanced CT (CE-CT) scans and further validated these results in an independent cohort.

2 Materials and methods

2.1 Patients

This was a retrospective analysis of patients with NSCLC treated with ICIs at Shaoxing Second Hospital between January 2016 and November 2022. Tumor staging was performed according to the 8th edition of the American Cancer Joint Committee TNM staging criteria (10). All patients were pathologically diagnosed with III–IV NSCLC. This study adhered to the principles of the Declaration of Helsinki and was approved by the hospital's Ethics Committee [Approval No. Ethics Approval (2022018)].

The inclusion criteria were as follows: (1) NSCLC confirmed by histology, (2) first- or later-line treatment with ICIs, and (3) complete baseline demographic data before treatment. The exclusion criteria were as follows: (1) baseline imaging (time point 0, TP0) or follow-up after 2–3 cycles of immunotherapy (time point 1, TP1) without CE-CT, (2) inability to accurately evaluate lesion boundaries on CE-CT images, (3) time interval between baseline imaging and immunotherapy exceeds 4 weeks; and (4) short axis of lymph nodes less than 15 mm.

2.2 CT image acquisition

A 64-slice CT scanner (Siemens SOMATOM Definition AS, Germany) was used to examine the patients who underwent routine respiration training. The scanning parameters were as follows: tube voltage = 120 kV, tube current = 200–300 mA, rotation time = 0.75 s, collimation = 32×1.25 mm, FOV = 360.0–500.0 mm, matrix = 512 × 512, slice thickness and interval = 5.0 mm, contrast agent injection rate = 2.5–3.0 mL/s, and injection volume = 1.1–1.7 mL/kg. After the routine scan, a thin-layer post-processing reconstruction of 0.6–1.5 mm was performed.

2.3 Image analysis

Two radiologists (A and B) with 15 years of experience in chest radiography independently evaluated the images, and the final results were obtained through consultation in cases of disagreement. The observed indicators included the selection of target lesions, target lesion boundaries, and TNM staging. This study evaluated whether the target lesions progressed after 6 months of treatment, based on the Response Evaluation Criteria in Solid Tumors (RECIST, version 1.1) (11).

2.4 Target lesion segmentation

ITK-SNAP software (version 3.6.0, http://www.itksnap.org/) was used for tumor segmentation. Radiologist A manually delineated the region of interest (ROI) for lesions on TP0 and TP1 CE-CT images, as shown in Figure 1I. To ensure reproducibility and accuracy, the radiologists separately segmented the lesion ROIs and extracted the features at TP0 and TP1 from 10 randomly selected patients. Interobserver interclass coefficient (ICC) was used to determine the consistency of these features, with an ICC value greater than 0.75 indicating higher repeatability of the results.

2.5 Image preprocessing and RFs extraction

The PyRadiomics package was used to analyze the segmentation data and isolate phenotypic features from the tumor regions after manual segmentation. To standardize all voxel sizes among the patients, the CT images were resampled to a 2-mm

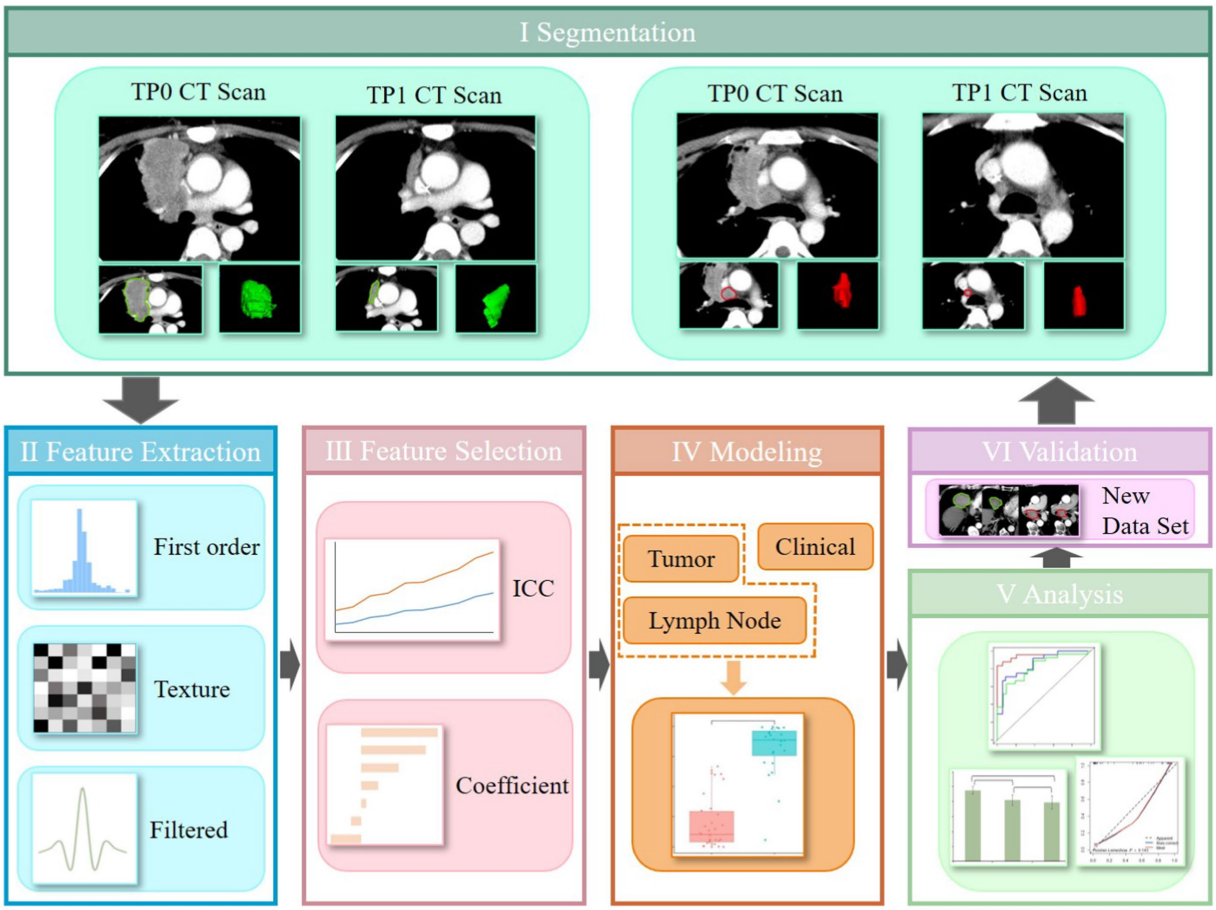

FIGURE 1
The workflow of this study, which mainly composed of six steps: data set, feature extraction, feature selection, model building, analysis, and validation.

resolution in all three directions (Figure 1II). To avoid redundancy with traditional radiological features and highlight texture differences within the target lesions, shape features were excluded from the RFs extraction. A total of 1,050 RFs were extracted for each 3D ROI, including the first-order features, grey-level co-occurrence matrix (GLCM), grey-level run length matrix (GLRLM), grey-level size zone matrix (GLSZM), grey-level dependence matrix (GLDM), and neighborhood grey-tone difference matrix (NGTDM). Delta-RFs were defined as the net change in RFs extracted at TP0 and TP1: Delta-RFs = Feature (TP1) − Feature (TP0). All features were normalized using the *Z*-score in Excel.

2.6 Delta-RFs and clinical features selection

2.6.1 Delta-RFs selection

A five-fold cross-validation method was used to assign training and validation cohorts using the same random seed in all splits to ensure consistency in grouping. Feature selection was performed using ICC and correlation analyses (Figure 1III). First, features with inter-observer instability (ICC <0.75) were excluded. Features with a high correlation (Pearson's correlation coefficient >0.9) were eliminated. The most significant predictive features and their corresponding weight coefficients were selected and the radiomics score (Rad score) for each patient was calculated to build the radiomics model.

2.6.2 Clinical features selection

Clinical feature selection involved statistical tests, multivariate analyses, and stepwise regression to select features associated with the six-month treatment response. These features were used to develop the clinical model.

2.7 Construction of radiomics prediction model

Significant radiomics and clinical features were selected as independent variables, while the six-month treatment response was the dependent variable. Logistic regression (LR) was used to establish a multivariate regression model to predict the treatment response (Figure 1IV). Nodal, tumor, and clinical models were constructed, and the receiver operating characteristic (ROC) curve and area under the curve (AUC) were used to evaluate the predictive performance of the rad-score for immunotherapy efficacy in advanced lung cancer.

2.8 Model comparison and evaluation

The performance of the three classifiers was comprehensively evaluated using ROC curves, AUC, accuracy (ACC), sensitivity (SEN), specificity (SPE), negative predictive value (NPV), and positive predictive value (PPV) (Figure 1V). The DeLong's test was used to compare the ROC curves of the three models. Calibration curves were used to describe the predictive accuracy of the three models. All the models were validated using a validation cohort (Figure 1VI).

2.9 Statistical methods

Data analysis was performed using SPSS (version 26.0) and R (version 4.1.2; https://www.r-project.org/). Continuous data are presented as mean ± standard deviation ($\bar{x} \pm s$) and were analyzed using independent sample *t*-tests. Categorical data are presented as percentages [*n* (%)] and were analyzed using chi-square or Fisher's exact tests. Univariate and multivariate LR analyses were conducted, and the backward stepwise variable elimination method was used to select clinically significant features to build the clinical prediction model. Statistical significance was set at $p < 0.05$.

3 Results

3.1 Population demographics

A total of 83 NSCLC patients were included in this study, including 69 (83.1%) males and 14 (16.9%) females, with an age range of 36 to 85 years, and a median age of 67 years. The demographic and clinicopathological characteristics of the 83 patients are presented in Table 1. Among them, 48 (57.8%) were in the responder group and 35 (42.2%) were in the non-responder group. Fifty-three (54.6%) of all patients received PD-1 ICIs (camrelizumab, sintilimab, tislelizumab or nivolumab) or PD-L1 ICIs (atezolizumab) monotherapy. The remaining 44 (45.4%) patients were treated with the combination of immunotherapies, ICIs in combination with chemotherapeutic agents (gemcitabine + cisplatin, paclitaxel + carboplatin) and/or antiangiogenic agents (mainly bevacizumab, endo, anlotinib, and afatinib). However, there were statistically significant differences in tumor diameter and lymph node diameter between the responder and non-responder groups ($p < 0.05$).

3.2 Delta-RFs selection and model construction

A total of 1,050 delta-RFs were extracted, and four key RFs (nodal model) and five key RFs (tumor model) were selected after ICC and correlation analysis, as shown in Table 2. Based on these features, the LR algorithm was applied to train the delta-RF sets of each lymph node and primary tumor, construct the nodal and tumor models, and convert the output probability scores into delta rad-scores. There were significant differences in the delta rad-scores between the responder and non-responder groups (Figure 2).

3.3 Clinical prediction model establishment

The results of the multivariate LR analysis showed that Δ Tumor diameter was an independent prognostic factor affecting the efficacy of ICIs treatment in patients with NSCLC ($p < 0.05$), as shown in Table 3. A clinical prediction model (clinical model) was established based on the selected independent variables.

3.4 The performance of the nodal model, tumor model, and clinical model

In the training set, the nodal model had the highest AUC of 0.96 (95% CI = 0.90–1.00), significantly higher than the tumor (0.86, 95% CI = 0.76–0.95) (DeLong test, $p < 0.05$) and clinical models (0.82, 95% CI = 0.71–0.93) (DeLong test, $p < 0.05$). The AUC of the tumor model was higher than that of the clinical model (DeLong's test, $p > 0.05$). In the validation set, the AUC of the nodal model (0.94, 95% CI = 0.85–1.00) was higher than the tumor model (0.77, 95% CI = 0.56–0.98) and the clinical model (0.74, 95% CI = 0.48–1.00), but the differences were not statistically significant (DeLong test, $p > 0.05$). Finally, the AUC of the tumor model was higher than that of the clinical model (DeLong's test, $p > 0.05$) (Figure 3). The calibration curve along with the Hosmer–Lemeshow test ($p > 0.05$) demonstrated good consistency between the predictions and observations in the three models (Supplementary Figure 1).

Using the Youden index to determine the cutoff value of the ROC curve, the ACC, SEN, SPE, NPV, and PPV of the nodal, tumor, and clinical models were calculated. The results are summarized in Table 4. Except for SPE and PPV, which were the highest in the clinical model, all other indicators were the highest in the nodal model.

4 Discussion

The data of the SEER (surveillance, epidemiology, and end results) database in the United States in 2018 showed that the overall 5-year survival rate of lung cancer patients was 18.6%, while the 5-year survival rate of advanced lung cancer patients with distant metastases was only 4.7%. With the advent of ICIs, the 5-year survival rate of patients with advanced lung cancer increased to 16% for the first time (12), which became a breakthrough in the treatment of advanced NSCLC. The ICI response of NSCLC patients varies widely among individuals, and the prognosis is influenced by a variety of factors, so it is necessary to find reliable biomarkers to screen the population that may benefit from ICIs (13).

Despite the availability of new treatment methods, patient survival rates remain relatively low (14). Although many clinical and histopathological features, laboratory markers, molecular biomarkers, and genetic markers have been tested for potential prognostic value, few effective and accurate prognostic factors are currently used in clinical practice to manage or predict individual patient prognosis. Clinical trials (15) have shown that lymph node clearance is closely related to patients' overall survival. Lymph nodes are common sites of regional metastases and are crucial for cancer staging. Lymph node phenotypic characteristics contain valuable information that is particularly relevant to patients with advanced NSCLC and can effectively predict clinical endpoints. There is also evidence that lymph

10.3389/fmed.2025.1541376

TABLE 1 Baseline data of the responders and non-responders.

Demographic or clinicopathologic characteristic	Responders (*N* = 48)	Non-responders (*N* = 35)	*p*-value
Gender, No. (%)			0.213
Female	6 (12.5%)	8 (22.9%)	
Male	42 (87.5%)	27 (77.1%)	
Age, [M (Q1, Q3)]	67 (59, 73)	67 (62, 71)	0.969
Tobacco use, No. (%)			0.564
Never smoker	24 (50.0%)	16 (45.7%)	
Current smoker	15 (31.3%)	9 (25.7%)	
Former smoker	9 (18.8%)	10 (28.6%)	
Pathological type, No. (%)			0.329
Squamous cell	35 (72.9%)	22 (62.1%)	
Adenocarcinoma	13 (27.1%)	13 (37.1%)	
Pathologic N stage, No. (%)			0.238
N1	2 (4.2%)	1 (2.9%)	
N2	22 (45.8%)	10 (28.6%)	
N3	24 (50.0%)	24 (68.6%)	
TNM stage, No. (%)			0.622
III	19 (39.6%)	12 (34.3%)	
IV	29 (60.4%)	23 (65.7%)	
Line of treatment, No. (%)			0.098
First line	32 (66.7%)	17 (48.6%)	
Later line	16 (33.3%)	18 (51.4%)	
Treatment strategy, No. (%)			0.309
Monotherapy	22 (45.8%)	20 (57.1%)	
Combination therapy	26 (54.2%)	15 (42.9%)	
Tumor diameter at pre-treatment (mm)	55.3 ± 19.7	58.7 ± 22.1	0.540
Lymph nodal diameter at pre-treatment (mm)	19.5 ± 6.2	20.4 ± 7.0	0.534
Δ Tumor diameter (mm)	−13.4 ± 9.5	0.3 ± 14.1	0.000**
Δ Lymph nodal diameter (mm)	−5.8 ± 5.6	1.6 ± 7.4	0.000**

**$p < 0.001$.

TABLE 2 Results of logistic regression analysis of screened radiomics features.

Models	Screened radiomics features	Odds ratio	OR 95%CI	*p*-value
Node model	wavelet-LLL_glszm_ZoneEntropy	11.113	3.293–37.506	0.000**
	log-sigma-4-0-mm-3D_glszm_ZoneEntropy	10.388	2.865–37.673	0.000**
	log-sigma-4-0-mm-3D_glszm_GrayLevelNonUniformity	1.706	1.265–2.300	0.000**
	log-sigma-3-0-mm-3D_glrlm_RunLengthNonUniformity	1.022	1.010–1.035	0.000**
Tumor model	log-sigma-2-0-mm-3D_glszm_ZoneEntropy	6.507	2.286–18.525	0.000 **
	log-sigma-3-0-mm-3D_glrlm_RunEntropy	5.153	1.953–13.597	0.001*
	log-sigma-4-0-mm-3D_glrlm_LongRunHighGrayLevelEmphasis	1.015	1.007–1.023	0.000**
	log-sigma-4-0-mm-3D_glrlm_LongRunEmphasis	1.023	1.010–1.036	0.001*
	wavelet-LLL_gldm_DependenceNonUniformityNormalized	3.489	1.608–7.570	0.002*

*$p < 0.05$ and **$p < 0.01$. HR, hazard ratio; CI, confidence interval.

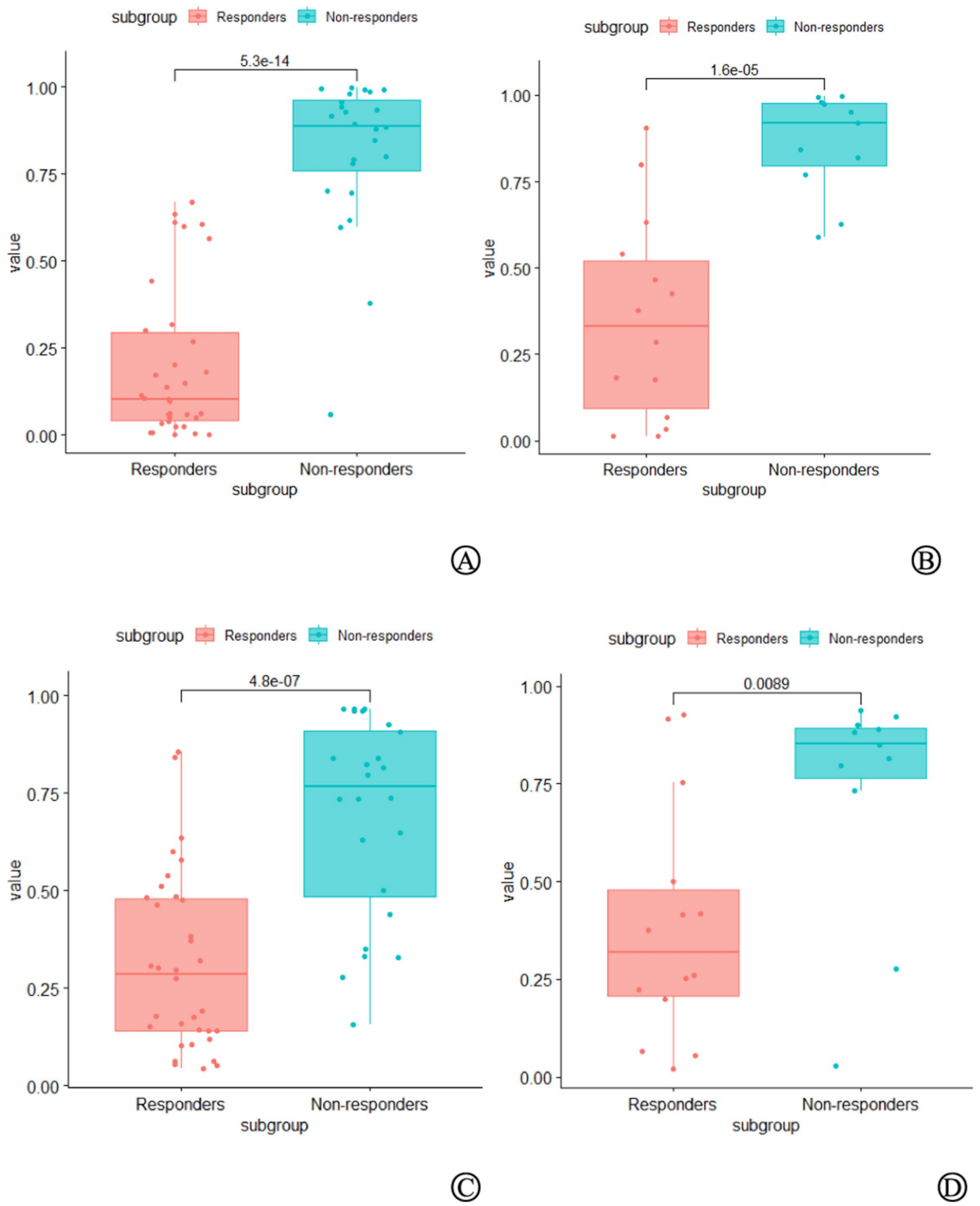

FIGURE 2
Comparison of delta radiomics scores between the non-responders group and the responders group in the training set **(A)** and validation set **(B)** of the nodal model, as well as in the training set **(C)** and validation set **(D)** of the tumor model. In both groups, the delta radiomics scores of the non-responders group were significantly higher than those of the responders group ($p < 0.05$).

node imaging features have a higher prognostic value than primary tumors in patients with lung, head, and neck cancers (16, 17). However, despite extensive research investigating the relationship between primary tumor phenotypes and clinical outcomes, there has been little quantitative analysis of the correlation between NSCLC lymph node characteristics and clinical outcomes. Coroller et al. (17) conducted the first study using quantitative lymph node imaging features to predict tumor response to radiochemotherapy. Carvalho et al. (18) found that common standard uptake value (SUV) descriptors from metastatic lymph nodes were associated with overall patient survival in NSCLC. Furthermore, compared to positron emission tomography (PET) information extracted solely from primary tumors, PET information extracted from metastatic lymph nodes had a higher prognostic value (*C*-index: 0.62 vs. 0.53, 0.56 vs.

TABLE 3 Results of logistic regression analysis of clinical variables in the training set.

Demographic or clinicopathologic characteristic	Odds ratio	OR 95% CI	*p*-value
Gender (male vs. female)	8.900	0.634–124.867	0.105
Age	1.026	0.937–1.125	0.577
Tobacco use never smoker vs. current smoker	0.464	0.051–4.205	0.495
Former smoker	1.636	0.239–11.189	0.616
Pathological type (squamous cell vs. adenocarcinoma)	1.716	0.286–10.313	0.555
Pathologic N stage N1 vs. N2	0.483	0.014–16.939	0.688
N3	2.925	0.114–75.353	0.517
TNM stage (III vs. IV)	0.466	0.059–3.670	0.469
Line of treatment (first line vs. later line)	0.726	0.095–5.581	0.759
Tumor diameter at pre-treatment	1.042	0.999–1.087	0.055
Lymph node diameter at pre-treatment	1.033	0.923–1.156	0.571
Δ Tumor diameter	0.878	0.794–0.970	0.011
Δ Lymph node diameter	0.879	0.765–1.010	0.070

CI, confidence interval.

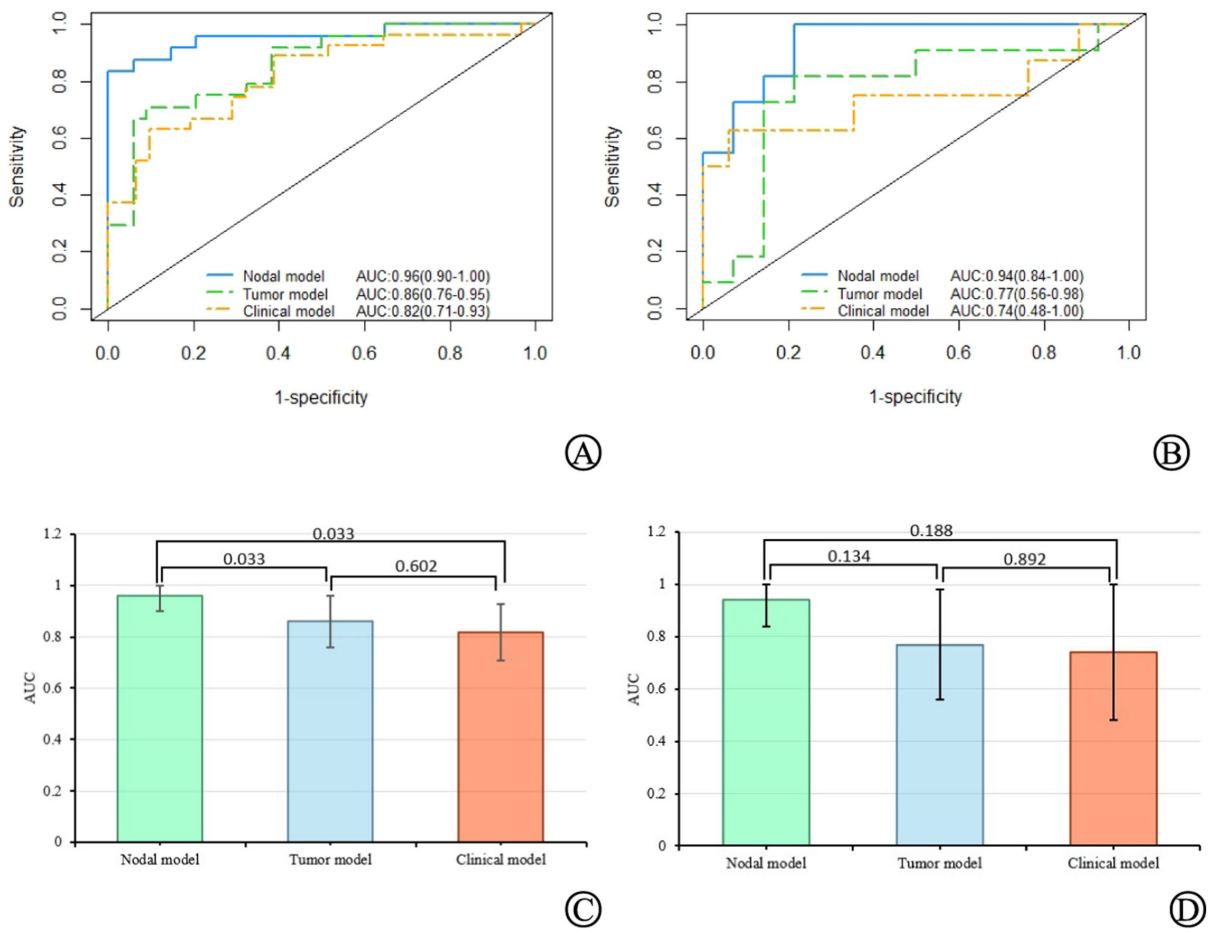

FIGURE 3
The AUC values of the nodal, tumor, and clinical models, as well as their comparisons in the training set **(A,C)** and validation set **(B,D)**.

TABLE 4 Performance metrics of the models.

Model	Training set						Validation set					
	AUC	ACC	SEN	SPE	NPV	PPV	AUC	ACC	SEN	SPE	NPV	PPV
Nodal	0.96	0.86	0.92	0.82	0.93	0.79	0.94	0.84	1.00	0.86	1.00	0.82
Tumor	0.86	0.78	0.75	0.79	0.82	0.72	0.77	0.80	0.82	0.79	0.85	0.75
Clinical	0.82	0.69	0.67	0.71	0.71	0.67	0.74	0.84	0.50	1.00	0.81	1.00

0.54, respectively). Our study is based on the fundamental principle that disease progression and metastatic ability are closely related to the presence of metastatic lymph nodes. We extracted quantitative features related to immunotherapy response from CE-CT images of both primary tumors and affected lymph nodes. We found that the predictive efficacy of the nodal model was superior to that of the tumor model (AUC: 0.96 vs. 0.86, 0.94 vs. 0.77, respectively). Although there was no statistically significant difference in the validation group, the tumor model had a lower 95% CI limit of only 0.56 with a wide interval, indicating that the predictive efficacy of the tumor model was relatively low. The clinical model also exhibited a similarly poor performance, confirming that lymph node radiomic information based on CE-CT scans provides additional prognostic information to that obtained from primary tumors (19). Coroller et al. (17) demonstrated that the optimal radiomics features extracted from metastatic lymph nodes can predict the pathological response after radiochemotherapy in patients with NSCLC, and this performance is higher than that of the optimal radiomics features extracted from primary tumors (AUC: 0.75 vs. 0.61, $p = 0.03$), further confirming the point above.

Moreover, previous radiomics studies have mainly focused on analyzing pretreatment imaging features. In our study, we provided a more comprehensive description of the rich temporal dependence between primary tumors and lymph nodes in pre-treatment and mid-treatment scans. This information can provide insights into treatment-induced changes, dynamically evaluate tumor burden, and better align with the evaluation of immunotherapy efficacy in clinical practice, which is consistent with recent reports (20, 21). In a similar study, Liu et al. (20) extracted delta-RFs from primary lesions and mediastinal metastatic lymph nodes in patients with late-stage NSCLC to predict the response status to ICIs treatment after 6 months. They found that the predictive performance of delta-RFs (AUC: 0.80–0.82) was significantly higher than that of baseline radiomics features (AUC: 0.51–0.59). In the present study, the predictive performance of the delta radiomics model reached a maximum of 0.96. Delta radiomics has been proposed to evaluate the changes that occurred during treatment after time by accessing changes in RFs of different timeline CT scans. Delta-radiomics has greater reproducibility and stability than conventional imaging histology (22). In addition to the fact that delta-RFs have been shown to be effective in differentiating responders from non-responders in advanced non-small cell lung cancer undergoing immunotherapy, delta-RFs have also shown good efficacy in treatment response assessment in patients with metastatic melanoma (23). In a recent study, Fan et al. (24) for the first time assessed tumor response in patients with esophageal squamous cell carcinoma undergoing neoadjuvant chemoradiotherapy based on delta-RFs of CT images. The model based on delta-RFs had higher predictive power than previous studies, especially when combined with clinical factors, further improving the predictive performance with an AUC of 0.963. In the clinical model, Δ Tumor diameter was an independent risk factor for prognosis. This represents the change in the diameter of the primary tumor caused by treatment, indicating that mid-treatment scans can provide important information related to clinical outcomes, supplementing the information provided by pretreatment imaging features.

Owing to the large number of features included in radiomics, we used the ICC and Pearson correlation analysis to select the most critical delta-RFs. Four and five optimal features were selected to construct the nodal and tumor models, respectively. Interestingly, we found that the zone entropy (ZE) of the GLSZM was the highest-weighted delta-RF regardless of the nodal or tumor model. The ZE measures the uncertainty/randomness in the distribution of zone sizes and grey levels, with a higher value indicating greater heterogeneity in the texture patterns. In our cohort, the ZE values were significantly higher in the non-responder group than in the responder group, both in the nodal model and the tumor model. The level of the ZE value may reflect the heterogeneity of the target lesions, with higher ZE values indicating higher heterogeneity of the target lesions, which is more likely to cause drug resistance.

Our study had certain limitations. First, this was a retrospective study based on a single medical center, and our model lacked external validation. Studies have shown that variations in scanning devices, acquisition methods, reconstruction parameters, and scanning protocols may affect the subsequent feature analysis (25, 26). Therefore, we believe that designing prospective trials and standardizing imaging scans for all patients from different research institutions is necessary. Secondly, the sample size of our cohort was relatively small, and the robustness and effectiveness of the model must be validated using larger datasets. Nevertheless, our study included a larger dataset (83 patients) than previous studies on lymph nodes (27, 28) (which included 25 and 43 patients). Third, limited follow-up was conducted in some patients; therefore, PFS and OS analyses were not performed on this dataset. However, due to the advanced stage of the tumors, our follow-up period was sufficient to provide clinically relevant information. Fourth, the included lymph nodes in this study were not confirmed by pathology but were included based on the diagnostic criteria of RECIST 1.1 for pathological lymph nodes (short axis greater than 15 mm). The diagnosis of mediastinal/hilar lymph node metastasis is usually performed through ^{18}F-fluorodeoxyglucose positron-emission tomography/computed tomography (^{18}F-FDG PET/CT), endobronchial ultrasound/endoscopic ultrasound (EBUS/EUS), or mediastinoscopy (29). However, ^{18}F-FDG PET/CT has significant limitations, particularly regarding the uptake of glucose-like FDG in benign inflammatory lymph nodes, which may lead to false-positive results (30). In addition, the low spatial resolution of PET/CT hinders the detection of small metastatic lymph nodes. Invasive examinations are often constrained by the anatomy and are only limited to nodes

accessible through this approach. CE-CT can help reduce the number of invasive surgeries required to confirm lymph node metastasis, thereby reducing the complications associated with invasive procedures. Therefore, CE-CT has a wider potential for clinical applications, does not require additional ionizing radiation, and does not incur significant additional costs. Fifth, in the clinical model of this study, wide confidence intervals were observed. Due to the small sample size, when using 5-fold cross-validation to evaluate model performance, the limited sample size in each fold may not fully represent the overall data, which could affect the stability of the model's performance. In future research, we aim to explore other methods, such as bootstrapping, to increase the diversity of the sample size through repeated sampling, thus mitigating the fluctuations caused by the small sample size.

In conclusion, this study demonstrated that lymph node-based phenotypic features are superior in reflecting the potential sensitivity of patients to immunotherapy than primary tumor sites. This allows for the early detection of patients with a high likelihood of rapid progression to ICIs treatment. Predicting the tumor response early during immunotherapy has potentially significant clinical implications for precision medicine. If the model predicts a poor response to immunotherapy, clinicians can consider pausing or switching the treatment plan, thereby avoiding continued use of potentially ineffective therapy, saving treatment resources, and minimizing side effects. Additionally, the model can help identify patients who require treatment adjustments, such as through combination therapy or changing the immunotherapy approach. Based on the early response predicted by the model, clinicians can develop a personalized management plan for the patient. This may include enhanced monitoring, regular evaluations, and treatment adjustments to ensure the optimal therapeutic outcome.

Data availability statement

The original contributions presented in the study are included in the article/Supplementary material, further inquiries can be directed to the corresponding author.

Ethics statement

The studies involving humans were approved by the Shaoxing Second Hospital Ethics Committee (Approval No. 2022018). The studies were conducted in accordance with the local legislation and institutional requirements. Written informed consent from the patients/participants or patients/participants legal guardian/next of kin was not required to participate in this study in accordance with the national legislation and the institutional requirements.

Author contributions

DX: Conceptualization, Data curation, Funding acquisition, Methodology, Software, Visualization, Writing – original draft, Writing – review & editing. JY: Conceptualization, Formal analysis, Methodology, Writing – review & editing. CH: Data curation, Software, Visualization, Writing – review & editing. HJ: Conceptualization, Data curation, Investigation, Methodology, Writing – review & editing. YQ: Data curation, Software, Visualization, Writing – review & editing. LF: Validation, Writing – review & editing. LK: Validation, Writing – review & editing. HX: Validation, Writing – review & editing.

Funding

The author(s) declare that financial support was received for the research and/or publication of this article. This research was supported by Keqiao District 2022 Self-Financing Science and Technology Plan for Social Development under Grant No. 2022KZ03.

Conflict of interest

The authors declare that the research was conducted in the absence of any commercial or financial relationships that could be construed as a potential conflict of interest.

Publisher's note

All claims expressed in this article are solely those of the authors and do not necessarily represent those of their affiliated organizations, or those of the publisher, the editors and the reviewers. Any product that may be evaluated in this article, or claim that may be made by its manufacturer, is not guaranteed or endorsed by the publisher.

Supplementary material

The Supplementary material for this article can be found online at: https://www.frontiersin.org/articles/10.3389/fmed.2025.1541376/full#supplementary-material

References

1. Sung H, Ferlay J, Siegel RL, Laversanne M, Soerjomataram I, Jemal A, et al. Global cancer statistics 2020: GLOBOCAN estimates of incidence and mortality worldwide for 36 cancers in 185 countries. *CA Cancer J Clin*. (2021) 71:209–49. doi: 10.3322/caac.21660

2. Soo RA, Lim SM, Syn NL, Teng R, Soong R, Mok TSK, et al. Immune checkpoint inhibitors in epidermal growth factor receptor mutant non-small cell lung cancer: current controversies and future directions. *Lung Cancer*. (2018) 115:12–20. doi: 10.1016/j.lungcan.2017.11.009

3. Horn L, Spigel DR, Vokes EE, Holgado E, Ready N, Steins M, et al. Nivolumab versus docetaxel in previously treated patients with advanced non-small-cell lung cancer: two-year outcomes from two randomized, open-label, phase III trials (check mate 017 and check mate 057). *J Clin Oncol*. (2017) 35:3924–33. doi: 10.1200/JCO.2017.74.3062

4. Herbst RS, Baas P, Kim DW, Felip E, Pérez-Gracia JL, Han JY, et al. Pembrolizumab versus docetaxel for previously treated, PD-L1-positive, advanced non-small-cell lung

cancer (KEYNOTE-010): a randomised controlled trial. *Lancet*. (2016) 387:1540–50. doi: 10.1016/S0140-6736(15)01281-7

5. Gillies RJ, Kinahan PE, Hricak H. Radiomics: images are more than pictures, they are data. *Radiology*. (2016) 278:563–77. doi: 10.1148/radiol.2015151169

6. Liu C, Gong J, Yu H, Liu Q, Wang S, Wang J. A CT-based radiomics approach to predict nivolumab response in advanced non-small-cell lung cancer. *Front Oncol*. (2021) 11:544339. doi: 10.3389/fonc.2021.544339

7. Khorrami M, Prasanna P, Gupta A, Patil P, Velu PD, Thawani R, et al. Changes in CT radiomic features associated with lymphocyte distribution predict overall survival and response to immunotherapy in non-small cell lung cancer. *Cancer Immunol Res*. (2020) 8:108–19. doi: 10.1158/2326-6066.CIR-19-0476

8. Bera K, Velcheti V, Madabhushi A. Novel quantitative imaging for predicting response to therapy: techniques and clinical applications. *Am Soc Clin Oncol Educ Book*. (2018) 38:1008–18. doi: 10.1200/EDBK_199747

9. Fried DV, Mawlawi O, Zhang L, Fave X, Zhou S, Ibbott G, et al. Stage III non-small cell lung cancer: prognostic value of FDG PET quantitative imaging features combined with clinical prognostic factors. *Radiology*. (2016) 278:214–22. doi: 10.1148/radiol.2015142920

10. Borghaei H, Paz-Ares L, Horn L, Spigel DR, Steins M, Ready NE, et al. Nivolumab versus docetaxel in advanced nonsquamous non-small-cell lung cancer. *N Engl J Med*. (2015) 373:1627–39. doi: 10.1056/NEJMoa1507643

11. Rittmeyer A, Barlesi F, Waterkamp D, Park K, Ciardiello F, von Pawel J, et al. Atezolizumab versus docetaxel in patients with previously treated non-small-cell lung cancer (OAK): a phase 3, open-label, multicentre randomised controlled trial. *Lancet*. (2017) 389:255–65. doi: 10.1016/S0140-6736(16)32517-X

12. Gettinger S, Horn L, Jackman D, Spigel D, Antonia S, Hellmann M, et al. Five-year follow-up of nivolumab in previously treated advanced non-small-cell lung cancer: results from the CA209-003 study. *J Clin Oncol*. (2018) 36:1675–84. doi: 10.1200/JCO.2017.77.0412

13. Abbas E, Fanni SC, Bandini C, Francischello R, Febi M, Aghakhanyan G, et al. Delta-radiomics in cancer immunotherapy response prediction: a systematic review. *Eur J Radiol Open*. (2023) 11:100511. doi: 10.1016/j.ejro.2023.100511

14. Siegel RL, Miller KD, Jemal A. Cancer statistics, 2020. *CA Cancer J Clin*. (2020) 70:7–30. doi: 10.3322/caac.21590

15. Suntharalingam M, Paulus R, Edelman MJ, Krasna M, Burrows W, Gore E, et al. Radiation therapy oncology group protocol 02-29: a phase II trial of neoadjuvant therapy with concurrent chemotherapy and full-dose radiation therapy followed by surgical resection and consolidative therapy for locally advanced non-small cell carcinoma of the lung. *Int J Radiat Oncol Biol Phys*. (2012) 84:456–63. doi: 10.1016/j.ijrobp.2011.11.069

16. Wu J, Gensheimer MF, Zhang N, Han F, Liang R, Qian Y, et al. Integrating tumor and nodal imaging characteristics at baseline and mid-treatment computed tomography scans to predict distant metastasis in oropharyngeal cancer treated with concurrent chemoradiotherapy. *Int J Radiat Oncol Biol Phys*. (2019) 104:942–52. doi: 10.1016/j.ijrobp.2019.03.036

17. Coroller TP, Agrawal V, Huynh E, Narayan V, Lee SW, Mak RH, et al. Radiomic-based pathological response prediction from primary tumors and lymph nodes in NSCLC. *J Thorac Oncol*. (2017) 12:467–76. doi: 10.1016/j.jtho.2016.11.2226

18. Carvalho S, Leijenaar RTH, Troost EGC, van Timmeren JE, Oberije C, van Elmpt W, et al. ^{18}F-fluorodeoxyglucose positron-emission tomography (FDG-PET)-radiomics of metastatic lymph nodes and primary tumor in non-small cell lung cancer (NSCLC)—a prospective externally validated study. *PLoS One*. (2018) 13:e192859. doi: 10.1371/journal.pone.0192859

19. Paesmans M, Garcia C, Wong CY, Patz EF Jr, Komaki R, Eschmann S, et al. Primary tumour standardised uptake value is prognostic in nonsmall cell lung cancer: a multivariate pooled analysis of individual data. *Eur Respir J*. (2015) 46:1751–61. doi: 10.1183/13993003.00099-2015

20. Liu Y, Wu M, Zhang Y, Luo Y, He S, Wang Y, et al. Imaging biomarkers to predict and evaluate the effectiveness of immunotherapy in advanced non-small-cell lung cancer. *Front Oncol*. (2021) 11:657615. doi: 10.3389/fonc.2021.657615

21. Lin P, Yang PF, Chen S, Shao YY, Xu L, Wu Y, et al. A delta-radiomics model for preoperative evaluation of neoadjuvant chemotherapy response in high-grade osteosarcoma. *Cancer Imaging*. (2020) 20:7. doi: 10.1186/s40644-019-0283-8

22. Nardone V, Reginelli A, Guida C, Belfiore MP, Biondi M, Mormile M, et al. Delta-radiomics increases multicentre reproducibility: a phantom study. *Med Oncol*. (2020) 37:38. doi: 10.1007/s12032-020-01359-9

23. Guerrisi A, Russillo M, Loi E, Ganeshan B, Ungania S, Desiderio F, et al. Exploring CT texture parameters as predictive and response imaging biomarkers of survival in patients with metastatic melanoma treated with PD-1 inhibitor nivolumab: a pilot study using a delta-radiomics approach. *Front Oncol*. (2021) 11:704607. doi: 10.3389/fonc.2021.704607

24. Fan L, Yang Z, Chang M, Chen Z, Wen Q. CT-based delta-radiomics nomogram to predict pathological complete response after neoadjuvant chemoradiotherapy in esophageal squamous cell carcinoma patients. *J Transl Med*. (2024) 22:579. doi: 10.1186/s12967-024-05392-4

25. Midya A, Chakraborty J, Gönen M, Do RKG, Simpson AL. Influence of CT acquisition and reconstruction parameters on radiomic feature reproducibility. *J Med Imaging*. (2018) 5:11020. doi: 10.1117/1.JMI.5.1.011020

26. Huynh E, Coroller TP, Narayan V, Agrawal V, Romano J, Franco I, et al. Associations of radiomic data extracted from static and respiratory-gated CT scans with disease recurrence in lung cancer patients treated with SBRT. *PLoS One*. (2017) 12:e169172. doi: 10.1371/journal.pone.0169172

27. Bayanati H, Thornhill RE, Souza CA, Sethi-Virmani V, Gupta A, Maziak D, et al. Quantitative CT texture and shape analysis: can it differentiate benign and malignant mediastinal lymph nodes in patients with primary lung cancer? *Eur Radiol*. (2015) 25:480–7. doi: 10.1007/s00330-014-3420-6

28. Li H, Becker N, Raman S, Chan TCY, Bissonnette JP. The value of nodal information in predicting lung cancer relapse using 4DPET/4DCT. *Med Phys*. (2015) 42:4727–33. doi: 10.1118/1.4926755

29. Grootjans W, de Geus-Oei LF, Troost EG, Visser EP, Oyen WJ, Bussink J. PET in the management of locally advanced and metastatic NSCLC. *Nat Rev Clin Oncol*. (2015) 12:395–407. doi: 10.1038/nrclinonc.2015.75

30. Flechsig P, Kratochwil C, Schwartz LH, Rath D, Moltz J, Antoch G, et al. Quantitative volumetric CT-histogram analysis in N-staging of ^{18}F-FDG-equivocal patients with lung cancer. *J Nucl Med*. (2014) 55:559–64. doi: 10.2967/jnumed.113.128504

frontiers | Frontiers in Immunology

TYPE Review
PUBLISHED 08 April 2025
DOI 10.3389/fimmu.2025.1563725

Check for updates

OPEN ACCESS

EDITED BY
Andrés Méndez Lucas,
University of Barcelona, Spain

REVIEWED BY
Paula Dobosz,
Poznan University of Medical Sciences, Poland
Nikita Kotlov,
BostonGene, Inc., United States

*CORRESPONDENCE
Wence Zhou
zhouwc129@163.com

†These authors have contributed equally to this work and share co-first authorship

RECEIVED 20 January 2025
ACCEPTED 17 March 2025
PUBLISHED 08 April 2025

CITATION
Fan Z, Xiao Y, Du Y, Zhang Y and Zhou W (2025) Pancreatic cancer subtyping - the keystone of precision treatment.
Front. Immunol. 16:1563725.
doi: 10.3389/fimmu.2025.1563725

COPYRIGHT
© 2025 Fan, Xiao, Du, Zhang and Zhou. This is an open-access article distributed under the terms of the Creative Commons Attribution License (CC BY). The use, distribution or reproduction in other forums is permitted, provided the original author(s) and the copyright owner(s) are credited and that the original publication in this journal is cited, in accordance with accepted academic practice. No use, distribution or reproduction is permitted which does not comply with these terms.

Pancreatic cancer subtyping - the keystone of precision treatment

Zeyang Fan[1†], Yao Xiao[1†], Yan Du[1], Yan Zhang[1] and Wence Zhou[2*]

[1]The Second Clinical Medical School, Lanzhou University, Lanzhou, China, [2]Department of General Surgery , The Second Hospital of Lanzhou University & The Second Clinical Medical School, Lanzhou University, Lanzhou, China

In recent years, the incidence and mortality rates of pancreatic cancer have been rising, posing a severe threat to human health. Tumor heterogeneity remains a critical barrier to advancing diagnosis and treatment efforts. The lack of specific early symptoms, limited early diagnostic methods, high biological complexity, and restricted therapeutic options contribute to the poor outcomes and prognosis of pancreatic cancer. Therefore, there is an urgent need to explore the different subtypes in-depth and develop personalized therapeutic strategies tailored to each subtype. Increasing evidence highlights the pivotal role of molecular subtyping in treating pancreatic cancer. This review focuses on recent advancements in classifying molecular subtypes and therapeutic approaches, discussed from the perspectives of gene mutations, genomics, transcriptomics, proteomics, metabolomics, and immunomics.

KEYWORDS

pancreatic cancer, subtypes, genomics, transcriptomics, proteomics, metabolomics, immunomics

1 Introduction

Recent epidemiological data indicate that pancreatic cancer is a highly lethal disease, with a 5-year survival rate of approximately 13% at diagnosis, and it is gradually becoming one of the most common causes of cancer-related death (1). Pancreatic cancer causes over 400,000 deaths annually and has already become the third leading cause of cancer-related deaths worldwide (1). By 2030, it is projected to become the second leading cause of cancer-related mortality (2). Among pancreatic cancers, pancreatic ductal adenocarcinoma (PDAC) accounts for approximately 90% of cases (3).

The clinical management of pancreatic cancer currently relies on a four-tier staging system (resectable, borderline resectable, locally advanced, and metastatic) (4, 5). Apart from surgical resection combined with chemotherapy, no other approaches have been shown to significantly prolong patient survival (6). In fact, only 10%-15% of patients present with resectable disease at the time of diagnosis (5). Even among patients who undergo surgical treatment, the 5-year survival rate is only 20% (4), and 69%-75% of these

patients eventually experience recurrence within two years, while 80%-90% relapse within five years (7). Despite advances in multidisciplinary treatment strategies, pancreatic cancer remains a systemic disease with no substantial improvement in prognosis (8).

Currently, two main factors contribute to the poor prognosis of PDAC. The first is the structural characteristics of PDAC itself: its complex tumor composition and architecture create a hypoxic microenvironment while isolating the tumor mass from external interactions, leading to drug resistance. The second factor is the intrinsic heterogeneity of pancreatic cancer, which includes intertumoral and intratumoral structural heterogeneity, molecular heterogeneity, subtype interconversion, and subtype transitions during disease progression (9). Therefore, addressing tumor heterogeneity to develop personalized treatments for individual patients has become a major focus of current research. This approach has already been validated in other solid tumors, such as targeting human epidermal growth factor receptor-2 (*HER2*) to treat *HER2*-overexpressing breast cancer. However, molecular subtyping of pancreatic cancer remains in its infancy, and clinically actionable subtypes for guiding therapeutic decisions have yet to be defined (5, 10).

Translating the latest advances in the molecular characteristics of pancreatic cancer into targeted therapies is an active area of ongoing research (4). In the coming years, the development of drugs designed to target specific molecular subtypes and associated pathways of pancreatic cancer is expected to make significant contributions to personalized and subtype-specific treatments. These novel drugs may be used in combination with certain first-line therapies to reduce mortality, extend overall survival (OS), and potentially address resistance to some first-line treatments. Subtyping pancreatic cancer based on different criteria holds potential clinical applications, as precision therapy focuses on distinguishing specific groups of patients with unique characteristics and treating them by targeting their specific molecular targets (10).

Currently, the classification criteria for pancreatic cancer subtypes are highly diverse. This review aims to summarize and discuss the most recent and influential subtyping strategies from multiple perspectives, including gene mutations, genomics, transcriptomics, proteomics, metabolomics, and immunomics (Figure 1, Table 1). Additionally, it provides a more comprehensive discussion of metabolomics and immunomics, which have been relatively underexplored in previous reviews.

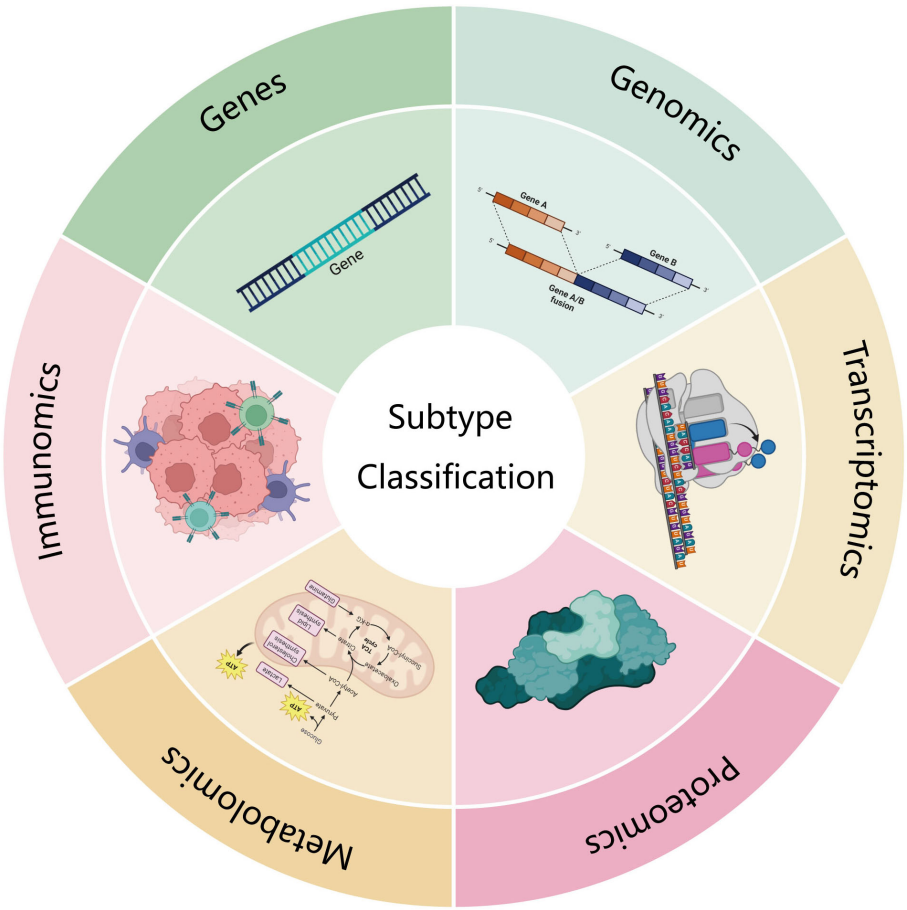

FIGURE 1
This review looks at several aspects of gene mutation, genomics, transcriptomics, proteomics, metabolomics and immunomics.

TABLE 1 Major subtype classification.

Classification	Author	Samples	Subtype	Ref
Genomics	Waddell, Pajic, Grimmond et al	100PDAC	Stable Locally rearranged Scattered Unstable	(26)
	Connor, Denroche, Gallinger et al	discovery cohort comprised 160 PDAC cases from 154 patients replication cohort comprised 95 primary PDAC.	Age-related DSBR MMR Signature 8	(52)
Transcriptomics	Collisson, Sadanandam, Gray et al	PDAC from UCSF and several microarray datasets Human and mouse cell lines	Classical Exocrine-like QM-PDA	(54)
	Moffitt, Marayati, Yeh et al	145 primary and 61 metastatic PDAC	classical basal-like	(56)
	Noll, Eisen, Sprick et al	8 PACO cell systems and their PT and DT allografts	KRT81+HNF1A− KRT81−HNF1A+ KRT81−HNF1A−	(58)
	Bailey, Chang, Grimmond et al	456 PDAC	pancreatic progenitor squamous ADEX immunogenic	(59)
	Sivakumar, de Santiago, Markowetz et al	242 pancreatic cancers from ICGC 178 pancreatic cancers from TCGA 5 pancreatic cancer related datasets from GEO	Hedgehog/Wnt NOTCH cell cycle	(66)
	Puleo, Nicolle, Maréchal et al	309 paraffin embedded PDAC samples	pure classical immune classical pure basal like stroma activated desmoplastic	(61)
	Mueller, Engleitner, Rad et al	38 PK mice 19 PanIN patients	C1/C2	(67)
	Chan, Kim, Notta et al	317 PDAC	Basal-like-A Basal-like-B Hybrid Classical-A Classical-B	(43)
	Birnbaum, Begg, Liss et al	28 PDAC	C1/C2/C3/C4	(65)
	Shi, Li, Gao et al	84 pancreatic cancer-like organs	Classical-like Basal-like Classical-Progenitor Glycomet	(70)
	Kim, Leem, Park et al	17 PDAC	Ep_TRIM54 Ep_KRT6A Ep_PIFO Ep_MSMB Ep_VGLL1	(72)
Proteomics	Zhao, Zhao, Yan	1200 PDAC	L1/L2/L6	(87)
		68 PDAC	Metabolic Progenitor-like	(88)

(Continued)

TABLE 1 Continued

Classification	Author	Samples	Subtype	Ref
	Law, Lagundžin, Woods et al		Proliferative Inflammatory	
	Son, Kim, Kim et al	225 PDAC	stable exocrine-like activated ECM remodeling	(89)
	Tong, Sun, Ding et al	217 PDAC	S-I/S-II/S-III	(90)
	Hyeon, Nam, Lee et al	196PDAC	TS1/TS2/TS3/TS4/IS1/IS2	(92)
Metabolomics	Daemen, Peterson, Evangelista et al	38 PDAC	reduced proliferative capacity glycolytic lipogenic	(94)
	Karasinska, Topham, Schaeffer et al	325 PDAC	quiescent glycolytic cholesterogenic mixed	(96)
	Li, Du, Zhang et al	20 PAAD and 10 normal tissues	quiescent pyruvate GG mixed	(99)
	Li, Tang, Jin et al	28 PDAC	glucomet-PDAC lipomet-PDAC	(101)
Immunomics	Knudsen, Vail, Witkiewicz et al	109 PDAC	hot cold mutationally cold mutationally active	(105)
	Wartenberg, Cibin, Karamitopoulou et al	110 PDAC	immune escape immune rich immune exhausted	(106)
	Danilova, Ho, Yarchoan et al	152 PAAD	PD-L1+/CD8high PD-L1+/CD8low PD-L1-/CD8high PD-L1-/CD8low	(107)
	de Santiago, Yau, Sivakumar et al	353 PDAC	innate immune T cell dominant tumor dominant	(108)
	Hwang, Jagadeesh, Regev et al	43 PDAC	treatment-enriched squamoid-basaloid classical	(111)
	Tong, Sun, Ding et al	217 PDAC	Im-S-I/Im-S-II/Im-S-III/ Im-S-IV/Im-S-V	(90)

2 Subtype classification

2.1 Gene mutation and applications

KRAS is the most commonly mutated oncogene in pancreatic cancer and represents one of the earliest alterations observed in pancreatic intraepithelial neoplasia (Pan IN) (Figure 2), where *KRAS* mutations lead to the activation of downstream effectors, driving various pro-tumorigenic processes (11). Approximately 90% of pancreatic cancer patients harbor *KRAS* mutations (12). While *KRAS* was previously considered undruggable, the past decade has witnessed the emergence of several promising molecular therapies targeting *KRAS*. These include MRTX1133 (a $KRAS^{G12D}$ inhibitor) (13), RMC-6236 (14), ASP3082 (15), and

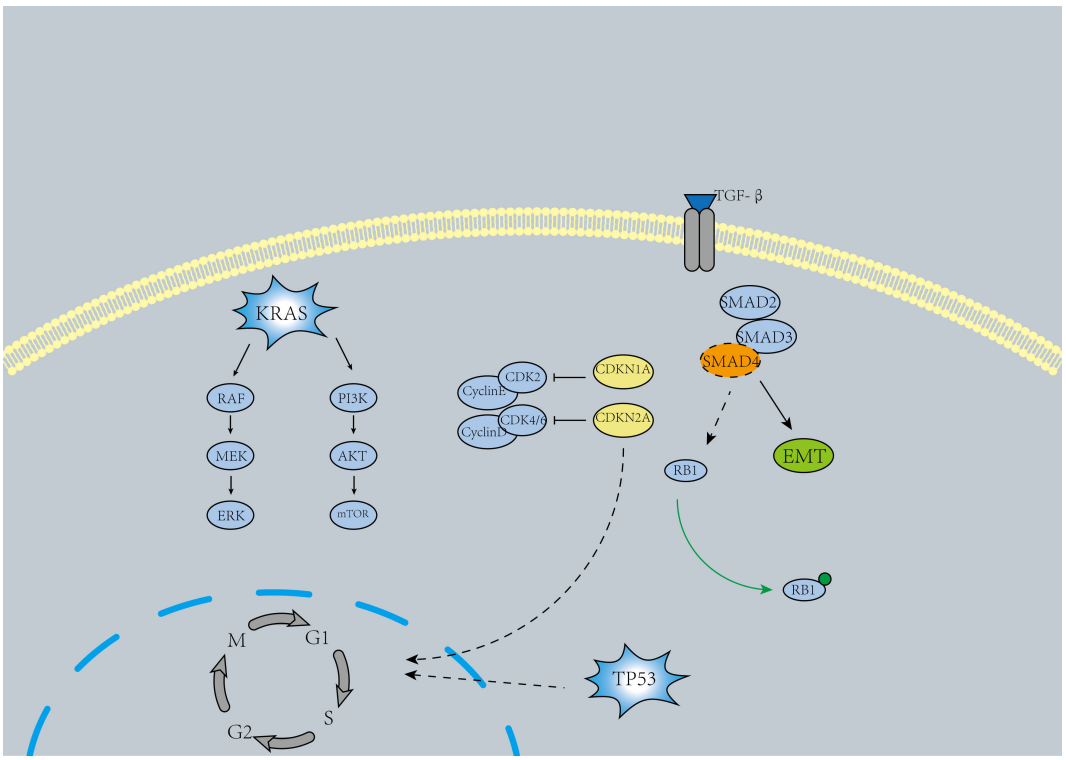

FIGURE 2
A mechanism map of the major pancreatic cancer causing genes.

BI1701963 (a pan-*KRAS* SOS1 inhibitor) (16). Notably, targeted therapies for the rare $KRAS^{G12C}$ mutant, such as Sotorasib, have shown therapeutic potential (17). Some researchers have shifted their focus to downstream molecules of *KRAS*, such as *EGFR*, *MEK*, and *PI3K*. However, results indicate that most *EGFR* and *MEK* inhibitors have not significantly improved patient outcomes (18). Interestingly, a recent study demonstrated that *EGFR* inhibition may provide tangible benefits in a selected subgroup of *KRAS* wild-type PDAC patients (19). Therefore, multiple drug combinations and further exploration of *KRAS* and its downstream signaling therapies may remain a hotspot for future research.

In pancreatic cancer, the inactivation of tumor suppressor genes *TP53*, *SMAD4*, and *CDKN2A* is another major oncogenic driver (4) (Figure 2). Inactivating mutations of *TP53* are identified in 50%-74% of pancreatic cancers (5, 18). Similar to *KRAS*, *TP53* mutations arise in Pan IN lesions and accumulate over time, ultimately driving the progression to pancreatic ductal adenocarcinoma (PDAC) (20). The primary oncogenic mechanism of *TP53* inactivation involves defective DNA damage recognition and the prevention of cell cycle arrest (4, 5).*TP53* reactivators include Cys-targeting compounds such as APR-246 (21), the compound ATO (22), and the antiparasitic drug sodium stibogluconate (SSG) (23). However, the applicability of these reactivators in pancreatic cancer treatment remains uncertain. Ongoing clinical trials may shed light on their potential to improve the prognosis of patients with *TP53* mutations.

The loss of *SMAD4* expression occurs in the late stages of PDAC tumor progression (24). Approximately 31%–38% of individuals with pancreatic cancer harbor *SMAD4* mutations, which are frequently lost through homozygous deletions or mutations. This results in the weakening of *SMAD4*-dependent inhibitory effects of transforming growth factor-β (TGF-β), thereby enhancing non-canonical TGF-β signaling and promoting pro-tumorigenic responses (25, 26). The loss of *SMAD4* is associated with disease metastasis (27). Disruption of the TGF-β-*SMAD4* signaling pathway in PDAC may induce epithelial-mesenchymal transition (EMT) (28). Cancer-associated fibroblasts (CAFs) secreting TGF-β may promote the proliferative phenotype of transformed PDAC cells, contributing to the heterogeneity of PDAC (29). In some studies, drugs targeting TGF-β, such as NIS793 (30) and Vactosertib (31), have shown promising efficacy.

In 46%–60% of pancreatic cancers, inactivating mutations of *CDKN2A* have been detected (4). The inactivation of *CDKN2A* is primarily caused by homozygous deletions, hypermethylation, or mutations combined with the loss of the wild-type allele, leading to dysregulation of the cell cycle in cancer cells (25, 32). The combined use of *CDK4/6* inhibitors and *ERK-MAPK* inhibitors may be effective for patients with *CDKN2A* and *KRAS* co-mutations (33).

Recent studies have identified several novel mutation/variant genes with frequencies below 20%, including *KDM6A*, *RAC1*, *RNF43*, *ARID1A*, *BRAF*, *TGFBR2*, *MAP3K21*, *SWI/SNF*-related, matrix-associated, *SMARCA4*, *ACVR2A*, *ACVR1B*, *NRAS*, *FAM133A*, *ZMAT2*, and *STAT3* (32, 34–37).PDAC is also

associated with germline and somatic mutations in the homologous recombination repair pathway, including *BRCA2*, *ATM*, *BRCA1*, and *PALB2* (38). Individuals carrying *BRCA* germline mutations have a significantly increased risk of developing pancreatic cancer (39). Tumors with homologous recombination deficiencies due to *BRCA1/2* mutations exhibit heightened sensitivity to poly (ADP-ribose) polymerase (PARP) inhibitors (40). A pivotal phase 3 randomized trial demonstrated that PARP inhibitors can prolong progression-free survival in patients with *BRCA1/2* mutations (40).

Recent studies on MTAP deletion mutations may provide new ideas for pancreatic cancer treatment. MTAP deletion plays a crucial role in pancreatic cancer research, with approximately 20–30% of pancreatic cancers exhibiting this genetic loss. This deletion is closely associated with poor patient prognosis. Regarding sensitivity to PRMT5 inhibitors, MTAP deletion renders cancer cells more susceptible to these inhibitors. This increased sensitivity is attributed to metabolic reprogramming induced by MTAP loss, which enhances glycolysis and *de novo* purine biosynthesis, thereby increasing cellular dependence on PRMT5. PRMT5 inhibitors may suppress cancer cell growth by targeting these processes. Combination treatment strategies have shown promise for MTAP-deficient pancreatic cancer. For instance, the combined use of 2-deoxy-D-glucose (2-DG) and L-alanosine has demonstrated synergistic lethality against MTAP-deficient pancreatic cancer cells. Furthermore, clinical trials combining PRMT5 inhibitors with agents such as 5-azacitidine and pembrolizumab may enhance therapeutic efficacy, paving the way for new treatment strategies for pancreatic cancer (41, 42).

Overall, the current drugs directly targeting *KRAS*, *TP53*, *SMAD4*, and *CDKN2A* have shown limited efficacy. However, further studies are needed to evaluate the effectiveness of drugs targeting the upstream and downstream factors of these genes, which is expected to become a major research focus in the coming years. Additionally, designing drugs based on low-frequency mutated genes, such as *BRCA* and *STAT3*, may offer promising and feasible approaches for pancreatic cancer treatment. In summary, specific therapeutic strategies targeting different mutated gene subtypes in pancreatic cancer require further in-depth investigation.

2.2 Genomics subtyping and applications

It is well known that the accumulation of genomic aberrations in tumors leads to the classification of different genomic subtypes and contributes to disease heterogeneity. This heterogeneity arises from the persistent genomic instability during tumor progression (43). Structural variations (SV) are a specific category of chromosomal alterations that can induce various gene changes, including deletions, rearrangements, amplifications, and fusions. These changes have significant biological implications and potential pathogenic associations at the molecular genetic level, playing a crucial role in understanding the mechanisms of tumorigenesis. Early studies have demonstrated the presence of multiple gene alterations caused by chromosomal structural variations in PDAC (44). Most structural variations are intra-chromosomal and can be classified into seven types: intra-chromosomal rearrangements, deletions, duplications, tandem duplications, inversions, fold-back inversions, and amplified inversions. Inter-chromosomal translocations are less common (26).

In 2015, Waddell et al. conducted whole-genome sequencing of 100 PDAC samples (26). Their study defined four pancreatic cancer subtypes: Stable, Locally Rearranged, Scattered, and Unstable. The Stable subtype accounted for 20% of the samples and typically exhibited widespread aneuploidy. These tumor genomes contained fewer than 50 SV events and were often associated with mitotic defects (26). The Locally Rearranged subtype comprised approximately 30% of the samples. About one-third of these genomes displayed copy number amplifications in known oncogenes, such as *KRAS*, SOX9, and *GATA6*, along with therapeutic targets like *ERBB2*, *CDK6*, *MET*, *PIK3CA*, and *PIK3R3* (45–49). The remaining locally rearranged genomes involved complex genomic events such as breakage–fusion–bridge cycles, chromothripsis, and ring chromosomes (26). The other two subtypes were the Scattered subtype (<200 SV events) and the Unstable subtype (>200 SV events), accounting for 36% and 14% of the samples, respectively. The Unstable subtype indicated defective DNA maintenance, which might render these tumors sensitive to DNA-damaging agents (50). Additionally, the Unstable subtype was associated with deleterious mutations in *BRCA1*, *BRCA2*, and *PALB2*, as the unstable genomes tend to recruit patients with *BRCA1* or *BRCA2* mutations (5). Current *PARP* inhibitor trials recruit patients based on *BRCA1* and *BRCA2* germline deficiencies, and these patients may exhibit susceptibility to platinum-based drugs and PARP inhibitors (26). Other chromosomal stability maintenance genes, such as *XRCC4* and *XRCC6*, have also been detected in the Unstable subtype or tumors with *BRCA*-mutated features (51). These findings suggest that the Unstable subtype may be a suitable candidate for precision therapies involving platinum-based drugs and *PARP* inhibitors.

In 2017, Connor et al. (52) performed whole-genome sequencing on 154 patients and combined their data with samples from 95 pancreatic cancer patients in the ICGC cohort. They proposed classifying PDAC into four subtypes: Age-related, Double-Strand Break Repair (DSBR), Mismatch Repair (MMR), and Unknown Etiology (Signature 8). The Age-related subtype arises from the gradual accumulation of damage during cell division. DSBR is primarily caused by defects in homologous recombination repair (HRR) of double-strand breaks. This subtype is associated with enhanced local anti-tumor immunity, where infiltrating CD8+ T cells show increased cytolytic activity, accompanied by increased expression of co-regulatory molecules (*CTLA-4*, *PD-L1*, *PD-L2*, and *IDO-1*). This scenario is similar to the response of melanoma to checkpoint inhibitors, suggesting that this subtype may respond to immunotherapy (53).MMR arises from defects in DNA mismatch repair, and its characteristics are similar to those of DSBR. As for the Unknown Etiology subtype, its origin remains poorly understood. Although some studies have suggested that smoking may be its cause, the data from Connor et al.'s research could not substantiate this epidemiological link.

With the continuous advancement of genomic analysis technologies in both depth and breadth, more refined and comprehensive genomic-based classifications will likely emerge in the future. These classifications will provide strong evidence and guidance for developing disease treatment plans, facilitating the transition from traditional empirical treatment models to precision medicine based on genomic profiling.

2.3 Transcriptomics subtyping and applications

Although we have summarized the genes and genomic phenotypes of pancreatic cancer, it is clear that these findings do not fully capture the entire spectrum of pancreatic ductal adenocarcinoma (PDAC), and their therapeutic efficacy remains limited. Given that various cellular processes can influence gene expression, screening for differentially expressed transcripts can aid in better identifying potential therapeutic targets for PDAC. Over years of research, several classification schemes for transcriptional subtypes have been published, and we will discuss some of the key classifications and their associated therapeutic applications.

In 2011, Collisson et al. proposed classifying pancreatic cancer into three subtypes: classical, quasi-mesenchymal (QM-PDA), and exocrine-like, each with its distinct characteristics (54). The classical subtype exhibits high expression of adhesion-related genes and epithelial genes, along with high *GATA6* expression, and is sensitive to erlotinib. The QM-PDA subtype shows high expression of stromal-related genes and is sensitive to gemcitabine. In the exocrine-like subtype, tumor cell-derived digestive enzyme genes are expressed at relatively high levels.

In 2014, Kim et al. identified three subtypes of pancreatic cancer. For subtype 1, the enriched pathways are closely related to the immune system, including hematopoietic cell lineage, cytokine-cytokine receptor interactions, and calcium signaling pathways. This subtype is associated with a high R0 resection rate and better prognosis. Subtype 2's enriched pathways are linked to fatal diseases like pancreatic cancer, renal cell carcinoma, and chronic myelogenous leukemia, and are often associated with poor prognosis. Subtype 3, which had a smaller sample size, showed gene overlap with Collisson et al.'s exocrine-like subtype through gene enrichment analysis (55).

In 2015, Moffitt divided pancreatic cancer into "classical" and "basal-like" subtypes (56). The classical subtype exhibited characteristics similar to the classical subtype defined by Collisson et al., with high expression of *GATA6*, which serves as a key marker to distinguish advanced pancreatic cancer classical subtypes from basal-like subtypes (57). The basal-like subtype was characterized by high expression of genes related to cadherins and keratins, along with high $KRAS^{G12D}$ expression. This subtype is typically associated with poorer prognosis but shows a better response to adjuvant therapy compared to the classical subtype. Moffitt also identified two stromal subtypes: "normal" and "activated." The "normal" stromal subtype was marked by elevated expression of markers such as pancreatic stellate cells, smooth muscle actin, vimentin, and desmin (*ACTA2*, *VIM*, *DES*). Patients with this type of stroma typically had a better prognosis. The "activated" stromal subtype was characterized by the expression of macrophage-related genes, such as integrin *ITGAM* and chemokine ligands *CCL13* and *CCL18*, as well as other genes like the secreted protein *SPARC* and *WNT* family members *WNT2* and *WNT5A*, indicating its significant role in promoting tumor growth. Interestingly, Moffitt et al. found a high overlap between the genes expressed by basal-like tumors and stromal subtypes and the QM-PDA genes proposed by Collisson et al.

In 2016, Noll et al. used an immunohistochemical classification based on markers *KRT81* and *HNF1A* to classify pancreatic cancer (58). The classification included the following subtypes: *KRT81+HNF1A−* for the QM-PDA subtype, *KRT81−HNF1A+* for the exocrine-like subtype, and *KRT81−HNF1A−* for the classical subtype. In this study, the exocrine-like subtype was found to be resistant to paclitaxel tyrosine kinase inhibitors due to the expression of CYP3A5.

In 2016, Bailey et al. analyzed 96 tumors with over 40% epithelial content and identified four subtypes: pancreatic progenitor, squamous, aberrantly differentiated endocrine exocrine (ADEX), and immunogenic (59). The squamous subtype was associated with mutations in *TP53* and *KDM6A*, and it exhibited a series of biological phenomena, including inflammation, hypoxic response, metabolic reprogramming, activation of the TGF-β signaling pathway, MYC pathway activation, autophagy, and upregulation of *TP63*ΔN and its target genes. This subtype was also closely related to hypermethylation and consistent downregulation of genes controlling pancreatic endodermal cell fate. The pancreatic progenitor subtype was linked to the expression of early pancreatic differentiation genes and showed upregulation of genes associated with fatty acid oxidation, steroid hormone biosynthesis, drug metabolism, and mucin O-linked glycosylation. ADEX played a significant role in the terminal differentiation phase of the pancreas, characterized by the upregulation of endocrine-exocrine differentiation genes. The immunogenic subtype was closely related to immune infiltration, particularly with infiltrating B and T cells, suggesting potential sensitivity to immune modulators. Notably, except for the immunogenic subtype, the other three subtypes defined in this study overlapped with those proposed by Collisson et al. Specifically, the "quasi-mesenchymal" subtype in Collisson's study was renamed "squamous" in this research, the "classical" subtype became "pancreatic progenitor," and the "exocrine-like" subtype was renamed ADEX. The existence of ADEX/exocrine-like subtype is still debated, with some theories suggesting it may be due to contamination by surrounding pancreatic tissue (56, 60–62), but some studies support its existence (63–65). Collisson et al. did not find evidence of the exocrine-like subtype in human and mouse cell lines, but it was observed in microanatomical samples (54).

In 2017, Sivakumar et al. combined the three biological processes regulated by *KRAS* with the classification system proposed by Bailey et al. Their research revealed several important findings. In squamous subtype samples, there was an overexpression of the Hedgehog/Wnt pathways, along with an accumulation of M2 macrophages. Despite the squamous subtype having the poorest prognosis, emerging evidence suggests that

targeted therapies could apply to this subtype, offering the potential for improved treatment outcomes. In the immunogenic subtype, cell cycle processes were overexpressed in the samples. However, an interesting paradox arose: patients in this subtype exhibited almost no noticeable immune activity. This contradiction challenges the conventional understanding of immune-related subtypes and emphasizes the need for further research to explore the underlying mechanisms, which could provide deeper insights into the biological features of this subtype. For the ADEX samples, there was an overexpression of the Notch pathway. Furthermore, the study discovered a positive correlation between immune therapy targets, such as programmed cell death protein 1 (*PD-1*) and cytotoxic T lymphocyte-associated protein 4 (*CTLA4*), and Notch pathway activity, along with an enrichment of CD8+ T cells. These findings suggest that patients in the Notch group may be more suitable for immune therapy (66).

In 2018, Puleo et al. conducted an RNA chip analysis on 309 paraffin-embedded samples, integrating the tumor microenvironment and epithelial components of tumors to distinguish five subtypes (61). The pure classical subtype they defined is composed of classic tumors with both normal and activated stroma, as defined by Moffitt et al. The activated stroma refers to the presence of fibroblasts in an activated state, which undergoes phenotypic changes to become myofibroblasts. This transformation process imparts unique histological and cellular characteristics to the pure classical subtype. The immune classical subtype is composed of classic tumors and normal stroma, as identified by Moffitt et al., which gives this subtype its distinct features. The pure basal-like subtype, defined by Moffitt et al., consists of basal tumors and activated stroma. It is characterized by the absence of cellular stroma and the occurrence of tumor metastatic spread, reflecting the subtype's unique biological behavior and providing a key entry point for subsequent studies on tumor metastasis mechanisms and the development of targeted therapeutic strategies. The stroma-activated subtype is composed of basal or classical tumors and activated stroma, which is described by Moffitt et al., reflecting the complex and diverse interactions between different tumor cell types and stroma components during tumorigenesis and progression. The desmoplastic subtype mainly consists of basal or classical tumors and normal stroma which is mentioned by Moffitt et al., and is notably characterized by low tumor content and high expression of vascularized stromal components (such as elastin), along with the highest degree of immune cell infiltration. Moreover, they observed a significant correlation between the expression of *MET* and nuclear *GLI1* with the stroma-activated and pure basal-like subtypes, suggesting that the MET and Hedgehog signaling pathways are activated in these subtypes. Additionally, human equilibrative nucleoside transporter 1 (*hENT1*) is expressed at relatively high levels in the classical subtype (including pure classical and immune classical), and since *hENT1* is a marker for gemcitabine sensitivity, this suggests that the classical subtype may be more sensitive to gemcitabine. The expression of *CTLA4* is higher in the immune classical and desmoplastic subtypes, which makes these two subtypes potentially more suitable for anti-*CTLA4* therapy. Furthermore, all other subtypes, except for the classical subtype, exhibit high expression of relevant immune checkpoints, indicating that these subtypes may be suitable for immune checkpoint inhibition therapy. These findings provide an important theoretical basis for the application of different therapies in various tumor subtypes and for optimizing treatment plans, significantly contributing to the advancement of personalized immunotherapy for pancreatic cancer.

In 2018, a study by Mueller et al. classified pancreatic cancer into two subgroups, C1 and C2 (67). C1 exhibits distinct epithelial-mesenchymal transition (EMT) characteristics, which are closely associated with the high expression of $KRAS^{G12D}$ and Ras-related transcriptional programs. In contrast, C2 is characterized by the high expression of epithelial differentiation genes. At the cellular morphology level, all C1 cell lines display mesenchymal cell characteristics, while C2 cell lines present typical epithelial cell morphology, creating a clear contrast between the two.

In a 2020 study, Dijk et al. classified PDAC into four subtypes: secretory, epithelial, compound pancreatic, and mesenchymal (64). The secretory subtype exhibits enrichment in both the endocrine and exocrine functions of the pancreas. The epithelial subtype is characterized by high expression of mitochondrial components and ribosomal-related features. The mesenchymal subtype displays characteristics associated with epithelial-mesenchymal transition, stromal interactions, and TGF-β signaling. The compound pancreatic subtype shares some similarities with the previously published classical subtype and ADEX/exocrine-like subtype, but enrichment analysis revealed that it more closely resembles the mesenchymal subtype. These findings are likely related to tumor heterogeneity and lay the foundation for further investigation into the complex and diverse mechanisms of intratumoral heterogeneity, as well as the development of more targeted diagnostic and therapeutic strategies.

In 2020, Chan et al. performed sequencing analysis on 248 purified primary and metastatic pancreatic cancer epithelial cell samples, identifying five subtypes: "Basal-like-A," "Basal-like-B," "Hybrid," "Classical-A," and "Classical-B" (43). The development of Classical-A/B tumors was associated with *GATA6* amplification and complete *SMAD4* loss, whereas Basal-like-A/B tumors were strongly correlated with complete *CDKN2A* loss and an increased frequency of *TP53* mutations. Metastatic basal-like tumors were often enriched with mutated *KRAS* and exhibited greater resistance to chemotherapy. Among these, Basal-like-A tumors demonstrated poor response to gemcitabine-based and mFOLFIRINOX chemotherapy regimens. Therefore, distinguishing the basal-like-A subtype from the basal-like subtype identified by Collisson et al. allows for a more precise prediction of chemotherapy sensitivity across subtypes. These features are of significant importance both for deepening the understanding of tumor biology and for identifying potential targeted therapies specific to each subtype (5). Furthermore, single-cell RNA sequencing of tumors from 15 patients revealed the coexistence of basal-like and classical expression features within individual tumors, providing direct evidence of intratumoral heterogeneity.

In 2021, Birnbaum et al. employed LCM and RNA-seq analysis to identify four cancer cell subtypes (C1–C4) and three peritumoral stromal subtypes (S1–S3), among which S1 was associated with better prognosis when paired with C1 and C2 subtypes (65). The C1 subtype was linked to genes involved in protein folding and leukocyte chemotaxis, whereas the C2 subtype showed a strong association with gene programs essential for pancreatic endocrine cell development and neuronal membrane signaling. The C3 subtype was related to nucleotide biosynthesis and protein translation regulation, while the C4 subtype was associated with oncogenic signaling pathways, highlighting its critical role in tumorigenic signaling mechanisms. The S1 subtype was related to developmental and cell differentiation pathways, S2 was linked to antigen processing and presentation, and S3 was associated with phospholipid synthesis and macromolecule modification. Further analysis revealed that the C1 and C3 subtypes correlated with the classical/pancreatic progenitor subtype, the C2 subtype aligned with the ADEX/exocrine-like subtype, and the C4 subtype was associated with the squamous/basal-like/quasi-mesenchymal subtype. Additionally, the S1 and S2 subtypes exhibited enrichment of normal and activated stromal subtypes, respectively. These intricate associations provide valuable insights into the biological heterogeneity of tumors, the interplay between subtypes, and the foundation for developing precise therapeutic strategies.

Espinet et al. classified pancreatic cancer into MC1 and MC2 subtypes, which were found to be associated with IFN expression, suggesting that effective inhibition of intrinsic interferon signaling could serve as a potential therapeutic approach for targeting these tumors (MC1) with minimal side effects on normal cells (68).

Ju et al. categorized pancreatic cancer into aggressive and moderate subtypes. The aggressive subtype was associated with pathways overlapping with DNA damage repair (DDR) mechanisms, including DNA replication, homologous recombination, mismatch repair, and upregulation of the P53 signaling pathway. This finding suggests that targeting repair proteins involved in DDR mechanisms may be a viable therapeutic strategy. In contrast, the moderate subtype exhibited upregulation of immune response-related pathways, including chemokine signaling, cell adhesion molecule (CAMs) pathways, and cytokine-cytokine receptor interaction pathways. For this subtype, immunotherapy could be considered as a potential treatment option (69).

Shi et al. identified four subtypes of pancreatic cancer: Classical-like, Basal-like, Classical-Progenitor, and Glycomet (70). The Classical-Progenitor subtype was significantly enriched for transcription factors such as *MYC*, *MYB*, and *ATOH1*, indicating specific progenitor cell characteristics. This subtype was associated with a significantly better prognosis compared to the other subtypes. The Glycomet subtype was characterized by enrichment of pathways related to glucose metabolism.

In 2023, Zheng et al. identified two subtypes, S1 and S2, based on N6-methyladenosine (m6A) transcriptomic modifications (71). The S2 subtype exhibited a distinct m6A modification pattern compared to S1. Notably, genes associated with the Squamous subtype described by Bailey et al. and the Classical subtype defined by Collisson et al. were more enriched in S2 than in S1. Additionally, the median progression-free survival (PFS) and overall survival (OS) times of S2 were significantly shorter than those of S1. Moreover, S2 exhibited relatively lower levels of T-cell and B-cell markers compared to the S1 subtype.

In 2024, Kim et al. performed single-cell sequencing on 17 pancreatic cancer samples and identified five distinct functional subpopulations of pancreatic cancer cells (72). These included Ep_TRIM54, associated with the Classical subtype, and Ep_KRT6A, associated with the Basal-like subtype (or quasi-mesenchymal subtype). They also identified Ep_PIFO, a Basal-like cluster with unique ciliary features previously mentioned in earlier studies (43, 73), as well as Ep_MSMB, a cancer cell cluster highly associated with intraductal papillary mucinous neoplasm (IPMN). Additionally, a previously unreported cluster, Ep_VGLL1, was identified. This subpopulation exhibited basic characteristics of the Classical subtype, such as high expression of tight junction genes (*TJP1* and *OCLN*) and low expression of mesenchymal markers (VIM and S100A4), along with Basal-like subtype features, such as low expression of *SMAD4* and *GATA6*. Furthermore, their study revealed that Ep_VGLL1 spatially correlates with both Classical (Ep_TRIM54) and Basal-like (Ep_KRT6A) clusters. Based on these findings, targeting Ep_VGLL1 to block the transition from the Classical to the Basal-like subtype could become a promising new therapeutic strategy, offering novel insights and directions for the treatment of related diseases.

Several molecular markers have also been used to classify previously identified subtypes of pancreatic cancer, including *HMGA1/2* and *FGF19* (74, 75), *HAPLN1* (76), *SPDEF* (77), *SEMA3A* (78), *KRT17high*/*CXCL8+* (79), *TEAD2* (80), *HOXA10* (81), *IRF1* (82), and *RBFOX2* (83), among others.

In recent years, with the help of advanced molecular biology techniques, a series of distinct subtypes associated with methylation modifications have been successfully identified (84, 85). These newly discovered subtypes exhibit distinct differences in the distribution of methylation sites, modification levels, and the regulatory patterns of gene expression, providing new insights into the complex pathogenic mechanisms of the disease. With the continuous innovation and development of DNA and RNA sequencing technologies, significant progress has been made in the transcriptomic classification of pancreatic cancer, which has driven the implementation of precision medicine for different transcriptomic subtypes. These transcriptomic subtypes show both commonalities and unique characteristics, yet a unified classification is still lacking. Future research needs to be extensive and systematic, aiming to accurately define transcriptomic subtypes, thereby providing molecular-level guidance for the precise treatment of pancreatic cancer.

2.4 Proteomic subtyping and its applications

As we have previously discussed the genetic and transcriptomic classifications of pancreatic cancer, the next topic to address is the

proteomic classification, which is downstream in the central dogma. PDAC is caused by DNA alterations, which subsequently promote tumor malignancy through RNA transcription and protein translation. Therefore, a comprehensive analysis of the functional proteomic changes in each tumor can deepen our understanding of disease progression and identify potential therapeutic targets (Figure 3). In recent years, advancements in various technologies have enabled the transition from identifying a limited number of proteins to conducting proteomic analyses. For PDAC, proteomic technologies have also been used to explore pathological mechanisms, diagnostic biomarkers, and therapeutic targets (86).

In 2018, Zhao et al. classified PDAC into tumor-specific subtypes (L1, L2, and L6) and stroma-specific subtypes (L3, L4, and L5) (87). L1 is enriched with carbohydrate metabolism-related gene sets and resembles the classical subtype identified by Collisson, while L6 is abundant in lipid and protein metabolism-related gene sets and aligns with Collisson's exocrine-like subtype. These metabolism-related subtypes could potentially be targeted using metabolic drugs for therapeutic intervention. L2, characterized by epithelial and cell proliferation gene profiles associated with poor prognosis, shows similarities to Bailey's squamous subtype. Given the high proportion of malignant epithelial cells in L2, patients with this subtype may benefit from intensified therapeutic strategies. L3 is enriched with collagen-related gene sets and is associated with poor prognosis, bearing resemblance to Bailey's pancreatic progenitor subtype. For patients with this subtype, treatments targeting collagen may be effective. L4, which contains a variety of immune-related gene sets and is linked to relatively favorable survival outcomes, shows good responsiveness to immunotherapy. L5, enriched with neurotransmitter and insulin secretion-related gene sets and characterized by high expression of *FGFR1* pathway-associated genes, may be sensitive to neuroendocrine therapies.

In 2020, Law et al. conducted a quantitative analysis of 916 proteins from a total of 68 tissue samples to characterize four distinct PDAC liver metastasis subtypes (88): Metabolic, Progenitor-like, Proliferative, and Inflammatory. The Metabolic and Progenitor-like subtypes are characterized by an enrichment of metabolism-related proteins, including those involved in the ethanol oxidation pathway, mitochondrial fatty acid β-oxidation pathway, and retinoic acid signaling pathway. The Proliferative subtype is rich in ribonucleoproteins and Cajal body proteins, which are closely associated with translation processes, cellular proliferation, and telomere maintenance, playing a crucial role in cancer cell growth and progression. The Inflammatory subtype is

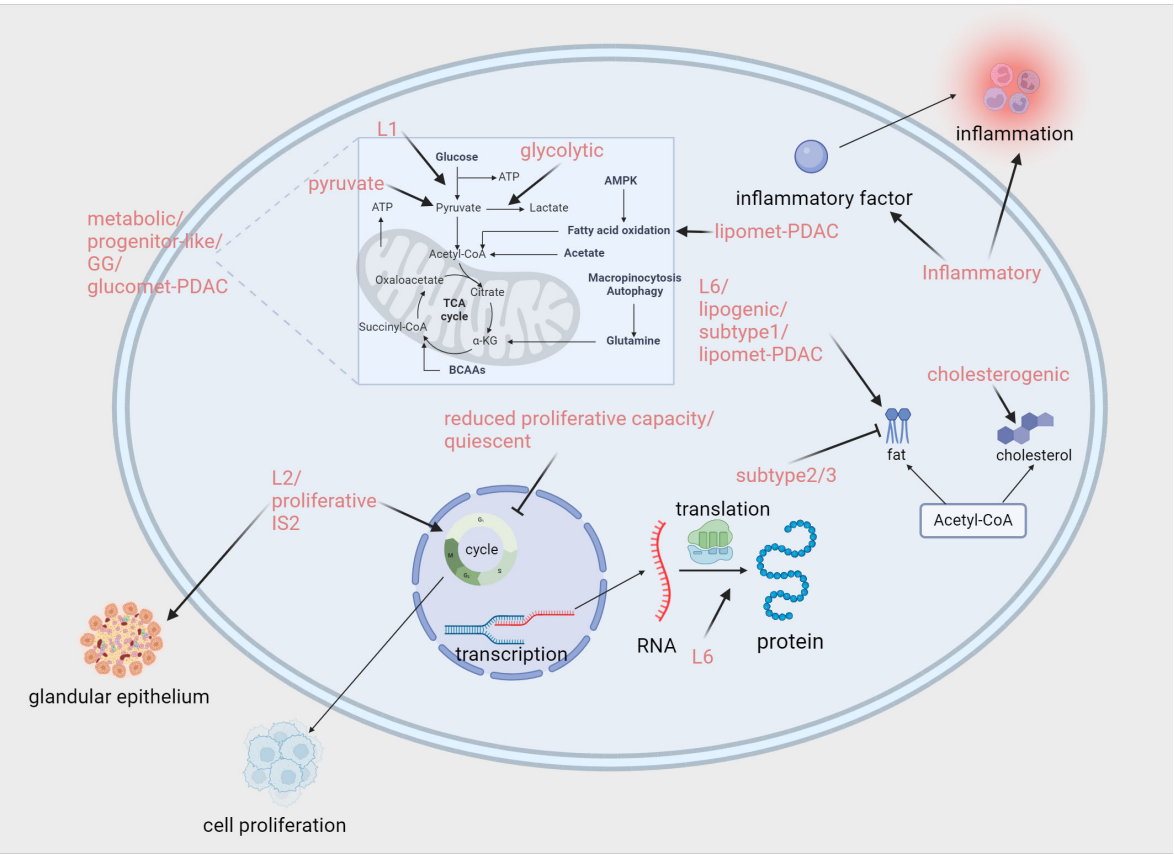

FIGURE 3
Proteomics and metabolomics-associated subtypes enriched or down-regulated pathways. Zhao (87):L1/L2/L6. Law (88): Metabolic/Progenitor-like/ Proliferative/Inflammatory. Daemen (94): reduced proliferative capacity/glycolytic/lipogenic. Karasinska (96): quiescent/glycolytic/cholesterogenic. Mahajan (97): Subtype 1./Subtype 2/Subtype 3. Li (99): quiescent/pyruvate/GG. Li (101): glucomet-PDAC/lipomet-PDAC. Hyeon (92): IS2. Created in https://BioRender.com.

enriched in proteins related to the pentose phosphate pathway, adaptive immune response, complement activation, *IL-8* production, and extracellular matrix organization. Moreover, the study revealed that the Proliferative and Inflammatory subtypes together correspond to the squamous subtype proposed by Bailey et al. In terms of chemotherapy, it is noteworthy that patients with the Metabolic and Progenitor-like subtypes demonstrated a survival advantage when treated with a combination of FOLFIRINOX and gemcitabine compared to gemcitabine alone. This finding provides valuable insights for optimizing clinical treatment strategies.

In 2021, Son et al. classified PDAC into four subtypes based on 24 protein features: stable, exocrine-like, activated, and extracellular matrix (ECM) remodeling. The stable subtype is so named because of its relatively stable disease progression and better prognosis. This subtype predominantly overlaps with the classical subtype proposed by Puleo et al., characterized by *GATA6* expression and an abundance of stromal components and pancreatic enzymes. Patients with this subtype show significantly improved survival outcomes when treated with first-line chemotherapy regimens. The exocrine-like subtype is characterized by high expression of pancreatic enzymes and is associated with the exocrine-like subtype identified by Moffitt et al. Enzyme replacement therapy may be effective for this subtype. The activated subtype is enriched in the *PI3K-AKT* and *MAPK/ERK* signaling pathways. This feature suggests that targeted therapies against receptor tyrosine kinases (RTKs) could benefit patients with this subtype. The ECM remodeling subtype is characterized by the enrichment of WNT/β-catenin and Notch signaling pathways. Targeting these two pathways may provide therapeutic benefits for patients with this subtype. Notably, the activated and ECM remodeling subtypes are highly correlated with the basal-like subtype, both of which are associated with poorer prognoses (89).

In 2022, Tong et al. conducted a comprehensive multi-omics analysis of 217 PDAC tumors and their paired non-tumor adjacent tissues, classifying PDAC into three subtypes based on proteomics: S-I, S-II, and S-III (90). The S-I subtype was associated with various metabolic processes, including the tricarboxylic acid (TCA) cycle, fatty acid metabolism, and glycolysis. The S-II subtype was closely linked to coagulation-related processes, while the S-III subtype was characterized by features such as the *ERBB2* signaling pathway and DNA damage response. Notably, these subtypes demonstrated significant overlap with those identified by Collisson et al. Specifically, the S-I subgroup overlapped with the "classical" subtype, with a concordance rate of 80.7%; the S-II subgroup overlapped with the "exocrine-like" subtype, with a concordance rate of 62.3%; and the S-III subgroup largely overlapped with the "QM-PDA" subtype, with a concordance rate of 98.1%. Furthermore, glycolysis-related proteins such as *PFKL* and *MDH2* were enriched in the S-I subtype, coagulation-related proteins such as *FGG* and *GP1BA* were enriched in the S-II subtype, and proteins like *MCM2* and *NCF1* were highly expressed in the S-III subtype. Based on these characteristics, therapeutic strategies targeting the relevant proteins and kinases within the pathways specific to each subgroup could potentially serve as viable treatment options.

In 2023, Swietlik analyzed more than 10,000 PDAC cell-derived proteins and uncovered distinct protein differences that segregate classical and mesenchymal subtypes. The classical and mesenchymal subtypes exhibited differences in secreted proteins, which were associated with immune cell recruitment and the composition of the tumor microenvironment. When interacting with macrophages, the two subtypes demonstrated distinct immunomodulatory and stromal remodeling characteristics (91).

In 2023, Hyeon performed a proteomic analysis of 171,272 peptides and 49,651 phosphopeptides derived from 196 PDAC patients from Asia, classifying PDAC into four subtypes: classical progenitor (TS1), squamous (TS2–4), immunogenic progenitor (IS1), and exocrine-like (IS2). The squamous subtype was further divided into activated stroma-enriched (TS2), invasive (TS3), and invasive-proliferative (TS4) subtypes. TS1 corresponded to the pancreatic progenitor subtype, while IS1 and IS2 corresponded to the immunogenic and exocrine-like subtypes, respectively. Tumors of the TS1 subtype were characterized by a high proportion of tumor cells, low proportions of fibroblasts and T cells, and activation of the mucin (*MUC1/4/5AC*) pathway, suggesting that targeting the mucin pathway in combination with chemotherapy could be effective. TS2–4 subtypes belong to the squamous subtype and demonstrated high proportions of tumor cells, low T cell infiltration, and enhanced activity of EMT-related pathways, such as the RhoA signaling and metalloproteinase pathways. Among these, TS4 showed the worst prognosis, potentially due to an increased proportion of polymorphonuclear myeloid-derived suppressor cells (PMN-MDSCs) that inhibit cytotoxic CD8+ T cells. These subtypes may benefit from a combination of RHOA signaling inhibitors and conventional cytotoxic chemotherapy. The squamous subtype subgroups identified through proteomics provide unique insights into therapeutic strategies for treating aggressive squamous tumors. A network model revealed increased mRNA expression of genes involved in phagocytosis, antigen presentation, and T cell receptor signaling in IS1 and IS2 subtypes. Correspondingly, proteins and phosphorylation levels within these pathways were also elevated. Additionally, IS2 exhibited increased abundance and phosphorylation levels of proteins involved in pancreatic secretion pathways, affirming its exocrine-like characteristics. Tailoring therapeutic approaches to the specific proteomic profiles of these subtypes may offer significant benefits to these patients (92).

In recent years, mass spectrometry technology has made rapid advancements, and bioinformatics engineering has seen extensive applications, providing strong impetus for the development of proteomics in the precision treatment of pancreatic ductal adenocarcinoma (PDAC). Proteomics allows for a comprehensive study of PDAC at the protein level, enabling the precise identification of protein changes closely associated with the onset and progression of the disease. This offers rich and accurate information resources for early diagnosis, the identification of therapeutic targets, and the monitoring of treatment efficacy. It is foreseeable that in future medical practice, proteomics will play an even more critical role in the precision treatment of PDAC, contributing significantly to improving patient prognosis, enhancing the effectiveness and specificity of treatment, and becoming a powerful tool in the fight against PDAC.

2.5 Metabolomics subtyping and applications

Metabolic reprogramming is a hallmark that regulates invasiveness and treatment response during cancer development and progression (93). In pancreatic cancer, a highly heterogeneous tumor, there are significant differences between tumor cells, which means that treatment strategies developed for a specific metabolic feature are often only effective in a subset of cancer patients. Therefore, conducting a systematic classification study of the metabolic reprogramming process in pancreatic cancer, and developing precision treatment strategies based on its unique metabolic characteristics, is of great significance and urgency (Figure 3). This not only helps deepen the understanding of the complex metabolic mechanisms in pancreatic cancer but also opens new avenues for achieving precision medicine in the treatment of pancreatic cancer.

In 2015, Daemen et al. conducted a quantitative analysis of 256 metabolites in 38 pancreatic cancer cell lines and identified three subtypes using non-negative matrix factorization (NMF) clustering: reduced proliferative capacity, glycolytic, and lipogenic (94). The reduced proliferative capacity subtype accounted for 34% of all lines, characterized by low levels of amino acids and carbohydrates, and a significantly longer doubling time compared to other subtypes. The glycolytic subtype exhibited elevated levels of components related to glycolysis and the serine pathway, including phosphoenolpyruvate (PEP), glyceraldehyde-3-phosphate, lactate, and serine. Additionally, this subtype demonstrated a notable feature: metabolites crucial for maintaining redox potential, such as NADH, NADP, and NADPH, were relatively low. Furthermore, genes associated with glycolysis and the pentose phosphate pathway were also expressed at higher levels in this subtype. The lipogenic subtype was enriched with various lipid metabolites, including palmitic acid, oleic acid, and palmitoleic acid, along with oxidative phosphorylation (OXPHOS) metabolites like coenzyme Q10 and coenzyme Q9. At the same time, cholesterol and lipid synthesis-related genes were upregulated in this subtype. Notably, the lipogenic subtype was associated with the epithelial (classical) subtype, while the glycolytic subtype was closely linked to the mesenchymal (QM-PDA) subtype, which aligns with the poorer prognosis associated with the glycolytic subtype. In terms of therapeutic applications, the glycolytic and lipogenic subtypes exhibited varying sensitivities to inhibitors targeting glycolysis, glutamine metabolism, lipid synthesis, and redox balance. Based on this, selecting appropriate drugs tailored to each subtype could enhance treatment efficacy for different patients, thus offering a potential strategy for personalized treatment.

In 2017, Nicolle et al. identified two metabolism-related subtypes, defined as Basal and Classical (95). Similar to the characteristics identified in previous studies, the Basal subtype exhibited stronger invasiveness and poorer prognosis, while the Classical subtype showed the opposite characteristics. Notably, this study found that the Basal subtype was associated with upregulation of genes related to the glycolytic pathway, whereas the Classical subtype exhibited a general increase in redox-related metabolites and widespread dysregulation of lipid metabolism, including a decrease in triglycerides, increased levels of fatty acids, and an increase in glycerophospholipids. Additionally, cholesterol transport proteins were significantly upregulated, and cholesterol ester levels were markedly higher, all of which indicated enhanced cholesterol uptake activity in the Classical subtype. This study suggests that targeting the metabolic characteristics of transcriptomic subtypes could be a promising and viable therapeutic approach.

In 2019, Karasinska et al. conducted a bioinformatics analysis of genomic, transcriptomic, and clinical data from a cohort of 325 PDAC cases, identifying four subtypes: Quiescent, Glycolytic, Cholesterogenic, and Mixed (96). The Quiescent subtype, as the name suggests, is characterized by low metabolic activity. Specifically, the expression of genes involved in amino acid catabolism, nucleotide metabolism, and the pentose phosphate pathway was significantly reduced, reflecting a relatively inactive metabolic state at the gene expression level. Notably, the Quiescent subtype was closely associated with the Classical subtype identified by Collisson et al. The Glycolytic subtype has distinct features, most notably a high enrichment of glycolysis-related pathways, along with amplification of the *KRAS* and *MYC* genes. Additionally, the expression levels of the mitochondrial pyruvate carriers *MPC1* and *MPC2* were significantly reduced. This subtype has been largely associated with the Basal/mesenchymal/squamous subtype in previous classifications and is clinically linked to poorer prognosis. The Cholesterogenic subtype is characterized by increased expression of MPC1 and MPC2 and enrichment of lipid metabolism-related pathways. It aligns with the pancreatic progenitor subtype and is associated with a better prognosis. The Mixed subtype combines characteristics of the aforementioned subtypes, resembling a complex "hybrid" with more diverse and complex biological features. Furthermore, an important finding of this study was that in Glycolytic PDAC cases, increasing the expression of *MPC1* and *MPC2* could potentially improve patient prognosis by promoting a transition of the tumor to a Cholesterogenic subtype.

In 2021, Mahajan studied the metabolic plasma profiles of 361 PDAC patients and identified three subtypes based on distinct lipid metabolism patterns (97). Subtype 1 exhibited elevated triglyceride levels and reduced ceramide levels. Subtype 2 showed the opposite pattern, with increased ceramide levels. Subtype 3 was characterized by significant decreases in both ceramide and triglyceride levels, along with complex fluctuations in the levels of various sphingolipid species, some of which increased and others decreased. The differences observed among these subtypes in lipid metabolism-related markers suggest that lipid metabolism plays a crucial role in the growth of pancreatic cancer. Therefore, future research may focus on investigating how lipids regulate cancer progression and exploring whether they can serve as potential targets for novel therapeutic strategies.

In 2022, Rodriguez et al. identified three distinct glycometabolic subtypes based on specific glycometabolism-related genes (98). The Fucosylated subtype was characterized by increased expression of

genes involved in fucosylation (*GMDS*) and O-glycosylation (*GALNT4*). This subtype was associated with the classical/progenitor subtype identified in previous studies and correlated with better prognosis. The Basal subtype displayed elevated expression of genes encoding galectin-1 (*LGALS1*), mucin *MUC4*, and *MUC16*. It was highly correlated with mesenchymal/basal-like/squamous subtypes, which are associated with poor prognosis. The Mixed/low tumor content subtype exhibited a lower tumor cell content and was linked to the previously identified ADEX/exocrine-like subtype. The study also demonstrated that the ADEX/exocrine-like subtype frequently occurs in samples with low tumor purity.

In 2023, our team conducted proteomic and metabolomic analyses on 20 PAAD tissues and 10 normal pancreatic tissues, classifying pancreatic cancer into four TAM2-associated metabolic subtypes based on the expression profiles of pyruvate and glycolysis/gluconeogenesis (CG)-related genes: Quiescent, Pyruvate, GG (glycolysis/gluconeogenesis), and Mixed subtypes (99). The Quiescent subtype was primarily enriched in KEGG pathways related to glucose, amino acid, and lipid metabolism and characterized by serine-type endopeptidase activity, hormone secretion, zymogen activation, and immune response. The Pyruvate subtype was closely associated with the *MAPK* and *cAMP* signaling pathways and featured cation channel complexes, vesicle-mediated transport, and insulin secretion. The GG subtype showed enrichment in KEGG pathways related to glucose metabolism and was characterized by exogenous metabolic processes, detoxification, and tissue homeostasis. The Mixed subtype participated in KEGG pathways associated with immune-related biological processes and signal molecules, featuring extracellular matrix organization, antigen presentation, and serine/threonine kinase signaling pathways. Our team also investigated the efficacy of various chemotherapeutic agents across these subtypes, providing practical insights for future pancreatic cancer treatment strategies. These findings offer new directions for addressing the challenges posed by pancreatic cancer.

In 2023, a study divided 930 pancreatic cancer samples into three clusters based on the expression profiles of oxidative stress and phospholipid metabolism (OSPM)-related genes: C1 (OSPM-active), C2 (OSPM-inactive), and C3 (OSPM-normal) (100). Among these, C1 displayed the highest OSPM functional score. Importantly, the OSPM functional score was negatively correlated with tumor-infiltrating lymphocytes (TILs), T-cell co-stimulation, plasmacytoid dendritic cells, and mast cells. Moreover, C1 was characterized by the elevated expression of numerous immune checkpoint molecules, such as *HAVCR2* and *TNFSF4*. These observations suggest that C1 might be more responsive to immunotherapy due to its unique immunosuppressive microenvironment and high levels of immune checkpoint expression.

In 2023, Li et al. described the metabolomic characteristics of PDAC organoids and classified them into two distinct subtypes: glucomet-PDAC (high glucose metabolism levels) and lipomet-PDAC (high lipid metabolism levels). Glucomet-PDAC was significantly enriched in glucose metabolism, energy metabolism, and nucleotide metabolism, with pentose phosphate pathway (PPP) metabolites highly accumulated in the corresponding organoids. This subtype exhibited resistance to chemotherapy, suggesting that conventional chemotherapeutic approaches might be less effective for treating this subtype. In contrast, lipomet-PDAC was characterized by increased expression of genes associated with lipid metabolism and glycan biosynthesis. Importantly, their study identified the *GLUT1/ALDOB/G6PD* axis as a key regulator that remodels glucose metabolism in glucomet-PDAC, ultimately driving chemoresistance in this subtype. This finding offers a novel strategy to address chemoresistance in glucomet-PDAC, positioning *GLUT1* as a promising therapeutic target to overcome this challenge (101).

In recent years, significant progress has been made in the study of metabolic characteristics in pancreatic cancer, particularly in theories based on metabolomics, which have garnered widespread attention. However, due to limitations in technology and other factors, translating these research findings into effective clinical treatment strategies remains a considerable challenge. Future studies focused on metabolomics are urgently needed to foster consensus among researchers on key issues and facilitate the application of these findings in clinical practice. Only through such efforts can patients truly benefit, offering new hope in the fight against pancreatic cancer.

2.6 Immunomics subtyping and applications

In recent years, significant progress has been made in the application of immunotherapy in the field of cancer. In 2018, the Nobel Prize in Physiology or Medicine was awarded to James P. Allison and Tasuku Honjo for their discovery of immune checkpoint blockade (ICB) therapy. Although this therapy has benefited some patients with solid tumors (102), a substantial proportion of "cold" tumors show limited response to ICB therapy (103), possibly due to the diversity of immune evasion mechanisms. Currently, there are several treatment methods for pancreatic cancer, such as oncolytic viruses, modified T cells (T-cell receptor (TCR) engineering and chimeric antigen receptor (CAR) T cell therapy), CAR natural killer cell therapy, cytokine-induced killing cells, immune checkpoint inhibitors, immune modulators, cancer vaccines, and strategies targeting bone marrow cells in the contemporary context (104). However, these have shown limited effectiveness in pancreatic cancer. Many immunotherapies that are effective in other solid tumors have proven to be less effective in pancreatic cancer treatment. The current focus of immune research is to develop various immune modulation strategies to enhance T cell function, initiate or strengthen tumor-specific T cell immunity, and convert the tumor microenvironment from immune "cold" to "hot," thereby improving the clinical treatment outlook for pancreatic cancer (103). Clearly, precision therapy is crucial at this point. Increasing evidence points to the same fact: in-depth exploration of tumor immune classification can provide valuable insights and strategies for designing more effective anti-cancer treatments, which is of great significance in improving cancer treatment outcomes and patient prognosis (Figure 4).

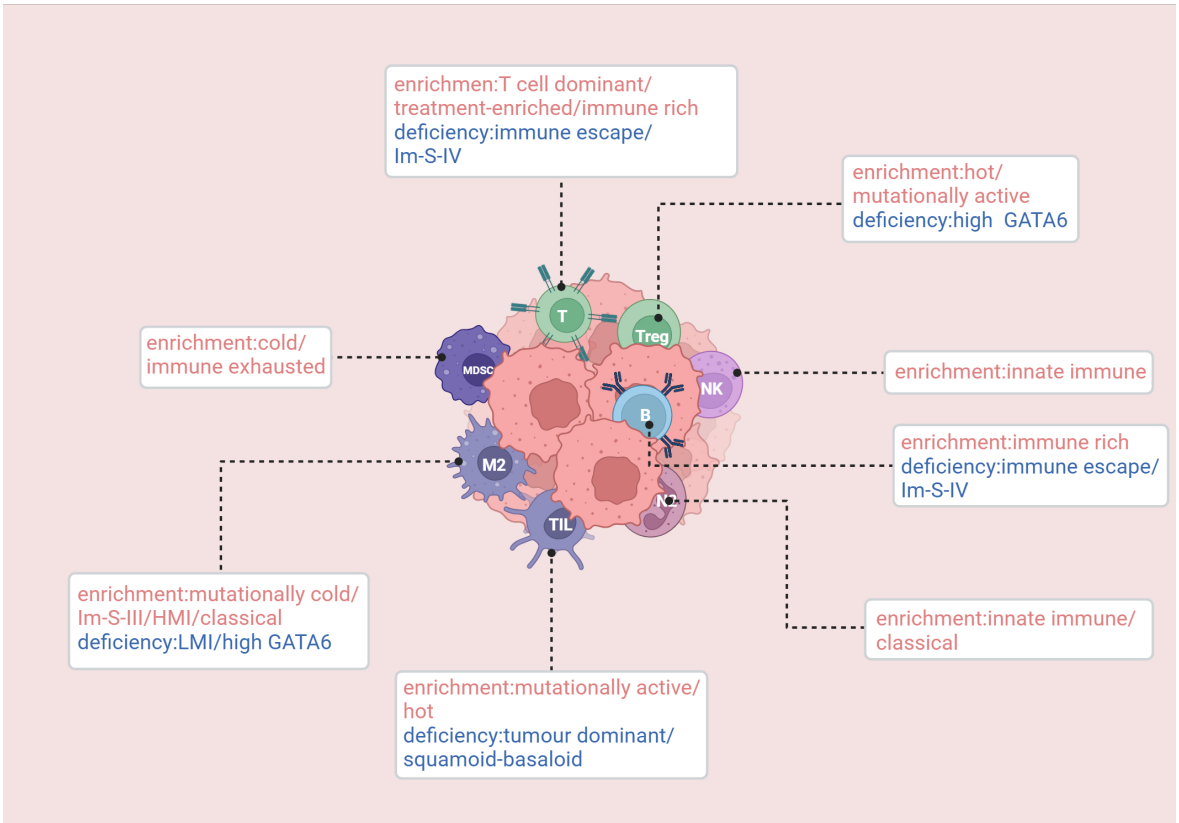

FIGURE 4
Enrichment and deficiency of immune cells in relevant immune subtypes. Knudsen (105): hot/cold/mutationally cold/mutationally active. Wartenberg (106): immune escape/immune rich/immune exhausted. de Santiago (108): innate immune/T cell dominant/tumor dominant. Hwang: treatment-enriched/squamoid-basaloid/classical. Tong (90): Im-S-IV(Metabolic-Neuron-Inflamed). Du (113): HMI/LMI. van Eijck (57): High GATA6. Created in https://BioRender.com.

In 2017, Knudsen et al. conducted a multi-omics analysis of a cohort of 109 PDAC patients and defined four immune subtypes of PDAC: hot, cold, mutationally cold, and mutationally active (105). Both the hot and mutationally active subtypes exhibit high mutational burdens, more tumor-infiltrating lymphocytes (TILs), and peritumoral lymphocytes, along with upregulated immune checkpoints (*CTLA-4* and *PDL-1*) and regulatory T cells. However, they differ in terms of tumor-associated macrophage levels. The cold subtype is characterized by low mutational burden, low levels of immune effector and suppressive cells, mature stromal types, high stromal volume, and low numbers of neoantigens. Notably, the cold subtype is associated with increased overall survival. Given these characteristics, treatment strategies that activate the immune system, such as cancer vaccines (*MUC1*, *GVAX*) or chimeric antigen receptor T cell therapy combined with immune modulators to counteract immune suppression mechanisms, may be more suitable. The mutationally cold subtype has fewer mutations, low stromal volume, and an immature stromal type, along with high levels of *MCT4*. Its microenvironment is glycolytic and acidic, and the immune infiltration is primarily composed of macrophages.

In 2018, Wartenberg et al. identified three immune subtypes of PDAC by performing immunohistochemical staining on immune cells within the tumor microenvironment: immune escape, immune rich, and immune exhausted (106). The immune escape phenotype is characterized by low levels of T cells and B cells, with a high infiltration of *FOXP3*+ regulatory T cells (Tregs), a higher tumor budding rate, and mutations in *CDKN2A*, *SMAD4*, and *PIK3CA*. Notably, this subtype displays significantly higher levels of CA19-9, which is typically associated with poor prognosis. This subtype is strongly correlated with the previously identified squamous/mesenchymal subtype. Moreover, their study suggests that targeting the MET pathway may be effective for the immune escape subtype. The immune rich phenotype is characterized by abundant T cell and B cell infiltration, with fewer *FOXP3*+ Tregs, lower tumor budding frequency, and low mutations in *CDKN2A* and *PIK3CA*. The CA19-9 levels are the lowest among the three groups, which correlates with the best prognosis. This subtype is associated with the pancreatic progenitor subtype. The immune exhausted subtype is characterized by an immunogenic microenvironment and includes two distinct subgroups. One subgroup shows *PD-L1* expression and higher *PIK3CA* mutations, while the other is a microsatellite unstable subgroup with higher *JAK3* mutations. Interestingly, despite being classified as immune exhausted, this subtype has a relatively better overall prognosis. Furthermore, this immune exhausted subtype is highly correlated with the immunogenic subtype proposed by Bailey et al.

In 2019, Danilova et al. defined four immune subtypes of pancreatic cancer based on the expression of *CD8* and *PD-L1*: *PD-L1+/CD8high*, *PD-L1+/CD8low*, *PD-L1-/CD8high*, and *PD-L1-/CD8low* (107). *PD-L1* expression is associated with poor prognosis, while CD8+ T cell infiltration correlates with better prognosis.

In 2019, a meta-analysis based on 353 pancreatic cancer patients classified the disease into three subtypes: innate immune, T cell dominant, and tumor dominant (108). The innate immune subtype shows enrichment of natural killer (NK) cells and neutrophils, accompanied by reactive stromal proliferation. The neutrophil enrichment suggests its potential as a biomarker and clinical therapeutic target. This subtype is most strongly associated with the squamous subtype identified by Bailey et al. and is correlated with better prognosis. The T cell dominant subtype is characterized by the accumulation of many tumor-infiltrating immune subpopulations related to adaptive immunity, including activated CD8+ and CD4+ T cells as well as B cells. Moreover, genes involved in immune checkpoint inhibition, such as *CTLA4* and *BTLA*, are significantly upregulated, suggesting potential responsiveness to ICB therapy. This subtype is closely associated with previously identified "exocrine-like," "ADEX," and "Notch" subtypes and shows a better prognosis than the innate immune subtype. The tumor dominant subtype is characterized by a unique microenvironment with a lack of tumor-infiltrating lymphocytes, high expression of adhesion-related and epithelial genes, and high expression of *GATA6*. This subtype overlaps with the classical subtype identified by Collisson et al.

In 2020, a study integrating genomic, epigenomic, transcriptomic, and clinical data from 161 pancreatic cancer patients established four molecular subgroups (iC1/iC2/iC3/iC4) (109). The study found that the iC1 subgroup exhibited significantly higher immune scores in B cells, CD4+ T cells, neutrophils, macrophages, and dendritic cells compared to the other three subgroups. The immune characteristic scores for macrophage regulation, lymphocyte infiltration, IFN-γ response, and TGF-β response were also higher in the iC1 subgroup, suggesting its potential applicability for immune therapy.

In 2022, a clustering analysis of 176 PAAD samples from the TCGA cohort identified two CD8+ T cell-related subtypes, IC1 and IC2 (110). Among the 10 oncogenic pathways, four pathways showed significant differences between the two subtypes: cell cycle, Hippo, Nrf1, and Wnt pathways. In the IC1 subtype, the enrichment scores for these pathways were markedly higher than those in the IC2 subtype. However, the IC2 subtype displayed its own characteristics, with higher immune infiltration scores compared to IC1. Additionally, the expression levels of most immune checkpoint-related genes were significantly higher in IC2, indicating its potential suitability for immune therapy. Regarding chemotherapy, IC1 demonstrated greater sensitivity to traditional chemotherapeutic drugs.

In 2022, a study by Hwang et al. performed RNA sequencing on 43 tumor samples and successfully identified three distinct clusters: "treatment-enriched," "squamoid-basaloid," and "classical" (111). The "treatment-enriched" cluster was closely associated with neuroendocrine-like malignant programs, neurotrophic CAF programs, and CD8+ T cells. The "squamoid-basaloid" cluster was linked to squamous, basaloid malignant programs, and various lymphoid and myeloid cells. The "classical" cluster was associated with classical malignant programs, myofibroblast progenitor cells, adhesion CAF programs, macrophages, neutrophils, and type 2 dendritic cells.

In 2022, Tong et al. identified five tumor subgroups with distinct immune and stromal features through multi-omics analysis: Im-S-I (Stromal), Im-S-II (Monocyte-Inflamed), Im-S-III (Macrophage-Inflamed), Im-S-IV (Metabolic-Neuron-Inflamed), and Im-S-V (Metabolic-cDC-Inflamed) (90). The stromal subgroup was characterized by elevated expression of endothelial cells and stromal-associated proteins (*COL17A1*, *COL7A1*, *ITGA3*, etc.), along with upregulated *EGFR* and *ERBB2* signaling pathways. The monocyte-inflamed subgroup was characterized by high monocyte infiltration levels. The macrophage-inflamed subgroup displayed tumor-associated macrophage (TAM) infiltration, with increased expression of immune evasion markers like *HAVCR2* (*TIM-3*), and had a relatively poorer prognosis. The metabolic-neuron-inflamed subgroup was characterized by neuronal features, with upregulated neuronal receptors and channels. The metabolic-cDC-inflamed subgroup was marked by increases in cDCs, CD4+ T cells, and B cells, and pathway analysis indicated upregulation of triglyceride and lipid breakdown processes. Furthermore, antigen-presentation MHC molecules, including *HLA-E*, *HLA-DQA1*, *HLA-DQB1*, and *HLA-DRA*, were also enhanced in this subgroup. Additionally, the study explored the relationship between these subtypes and age, revealing that older patients had more immune cell infiltration than younger patients, suggesting that immune therapy may be more beneficial for older patients.

In 2022, Wang et al. used the ICGC database to classify the PDAC cohort into four subtypes: Immune-enrich-Stroma, Non-immune-Stroma, Immune-enrich-non-Stroma, and Nonimmune-non-Stroma (112). The Immune- enrich -Stroma subtype was primarily enriched in tumor immune-related molecular features. The Non- immune -Stroma subtype was characterized by features such as *PD-1* resistance, activated stroma, CAF stimulation, and normal stroma, with very low immune-related characteristics. The Immune-enrich-non-Stroma subtype was mainly enriched in tumor immune-related features, with very low expression of stromal characteristics. The Nonimmune-non-Stroma subtype exhibited few immune and stromal features.

In 2023, our team performed clustering analysis on 178 samples from the TCGA database and identified two subtypes: High TAM2 Infiltration (HMI) and Low TAM2 Infiltration (LMI) (113). The HMI cluster was characterized by genes involved in various classical tumor signaling pathways and immune processes, including *PI3K-AKT*, *NF-κB*, and *IL-17* signaling pathways, and showed a low response rate to immunotherapy, possibly related to TAM2 enrichment. However, the KEGG pathways involved in the LMI cluster were not related to tumor progression or immune response, but this subtype was sensitive to traditional chemotherapy drugs such as oxaliplatin and exhibited a better response to immunotherapy than the HMI subtype.

In 2023, Zheng et al. classified patients into two molecular subtypes of PDAC based on T cell marker genes (TMGs): Proliferative PDAC (C1) and Immune PDAC (C2) (114). The C1 group (high TMGs) was significantly enriched in cell cycle and cell proliferation-related pathways, while the C2 group (low TMGs) was enriched in immune-related pathways. The high TMGs group was significantly associated with poor overall survival (OS), suggesting that TMGs may serve as a reliable prognostic biomarker for PDAC.

In 2024, van Eijck et al. demonstrated that tumors with high *GATA6* expression exhibited reduced infiltration of immunosuppressive regulatory T cells and M2 macrophages while showing increased infiltration of immune-stimulating, antigen-presenting, and activated T cells. This study suggested that *GATA6* defines an immune-enriched phenotype, which is associated with favorable outcomes for pancreatic cancer patients undergoing preoperative treatment (57).

In 2024, George B et al. conducted a transcriptomic analysis of the tumor microenvironment (TME) in 1,657 pancreatic cancer samples from public databases and validated their findings using an independent cohort of 79 patients. Based on their analysis, the TME was classified into four subtypes: immune enriched (IE), immune enriched with fibrosis (IE/F), fibrotic (F), and immune depleted (D). The IE subtype exhibited the highest levels of anti-tumor immune components, including T cells, B cells, and natural killer cells, while also showing elevated tumor-promoting immune components, such as regulatory T cells and immune checkpoint molecules. However, the anti-tumor immune signals remained predominant. The IE/F subtype was characterized by a balanced activation of both anti-tumor and tumor-promoting immune components, with the highest activation of the WNT signaling pathway. The F subtype displayed the strongest enrichment of cancer-associated fibroblast (CAF) pathways and angiogenesis-related signals. In contrast, the D subtype exhibited the highest levels of proliferative gene signatures. Additionally, the study revealed that most lung metastases were classified as the IE subtype, whereas liver metastases were predominantly of the D subtype. The IE/F subtype showed a strong resemblance to Bailey's ADEX subtype, while Bailey's immunogenic subtype largely overlapped with the IE and IE/F subtypes identified in this study. The F and D TME subtypes were associated with Moffitt's and Bailey's classifications (basal-like and squamous subtypes, respectively) and were linked to the poorest prognosis. Furthermore, differences in surface biomarkers were observed among the TME subtypes, providing potential therapeutic implications for PDAC patients. Specifically, immune-regulatory surface biomarkers were most highly expressed in the IE and IE/F subtypes, stromal proteins were predominantly expressed in the F subtype, and signaling molecules associated with tumor invasion and survival were highly expressed in the D subtype (115).

In these studies, each subtype exhibits distinct immune characteristics, including but not limited to tumor mutational burden (TMB), *PD-1/PD-L1* levels, mismatch repair (MMR), immune checkpoint inhibitors, stromal components, and TGF-β responses. For tumor subtypes with high TMB, vaccine-based therapies may be a more suitable option, as a higher TMB indicates the presence of more genetic mutations within tumor cells, providing additional targets for vaccine-induced immune responses. In cases where a tumor subtype exhibits a higher expression of immune checkpoints, this subtype may be more sensitive to immune checkpoint blockade (ICB) therapy. Immunotherapy may be effective for subtypes with elevated expression of immune cell death regulators (5). With the growing research on immune-related mechanisms, immune subtype-based therapies are expected to bring new hope to pancreatic cancer patients in the future.

3 Discussion

In pancreatic cancer research, molecular subtyping plays a central role in advancing precision medicine. However, current efforts to classify pancreatic cancer face significant challenges alongside emerging opportunities. Subtypes are primarily defined based on multiple dimensions, including gene mutations, genomics, transcriptomics, proteomics, metabolomics, and immunomics. Despite these classifications, no unified consensus has been established in the medical field, and progress in translating these classifications into clinical practice remains slow, significantly hindering the development of precision medicine for pancreatic cancer.

From the perspective of multi-omics clinical trials, genomics-related trials such as NCT02869802, NCT05380414, and NCT04484636 provide crucial avenues for exploring the molecular mechanisms of pancreatic cancer. An in-depth analysis of multi-omics data from pancreatic cancer patients in the TCGA database—including gene expression profiles, methylation microarray data, and histone modification data—has led to the identification of multiple epigenetically dysregulated lncRNAs (epi - lncRNAs). These epi - lncRNAs exhibit significant genomic differences from non - epi - lncRNAs, such as increased length, a higher number of transcripts, and more exons. Further screening identified five pancreatic cancer-specific epi-lncRNA genes (AL161431.1, LINC00663, LINC00941, SNHG10, and TM4SF1-AS1), which were used to construct a prognostic model. This model demonstrated strong prognostic predictive performance across different datasets, highlighting the critical role of genomics in pancreatic cancer subtyping research (116). Additionally, immunotherapy-related trials such as NCT01072981 and NCT06370754 have injected new momentum into research on immune-related pancreatic cancer subtypes.

The integration of multi-omics approaches offers promising prospects for pancreatic cancer subtyping. However, its clinical application presents both advantages and challenges. One of its key benefits is the ability to provide a comprehensive understanding of the molecular characteristics of pancreatic cancer, enabling more precise subtyping. By integrating genomics, transcriptomics, proteomics, metabolomics, and immunomics, researchers can conduct a holistic analysis of the complex biological processes underlying pancreatic cancer. For example, the combined use of the UK Biobank and multi-omics analyses has yielded significant findings. In one study (117), researchers integrated multi-omics

data from biobanks such as the UK Biobank, incorporating 4,611 genome-wide association studies (GWAS) and meta-analyses. By applying Mendelian randomization and colocalization analyses, they identified numerous disease-associated genetic loci, providing valuable insights for pancreatic cancer gene-disease association studies. Another multi-omics study (118) utilized UK Biobank data to train genetic scores for predicting multi-omics traits, conducting a phenome-wide association study that uncovered strong associations between multiple diseases and multi-omics characteristics. These findings contribute to a more comprehensive foundation for pancreatic cancer subtyping, facilitating the development of personalized treatment strategies and improving therapeutic outcomes.

Nevertheless, several challenges hinder the clinical application of multi-omics approaches. First, the acquisition and analysis of multi-omics data are costly. Genomic testing requires advanced sequencing platforms and substantial reagent investments, while proteomic and metabolomic analyses demand specialized equipment and intricate experimental procedures, limiting their widespread clinical adoption, particularly in resource-limited settings. Second, the interpretation of multi-omics data is highly complex. The vast amount of multi-dimensional data necessitates sophisticated analytical methods to extract clinically relevant insights. However, the intricate interconnections between different omics layers remain challenging to decipher, and the lack of standardized analytical approaches may lead to misinterpretation. Lastly, the standardization of multi-omics testing techniques remains insufficient. Variations in laboratory methodologies, workflows, and quality control standards contribute to inconsistencies in results, undermining the accuracy and reliability of multi-omics applications in clinical practice.

A detailed investigation has revealed that the difficulties associated with multi-omics-based subtyping are influenced by multiple complex factors. One of the most significant factors is sample purity. Pancreatic tumor samples often consist of a mixture of different cell types, and when purity is low, interference from non-tumor cells may obscure the molecular characteristics of tumor cells, leading to misclassification and a reduction in subtyping accuracy. Another important factor is the variability in analytical methodologies. Differences in experimental techniques and analytical algorithms across laboratories may lead to inconsistencies in the classification of the same tumor sample.

In addition, differences in sample composition may also interfere with subtyping. Cellular heterogeneity exists across different regions of a tumor, and variations in molecular characteristics between regions may introduce bias in classification if not adequately accounted for. Furthermore, tumor samples obtained through surgical procedures are often divided into separate sections for different types of analysis. This fragmented approach means that subtyping is frequently conducted on only part of a tumor rather than the entire tumor, which may lead to discrepancies in classification results. For example, transcriptomic analysis of one tumor section may identify a particular subtype, while proteomic analysis of another section may suggest a different classification. These findings highlight the necessity of conducting comprehensive and systematic analyses of whole tumor samples. Since tumors are complex mixtures of multiple cellular components, accurate classification requires considering them as integrated biological systems rather than isolated parts. Moreover, increasing sample size is essential to minimize the impact of individual heterogeneity. Conducting large-scale analyses across a substantial number of samples is crucial for accurately characterizing the molecular subtypes and biological patterns of pancreatic cancer.

Currently, combination therapy centered around chemotherapy remains the primary treatment for patients with advanced pancreatic cancer. As a result, many existing classification systems have been designed to predict chemotherapy response, providing a basis for clinical decision-making. By analyzing tumor gene expression profiles and proteomic features, these models can help predict a patient's sensitivity to different chemotherapy agents, thereby guiding the selection of the most appropriate treatment regimen.

At the same time, targeted therapy and immunotherapy have emerged as key areas of research. Targeted therapies selectively inhibit specific molecular targets unique to tumor cells, while immunotherapies activate the patient's immune system to combat cancer. These approaches are expected to expand treatment options and improve outcomes for pancreatic cancer patients. However, in clinical practice, tumor subtypes may change over the course of disease progression, which presents a significant challenge for precision medicine. A treatment strategy based on a patient's initial tumor subtype may lose effectiveness if the tumor undergoes subtype transformation. For instance, a tumor that initially responds well to a targeted therapy may develop resistance due to changes in its molecular subtype, ultimately reducing treatment efficacy.

Given these challenges, the development of low-cost, minimally invasive subtyping techniques is essential. Liquid biopsy (119) and circulating DNA (120) analysis have shown great potential. Liquid biopsy enables real-time, dynamic monitoring of tumor molecular characteristics by detecting tumor cells, tumor-derived DNA, RNA, and proteins in a patient's blood, providing a convenient and efficient approach for pancreatic cancer subtyping. Circulating DNA, which consists of DNA fragments released by tumor cells into the bloodstream, can be analyzed to identify tumor-specific mutations and methylation patterns, facilitating accurate subtype classification. For example, the detection of specific gene mutations in circulating DNA may enable rapid determination of a patient's tumor subtype, thereby offering timely guidance for precision treatment.

In the future, we hope to achieve a broad consensus on subtype-based treatments for pancreatic cancer, establish unified classification standards through multi-omics integration, and provide robust guidance for clinical management. Such advancements would bring renewed hope to pancreatic cancer patients and contribute to improving their quality of life.

Author contributions

ZF: Data curation, Visualization, Writing – original draft, Writing – review & editing. YX: Writing – review & editing. YD: Writing – review & editing. YZ: Software, Writing – review & editing. WZ: Funding acquisition, Supervision, Writing – review & editing.

Funding

The author(s) declare that financial support was received for the research and/or publication of this article. This study was supported by grants from National Natural Science Foundation of China (NO. 82260555), Gansu Provincial Top-notch Talent Program (NO (2023).9), Gansu Youth Science and Technology Foundation (NO.24JRRA374), Cuiying Science and Technology Innovation Project of the Second Hospital of Lanzhou University (NO.CY2024-CQ-01& CY2023-YB-A02).

Acknowledgments

We would like to express our sincere gratitude to all those who contributed to this study. Special thanks to D.Y. for providing the conceptual framework and guiding the overall direction of the research. We would also like to acknowledge X.Y. for their valuable input in revising the manuscript and Z.Y. for their meticulous work in preparing the figures and tables. Furthermore, we would like to thank BioRender (www.biorender.com) for providing the professional illustration tools used in the creation of the figures in this manuscript. Finally, Z.W.C. would like to acknowledge the support from their respective institutions, as well as the valuable feedback from the reviewers.

Conflict of interest

The authors declare that the research was conducted in the absence of any commercial or financial relationships that could be construed as a potential conflict of interest.

Generative AI statement

The author(s) declare that no Generative AI was used in the creation of this manuscript.

Publisher's note

All claims expressed in this article are solely those of the authors and do not necessarily represent those of their affiliated organizations, or those of the publisher, the editors and the reviewers. Any product that may be evaluated in this article, or claim that may be made by its manufacturer, is not guaranteed or endorsed by the publisher.

References

1. Siegel RL, Giaquinto AN, Jemal A. Cancer statistics, 2024. *CA Cancer J Clin*. (2024) 74:12–49. doi: 10.3322/caac.21820

2. Rahib L, Smith BD, Aizenberg R, Rosenzweig AB, Fleshman JM, Matrisian LM. Projecting cancer incidence and deaths to 2030: the unexpected burden of thyroid, liver, and pancreas cancers in the United States. *Cancer Res*. (2014) 74:2913–21. doi: 10.1158/0008-5472.CAN-14-0155

3. Backx E, Coolens K, Van den Bossche J-L, Houbracken I, Espinet E, Rooman I. On the origin of pancreatic cancer: molecular tumor subtypes in perspective of exocrine cell plasticity. *Cell Mol Gastroenterol Hepatol*. (2022) 13:1243–53. doi: 10.1016/j.jcmgh.2021.11.010

4. Mizrahi JD, Surana R, Valle JW, Shroff RT. Pancreatic cancer. *Lancet*. (2020) 395:2008–20. doi: 10.1016/S0140-6736(20)30974-0

5. Huang X, Zhang G, Liang T. Subtyping for pancreatic cancer precision therapy. *Trends Pharmacol Sci*. (2022) 43:482–94. doi: 10.1016/j.tips.2022.03.005

6. Hu ZI, O'Reilly EM. Therapeutic developments in pancreatic cancer. *Nat Rev Gastroenterol Hepatol*. (2024) 21:7–24. doi: 10.1038/s41575-023-00840-w

7. Lambert A, Schwarz L, Borbath I, Henry A, Van Laethem J-L, Malka D, et al. An update on treatment options for pancreatic adenocarcinoma. *Ther Adv Med Oncol*. (2019) 11:1758835919875568. doi: 10.1177/1758835919875568

8. Wang J, Yang J, Narang A, He J, Wolfgang C, Li K, et al. Consensus, debate, and prospective on pancreatic cancer treatments. *J Hematol Oncol*. (2024) 17:92. doi: 10.1186/s13045-024-01613-x

9. Wang X, Yang J, Ren B, Yang G, Liu X, Xiao R, et al. Comprehensive multi-omics profiling identifies novel molecular subtypes of pancreatic ductal adenocarcinoma. *Genes Dis*. (2024) 11:101143. doi: 10.1016/j.gendis.2023.101143

10. Collisson EA, Bailey P, Chang DK, Biankin AV. Molecular subtypes of pancreatic cancer. *Nat Rev Gastroenterol Hepatol*. (2019) 16:207–20. doi: 10.1038/s41575-019-0109-y

11. Wasko UN, Jiang J, Dalton TC, Curiel-Garcia A, Edwards AC, Wang Y, et al. Tumour-selective activity of RAS-GTP inhibition in pancreatic cancer. *Nature*. (2024) 629:927–36. doi: 10.1038/s41586-024-07379-z

12. Wang S, Zheng Y, Yang F, Zhu L, Zhu X-Q, Wang Z-F, et al. The molecular biology of pancreatic adenocarcinoma: translational challenges and clinical perspectives. *Signal Transduct Target Ther*. (2021) 6:249. doi: 10.1038/s41392-021-00659-4

13. Wang X, Allen S, Blake JF, Bowcut V, Briere DM, Calinisan A, et al. Identification of MRTX1133, a noncovalent, potent, and selective KRAS(G12D) inhibitor. *J Med Chem*. (2022) 65:3123–33. doi: 10.1021/acs.jmedchem.1c01688

14. Jiang J, Jiang L, Maldonato BJ, Wang Y, Holderfield M, Aronchik I, et al. Translational and therapeutic evaluation of RAS-GTP inhibition by RMC-6236 in RAS-driven cancers. *Cancer Discovery*. (2024) 14:994–1017. doi: 10.1158/2159-8290.CD-24-0027

15. Nagashima T, Inamura K, Nishizono Y, Suzuki A, Tanaka H, Yoshinari T, et al. ASP3082, a First-in-class novel KRAS G12D degrader, exhibits remarkable anti-tumor activity in KRAS G12D mutated cancer models. *Eur J Cancer*. (2022). https://api.semanticscholar.org/CorpusID:253220097.

16. Hofmann MH, Gmachl M, Ramharter J, Savarese F, Gerlach D, Marszalek JR, et al. BI-3406, a potent and selective SOS1-KRAS interaction inhibitor, is effective in KRAS-driven cancers through combined MEK inhibition. *Cancer Discovery*. (2021) 11:142–57. doi: 10.1158/2159-8290.CD-20-0142

17. Strickler JH, Satake H, George TJ, Yaeger R, Hollebecque A, Garrido-Laguna I, et al. Sotorasib in KRAS p.G12C-mutated advanced pancreatic cancer. *N Engl J Med*. (2023) 388:33–43. doi: 10.1056/NEJMoa2208470

18. Qian Y, Gong Y, Fan Z, Luo G, Huang Q, Deng S, et al. Molecular alterations and targeted therapy in pancreatic ductal adenocarcinoma. *J Hematol Oncol*. (2020) 13:130. doi: 10.1186/s13045-020-00958-3

19. Qin S, Li J, Bai Y, Wang Z, Chen Z, Xu R, et al. Nimotuzumab plus gemcitabine for K-ras wild-type locally advanced or metastatic pancreatic cancer. *J Clin Oncol*. (2023) 41:5163–73. doi: 10.1200/JCO.22.02630

20. Murphy SJ, Hart SN, Lima JF, Kipp BR, Klebig M, Winters JL, et al. Genetic alterations associated with progression from pancreatic intraepithelial neoplasia to invasive pancreatic tumor. *Gastroenterology*. (2013) 145:1098–1109.e1. doi: 10.1053/j.gastro.2013.07.049

21. Sallman DA, DeZern AE, Garcia-Manero G, Steensma DP, Roboz GJ, Sekeres MA, et al. Eprenetapopt (APR-246) and azacitidine in TP53-mutant myelodysplastic syndromes. *J Clin Oncol*. (2021) 39:1584–94. doi: 10.1200/JCO.20.02341

22. Song H, Wu J, Tang Y, Dai Y, Xiang X, Li Y, et al. Diverse rescue potencies of p53 mutations to ATO are predetermined by intrinsic mutational properties. *Sci Transl Med*. (2023) 15:eabn9155. doi: 10.1126/scitranslmed.abn9155

23. Tang Y, Song H, Wang Z, Xiao S, Xiang X, Zhan H, et al. Repurposing antiparasitic antimonials to noncovalently rescue temperature-sensitive p53 mutations. *Cell Rep*. (2022) 39:110622. doi: 10.1016/j.celrep.2022.110622

24. Yamada S, Fujii T, Shimoyama Y, Kanda M, Nakayama G, Sugimoto H, et al. SMAD4 expression predicts local spread and treatment failure in resected pancreatic cancer. *Pancreas*. (2015) 44:660–4. doi: 10.1097/MPA.0000000000000315

25. Christenson ES, Jaffee E, Azad NS. Current and emerging therapies for patients with advanced pancreatic ductal adenocarcinoma: a bright future. *Lancet Oncol*. (2020) 21:e135–45. doi: 10.1016/S1470-2045(19)30795-8

26. Waddell N, Pajic M, Patch A-M, Chang DK, Kassahn KS, Bailey P, et al. Whole genomes redefine the mutational landscape of pancreatic cancer. *Nature*. (2015) 518:495–501. doi: 10.1038/nature14169

27. Shi S, Ji S, Qin Y, Xu J, Zhang B, Xu W, et al. Metabolic tumor burden is associated with major oncogenomic alterations and serum tumor markers in patients with resected pancreatic cancer. *Cancer Lett*. (2015) 360:227–33. doi: 10.1016/j.canlet.2015.02.014

28. Lee M, Ham H, Lee J, Lee ES, Chung CH, Kong D-H, et al. TGF-β-induced PAUF plays a pivotal role in the migration and invasion of human pancreatic ductal adenocarcinoma cell line panc-1. *Int J Mol Sci*. (2024) 25. doi: 10.3390/ijms252111420

29. Ligorio M, Sil S, Malagon-Lopez J, Nieman LT, Misale S, Di Pilato M, et al. Stromal microenvironment shapes the intratumoral architecture of pancreatic cancer. *Cell*. (2019) 178:160–175.e27. doi: 10.1016/j.cell.2019.05.012

30. Qiang L, Hoffman MT, Ali LR, Castillo JI, Kageler L, Temesgen A, et al. Transforming growth factor-β Blockade in pancreatic cancer enhances sensitivity to combination chemotherapy. *Gastroenterology*. (2023) 165:874–890.e10. doi: 10.1053/j.gastro.2023.05.038

31. Hong E, Barczak W, Park S, Heo JS, Ooshima A, Munro S, et al. Combination treatment of T1-44, a PRMT5 inhibitor with Vactosertib, an inhibitor of TGF-β signaling, inhibits invasion and prolongs survival in a mouse model of pancreatic tumors. *Cell Death Dis*. (2023) 14:93. doi: 10.1038/s41419-023-05630-5

32. Connor AA, Denroche RE, Jang GH, Lemire M, Zhang A, Chan-Seng-Yue M, et al. Integration of genomic and transcriptional features in pancreatic cancer reveals increased cell cycle progression in metastases. *Cancer Cell*. (2019) 35:267–282.e7. doi: 10.1016/j.ccell.2018.12.010

33. Goodwin CM, Waters AM, Klomp JE, Javaid S, Bryant KL, Stalnecker CA, et al. Combination therapies with CDK4/6 inhibitors to treat KRAS-mutant pancreatic cancer. *Cancer Res*. (2023) 83:141–57. doi: 10.1158/0008-5472.CAN-22-0391

34. Ying H, Kimmelman AC, Bardeesy N, Kalluri R, Maitra A, DePinho RA. Genetics and biology of pancreatic ductal adenocarcinoma. *Genes Dev*. (2025) 39:36–63. doi: 10.1101/gad.351863.124

35. Ying H, Dey P, Yao W, Kimmelman AC, Draetta GF, Maitra A, et al. Genetics and biology of pancreatic ductal adenocarcinoma. *Genes Dev*. (2016) 30:355–85. doi: 10.1101/gad.275776.115

36. Shen G-Q, Aleassa EM, Walsh RM, Morris-Stiff G. Next-generation sequencing in pancreatic cancer. *Pancreas*. (2019) 48:739–48. doi: 10.1097/MPA.0000000000001324

37. Li X, Jiang W, Dong S, Li W, Zhu W, Zhou W. STAT3 inhibitors: A novel insight for anticancer therapy of pancreatic cancer. *Biomolecules*. (2022) 12. doi: 10.3390/biom12101450

38. Shindo K, Yu J, Suenaga M, Fesharakizadeh S, Cho C, Macgregor-Das A, et al. Deleterious germline mutations in patients with apparently sporadic pancreatic adenocarcinoma. *J Clin Oncol*. (2017) 35:3382–90. doi: 10.1200/JCO.2017.72.3502

39. Boursi B, Wileyto EP, Mamtani R, Domchek SM, Golan T, Hood R, et al. Analysis of BRCA1- and BRCA2-related pancreatic cancer and survival. *JAMA Netw Open*. (2023) 6:e2345013. doi: 10.1001/jamanetworkopen.2023.45013

40. Golan T, Hammel P, Reni M, Van Cutsem E, Macarulla T, Hall MJ, et al. Maintenance olaparib for germline BRCA-mutated metastatic pancreatic cancer. *N Engl J Med*. (2019) 381:317–27. doi: 10.1056/NEJMoa1903387

41. Hu Q, Qin Y, Ji S, Shi X, Dai W, Fan G, et al. MTAP deficiency-induced metabolic reprogramming creates a vulnerability to cotargeting *de novo* purine synthesis and glycolysis in pancreatic cancer. *Cancer Res*. (2021) 81:4964–80. doi: 10.1158/0008-5472.CAN-20-0414

42. Lee MKC, Grimmond SM, McArthur GA, Sheppard KE. PRMT5: an emerging target for pancreatic adenocarcinoma. *Cancers (Basel)*. (2021) 13. doi: 10.3390/cancers13205136

43. Chan-Seng-Yue M, Kim JC, Wilson GW, Ng K, Figueroa EF, O'Kane GM, et al. Transcription phenotypes of pancreatic cancer are driven by genomic events during tumor evolution. *Nat Genet*. (2020) 52:231–40. doi: 10.1038/s41588-019-0566-9

44. Molenaar JJ, Koster J, Zwijnenburg DA, van Sluis P, Valentijn LJ, van der Ploeg I, et al. Sequencing of neuroblastoma identifies chromothripsis and defects in neuritogenesis genes. *Nature*. (2012) 483:589–93. doi: 10.1038/nature10910

45. Li E, Huang X, Zhang G, Liang T. Combinational blockade of MET and PD-L1 improves pancreatic cancer immunotherapeutic efficacy. *J Exp Clin Cancer Res*. (2021) 40:279. doi: 10.1186/s13046-021-02055-w

46. Peng Y-P, Zhu Y, Yin L-D, Wei J-S, Liu X-C, Zhu X-L, et al. PIK3R3 promotes metastasis of pancreatic cancer via ZEB1 induced epithelial-mesenchymal transition. *Cell Physiol Biochem*. (2018) 46:1930–8. doi: 10.1159/000489382

47. Lin T, Ren Q, Zuo W, Jia R, Xie L, Lin R, et al. Valproic acid exhibits anti-tumor activity selectively against EGFR/ErbB2/ErbB3-coexpressing pancreatic cancer via induction of ErbB family members-targeting microRNAs. *J Exp Clin Cancer Res*. (2019) 38:150. doi: 10.1186/s13046-019-1160-9

48. Sivaram N, McLaughlin PA, Han HV, Petrenko O, Jiang Y-P, Ballou LM, et al. Tumor-intrinsic PIK3CA represses tumor immunogenecity in a model of pancreatic cancer. *J Clin Invest*. (2019) 129:3264–76. doi: 10.1172/JCI123540

49. Huang X, Zhang G. Split cyclin-dependent kinase 4/6-retinoblastoma 1 axis in pancreatic cancer. *Front Cell Dev Biol*. (2020) 8:602352. doi: 10.3389/fcell.2020.602352

50. Tutt A, Gabriel A, Bertwistle D, Connor F, Paterson H, Peacock J, et al. Absence of Brca2 causes genome instability by chromosome breakage and loss associated with centrosome amplification. *Curr Biol*. (1999) 9:1107–10. doi: 10.1016/s0960-9822(99)80479-5

51. Safarzad M, Besharat S, Salimi S, Azarhoush R, Behnampour N, Joshaghani HR. Association between selenium, cadmium, and arsenic levels and genetic polymorphisms in DNA repair genes (XRCC5, XRCC6) in gastric cancerous and non-cancerous tissue. *J Trace Elem Med Biol*. (2019) 55:89–95. doi: 10.1016/j.jtemb.2019.06.003

52. Connor AA, Denroche RE, Jang GH, Timms L, Kalimuthu SN, Selander I, et al. Association of distinct mutational signatures with correlates of increased immune activity in pancreatic ductal adenocarcinoma. *JAMA Oncol*. (2017) 3:774–83. doi: 10.1001/jamaoncol.2016.3916

53. Van Allen EM, Miao D, Schilling B, Shukla SA, Blank C, Zimmer L, et al. Genomic correlates of response to CTLA-4 blockade in metastatic melanoma. *Science*. (2015) 350:207–11. doi: 10.1126/science.aad0095

54. Collisson EA, Sadanandam A, Olson P, Gibb WJ, Truitt M, Gu S, et al. Subtypes of pancreatic ductal adenocarcinoma and their differing responses to therapy. *Nat Med*. (2011) 17:500–3. doi: 10.1038/nm.2344

55. Kim S, Kang M, Lee S, Bae S, Han S, Jang J-Y, et al. Identifying molecular subtypes related to clinicopathologic factors in pancreatic cancer. *BioMed Eng Online*. (2014) 13 Suppl 2:S5. doi: 10.1186/1475-925X-13-S2-S5

56. Moffitt RA, Marayati R, Flate EL, Volmar KE, Loeza SGH, Hoadley KA, et al. Virtual microdissection identifies distinct tumor- and stroma-specific subtypes of pancreatic ductal adenocarcinoma. *Nat Genet*. (2015) 47:1168–78. doi: 10.1038/ng.3398

57. van Eijck CWF, Real FX, Malats N, Vadgama D, van den Bosch TPP, Doukas M, et al. GATA6 identifies an immune-enriched phenotype linked to favorable outcomes in patients with pancreatic cancer undergoing upfront surgery. *Cell Rep Med*. (2024) 5:101557. doi: 10.1016/j.xcrm.2024.101557

58. Noll EM, Eisen C, Stenzinger A, Espinet E, Muckenhuber A, Klein C, et al. CYP3A5 mediates basal and acquired therapy resistance in different subtypes of pancreatic ductal adenocarcinoma. *Nat Med*. (2016) 22:278–87. doi: 10.1038/nm.4038

59. Bailey P, Chang DK, Nones K, Johns AL, Patch A-M, Gingras M-C, et al. Genomic analyses identify molecular subtypes of pancreatic cancer. *Nature*. (2016) 531:47–52. doi: 10.1038/nature16965

60. Raphael BJ, Hruban RH, Aguirre AJ, Moffitt RA, Yeh JJ, Stewart C, et al. Integrated genomic characterization of pancreatic ductal adenocarcinoma. *Cancer Cell*. (2017) 32:185–203.e13. doi: 10.1016/j.ccell.2017.07.007

61. Puleo F, Nicolle R, Blum Y, Cros J, Marisa L, Demetter P, et al. Stratification of pancreatic ductal adenocarcinomas based on tumor and microenvironment features. *Gastroenterology*. (2018) 155:1999–2013.e3. doi: 10.1053/j.gastro.2018.08.033

62. Maurer C, Holmstrom SR, He J, Laise P, Su T, Ahmed A, et al. Experimental microdissection enables functional harmonisation of pancreatic cancer subtypes. *Gut*. (2019) 68:1034–43. doi: 10.1136/gutjnl-2018-317706

63. Janky R, Binda MM, Allemeersch J, Van den Broeck A, Govaere O, Swinnen JV, et al. Prognostic relevance of molecular subtypes and master regulators in pancreatic ductal adenocarcinoma. *BMC Cancer*. (2016) 16:632. doi: 10.1186/s12885-016-2540-6

64. Dijk F, Veenstra VL, Soer EC, Dings MPG, Zhao L, Halfwerk JB, et al. Unsupervised class discovery in pancreatic ductal adenocarcinoma reveals cell-intrinsic mesenchymal features and high concordance between existing classification systems. *Sci Rep*. (2020) 10:337. doi: 10.1038/s41598-019-56826-9

65. Birnbaum DJ, Begg SKS, Finetti P, Vanderburg C, Kulkarni AS, Neyaz A, et al. Transcriptomic analysis of laser capture microdissected tumors reveals cancer- and stromal-specific molecular subtypes of pancreatic ductal adenocarcinoma. *Clin Cancer Res*. (2021) 27:2314–25. doi: 10.1158/1078-0432.CCR-20-1039

66. Sivakumar S, de Santiago I, Chlon L, Markowetz F. Master regulators of oncogenic KRAS response in pancreatic cancer: an integrative network biology analysis. *PloS Med*. (2017) 14:e1002223. doi: 10.1371/journal.pmed.1002223

67. Mueller S, Engleitner T, Maresch R, Zukowska M, Lange S, Kaltenbacher T, et al. Evolutionary routes and KRAS dosage define pancreatic cancer phenotypes. *Nature*. (2018) 554:62–8. doi: 10.1038/nature25459

68. Espinet E, Gu Z, Imbusch CD, Giese NA, Büscher M, Safavi M, et al. Aggressive PDACs show hypomethylation of repetitive elements and the execution of an intrinsic IFN program linked to a ductal cell of origin. *Cancer Discovery*. (2021) 11:638–59. doi: 10.1158/2159-8290.CD-20-1202

69. Ju J, Wismans LV, Mustafa DAM, Reinders MJT, van Eijck CHJ, Stubbs AP, et al. Robust deep learning model for prognostic stratification of pancreatic ductal adenocarcinoma patients. *iScience*. (2021) 24:103415. doi: 10.1016/j.isci.2021.103415

70. Shi X, Li Y, Yuan Q, Tang S, Guo S, Zhang Y, et al. Integrated profiling of human pancreatic cancer organoids reveals chromatin accessibility features associated with drug sensitivity. *Nat Commun*. (2022) 13:2169. doi: 10.1038/s41467-022-29857-6

71. Zheng Y, Li X, Deng S, Zhao H, Ye Y, Zhang S, et al. CSTF2 mediated mRNA N (6)-methyladenosine modification drives pancreatic ductal adenocarcinoma m(6)A subtypes. *Nat Commun*. (2023) 14:6334. doi: 10.1038/s41467-023-41861-y

72. Kim S, Leem G, Choi J, Koh Y, Lee S, Nam S-H, et al. Integrative analysis of spatial and single-cell transcriptome data from human pancreatic cancer reveals an intermediate cancer cell population associated with poor prognosis. *Genome Med*. (2024) 16:20. doi: 10.1186/s13073-024-01287-7

73. Barkley D, Moncada R, Pour M, Liberman DA, Dryg I, Werba G, et al. Cancer cell states recur across tumor types and form specific interactions with the tumor microenvironment. *Nat Genet*. (2022) 54:1192–201. doi: 10.1038/s41588-022-01141-9

74. Chia L, Wang B, Kim J-H, Luo LZ, Shuai S, Herrera I, et al. HMGA1 induces FGF19 to drive pancreatic carcinogenesis and stroma formation. *J Clin Invest*. (2023) 133. doi: 10.1172/JCI151601

75. Luo Z, Zheng Q, Ye S, Li Y, Chen J, Fan C, et al. HMGA2 alleviates ferroptosis by promoting GPX4 expression in pancreatic cancer cells. *Cell Death Dis*. (2024) 15:220. doi: 10.1038/s41419-024-06592-y

76. Wiedmann L, De Angelis Rigotti F, Vaquero-Siguero N, Donato E, Espinet E, Moll I, et al. HAPLN1 potentiates peritoneal metastasis in pancreatic cancer. *Nat Commun*. (2023) 14:2353. doi: 10.1038/s41467-023-38064-w

77. Tonelli C, Yordanov GN, Hao Y, Deschênes A, Hinds J, Belleau P, et al. A mucus production programme promotes classical pancreatic ductal adenocarcinoma. *Gut*. (2024) 73:941–54. doi: 10.1136/gutjnl-2023-329839

78. Lupo F, Pezzini F, Pasini D, Fiorini E, Adamo A, Veghini L, et al. Axon guidance cue SEMA3A promotes the aggressive phenotype of basal-like PDAC. *Gut*. (2024) 73:1321–35. doi: 10.1136/gutjnl-2023-329807

79. Carpenter ES, Kadiyala P, Elhossiny AM, Kemp SB, Li J, Steele NG, et al. KRT17high/CXCL8+ Tumor cells display both classical and basal features and regulate myeloid infiltration in the pancreatic cancer microenvironment. *Clin Cancer Res*. (2024) 30:2497–513. doi: 10.1158/1078-0432.CCR-23-1421

80. Yoo H-B, Moon JW, Kim H-R, Lee HS, Miyabayashi K, Park CH, et al. A TEAD2-driven endothelial-like program shapes basal-like differentiation and metastasis of pancreatic cancer. *Gastroenterology*. (2023) 165:133–148.e17. doi: 10.1053/j.gastro.2023.02.049

81. Kisling SG, Atri P, Shah A, Cox JL, Sharma S, Smith LM, et al. A novel HOXA10-associated 5-gene-based prognostic signature for stratification of short-term survivors of pancreatic ductal adenocarcinoma. *Clin Cancer Res*. (2023) 29:3759–70. doi: 10.1158/1078-0432.CCR-23-0825

82. Alfarano G, Audano M, Di Chiaro P, Balestrieri C, Milan M, Polletti S, et al. Interferon regulatory factor 1 (IRF1) controls the metabolic programmes of low-grade pancreatic cancer cells. *Gut*. (2023) 72:109–28. doi: 10.1136/gutjnl-2021-325811

83. Maurin M, Ranjouri M, Megino-Luque C, Newberg JY, Du D, Martin K, et al. RBFOX2 deregulation promotes pancreatic cancer progression and metastasis through alternative splicing. *Nat Commun*. (2023) 14:8444. doi: 10.1038/s41467-023-44126-w

84. Zhou D, Guo S, Wang Y, Zhao J, Liu H, Zhou F, et al. Functional characteristics of DNA N6-methyladenine modification based on long-read sequencing in pancreatic cancer. *Brief Funct Genomics*. (2024) 23:150–62. doi: 10.1093/bfgp/elad021

85. Yin X, Kong L, Liu P. Identification of prognosis-related molecular subgroups based on DNA methylation in pancreatic cancer. *Clin Epigenet*. (2021) 13:109. doi: 10.1186/s13148-021-01090-w

86. Coleman O, Henry M, McVey G, Clynes M, Moriarty M, Meleady P. Proteomic strategies in the search for novel pancreatic cancer biomarkers and drug targets: recent advances and clinical impact. *Expert Rev Proteomics*. (2016) 13:383–94. doi: 10.1586/14789450.2016.1167601

87. Zhao L, Zhao H, Yan H. Gene expression profiling of 1200 pancreatic ductal adenocarcinoma reveals novel subtypes. *BMC Cancer*. (2018) 18:603. doi: 10.1186/s12885-018-4546-8

88. Law HC-H, Lagundžin D, Clement EJ, Qiao F, Wagner ZS, Krieger KL, et al. The proteomic landscape of pancreatic ductal adenocarcinoma liver metastases identifies molecular subtypes and associations with clinical response. *Clin Cancer Res*. (2020) 26:1065–76. doi: 10.1158/1078-0432.CCR-19-1496

89. Son M, Kim H, Han D, Kim Y, Huh I, Han Y, et al. A clinically applicable 24-protein model for classifying risk subgroups in pancreatic ductal adenocarcinomas using multiple reaction monitoring-mass spectrometry. *Clin Cancer Res*. (2021) 27:3370–82. doi: 10.1158/1078-0432.CCR-20-3513

90. Tong Y, Sun M, Chen L, Wang Y, Li Y, Li L, et al. Proteogenomic insights into the biology and treatment of pancreatic ductal adenocarcinoma. *J Hematol Oncol*. (2022) 15:168. doi: 10.1186/s13045-022-01384-3

91. Swietlik JJ, Bärthel S, Falcomatà C, Fink D, Sinha A, Cheng J, et al. Cell-selective proteomics segregates pancreatic cancer subtypes by extracellular proteins in tumors and circulation. *Nat Commun*. (2023) 14:2642. doi: 10.1038/s41467-023-38171-8

92. Hyeon DY, Nam D, Han Y, Kim DK, Kim G, Kim D, et al. Proteogenomic landscape of human pancreatic ductal adenocarcinoma in an Asian population reveals tumor cell-enriched and immune-rich subtypes. *Nat Cancer*. (2023) 4:290–307. doi: 10.1038/s43018-022-00479-7

93. Weiss F, Lauffenburger D, Friedl P. Towards targeting of shared mechanisms of cancer metastasis and therapy resistance. *Nat Rev Cancer*. (2022) 22:157–73. doi: 10.1038/s41568-021-00427-0

94. Daemen A, Peterson D, Sahu N, McCord R, Du X, Liu B, et al. Metabolite profiling stratifies pancreatic ductal adenocarcinomas into subtypes with distinct sensitivities to metabolic inhibitors. *Proc Natl Acad Sci U.S.A*. (2015) 112: E4410–4417. doi: 10.1073/pnas.1501605112

95. Nicolle R, Blum Y, Marisa L, Loncle C, Gayet O, Moutardier V, et al. Pancreatic adenocarcinoma therapeutic targets revealed by tumor-stroma cross-talk analyses in patient-derived xenografts. *Cell Rep*. (2017) 21:2458–70. doi: 10.1016/j.celrep.2017.11.003

96. Karasinska JM, Topham JT, Kalloger SE, Jang GH, Denroche RE, Culibrk L, et al. Altered gene expression along the glycolysis-cholesterol synthesis axis is associated with outcome in pancreatic cancer. *Clin Cancer Res*. (2020) 26:135–46. doi: 10.1158/1078-0432.CCR-19-1543

97. Mahajan UM, Alnatsha A, Li Q, Oehrle B, Weiss F-U, Sendler M, et al. Plasma metabolome profiling identifies metabolic subtypes of pancreatic ductal adenocarcinoma. *Cells*. (2021) 10. doi: 10.3390/cells10071821

98. Rodriguez E, Boelaars K, Brown K, Madunić K, van Ee T, Dijk F, et al. Analysis of the glyco-code in pancreatic ductal adenocarcinoma identifies glycan-mediated immune regulatory circuits. *Commun Biol*. (2022) 5:41. doi: 10.1038/s42003-021-02934-0

99. Li X, Du Y, Jiang W, Dong S, Li W, Tang H, et al. Integrated transcriptomics, proteomics and metabolomics-based analysis uncover TAM2-associated glycolysis and pyruvate metabolic remodeling in pancreatic cancer. *Front Immunol*. (2023) 14:1170223. doi: 10.3389/fimmu.2023.1170223

100. Wang H, Guo H, Sun J, Wang Y. Multi-omics analyses based on genes associated with oxidative stress and phospholipid metabolism revealed the intrinsic molecular characteristics of pancreatic cancer. *Sci Rep*. (2023) 13:13564. doi: 10.1038/s41598-023-40560-4

101. Li Y, Tang S, Shi X, Lv J, Wu X, Zhang Y, et al. Metabolic classification suggests the GLUT1/ALDOB/G6PD axis as a therapeutic target in chemotherapy-resistant pancreatic cancer. *Cell Rep Med*. (2023) 4:101162. doi: 10.1016/j.xcrm.2023.101162

102. Dammeijer F, van Gulijk M, Mulder EE, Lukkes M, Klaase L, van den Bosch T, et al. The PD-1/PD-L1-checkpoint restrains T cell immunity in tumor-draining lymph nodes. *Cancer Cell*. (2020) 38:685–700.e8. doi: 10.1016/j.ccell.2020.09.001

103. Zhang J, Huang D, Saw PE, Song E. Turning cold tumors hot: from molecular mechanisms to clinical applications. *Trends Immunol*. (2022) 43:523–45. doi: 10.1016/j.it.2022.04.010

104. Farhangnia P, Khorramdelazad H, Nickho H, Delbandi A-A. Current and future immunotherapeutic approaches in pancreatic cancer treatment. *J Hematol Oncol*. (2024) 17:40. doi: 10.1186/s13045-024-01561-6

105. Knudsen ES, Vail P, Balaji U, Ngo H, Botros IW, Makarov V, et al. Stratification of pancreatic ductal adenocarcinoma: combinatorial genetic, stromal, and immunologic markers. *Clin Cancer Res*. (2017) 23:4429–40. doi: 10.1158/1078-0432.CCR-17-0162

106. Wartenberg M, Cibin S, Zlobec I, Vassella E, Eppenberger-Castori S, Terracciano L, et al. Integrated genomic and immunophenotypic classification of pancreatic cancer reveals three distinct subtypes with prognostic/predictive significance. *Clin Cancer Res*. (2018) 24:4444–54. doi: 10.1158/1078-0432.CCR-17-3401

107. Danilova L, Ho WJ, Zhu Q, Vithayathil T, De-Jesus-Acosta A, Azad NS, et al. Programmed cell death ligand-1 (PD-L1) and CD8 expression profiling identify an immunologic subtype of pancreatic ductal adenocarcinomas with favorable survival. *Cancer Immunol Res*. (2019) 7:886–95. doi: 10.1158/2326-6066.CIR-18-0822

108. de Santiago I, Yau C, Heij L, Middleton MR, Markowetz F, Grabsch HI, et al. Immunophenotypes of pancreatic ductal adenocarcinoma: Meta-analysis of transcriptional subtypes. *Int J Cancer*. (2019) 145:1125–37. doi: 10.1002/ijc.32186

109. Kong L, Liu P, Zheng M, Xue B, Liang K, Tan X. Multi-omics analysis based on integrated genomics, epigenomics and transcriptomics in pancreatic cancer. *Epigenomics*. (2020) 12:507–24. doi: 10.2217/epi-2019-0374

110. Xu D, Wang Y, Chen Y, Zheng J. Identification of the molecular subtype and prognostic characteristics of pancreatic cancer based on CD8 + T cell-related genes. *Cancer Immunol Immunother*. (2023) 72:647–64. doi: 10.1007/s00262-022-03269-3

111. Hwang WL, Jagadeesh KA, Guo JA, Hoffman HI, Yadollahpour P, Reeves JW, et al. Single-nucleus and spatial transcriptome profiling of pancreatic cancer identifies multicellular dynamics associated with neoadjuvant treatment. *Nat Genet*. (2022) 54:1178–91. doi: 10.1038/s41588-022-01134-8

112. Wang X, Li L, Yang Y, Fan L, Ma Y, Mao F. Reveal the heterogeneity in the tumor microenvironment of pancreatic cancer and analyze the differences in prognosis and immunotherapy responses of distinct immune subtypes. *Front Oncol*. (2022) 12:832715. doi: 10.3389/fonc.2022.832715

113. Du Y, Dong S, Jiang W, Li M, Li W, Li X, et al. Integration of single-cell RNA sequencing and bulk RNA sequencing reveals that TAM2-driven genes affect immunotherapeutic response and prognosis in pancreatic cancer. *Int J Mol Sci*. (2023) 24. doi: 10.3390/ijms241612787

114. Zheng H, Li Y, Zhao Y, Jiang A. Single-cell and bulk RNA sequencing identifies T cell marker genes score to predict the prognosis of pancreatic ductal adenocarcinoma. *Sci Rep*. (2023) 13:3684. doi: 10.1038/s41598-023-30972-7

115. George B, Kudryashova O, Kravets A, Thalji S, Malarkannan S, Kurzrock R, et al. Transcriptomic-based microenvironment classification reveals precision medicine strategies for pancreatic ductal adenocarcinoma. *Gastroenterology*. (2024) 166:859–871.e3. doi: 10.1053/j.gastro.2024.01.028

116. Ke M. Identification and validation of apparent imbalanced epi-lncRNAs prognostic model based on multi-omics data in pancreatic cancer. *Front Mol Biosci*. (2022) 9:860323. doi: 10.3389/fmolb.2022.860323

117. Lessard S, Chao M, Reis K, Beauvais M, Rajpal DK, Sloane J, et al. Leveraging large-scale multi-omics evidences to identify therapeutic targets from genome-wide association studies. *BMC Genomics*. (2024) 25:1111. doi: 10.1186/s12864-024-10971-2

118. Xu Y, Ritchie SC, Liang Y, Timmers PRHJ, Pietzner M, Lannelongue L, et al. An atlas of genetic scores to predict multi-omic traits. *Nature*. (2023) 616:123–31. doi: 10.1038/s41586-023-05844-9

119. Ben-Ami R, Wang Q-L, Zhang J, Supplee JG, Fahrmann JF, Lehmann-Werman R, et al. Protein biomarkers and alternatively methylated cell-free DNA detect early stage pancreatic cancer. *Gut*. (2024) 73:639–48. doi: 10.1136/gutjnl-2023-331074

120. Yu B, Shao S, Ma W. Frontiers in pancreatic cancer on biomarkers, microenvironment, and immunotherapy. *Cancer Lett*. (2025) 610:217350. doi: 10.1016/j.canlet.2024.217350

frontiers | Frontiers in Oncology

TYPE Review
PUBLISHED 21 May 2025
DOI 10.3389/fonc.2025.1564226

Check for updates

OPEN ACCESS

EDITED BY
Ana Luísa De Sousa-Coelho,
Algarve Biomedical Center Research Institute (ABC-RI), Portugal

REVIEWED BY
Niki Millward,
University of Texas MD Anderson Cancer Center, United States
Johann Matschke,
Essen University Hospital, Germany

*CORRESPONDENCE
Fang Xu
xu27002@126.com
Chunhui Yang
yangchunhui627@163.com

†These authors have contributed equally to this work

RECEIVED 21 January 2025
ACCEPTED 02 May 2025
PUBLISHED 21 May 2025

CITATION
Cai H, Zhang F, Xu F and Yang C (2025) Metabolic reprogramming and therapeutic targeting in non-small cell lung cancer: emerging insights beyond the Warburg effect. *Front. Oncol.* 15:1564226.
doi: 10.3389/fonc.2025.1564226

COPYRIGHT
© 2025 Cai, Zhang, Xu and Yang. This is an open-access article distributed under the terms of the Creative Commons Attribution License (CC BY). The use, distribution or reproduction in other forums is permitted, provided the original author(s) and the copyright owner(s) are credited and that the original publication in this journal is cited, in accordance with accepted academic practice. No use, distribution or reproduction is permitted which does not comply with these terms.

Metabolic reprogramming and therapeutic targeting in non-small cell lung cancer: emerging insights beyond the Warburg effect

Hong Cai[1†], Feng Zhang[2†], Fang Xu[1*] and Chunhui Yang[1*]

[1]Department of Clinical Laboratory, The Second Hospital of Dalian Medical University, Dalian, Liaoning, China, [2]Department of Clinical Laboratory, Affiliated Zhongshan Hospital of Dalian University, Dalian, Liaoning, China

Non-small cell lung cancer (NSCLC) remains a leading cause of cancer-related mortality worldwide. Recent advancements have illuminated the intricate metabolic reprogramming that underpins NSCLC progression and resistance to therapy. Beyond the classical Warburg effect, emerging evidence highlights the pivotal roles of altered lipid metabolism, amino acid utilization, and the metabolic crosstalk within the tumor microenvironment (TME). This review delves into the latest discoveries in NSCLC metabolism, emphasizing novel pathways and mechanisms that contribute to tumor growth and survival. We critically assess the interplay between cancer cell metabolism and the TME, explore the impact of metabolic heterogeneity, and discuss how metabolic adaptations confer therapeutic resistance. By integrating insights from cutting-edge technologies such as single-cell metabolomics and spatial metabolomics, we identify potential metabolic vulnerabilities in NSCLC. Finally, we propose innovative therapeutic strategies that target these metabolic dependencies, including combination approaches that enhance the efficacy of existing treatments and pave the way for personalized metabolic therapies.

KEYWORDS

non-small cell lung cancer, metabolic reprogramming, tumor microenvironment, therapeutic targeting, metabolic vulnerabilities

1 Introduction

Lung cancer remains a global health challenge, being the leading cause of cancer-related mortality worldwide, with an estimated 2.2 million new cases and 1.8 million deaths in 2020 (1). NSCLC accounts for approximately 85% of all lung cancer cases and includes various histological subtypes such as adenocarcinoma, squamous cell carcinoma, and large cell carcinoma (2). Despite significant advances in surgical techniques, chemotherapy, targeted therapies, and immunotherapy, the overall five-year survival rate for NSCLC patients remains

low, particularly in advanced stages where it drops below 10% (3). Late diagnosis, tumor heterogeneity, and the development of resistance to conventional treatments contribute to this poor prognosis (4). Therefore, a deeper understanding of the underlying mechanisms driving NSCLC progression and therapeutic resistance is crucial for developing more effective treatments.

One area of intense research is the metabolic reprogramming of cancer cells-a hallmark of cancer that supports rapid proliferation and survival under hostile conditions (5). Metabolic alterations enable cancer cells to meet the increased demands for energy and biosynthetic precursors required for continuous growth and division (6). Warburg effect, characterized by increased glycolysis even in the presence of oxygen, has been a focal point of cancer metabolism research (7), recent studies have uncovered a more complex metabolic landscape in NSCLC. Alterations in lipid metabolism, amino acid utilization, and metabolic interactions with the TME play significant roles in tumor progression, metastasis, and therapeutic resistance (8). Furthermore, metabolic heterogeneity within tumors and the metabolic plasticity of cancer cells allow them to adapt to changing environmental conditions and therapeutic pressures (9).

The TME, comprising stromal cells, immune cells, extracellular matrix (ECM) components, and vasculature, interacts dynamically with cancer cells, influencing their metabolic behavior and contributing to disease progression (10). Cancer-associated fibroblasts (CAFs) can alter the availability of nutrients and secrete metabolic intermediates that fuel tumor growth (11). Immune cells within the TME can have their function modulated by the metabolic activities of cancer cells, leading to immune evasion (12). Hypoxia, a common feature of solid tumors due to abnormal vasculature, further drives metabolic reprogramming by stabilizing hypoxia-inducible factors (HIFs) that regulate genes involved in glycolysis and angiogenesis (13).

This review aims to provide a comprehensive and up-to-date analysis of energy metabolism in NSCLC, highlighting novel insights and potential therapeutic opportunities. We focus on recent discoveries that shed light on the metabolic heterogeneity of NSCLC, the influence of the TME on metabolic adaptations, and the implications for therapy resistance. By integrating emerging technologies such as single-cell metabolomics, CRISPR-based metabolic screens, and systems biology approaches, and by adopting multidisciplinary perspectives, we propose innovative strategies to target metabolic vulnerabilities in NSCLC. Ultimately, we aim to bridge the gap between basic metabolic research and clinical applications, paving the way for more effective and personalized therapies for NSCLC patients.

2 Metabolic reprogramming in NSCLC: beyond the Warburg effect

2.1 The Warburg effect revisited

The Warburg effect, first described by Otto Warburg in the 1920s, refers to the observation that cancer cells preferentially utilize glycolysis for energy production even in the presence of adequate oxygen-a phenomenon known as aerobic glycolysis. This metabolic reprogramming allows cancer cells to rapidly generate ATP and accumulate intermediates for biosynthetic processes essential for proliferation (14). In NSCLC, there is significant upregulation of glycolytic enzymes such as hexokinase 2 (HK2) and pyruvate kinase M2 (PKM2), which facilitate increased glycolytic flux (15). However, this glycolytic shift is only part of the complex metabolic adaptations in NSCLC. Recent studies have revealed that mitochondrial oxidative phosphorylation (OXPHOS) remains active in many cancer cells, including NSCLC (16). This suggests that cancer cells exhibit metabolic flexibility, capable of utilizing both glycolysis and OXPHOS depending on environmental conditions and cellular demands (17). For instance, under hypoxic conditions commonly found within tumors, glycolysis is upregulated, while in oxygen-rich areas, OXPHOS can contribute significantly to adenosine triphosphate (ATP) production (18).

Moreover, the reliance on glycolysis is influenced by oncogenic signaling pathways. Mutations in genes such as kirsten rats arcomaviral oncogene homolog (KRAS) and epidermal growth factor receptor (EGFR), which are prevalent in NSCLC, activate downstream effectors like phosphatidylinositol 3-Kinase/protein kinase B/mammalian target of rapamycin (PI3K/AKT/mTOR) and mitogen-activated protein kinase (MAPK) pathways (19). These pathways upregulate glucose transporters (e.g., GLUT1) and glycolytic enzymes, enhancing glucose uptake and glycolysis (20). Additionally, HIFs, stabilized under low oxygen conditions, promote the expression of genes involved in glycolysis and suppress OXPHOS (21).

Understanding the nuances of the Warburg effect in NSCLC is crucial for therapeutic development. Targeting glycolytic enzymes has shown promise in preclinical models; however, due to the metabolic plasticity of cancer cells, inhibition of glycolysis alone may lead to compensatory upregulation of OXPHOS or other pathways. Therefore, combination therapies that target multiple metabolic pathways may be more effective in overcoming resistance and achieving sustained antitumor effects.

2.2 Mitochondrial metabolism and OXPHOS

Contrary to the traditional view that cancer cells have impaired mitochondrial function, recent studies have demonstrated that mitochondrial OXPHOS remains active and is essential for the survival and proliferation of NSCLC cells (22). Mitochondria play a pivotal role not only in energy production but also in biosynthesis, redox balance, and regulation of apoptosis (23). NSCLC cells exhibit remarkable metabolic flexibility, enabling them to switch between glycolysis and OXPHOS in response to environmental cues such as nutrient availability, oxygen levels, and therapeutic interventions (24). Figure 1 illustrates the dynamic interplay between these two energy-producing pathways and highlights the compensatory mechanisms that allow NSCLC cells to adapt their metabolism under stress conditions.

The metabolic adaptability contributes significantly to therapeutic resistance. For instance, when glycolysis is inhibited-either pharmacologically or due to nutrient scarcity-NSCLC cells can upregulate OXPHOS to meet their energy and biosynthetic demands (25). This compensatory increase in OXPHOS allows cancer cells to evade glycolysis-targeted therapies, highlighting the challenge of metabolic plasticity in effective cancer treatment (26). Additionally, some subpopulations of cancer stem cells within NSCLC have been found to rely heavily on OXPHOS, contributing to tumor heterogeneity and resistance to chemotherapy and radiotherapy (27).

Recent research has uncovered that oncogenic drivers common in NSCLC, such as mutations in the KRAS gene, can influence mitochondrial function. KRAS-mutant NSCLC cells demonstrate enhanced mitochondrial biogenesis and elevated OXPHOS activity, which supports their aggressive phenotype (28). Moreover, alterations in mitochondrial dynamics-processes that control mitochondrial fission and fusion-have been implicated in NSCLC progression. Dysregulated expression of proteins like dynamin-related protein 1 (DRP1) and mitofusins (MFN1 and MFN2) affects mitochondrial morphology and function, promoting cancer cell survival and metastasis (29). Targeting mitochondrial metabolism presents a promising therapeutic strategy. Inhibitors of OXPHOS components, such as complex I inhibitor IACS-010759, have shown antitumor activity in preclinical models of NSCLC by inducing energy stress and apoptosis (30). Furthermore, combining OXPHOS inhibitors with agents targeting glycolysis may overcome metabolic compensation mechanisms and enhance therapeutic efficacy (31). Agents that disrupt mitochondrial dynamics or promote mitochondrial dysfunction are also being explored as potential treatments (32).

The interplay between mitochondrial metabolism and the TME further complicates the metabolic landscape. Hypoxic regions within tumors can influence mitochondrial function and promote metabolic reprogramming (33). Additionally, interactions with stromal cells and immune cells can modulate mitochondrial activity in NSCLC cells, affecting tumor growth and response to therapy (34).

In summary, mitochondrial metabolism and OXPHOS play critical roles in NSCLC biology. Understanding the mechanisms underlying metabolic flexibility and mitochondrial function in cancer cells is essential for developing effective therapeutic strategies that can circumvent resistance and target the metabolic vulnerabilities of NSCLC.

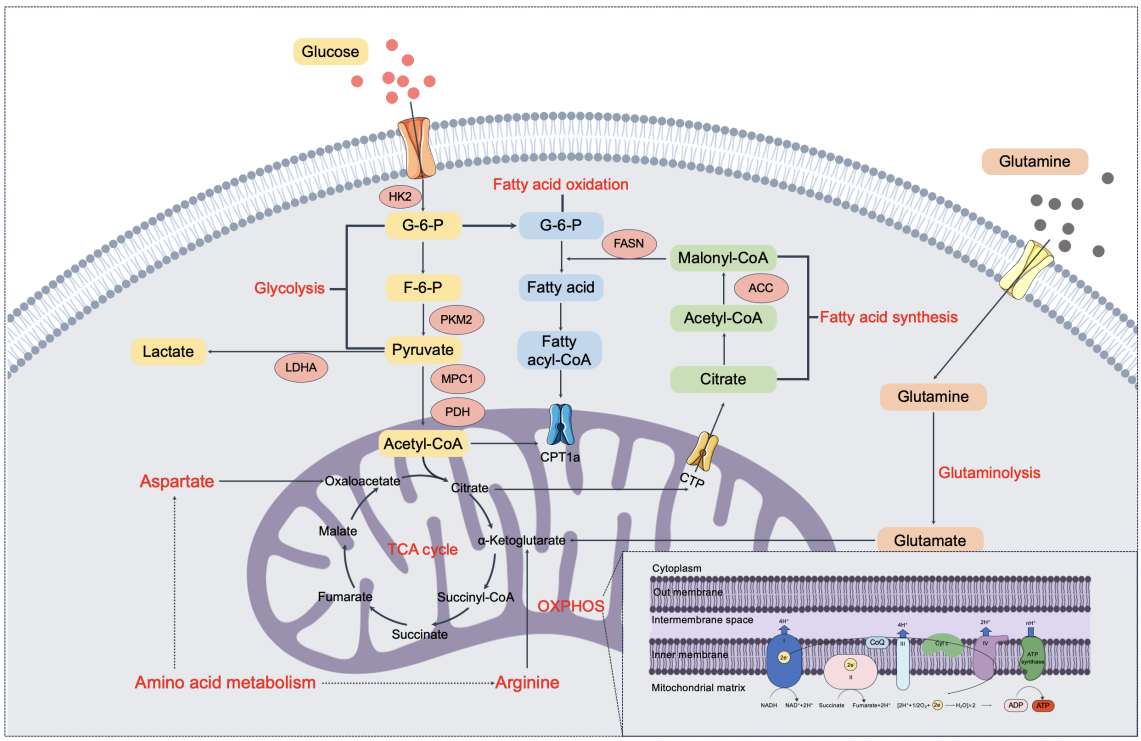

FIGURE 1
Integrated schematic of glycolysis, mitochondrial metabolism, and lipid pathways in NSCLC cells. This figure summarizes key metabolic processes in NSCLC cells, illustrating the interplay and compensatory mechanisms between glycolysis and OXPHOS, as well as the integration of lipid metabolism. Glucose is metabolized through glycolysis to produce pyruvate, which enters mitochondria to fuel the TCA cycle and OXPHOS for ATP production. Under certain conditions, pyruvate is diverted to lactate via LDHA. Glutamine contributes to TCA cycle intermediates through glutaminolysis, supporting biosynthesis and redox balance. Fatty acid metabolism is also reprogrammed in NSCLC: fatty acid synthesis, driven by enzymes such as ACC and FASN, converts citrate and acetyl-CoA into lipids, while FAO via CPT1a provides additional acetyl-CoA for mitochondrial respiration. Together, these interconnected pathways reflect the metabolic flexibility and adaptability of NSCLC cells in response to environmental and therapeutic pressures.

2.3 Lipid metabolism: a new frontier

Lipid metabolism has emerged as a critical aspect of NSCLC biology, influencing tumor growth, survival, and metastasis (35). Cancer cells require a continuous supply of lipids for the synthesis of cellular membranes and signaling molecules that support rapid proliferation. Enhanced *de novo* lipogenesis—the endogenous production of fatty acids from non-lipid precursors like glucose and glutamine—is a hallmark of metabolic reprogramming in cancer (36), and is particularly prominent in NSCLC.

This process is depicted in Figure 1, which illustrates key pathways involved in lipid synthesis and oxidation in NSCLC cells. This process provides not only structural components for membrane biogenesis but also lipid signaling molecules that can activate oncogenic pathways. Enzymes such as fatty acid synthase (FASN) and stearoyl-CoA desaturase-1 (SCD1) play pivotal roles in lipid synthesis and are overexpressed in NSCLC (37). FASN is responsible for the synthesis of palmitate, a saturated fatty acid that serves as a building block for more complex lipids. Overexpression of FASN has been associated with increased tumor aggressiveness, resistance to chemotherapy, and poorer prognosis in NSCLC patients (38). Targeting FASN with small-molecule inhibitors has shown promise in preclinical models, leading to reduced tumor growth and enhanced sensitivity to other therapies (39). SCD1 introduces a double bond into saturated fatty acyl-CoAs to produce MUFAs, which are essential for maintaining membrane fluidity and function. Elevated SCD1 expression has been linked to enhanced tumor growth, metastasis, and reduced survival rates in NSCLC. Inhibition of SCD1 can disrupt membrane composition, induce endoplasmic reticulum (ER) stress, and trigger apoptosis in cancer cells (40). Acetyl-CoA carboxylase (ACC) is a key rate-limiting enzyme in fatty acid synthesis, playing a critical role in cellular metabolism and tumor growth by converting acetyl-CoA to malonyl-CoA. ACC regulates *de novo* fatty acid synthesis to meet the biosynthetic demands of tumor growth, and its inhibitor ND-646 significantly suppresses the growth and viability of NSCLC cells while enhancing the efficacy of chemotherapy, making it a potential target for cancer metabolism therapy (41).

Beyond lipid synthesis, NSCLC cells can utilize lipid oxidation through fatty acid oxidation (FAO) pathways to meet their energy demands and maintain redox balance (42). FAO involves the breakdown of fatty acids in mitochondria to generate acetyl-CoA, nicotinamide adenine dinucleotide (NADH), and flavin adenine dinucleotide hydrogen ($FADH_2$), which feed into the tricarboxylic acid (TCA) cycle and electron transport chain to produce ATP (43). By relying on FAO, cancer cells can adapt to nutrient-deprived or hypoxic conditions where glycolysis may be less efficient (44). FAO also contributes to the maintenance of redox homeostasis by generating NADPH, a critical reducing agent that helps neutralize reactive oxygen species (ROS) and protect cells from oxidative stress (45). Enzymes like carnitine palmitoyltransferase 1 (CPT1), which regulates the transport of long-chain fatty acids into mitochondria, are often upregulated in NSCLC. Inhibition of CPT1 can impair FAO, leading to energy stress and increased sensitivity to oxidative damage (46).

NSCLC cells can enhance lipid uptake from the microenvironment by overexpressing lipid transporters such as cluster of differentiation 36 (CD36) and fatty acid-binding proteins (FABPs) (47). This uptake allows cancer cells to utilize exogenous fatty acids for energy production and membrane synthesis. Additionally, cancer cells can store excess lipids in lipid droplets, which serve as reservoirs that can be mobilized during times of metabolic stress (48). Alterations in lipid metabolism are often driven by oncogenic signaling pathways common in NSCLC. For example, activation of the PI3K/AKT/mTOR pathway can upregulate lipid synthesis by increasing the expression and activity of lipogenic enzymes (49). Mutations in KRAS, frequently observed in NSCLC, have been shown to enhance lipid metabolism, promoting tumor growth and survival (50). These signaling pathways not only stimulate lipid production but also integrate metabolic cues with cell proliferation and survival mechanisms.

2.4 Amino acid metabolism: beyond glutamine addiction

While glutamine metabolism is well-established in cancer biology due to its role in supporting rapid cell proliferation and survival (51), NSCLC cells also exploit other amino acids to meet their metabolic demands. Recent studies have highlighted alterations in the metabolism of amino acids such as serine, glycine, proline, and branched-chain amino acids (BCAAs), which contribute to nucleotide synthesis, redox balance, and energy production (52).

2.4.1 Serine and glycine metabolism

Serine and glycine are non-essential amino acids that play crucial roles in one-carbon metabolism, which is essential for nucleotide synthesis, methylation reactions, and antioxidant defense (53). NSCLC cells can upregulate enzymes involved in the serine-glycine synthesis pathway, such as phosphoglycerate dehydrogenase (PHGDH), phosphoserine aminotransferase (PSAT1), and serine hydroxymethyltransferase (SHMT) (54). Overexpression of PHGDH has been observed in NSCLC and is associated with enhanced tumor growth and poor prognosis (55). Targeting this pathway can disrupt nucleotide biosynthesis and reduce the proliferation of cancer cells. Moreover, serine and glycine contribute to the synthesis of glutathione, a major intracellular antioxidant that helps maintain redox homeostasis (56). By elevating serine and glycine metabolism, NSCLC cells enhance their capacity to detoxify ROS, thereby promoting survival under oxidative stress conditions induced by therapies (57).

2.4.2 Proline metabolism

Proline metabolism is another pathway exploited by NSCLC cells to support tumor growth and metastasis (58). Proline biosynthesis from glutamate involves the enzyme pyrroline-5-carboxylate synthase (P5CS), while its degradation is mediated by proline dehydrogenase (PRODH). Proline can serve as a source of energy and contribute to redox balance by generating $NADP^+$/

NADPH (59). Altered proline metabolism aids in the adaptation of cancer cells to hypoxic conditions and nutrient deprivation, facilitating tumor progression (60). Inhibiting key enzymes in proline metabolism may impair cancer cell survival and sensitize tumors to treatment (61).

2.4.3 BCAAs

BCAAs-leucine, isoleucine, and valine-are essential amino acids involved in protein synthesis and signaling pathways that regulate cell growth and metabolism (62). NSCLC cells can exhibit increased uptake and catabolism of BCAAs to fuel the TCA cycle and provide nitrogen for nucleotide and amino acid synthesis (52). Enzymes such as branched-chain amino acid transaminase 1 (BCAT1) are upregulated in NSCLC and have been associated with tumor aggressiveness and poor clinical outcomes (63). Targeting BCAA metabolism may disrupt energy production and biosynthesis, leading to reduced tumor growth.

2.4.4 Amino acid transporters

To support increased amino acid demands, NSCLC cells often upregulate amino acid transporters. Transporters like solute carrier family 1 member 5 (SLC1A5/ASCT2) and SLC7A5 (LAT1) facilitate the uptake of glutamine, serine, leucine, and other amino acids (64, 65). Overexpression of these transporters has been linked to enhanced tumor growth, metastasis, and resistance to chemotherapy (66). Inhibiting amino acid transporters can reduce the intracellular availability of critical nutrients, inducing metabolic stress and apoptosis in cancer cells (67).

2.5 Metabolic heterogeneity and plasticity

NSCLC exhibit significant metabolic heterogeneity, both between different tumors (intertumoral heterogeneity) and within individual tumors (intratumoral heterogeneity)[1]. This heterogeneity arises from a complex interplay of genetic mutations, epigenetic modifications, tumor microenvironmental factors, and cellular interactions, leading to diverse metabolic phenotypes among cancer cells (68).

2.5.1 Genetic mutations and metabolic diversity

Genetic mutations commonly found in NSCLC, such as alterations in KRAS, EGFR, anaplastic lymphoma kinase (ALK), and liver kinase B1 (LKB1), drive distinct metabolic reprogramming in tumor cells (69). For instance, KRAS-mutant NSCLC cells often exhibit enhanced glucose uptake and glycolysis, whereas EGFR-mutant cells may rely more on glutamine metabolism (70). Loss of LKB1 function is associated with defects in mitochondrial OXPHOS and increased dependency on alternative energy sources (71). These genetic differences contribute to metabolic heterogeneity, influencing how tumor cells utilize nutrients and respond to metabolic stress.

2.5.2 Microenvironmental influences

The TME significantly impacts metabolic heterogeneity. Factors such as hypoxia, nutrient availability, pH changes, and interactions with stromal cells create spatial metabolic gradients within tumors (72). Hypoxic regions often lead to increased glycolysis and lactate production, while well-oxygenated areas may favor OXPHOS (73). Additionally, the availability of nutrients like glucose, amino acids, and lipids can vary within the tumor, forcing cancer cells to adapt their metabolism accordingly (74).

2.5.3 Interactions with stromal cells

CAFs, immune cells, and endothelial cells within the TME modulate cancer cell metabolism through paracrine signaling and direct cell-cell interactions (75). For example, CAFs can secrete metabolites such as lactate, amino acids, and fatty acids, which cancer cells uptake and utilize for energy and biosynthesis (10). Immune cells like tumor-associated macrophages (TAMs) produce cytokines that alter metabolic pathways in cancer cells, promoting survival and proliferation (76). These interactions further enhance metabolic diversity within the tumor.

2.5.4 Metabolic plasticity and therapeutic resistance

Metabolic heterogeneity contributes to therapeutic resistance by enabling subpopulations of cancer cells to survive under treatment-induced stress (77). Cancer cells with different metabolic profiles may respond variably to therapies targeting specific metabolic pathways (78). Metabolic plasticity-the ability of cancer cells to switch between metabolic states-allows them to adapt to environmental changes or therapeutic pressures (79). For instance, inhibiting glycolysis may lead some cancer cells to increase OXPHOS or utilize alternative substrates like fatty acids and amino acids (80).

2.5.5 Implications for personalized medicine

The presence of metabolic heterogeneity underscores the need for personalized metabolic interventions in NSCLC (81). Therapeutic strategies that consider the specific metabolic dependencies of a patient's tumor may improve treatment efficacy (82). Techniques such as single-cell metabolomics and metabolic imaging can identify metabolic subtypes within tumors, guiding the selection of targeted therapies (83). Additionally, combining metabolic inhibitors with other treatments may overcome resistance by targeting multiple metabolic pathways simultaneously (84).

Understanding the mechanisms driving metabolic heterogeneity and plasticity is crucial for developing effective therapies. Integrating genomic, transcriptomic, and metabolomic data can provide a comprehensive view of tumor metabolism (85). Personalized approaches that tailor treatments based on individual metabolic profiles hold promise for improving outcomes in NSCLC patients.

3 The TME: metabolic crosstalk and therapeutic resistance

3.1 CAFs and metabolic support

CAFs are among the most abundant stromal cells within the TME of NSCLC and play a crucial role in supporting tumor metabolism and progression (86). CAFs undergo significant metabolic reprogramming that enables them to supply essential nutrients and metabolites to cancer cells, thereby promoting tumor growth and survival (51). One of the key phenomena illustrating this supportive role is the "reverse Warburg effect". Unlike the traditional Warburg effect, where cancer cells preferentially utilize glycolysis for energy production even in the presence of oxygen, the reverse Warburg effect describes how CAFs enhance their glycolytic activity to produce high-energy metabolites such as lactate and pyruvate (87). These metabolites are then secreted into the TME and taken up by cancer cells, which utilize them through OXPHOS to generate ATP and support anabolic processes. This metabolic coupling allows cancer cells to conserve glucose for biosynthetic pathways, thus facilitating rapid proliferation and growth (88).

Beyond lactate production, CAFs secrete a variety of nutrients, including amino acids (e.g., glutamine, alanine) and fatty acids, which cancer cells can exploit. CAF-derived glutamine serves as an anaplerotic substrate replenishing TCA cycle intermediates in cancer cells, supporting energy production and biosynthesis of nucleotides and amino acids (89). Alanine secreted by CAFs can be converted into pyruvate, further fueling the TCA cycle. CAFs can release free fatty acids that cancer cells uptake and utilize for β-oxidation, contributing to ATP generation and membrane synthesis (90).

CAFs also modulate the ECM and secrete cytokines and growth factors that influence cancer cell metabolism and behavior (91). Factors such as transforming growth factor-beta (TGF-β), hepatocyte growth factor (HGF), and interleukins secreted by CAFs can activate signaling pathways (e.g., PI3K/AKT, MAPK) in cancer cells, leading to enhanced glycolysis and survival (92).

3.2 Immune cell metabolism and immune evasion

The metabolic state of immune cells within the TME profoundly affects their function and the overall immune response against NSCLC (93). Effective antitumor immunity relies on the activity of various immune cells, particularly effector T cells and natural killer (NK) cells, which require substantial energy and biosynthetic materials to proliferate and exert their cytotoxic functions (94). However, the TME is often characterized by metabolic competition and deprivation, as rapidly proliferating tumor cells consume large amounts of glucose, amino acids, and other nutrients (95). As illustrated in Figure 2, this metabolic imbalance not only limits nutrient availability for immune cells but also drives the reprogramming of both effector and regulatory immune cell populations, ultimately shaping the immune landscape toward either tumor suppression or immune evasion.

3.2.1 Metabolic competition and nutrient deprivation

Tumor cells alter the availability of key nutrients in the TME by upregulating glucose transporters and amino acid transporters, leading to increased uptake and consumption of glucose and amino acids (96). This metabolic competition results in a nutrient-deprived environment for immune cells. Effector T cells rely on glycolysis for energy production and effector functions such as cytokine production and proliferation. Glucose deprivation impairs T cell receptor (TCR) signaling, reduces cytokine production (e.g., interferon-gamma), and diminishes cytotoxic activity (97). Amino acids like glutamine, arginine, and tryptophan are critical for T cell function and proliferation (98). Tumor cells can deplete these amino acids or produce immunosuppressive metabolites (e.g., kynurenine from tryptophan catabolism via indoleamine 2,3-dioxygenase [IDO]) that inhibit T cell activity (99).

3.2.2 Metabolic checkpoints and immune suppression

Metabolic reprogramming in lung cancer plays a pivotal role in immune regulation by inducing metabolic stress and activating metabolic checkpoints in immune cells, leading to immunosuppression. Tumor-induced energy stress activates key metabolic sensors such as AMP-Activated Protein Kinase (AMPK), which modulates T cell metabolism and reduces their effector functions. Similarly, nutrient deprivation within the TME inhibits mTOR signaling, impairing T cell growth and responses. Additionally, hypoxia stabilizes HIFs, which alter immune cell metabolism and promote an immunosuppressive phenotype (100).

Tumor cells exploit these metabolic pathways to evade immune responses through several mechanisms. First, the upregulation of immune checkpoint molecules such as programmed cell death ligand 1 (PD-L1) on tumor cells interacts with programmed cell death protein 1 (PD-1) on T cells, suppressing glucose uptake and glycolysis in T cells, thereby diminishing their effector functions (101). Second, tumor cells secrete immunosuppressive factors like TGF-β and adenosine, which further modulate immune cell metabolism and suppress antitumor immunity. These metabolic interactions underscore the critical role of metabolic reprogramming in shaping the immune landscape of lung cancer, presenting potential targets for therapeutic intervention (102).

3.3 Hypoxia and metabolic adaptations

Hypoxia, or low oxygen conditions, is a hallmark of the TME in solid cancers, including NSCLC (103). Rapid tumor growth often outpaces the development of new blood vessels, leading to regions of insufficient oxygen supply. Hypoxic conditions trigger the stabilization of HIFs, particularly HIF-1α and HIF-2α, which are key transcription factors orchestrating cellular responses to low

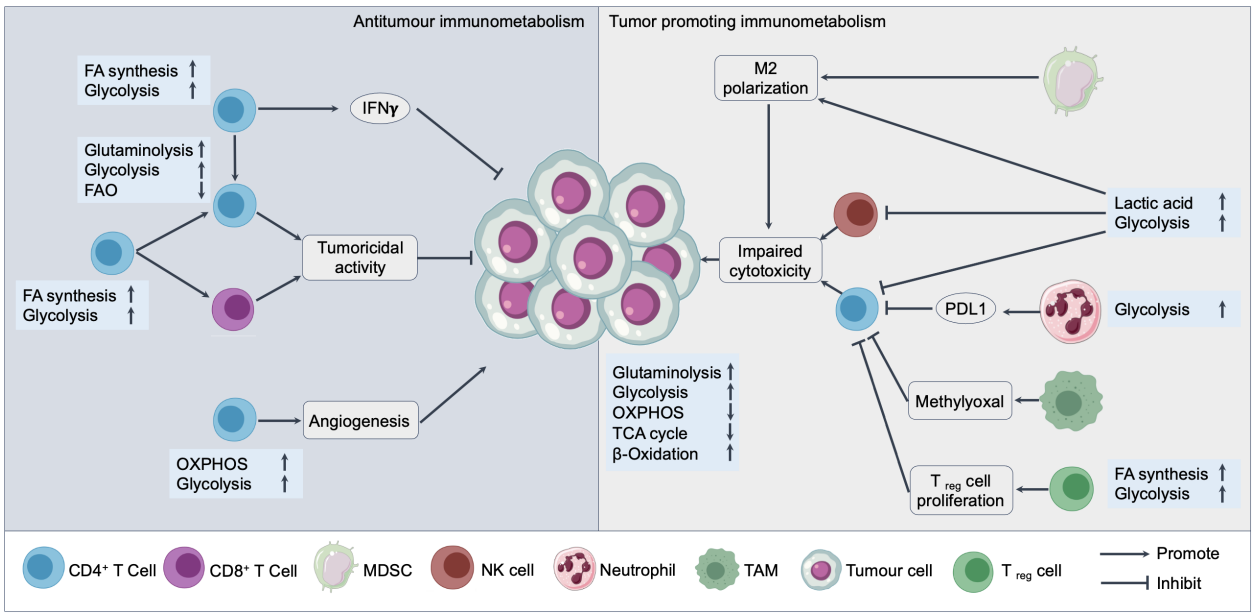

FIGURE 2
Immunometabolic interactions in the NSCLC TME.This schematic illustrates the dual roles of immune cell metabolism in either promoting or suppressing tumor growth in NSCLC. On the left, antitumor immunometabolism is driven by activated $CD4^+$ and $CD8^+$ T cells, NK cells, and other cytotoxic immune cells exhibiting increased glycolysis, fatty acid (FA) synthesis, OXPHOS, and glutaminolysis, supporting IFN-γ production, angiogenesis, and tumoricidal activity. On the right, tumor-promoting immunometabolism is characterized by immunosuppressive cells such as regulatory T cells (T_{reg} cell), myeloid-derived suppressor cells (MDSCs), TAMs, and neutrophils, which exploit elevated glycolysis, lactic acid production, and altered metabolic intermediates (e.g., methylglyoxal) to inhibit cytotoxic function and promote T_{reg} cell proliferation, PD-L1 expression, and M2 polarization. Tumor cells actively shape the metabolic landscape of the TME by rewiring their own metabolic programs (e.g., enhanced glycolysis, glutaminolysis, and β-oxidation) to suppress immune responses and sustain growth.

oxygen levels (104). Under normoxic conditions, HIF-α subunits are hydroxylated by prolyl hydroxylase domain proteins (PHDs), marking them for degradation via the von Hippel-Lindau (VHL) ubiquitin-proteasome pathway (105). Hypoxia inhibits PHD activity, preventing HIF-α degradation. Stabilized HIF-α translocates to the nucleus, dimerizes with HIF-1β, and activates the transcription of target genes involved in crucial processes such as metabolism, angiogenesis, erythropoiesis, and cell survival (106).

HIFs play a pivotal role in reprogramming cancer cell metabolism to adapt to hypoxic conditions (107). HIF-1α upregulates glycolytic enzymes, including HK2, phosphofructokinase 1 (PFK1), and lactate dehydrogenase A (LDHA), shifting the metabolic flux towards glycolysis despite the presence of oxygen (aerobic glycolysis) (108). This shift allows cancer cells to generate ATP efficiently under low oxygen conditions. Upregulation of glucose transporters such as GLUT1 enhances glucose uptake from the extracellular environment, providing substrates for glycolysis (109). HIF-1α induces pyruvate dehydrogenase kinase 1 (PDK1), which inhibits pyruvate dehydrogenase (PDH), decreasing the conversion of pyruvate to acetyl-CoA and thus reducing entry into the TCA cycle (110). This adaptation minimizes oxygen consumption and reduces ROS production from mitochondria. Increased LDHA activity converts pyruvate to lactate, which is exported out of the cell via monocarboxylate transporters (MCTs), contributing to the acidic TME (111).

4 Emerging technologies unveiling metabolic vulnerabilities

The rapid advancement of innovative technologies has significantly enhanced our ability to uncover metabolic vulnerabilities in cancer, providing new insights into tumor biology and therapeutic opportunities. Single-cell metabolomics has emerged as a powerful tool, enabling the analysis of metabolic heterogeneity at an unprecedented resolution (112). By profiling individual cells, researchers can identify distinct subpopulations with unique metabolic dependencies, which can inform the development of more precise and effective targeted therapies. Spatial metabolomics further expands this capability by detecting and imaging metabolites with spatial resolution at the tissue or cellular level (113). By combining mass spectrometry imaging with traditional metabolomics approaches, this technique allows for the visualization of metabolite distribution within biological tissues, offering a deeper understanding of the TME and its metabolic interactions.

The advent of high-resolution mass spectrometry (HRMS) has significantly enhanced the sensitivity and accuracy of metabolite detection. HRMS provides precise molecular weight measurements and detailed structural information, making it a cornerstone technology in metabolomics research (114). Finally, systems biology and computational modeling integrate multi-omics data to construct metabolic networks and predict therapeutic outcomes

(115). Computational tools enable the simulation of metabolic interventions and identification of synergistic drug combinations, paving the way for more strategic and effective treatment regimens. Together, these emerging technologies are revolutionizing our understanding of cancer metabolism and driving the discovery of novel therapeutic strategies.

5 Therapeutic implications and strategies

Recent advances in elucidating the metabolic landscape of NSCLC have highlighted several key pathways that are amenable to therapeutic intervention. Targeting metabolic dependencies represents a promising strategy to disrupt tumor growth and overcome resistance mechanisms (Figure 3). In this section, we discuss emerging therapeutic approaches aimed at modulating core metabolic processes in NSCLC. A summary of representative metabolic inhibitors and their targeted pathways is provided in Table 1, which offers a comprehensive overview of current therapeutic agents explored in NSCLC metabolic intervention.

5.1 Targeting glycolysis and OXPHOS

The metabolic reprogramming of NSCLC cells presents a strategic opportunity for therapeutic intervention by targeting key energy-producing pathways. Glycolysis and OXPHOS are central to cancer cell metabolism, providing ATP and metabolic intermediates necessary for rapid proliferation and survival. Inhibitors targeting these pathways have shown promise in preclinical models, but due to metabolic plasticity, cancer cells can switch between glycolysis and OXPHOS to compensate when one pathway is inhibited (129). Therefore, combination therapies targeting both pathways may be more effective in preventing metabolic compensation and inducing cancer cell death.

Key glycolytic enzymes such as HK2 and PKM2 are overexpressed in NSCLC and are critical for maintaining the high glycolytic flux observed in cancer cells. HK2 catalyzes the first step of glycolysis, phosphorylating glucose to glucose-6-phosphate. Inhibitors like 2-deoxy-D-glucose (2-DG) mimic glucose but cannot undergo further metabolism, effectively inhibiting HK2 activity (130). Preclinical studies have shown that 2-DG induces apoptosis and enhances the sensitivity of cancer cells to

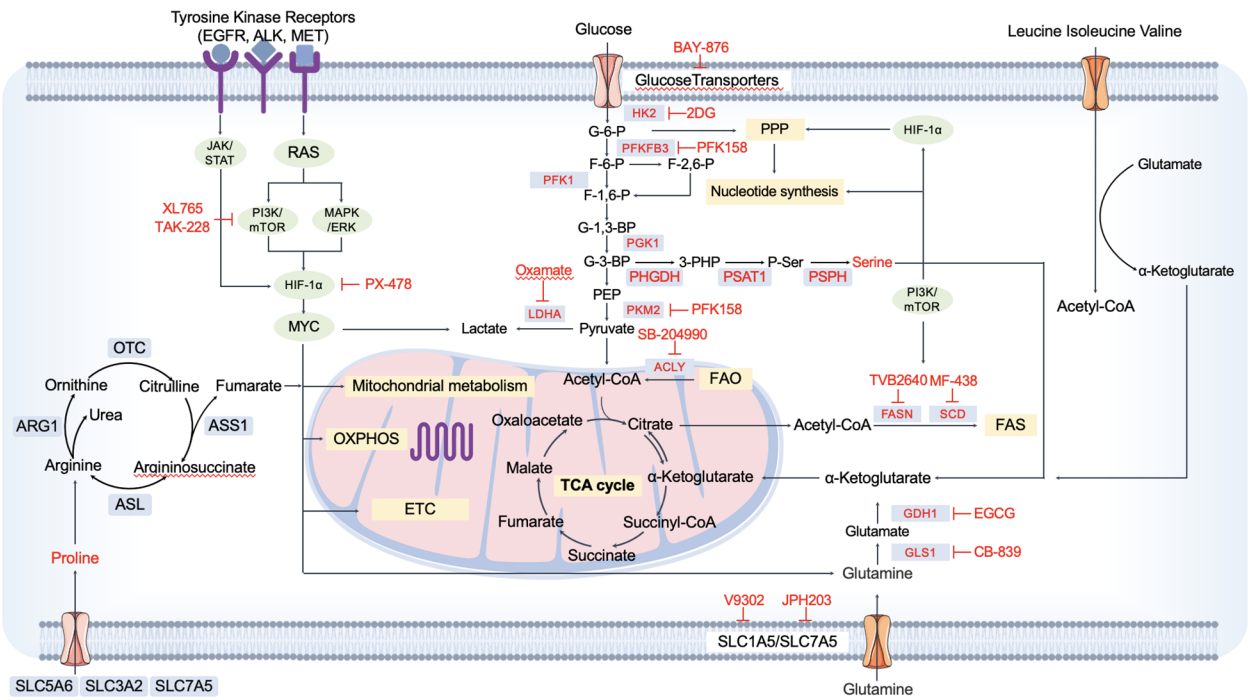

FIGURE 3
Targetable metabolic pathways and inhibitors in NSCLC.This schematic highlights key metabolic pathways reprogrammed in NSCLC cells and outlines current therapeutic targets under investigation. Central carbon metabolism—including glycolysis, the pentose phosphate pathway (PPP), TCA cycle, and OXPHOS—is regulated by oncogenic signaling pathways such as PI3K/mTOR and MAPK/ERK, often activated by mutations in receptor tyrosine kinases (EGFR, ALK, MET). Metabolic enzymes (e.g., HK2, PFKFB3, LDHA, PHGDH, PKM2, ACLY, FASN, SCD, GLS1) and transporters (e.g., SLC1A5/SLC7A5) are shown with corresponding small-molecule inhibitors (e.g., 2-DG, BAY-876, PFK158, Oxamate, PX-478, CB-839, TVB2640, MF-438, JPH203), many of which are being evaluated in preclinical or clinical settings. The diagram also illustrates amino acid metabolism (e.g., glutaminolysis, serine biosynthesis, arginine and proline metabolism), emphasizing the metabolic plasticity of NSCLC and the opportunities for combinatorial metabolic interventions. This comprehensive map provides a framework for rational design of therapies targeting metabolic vulnerabilities in NSCLC.

10.3389/fonc.2025.1564226

TABLE 1 Drugs/compounds targeting different proteins/enzymes of the metabolic pathway.

Pathways	Molecular target	Drugs/ compounds	Mechanism of action	Clinical trial status
Glucose metabolism pathway				
	GLUTS	BAY-876	selective GLUT1 inhibitor, inhibition of proliferation in NSCLC cells (20)	–
	PFK2/PFKFB3	PFK158	Inhibits growth of NSCLC (in vitro) (26)	Phase I NCT02044861
	HK2	2-DG	Specific HK2 inhibitor, induction apoptosis of lung cancer stem cells (116)	Phase I/II NCT00096707
	PKM2	TEPP-46 and DASA-58	Inhibits proliferation and induces apoptosis of NSCLC cells (117, 118)	–
	LDH-A	Oxamate	Enhances the efficacy of anti-PD-1 treatment in an NSCLC (119)	–
Mitochondrial metabolism				
	OXPHOS	Metformin Phenformin	Inhibit mitochondrial complex I, reducing ATP production and increasing ROS generation (120, 121)	Phase I/II NCT03086733 -
	ATP Synthase	Oligomycin	Inhibit ATP synthase (122)	–
	Bcl-2/Bcl-xL	venetoclax	Promote apoptosis (123)	Phase I NCT04274907
Lipid metabolism pathway				
	ACC	ND-646	Prevents ACC subunit dimerization (41)	Preclinical
	FASN	TVB2640 TVB3166	Selective FASN inhibitor (124) Selective FASN inhibitor (125)	Phase II (NCT03808558) Preclinical
	SCD1	MF-438	Specific SCD1 inhibitor, induction apoptosis lung cancer stem cells (126, 127)	Preclinical
	CPT1	Etomoxir	Irreversible inhibitor of CPT1B (46)	–
Amino acid metabolism pathway				
	SLC1A5	V9302	Inhibits proliferation and induces apoptosis of NSCLC cells (64)	–
	SLC7A5	JPH203	Selective SLC7A5 inhibitor (65)	–
	GLS1	CB-839	Induction apoptosis lung cancer stem cells (128)	Phase I/ II (NCT02071862) (NCT02771626)
Signaling proteins and transcription factors				
	mTORC1 and mTORC2	TAK-228	ATP-dependent mTOR1/2 inhibitor, inhibition of proliferation in NSCLC cells (49)	Phase II (NCT02503722)
	HIF-1α	PX-478	Induction apoptosis of NSCLC cells (104)	Preclinical
	PI3K and mTOR	XL765	A pan PI3K/mTOR inhibitor (19)	Phase I (NCT00777699)

chemotherapy and radiotherapy (116). However, its clinical application is limited by toxicity and lack of specificity. PKM2 controls the final step of glycolysis, converting phosphoenolpyruvate to pyruvate. PKM2 exists in both active tetrameric and less active dimeric forms, with cancer cells favoring the dimeric form to promote anabolic processes. Small-molecule activators like TEPP-46 and DASA-58 stabilize the tetrameric form, enhancing pyruvate production and reducing lactate formation (117, 118). This shift can suppress tumor growth and induce apoptosis.

Cancer cells can compensate for inhibited glycolysis by increasing reliance on mitochondrial OXPHOS. Targeting OXPHOS can disrupt this adaptive mechanism: 1. Complex I Inhibitors: Metformin and phenformin inhibit mitochondrial complex I, reducing ATP production and increasing ROS generation (120, 121). Phenformin has shown greater antitumor activity than metformin in preclinical models of NSCLC but with a higher risk of lactic acidosis (131). 2. ATP Synthase Inhibitors: Oligomycin and its derivatives inhibit ATP synthase, leading to

decreased ATP production (122). While effective *in vitro*, their clinical use is limited due to toxicity in normal cells. 3. B-cell lymphoma-2/-xL (Bcl-2/Bcl-xL) Inhibitors: Agents like venetoclax target anti-apoptotic proteins located on the mitochondrial membrane, promoting apoptosis in cancer cells (123). Combining these with OXPHOS inhibitors can enhance cancer cell death.

Combining glycolysis inhibitors with OXPHOS inhibitors may prevent cancer cells from switching energy sources and enhance therapeutic efficacy. Simultaneous targeting of HK2 and complex I can induce energetic crisis in cancer cells. For example, combining 2-DG with metformin has shown synergistic effects in reducing NSCLC cell viability (132). Inhibiting key enzymes in both pathways limits the ability of cancer cells to adapt metabolically. This approach can lead to increased ROS production, DNA damage, and activation of cell death pathways.

5.2 Targeting lipid metabolism

Lipid metabolism plays a crucial role in the growth and survival of NSCLC cells, as previously discussed. Targeting key enzymes involved in lipid synthesis and desaturation presents a promising therapeutic strategy. FASN and SCD1 are two pivotal enzymes in lipid metabolism that have gained significant attention as potential targets for cancer therapy.

FASN is an essential enzyme responsible for the *de novo* synthesis of long-chain fatty acids from acetyl-CoA and malonyl-CoA precursors. Overexpression of FASN has been observed in various cancers, including NSCLC, and is associated with poor prognosis and aggressive tumor behavior (133). By promoting lipid synthesis, FASN supports membrane biogenesis, energy storage, and the production of lipid signaling molecules that facilitate tumor growth and metastasis (134). TVB-2640 is a first-in-class, orally bioavailable, small-molecule inhibitor of FASN that has entered clinical trials. It selectively inhibits the enzymatic activity of FASN, leading to reduced fatty acid synthesis and accumulation of malonyl-CoA, which can induce apoptosis and inhibit tumor growth (124). In preclinical studies, TVB-2640 demonstrated significant antitumor activity in NSCLC models, both as a monotherapy and in combination with other agents (125). Clinical trials are currently evaluating the safety and efficacy of TVB-2640 in patients with advanced solid tumors, including NSCLC (124). Preliminary results have shown that TVB-2640 is well-tolerated and exhibits antitumor activity, especially when combined with other treatments such as chemotherapy or targeted therapies. These findings suggest that inhibiting FASN can disrupt lipid homeostasis in cancer cells, leading to growth inhibition and enhanced sensitivity to other anticancer agents.

SCD1 is a rate-limiting enzyme in the synthesis of monounsaturated fatty acids (MUFAs) from saturated fatty acids (SFAs). MUFAs are critical components of cellular membranes and play a role in lipid signaling and energy storage (126). Overexpression of SCD1 has been linked to increased proliferation, survival, and chemoresistance in NSCLC cells (135). Targeting SCD1 disrupts the balance of saturated and unsaturated fatty acids, affecting membrane fluidity and function. Inhibition of SCD1 leads to the accumulation of SFAs, which can cause ER stress and activate the unfolded protein response (UPR) (136). Prolonged ER stress can trigger apoptosis in cancer cells. Additionally, decreased levels of MUFAs impair membrane synthesis and the formation of lipid rafts, which are essential for signal transduction and the activation of oncogenic pathways. Several small-molecule inhibitors of SCD1 have been developed and shown to exhibit antitumor activity in preclinical models of NSCLC. For example, A939572 and MF-438 are potent SCD1 inhibitors that have demonstrated the ability to reduce tumor cell proliferation and induce apoptosis (126, 127). In combination with other treatments, such as chemotherapy or targeted therapies, SCD1 inhibitors may enhance therapeutic efficacy by sensitizing cancer cells to these agents. While targeting lipid metabolism shows promise, clinical outcomes have been variable. Some studies suggest that inhibiting FAO may impair T cell function and exacerbate inflammation, raising concerns about off-target effects. Moreover, conflicting evidence exists regarding the dependency of certain NSCLC subtypes on FAO versus lipogenesis, underscoring the need for subtype-specific therapeutic strategies.

5.3 Targeting amino acid metabolism

Amino acid metabolism plays a pivotal role in the growth and survival of NSCLC cells. Targeting key enzymes and pathways involved in amino acid utilization presents a promising therapeutic strategy. Glutaminase (GLS) inhibitors, such as CB-839 (telaglenastat), and inhibitors of serine and glycine synthesis pathways have shown potential in impairing tumor growth by disrupting critical metabolic processes (128). Glutamine is an essential nutrient for rapidly proliferating cancer cells, serving as a carbon and nitrogen source for nucleotide and amino acid synthesis, as well as maintaining redox balance through glutathione production. GLS catalyzes the conversion of glutamine to glutamate, a key step in glutamine metabolism. Overexpression of GLS has been observed in NSCLC and is associated with increased tumor aggressiveness (137). CB-839 is an orally bioavailable, selective GLS inhibitor that has demonstrated antitumor activity in preclinical models of NSCLC by blocking glutamine utilization (138). By inhibiting GLS, CB-839 reduces the production of glutamate and downstream metabolites, leading to impaired nucleotide synthesis, decreased glutathione levels, and increased oxidative stress (139). This can result in cancer cell death and reduced tumor growth.

Serine and glycine are non-essential amino acids integral to one-carbon metabolism, which is crucial for nucleotide synthesis, methylation reactions, and maintaining redox balance (54). NSCLC cells often upregulate enzymes involved in the serine-glycine synthesis pathway to meet the increased demands of rapid proliferation. PHGDH catalyzes the first step in the *de novo* serine synthesis pathway. Overexpression of PHGDH has been observed in NSCLC and is associated with enhanced tumor growth (140). Inhibitors targeting PHGDH can disrupt serine production, impair nucleotide biosynthesis, and induce cell cycle

arrest. Novel PHGDH inhibitors have shown efficacy in preclinical models, reducing tumor growth and enhancing sensitivity to chemotherapy (141). SHMT converts serine to glycine, contributing to one-carbon units necessary for thymidine and purine synthesis (142). Inhibiting SHMT disrupts DNA synthesis and can induce apoptosis in cancer cells. Agents targeting SHMT have demonstrated antitumor activity by inducing DNA damage and impairing cell proliferation (143).

Proline metabolism is another pathway exploited by NSCLC cells to support tumor growth and metastasis (144). Proline biosynthesis and degradation are linked to energy production and redox balance. Inhibiting key enzymes such as pyrroline-5-carboxylate reductase (PYCR) can disrupt proline metabolism, leading to increased oxidative stress and reduced tumor growth (145). Targeting proline metabolism may also impair the survival of cancer stem cells, which are often resistant to conventional therapies (146).

BCAAs-leucine, isoleucine, and valine-are essential amino acids involved in protein synthesis and signaling pathways that regulate cell growth (147). NSCLC cells may exhibit increased uptake and catabolism of BCAAs to fuel the TCA cycle and provide nitrogen for nucleotide and amino acid synthesis (148). BCAT1 catalyzes the first step in BCAA catabolism. Overexpression of BCAT1 has been associated with tumor aggressiveness and poor prognosis in NSCLC (149). Inhibiting BCAT1 can impair BCAA metabolism, suppress tumor growth, and reduce cancer cell proliferation. To support increased amino acid demands, NSCLC cells often upregulate amino acid transporters (150). Targeting these transporters can reduce the uptake of critical nutrients: ASCT2 is a glutamine transporter overexpressed in many cancers (151). Inhibiting ASCT2 can decrease glutamine uptake, leading to metabolic stress and sensitizing cancer cells to chemotherapy (152). LAT1 transports large neutral amino acids, including leucine (153). Targeting LAT1 can disrupt mTOR signaling pathways, reduce protein synthesis, and inhibit tumor growth (65). Similarly, targeting amino acid metabolism is not without limitations. For instance, while LAT1 inhibitors show antitumor potential, they may also impact immune cell metabolism or lead to resistance via transporter redundancy. Furthermore, some clinical trials targeting amino acid pathways have failed to show significant benefits, highlighting the complexity and redundancy of metabolic networks in cancer.

5.4 Combination therapies and immunometabolism

Combining metabolic inhibitors with immunotherapies has emerged as a promising strategy to enhance antitumor immune responses in NSCLC (154). Modulating tumor metabolism can improve the function of immune cells within the TME, representing a synergistic approach to NSCLC treatment. Tumor cells often create a metabolically hostile environment for immune cells by consuming large amounts of glucose and amino acids, leading to nutrient deprivation for tumor-infiltrating lymphocytes (TILs) (155). Additionally, tumor cells produce immunosuppressive metabolites like lactate and adenosine, which inhibit immune cell function (156). By targeting tumor metabolism, it is possible to alleviate these immunosuppressive conditions and enhance the efficacy of immunotherapies. Inhibiting glycolysis in tumor cells can reduce glucose competition, making it more available for effector T cells that rely on glycolysis for their function (157). Glycolytic inhibitors, such as 2-DG, may improve T-cell activity when combined with immune checkpoint inhibitors (116). IDO is an enzyme overexpressed in some tumors that depletes tryptophan and produces immunosuppressive metabolites (158). IDO inhibitors can restore tryptophan levels and enhance T-cell proliferation. Combining IDO inhibitors with PD-1/PD-L1 blockade has shown synergistic antitumor effects in preclinical models (159). As discussed previously, GLS inhibitors like CB-839 can reduce glutamine availability for tumor cells (128). Since glutamine is less critical for T-cell function than for tumor cells, GLS inhibition may preferentially affect cancer cells and improve immune responses.

Modulating the metabolism of immune cells themselves can also enhance antitumor immunity. The mTOR pathway regulates T-cell metabolism and function (160). Activating mTOR can promote T-cell glycolysis and effector functions. Agents that enhance mTOR signaling in T cells may boost their antitumor activity. AMPK activation can improve the metabolic fitness of T cells, enhancing their survival and function in the nutrient-deprived TME (161).

Combining metabolic inhibitors with immunotherapies aims to create a more favorable metabolic environment for immune cells while directly targeting tumor metabolism. Targeting metabolic checkpoints in tumor cells can sensitize them to immune-mediated killing. For example, inhibiting LDHA reduces lactate production, alleviating acid-mediated immunosuppression (119). Combining immune checkpoint inhibitors (e.g., anti-PD-1/PD-L1 antibodies) with metabolic modulators can enhance T-cell infiltration and activity. Clinical trials are exploring such combinations in NSCLC patients. Epacadostat, an IDO inhibitor, has been evaluated in combination with pembrolizumab (anti-PD-1) in clinical trials, showing promising results in some cancer types (162). However, results have been mixed, and further studies are needed to determine efficacy in NSCLC. Metformin, a complex I inhibitor, has immunomodulatory effects and may enhance responses to immunotherapy (132). Retrospective studies suggest that NSCLC patients taking metformin may have improved outcomes with immune checkpoint inhibitors.

5.5 Personalized metabolic therapies

The heterogeneity of metabolic profiles among NSCLC tumors underscores the need for personalized metabolic therapies (163). Metabolic profiling of tumors can identify patient-specific metabolic dependencies, enabling tailored treatment strategies that target the unique metabolic vulnerabilities of each tumor (164). Advanced technologies such as metabolomics, genomics, transcriptomics, and proteomics allow for comprehensive metabolic profiling of tumors. High-throughput techniques can analyze metabolic enzyme expression levels, metabolite concentrations, and metabolic fluxes within cancer cells (165).

These high-throughput techniques include: 1. Mass Spectrometry (MS) and Nuclear Magnetic Resonance (NMR) Spectroscopy: These techniques enable the identification and quantification of a wide range of metabolites in tumor samples. 2. Positron Emission Tomography (PET) Imaging: Metabolic imaging using tracers like 18F-fluorodeoxyglucose (FDG) can assess glucose uptake in tumors, providing insights into glycolytic activity. 3. Gene Expression Profiling: Analyzing the expression of genes involved in metabolic pathways can reveal overactive or dysregulated metabolic enzymes.

6 Challenges and future directions

Cancer cells' ability to adapt metabolically poses a significant challenge for metabolic therapies. Their metabolic plasticity enables them to switch between different energy sources and metabolic pathways, which can render single-agent treatments less effective. Future research should focus on understanding these resistance mechanisms and developing strategies to prevent or overcome them. Ensuring the safety and selectivity of metabolic inhibitors is also critical; these agents must selectively target cancer cells without harming normal tissues. Strategies to achieve this include exploiting cancer-specific metabolic pathways or employing delivery systems that preferentially target tumor cells.

Integrating metabolic biomarkers into clinical practice is essential for personalizing treatment and improving outcomes. Standardizing these biomarkers and incorporating them into clinical workflows require close collaboration between researchers and clinicians. Validation in large, diverse patient cohorts is necessary to ensure their reliability and effectiveness in clinical settings. Advancing the field further necessitates interdisciplinary collaboration among oncologists, biochemists, pharmacologists, and computational biologists. Integrating diverse expertise will accelerate the translation of metabolic discoveries into effective therapies, ultimately enhancing treatment strategies for NSCLC.

7 Conclusion

The metabolic reprogramming of NSCLC cells extends far beyond the Warburg effect, encompassing alterations in lipid and amino acid metabolism and dynamic interactions with the TME. These metabolic adaptations are not merely bystanders but are integral to tumor growth, survival, and therapeutic resistance. By leveraging emerging technologies and a deeper understanding of metabolic heterogeneity, we can identify novel vulnerabilities in NSCLC. Therapeutic strategies that target these metabolic dependencies offer promising avenues for improving patient outcomes. Combining metabolic inhibitors with existing treatments, such as immunotherapies and targeted therapies, may enhance efficacy and overcome resistance. Personalized metabolic therapies, guided by metabolic profiling, represent the next frontier in precision oncology. As we continue to unravel the complexities of NSCLC metabolism, we move closer to realizing the full potential of metabolic targeting in cancer therapy. The integration of cutting-edge research with clinical practice holds the promise of transforming NSCLC management and improving the lives of patients worldwide.

Author contributions

HC: Investigation, Writing – original draft. FZ: Investigation, Writing – original draft. FX: Investigation, Writing – review & editing. CY: Conceptualization, Funding acquisition, Project administration, Supervision, Writing – review & editing.

Funding

The author(s) declare that financial support was received for the research and/or publication of this article. This work was supported by a grant from the Dalian Science and Technology Innovation Fund Program (No. 2024JJ13PT070) and United Foundation for Dalian Institute of Chemical Physics, Chinese Academy of Sciences and the Second Hospital of Dalian Medical University (No. DMU-2&DICP UN202410), and National Natural Science Foundation of China (No. 82002211).

Conflict of interest

The authors declare that the research was conducted in the absence of any commercial or financial relationships that could be construed as a potential conflict of interest.

Generative AI statement

The author(s) declare that no Generative AI was used in the creation of this manuscript.

Publisher's note

All claims expressed in this article are solely those of the authors and do not necessarily represent those of their affiliated organizations, or those of the publisher, the editors and the reviewers. Any product that may be evaluated in this article, or claim that may be made by its manufacturer, is not guaranteed or endorsed by the publisher.

References

1. Thai AA, Solomon BJ, Sequist LV, Gainor JF, Heist RS. Lung cancer. *Lancet*. (2021) 398:535–54. doi: 10.1016/S0140-6736(21)00312-3

2. Megyesfalvi Z, Gay CM, Popper H, Pirker R, Ostoros G, Heeke S, et al. Clinical insights into small cell lung cancer: Tumor heterogeneity, diagnosis, therapy, and future directions. *CA Cancer J Clin*. (2023) 73:620–52. doi: 10.3322/caac.21785

3. Siegel RL, Miller KD, Fuchs HE, Jemal A. Cancer statistics, 2021. *CA Cancer J Clin*. (2021) 71:7–33. doi: 10.3322/caac.21654

4. Chaft JE, Shyr Y, Sepesi B, Forde PM. Preoperative and postoperative systemic therapy for operable non-small-cell lung cancer. *J Clin Oncol*. (2022) 40:546–55. doi: 10.1200/JCO.21.01589

5. Pavlova NN, Zhu J, Thompson CB. The hallmarks of cancer metabolism: Still emerging. *Cell Metab*. (2022) 34:355–77. doi: 10.1016/j.cmet.2022.01.007

6. Martínez-Reyes I, Chandel NS. Cancer metabolism: looking forward. *Nat Rev Cancer*. (2021) 21:669–80. doi: 10.1038/s41568-021-00378-6

7. Warburg O. On the origin of cancer cells. *Science*. (1956) 123:309–14. doi: 10.1126/science.123.3191.309

8. Faubert B, Solmonson A, DeBerardinis RJ. Metabolic reprogramming and cancer progression. *Science*. (2020) 368:eaaw5473. doi: 10.1126/science.aaw5473

9. Salcher S, Sturm G, Horvath L, Untergasser G, Kuempers C, Fotakis G, et al. High-resolution single-cell atlas reveals diversity and plasticity of tissue-resident neutrophils in non-small cell lung cancer. *Cancer Cell*. (2022) 40:1503–1520.e8. doi: 10.1016/j.ccell.2022.10.008

10. Li Z, Sun C, Qin Z. Metabolic reprogramming of cancer-associated fibroblasts and its effect on cancer cell reprogramming. *Theranostics*. (2021) 11:8322–36. doi: 10.7150/thno.62378

11. Mao X, Xu J, Wang W, Liang C, Hua J, Liu J, et al. Crosstalk between cancer-associated fibroblasts and immune cells in the tumor microenvironment: new findings and future perspectives. *Mol Cancer*. (2021) 20:131. doi: 10.1186/s12943-021-01428-1

12. Xia L, Oyang L, Lin J, Tan S, Han Y, Wu N, et al. The cancer metabolic reprogramming and immune response. *Mol Cancer*. (2021) 20:28. doi: 10.1186/s12943-021-01316-8

13. Jing X, Yang F, Shao C, Wei K, Xie M, Shen H, et al. Role of hypoxia in cancer therapy by regulating the tumor microenvironment. *Mol Cancer*. (2019) 18:157. doi: 10.1186/s12943-019-1089-9

14. Vander Heiden MG, Cantley LC, Thompson CB. Understanding the Warburg effect: the metabolic requirements of cell proliferation. *Science*. (2009) 324:1029–33. doi: 10.1126/science.1160809

15. Liang LJ, Yang FY, Wang D, Zhang YF, Yu H, Wang Z, et al. CIP2A induces PKM2 tetramer formation and oxidative phosphorylation in non-small cell lung cancer. *Cell Discov*. (2024) 10:13. doi: 10.1038/s41421-023-00633-0

16. Gonzalez MA, Lu DR, Yousefi M, Kroll A, Lo CH, Briseño CG, et al. Phagocytosis increases an oxidative metabolic and immune suppressive signature in tumor macrophages. *J Exp Med*. (2023) 220:e20221472. doi: 10.1084/jem.20221472

17. Rao S, Mondragón L, Pranjic B, Hanada T, Stoll G, Köcher T, et al. AIF-regulated oxidative phosphorylation supports lung cancer development. *Cell Res*. (2019) 29:579–91. doi: 10.1038/s41422-019-0181-4

18. Zhou Y, Guo Y, Ran M, Shan W, Granchi C, Giovannetti E, et al. Combined inhibition of pyruvate dehydrogenase kinase 1 and lactate dehydrogenase A induces metabolic and signaling reprogramming and enhances lung adenocarcinoma cell killing. *Cancer Lett*. (2023) 577:216425. doi: 10.1016/j.canlet.2023.216425

19. Ge W, Wang Y, Quan M, Mao T, Bischof EY, Xu H, et al. Activation of the PI3K/AKT signaling pathway by ARNTL2 enhances cellular glycolysis and sensitizes pancreatic adenocarcinoma to erlotinib. *Mol Cancer*. (2024) 23:48. doi: 10.1186/s12943-024-01965-5

20. Sun S, Zhang Y, Xu W, Yang R, Yang Y, Guo J, et al. Plumbagin reduction by thioredoxin reductase 1 possesses synergy effects with GLUT1 inhibitor on KEAP1-mutant NSCLC cells. *BioMed Pharmacother*. (2022) 146:112546. doi: 10.1016/j.biopha.2021.112546

21. Huang Y, Chen Z, Lu T, Bi G, Li M, Liang J, et al. HIF-1α switches the functionality of TGF-β signaling via changing the partners of smads to drive glucose metabolic reprogramming in non-small cell lung cancer. *J Exp Clin Cancer Res*. (2021) 40:398. doi: 10.1186/s13046-021-02188-y

22. Sainero-Alcolado L, Liaño-Pons J, Ruiz-Pérez MV, Arsenian-Henriksson M. Targeting mitochondrial metabolism for precision medicine in cancer. *Cell Death Differ*. (2022) 29:1304–17. doi: 10.1038/s41418-022-01022-y

23. Porporato PE, Filigheddu N, Pedro JMB, Kroemer G, Galluzzi L. Mitochondrial metabolism and cancer. *Cell Res*. (2018) 28:265–80. doi: 10.1038/cr.2017.155

24. Ashton TM, McKenna WG, Kunz-Schughart LA, Higgins GS. Oxidative phosphorylation as an emerging target in cancer therapy. *Clin Cancer Res*. (2018) 24:2482–90. doi: 10.1158/1078-0432.CCR-17-3070

25. Lin Z, Li J, Zhang J, Feng W, Lu J, Ma X, et al. Metabolic reprogramming driven by IGF2BP3 promotes acquired resistance to EGFR inhibitors in non-small cell lung cancer. *Cancer Res*. (2023) 83:2187–207. doi: 10.1158/0008-5472.CAN-22-3059

26. Thirusangu P, Ray U, Sarkar Bhattacharya S, Oien DB, Jin L, Staub J, et al. PFKFB3 regulates cancer stemness through the Hippo pathway in small cell lung carcinoma. *Oncogene*. (2022) 41:4003–17. doi: 10.1038/s41388-022-02391-x

27. Han M, Bushong EA, Segawa M, Tiard A, Wong A, Brady MR, et al. Spatial mapping of mitochondrial networks and bioenergetics in lung cancer. *Nature*. (2023) 615:712–9. doi: 10.1038/s41586-023-05793-3

28. Feng J, Lian Z, Xia X, Lu Y, Hu K, Zhang Y, et al. Targeting metabolic vulnerability in mitochondria conquers MEK inhibitor resistance in KRAS-mutant lung cancer. *Acta Pharm Sin B*. (2023) 13:1145–63. doi: 10.1016/j.apsb.2022.10.023

29. Rehman J, Zhang HJ, Toth PT, Zhang Y, Marsboom G, Hong Z, et al. Inhibition of mitochondrial fission prevents cell cycle progression in lung cancer. *FASEB J*. (2012) 26:2175–86. doi: 10.1096/fj.11-196543

30. Chen D, Barsoumian HB, Fischer G, Yang L, Verma V, Younes AI, et al. Combination treatment with radiotherapy and a novel oxidative phosphorylation inhibitor overcomes PD-1 resistance and enhances antitumor immunity. *J Immunother Cancer*. (2020) 8:e000289. doi: 10.1136/jitc-2019-000289

31. Lissanu Deribe Y, Sun Y, Terranova C, Khan F, Martinez-Ledesma J, Gay J, et al. Mutations in the SWI/SNF complex induce a targetable dependence on oxidative phosphorylation in lung cancer. *Nat Med*. (2018) 24:1047–57. doi: 10.1038/s41591-018-0019-5

32. Zhang J, Qiao W, Luo Y. Mitochondrial quality control proteases and their modulation for cancer therapy. *Med Res Rev*. (2023) 43:399–436. doi: 10.1002/med.21929

33. Joshi SR, Kitagawa A, Jacob C, Hashimoto R, Dhagia V, Ramesh A, et al. Hypoxic activation of glucose-6-phosphate dehydrogenase controls the expression of genes involved in the pathogenesis of pulmonary hypertension through the regulation of DNA methylation. *Am J Physiol Lung Cell Mol Physiol*. (2020) 318:L773–86. doi: 10.1152/ajplung.00001.2020

34. Parma B, Wurdak H, Ceppi P. Harnessing mitochondrial metabolism and drug resistance in non-small cell lung cancer and beyond by blocking heat-shock proteins. *Drug Resist Updat*. (2022) 65:100888. doi: 10.1016/j.drup.2022.100888

35. Lien EC, Westermark AM, Zhang Y, Yuan C, Li Z, Lau AN, et al. Low glycaemic diets alter lipid metabolism to influence tumour growth. *Nature*. (2021) 599:302–7. doi: 10.1038/s41586-021-04049-2

36. Bartolacci C, Andreani C, Vale G, Berto S, Melegari M, Crouch AC, et al. Targeting *de novo* lipogenesis and the Lands cycle induces ferroptosis in KRAS-mutant lung cancer. *Nat Commun*. (2022) 13:4327. doi: 10.1038/s41467-022-31963-4

37. Al-Jawadi A, Patel CR, Shiarella RJ, Romelus E, Auvinen M, Guardia J, et al. Cell-type-specific, ketohexokinase-dependent induction by fructose of lipogenic gene expression in mouse small intestine. *J Nutr*. (2020) 150:1722–30. doi: 10.1093/jn/nxaa113

38. Lyu Q, Zhu W, Wei T, Ding W, Cao M, Wang Q, et al. High mutations in fatty acid metabolism contribute to a better prognosis of small-cell lung cancer patients treated with chemotherapy. *Cancer Med*. (2021) 10:7863–76. doi: 10.1002/cam4.4290

39. Cao D, Yang J, Deng Y, Su M, Wang Y, Feng X, et al. Discovery of a mammalian FASN inhibitor against xenografts of non-small cell lung cancer and melanoma. *Signal Transduct Target Ther*. (2022) 7:273. doi: 10.1038/s41392-022-01099-4

40. Wohlhieter CA, Richards AL, Uddin F, Hulton CH, Quintanal-Villalonga À, Martin A, et al. Concurrent mutations in STK11 and KEAP1 promote ferroptosis protection and SCD1 dependence in lung cancer. *Cell Rep*. (2020) 33:108444. doi: 10.1016/j.celrep.2020.108444

41. Svensson RU, Parker SJ, Eichner LJ, Kolar MJ, Wallace M, Brun SN, et al. Inhibition of acetyl-CoA carboxylase suppresses fatty acid synthesis and tumor growth of non-small-cell lung cancer in preclinical models. *Nat Med*. (2016) 22:1108–19. doi: 10.1038/nm.4181

42. Peng F, Lu J, Su K, Liu X, Luo H, He B, et al. Oncogenic fatty acid oxidation senses circadian disruption in sleep-deficiency-enhanced tumorigenesis. *Cell Metab*. (2024) 36:1598–1618.e11. doi: 10.1016/j.cmet.2024.04.018

43. Ma Y, Temkin SM, Hawkridge AM, Guo C, Wang W, Wang XY, et al. Fatty acid oxidation: An emerging facet of metabolic transformation in cancer. *Cancer Lett*. (2018) 435:92–100. doi: 10.1016/j.canlet.2018.08.006

44. Nimmakayala RK, Leon F, Rachagani S, Rauth S, Nallasamy P, Marimuthu S, et al. Metabolic programming of distinct cancer stem cells promotes metastasis of pancreatic ductal adenocarcinoma. *Oncogene*. (2021) 40:215–31. doi: 10.1038/s41388-020-01518-2

45. Gao Y, Song Z, Jia L, Tang Y, Wang C, Zhao X, et al. Self-amplified ROS production from fatty acid oxidation enhanced tumor immunotherapy by atorvastatin/PD-L1 siRNA lipopeptide nanoplexes. *Biomaterials*. (2022) 291:121902. doi: 10.1016/j.biomaterials.2022.121902

46. Yan R, Zheng C, Qian S, Li K, Kong X, Liao S. The ZNF263/CPT1B axis regulates fatty acid β-oxidation to affect cisplatin resistance in lung adenocarcinoma. *Pharmacogenomics J*. (2024) 24:33. doi: 10.1038/s41397-024-00355-w

47. Liu LZ, Wang B, Zhang R, Wu Z, Huang Y, Zhang X, et al. The activated CD36-Src axis promotes lung adenocarcinoma cell proliferation and actin remodeling-

involved metastasis in high-fat environment. *Cell Death Dis*. (2023) 14:548. doi: 10.1038/s41419-023-06078-3

48. Gong Z, Li Q, Shi J, Liu ET, Shultz LD, Ren G. Lipid-laden lung mesenchymal cells foster breast cancer metastasis via metabolic reprogramming of tumor cells and natural killer cells. *Cell Metab*. (2022) 34:1960–1976.e9. doi: 10.1016/j.cmet.2022.11.003

49. Chen J, Zhao R, Wang Y, Xiao H, Lin W, Diao M, et al. G protein-coupled estrogen receptor activates PI3K/AKT/mTOR signaling to suppress ferroptosis via SREBP1/SCD1-mediated lipogenesis. *Mol Med*. (2024) 30:28. doi: 10.1186/s10020-023-00763-x

50. Anthiya S, Öztürk SC, Yanik H, Tavukcuoglu E, Şahin A, Datta D, et al. Targeted siRNA lipid nanoparticles for the treatment of KRAS-mutant tumors. *J Control Release*. (2023) 357:67–83. doi: 10.1016/j.jconrel.2023.03.016

51. Liu T, Han C, Fang P, Ma Z, Wang X, Chen H, et al. Cancer-associated fibroblast-specific lncRNA LINC01614 enhances glutamine uptake in lung adenocarcinoma. *J Hematol Oncol*. (2022) 15:141. doi: 10.1186/s13045-022-01359-4

52. Mayers JR, Torrence ME, Danai LV, Papagiannakopoulos T, Davidson SM, Bauer MR, et al. Tissue of origin dictates branched-chain amino acid metabolism in mutant Kras-driven cancers. *Science*. (2016) 353:1161–5. doi: 10.1126/science.aaf5171

53. Rachedi NS, Tang Y, Tai YY, Zhao J, Chauvet C, Grynblat J, et al. Dietary intake and glutamine-serine metabolism control pathologic vascular stiffness. *Cell Metab*. (2024) 36:1335–1350.e8. doi: 10.1016/j.cmet.2024.04.010

54. DeNicola GM, Chen PH, Mullarky E, Sudderth JA, Hu Z, Wu D, et al. NRF2 regulates serine biosynthesis in non-small cell lung cancer. *Nat Genet*. (2015) 47:1475–81. doi: 10.1038/ng.3421

55. Zhu J, Ma J, Wang X, Ma T, Zhang S, Wang W, et al. High expression of PHGDH predicts poor prognosis in non-small cell lung cancer. *Transl Oncol*. (2016) 9:592–9. doi: 10.1016/j.tranon.2016.08.003

56. He L, Endress J, Cho S, Li Z, Zheng Y, Asara JM, et al. Suppression of nuclear GSK3 signaling promotes serine/one-carbon metabolism and confers metabolic vulnerability in lung cancer cells. *Sci Adv*. (2022) 8:eabm8786. doi: 10.1126/sciadv.abm8786

57. Zhang B, Zheng A, Hydbring P, Ambroise G, Ouchida AT, Goiny M, et al. PHGDH defines a metabolic subtype in lung adenocarcinomas with poor prognosis. *Cell Rep*. (2017) 19:2289–303. doi: 10.1016/j.celrep.2017.05.067

58. Jing N, Zhang K, Chen X, Liu K, Wang J, Xiao L, et al. ADORA2A-driven proline synthesis triggers epigenetic reprogramming in neuroendocrine prostate and lung cancers. *J Clin Invest*. (2023) 133:e168670. doi: 10.1172/JCI168670

59. Elia I, Broekaert D, Christen S, Boon R, Radaelli E, Orth MF, et al. Proline metabolism supports metastasis formation and could be inhibited to selectively target metastasizing cancer cells. *Nat Commun*. (2017) 8:15267. doi: 10.1038/ncomms15267

60. Liu Y, Mao C, Wang M, Liu N, Ouyang L, Liu S, et al. Cancer progression is mediated by proline catabolism in non-small cell lung cancer. *Oncogene*. (2020) 39:2358–76. doi: 10.1038/s41388-019-1151-5

61. Mailloux RJ. Proline and dihydroorotate dehydrogenase promote a hyper-proliferative state and dampen ferroptosis in cancer cells by rewiring mitochondrial redox metabolism. *Biochim Biophys Acta Mol Cell Res*. (2024) 1871:119639. doi: 10.1016/j.bbamcr.2023.119639

62. Xu E, Ji B, Jin K, Chen Y. Branched-chain amino acids catabolism and cancer progression: focus on therapeutic interventions. *Front Oncol*. (2023) 13:1220638. doi: 10.3389/fonc.2023.1220638

63. Yao X, Deng Y, Zhou J, Jiang L, Song Y. Expression pattern and prognostic analysis of branched-chain amino acid catabolism-related genes in non-small cell lung cancer. *Front Biosci (Landmark Ed)*. (2023) 28:107. doi: 10.31083/j.fbl2806107

64. Hassanein M, Hoeksema MD, Shiota M, Qian J, Harris BK, Chen H, et al. SLC1A5 mediates glutamine transport required for lung cancer cell growth and survival. *Clin Cancer Res*. (2013) 19:560–70. doi: 10.1158/1078-0432.CCR-12-2334

65. Cormerais Y, Giuliano S, LeFloch R, Front B, Durivault J, Tambutté E, et al. Genetic disruption of the multifunctional CD98/LAT1 complex demonstrates the key role of essential amino acid transport in the control of mTORC1 and tumor growth. *Cancer Res*. (2016) 76:4481–92. doi: 10.1158/0008-5472.CAN-15-3376

66. Liu X, Qin H, Li Z, Lv Y, Feng S, Zhuang W, et al. Inspiratory hyperoxia suppresses lung cancer metastasis through a MYC/SLC1A5-dependent metabolic pathway. *Eur Respir J*. (2022) 60:2200062. doi: 10.1183/13993003.00062-2022

67. Hassanein M, Qian J, Hoeksema MD, Wang J, Jacobovitz M, Ji X, et al. Targeting SLC1a5-mediated glutamine dependence in non-small cell lung cancer. *Int J Cancer*. (2015) 137:1587–97. doi: 10.1002/ijc.29535

68. Groves SM, Ildefonso GV, McAtee CO, Ozawa PMM, Ireland AS, Stauffer PE, et al. Archetype tasks link intratumoral heterogeneity to plasticity and cancer hallmarks in small cell lung cancer. *Cell Syst*. (2022) 13:690–710.e17. doi: 10.1016/j.cels.2022.07.006

69. Li L, Bi Z, Wadgaonkar P, Lu Y, Zhang Q, Fu Y, et al. Metabolic and epigenetic reprogramming in the arsenic-induced cancer stem cells. *Semin Cancer Biol*. (2019) 57:10–8. doi: 10.1016/j.semcancer.2019.04.003

70. Galan-Cobo A, Sitthideatphaiboon P, Qu X, Poteete A, Pisegna MA, Tong P, et al. LKB1 and KEAP1/NRF2 pathways cooperatively promote metabolic reprogramming with enhanced glutamine dependence in KRAS-mutant lung adenocarcinoma. *Cancer Res*. (2019) 79:3251–67. doi: 10.1158/0008-5472.CAN-18-3527

71. Kaufman JM, Amann JM, Park K, Arasada RR, Li H, Shyr Y, et al. LKB1 loss induces characteristic patterns of gene expression in human tumors associated with NRF2 activation and attenuation of PI3K-AKT. *J Thorac Oncol*. (2014) 9:794–804. doi: 10.1097/JTO.0000000000000173

72. Zhang S, Liu Y, Sun Y, Liu Q, Gu Y, Huang Y, et al. Aberrant R-loop-mediated immune evasion, cellular communication, and metabolic reprogramming affect cancer progression: a single-cell analysis. *Mol Cancer*. (2024) 23:11. doi: 10.1186/s12943-023-01924-6

73. Chen PH, Cai L, Huffman K, Yang C, Kim J, Faubert B, et al. Metabolic diversity in human non-small cell lung cancer cells. *Mol Cell*. (2019) 76:838–851.e5. doi: 10.1016/j.molcel.2019.08.028

74. Choi KM, Kim JJ, Yoo J, Kim KS, Gu Y, Eom J, et al. The interferon-inducible protein viperin controls cancer metabolic reprogramming to enhance cancer progression. *J Clin Invest*. (2022) 132:e157302. doi: 10.1172/JCI157302

75. Gu M, Liu Y, Zheng W, Jing Z, Li X, Guo W, et al. Combined targeting of senescent cells and senescent macrophages: A new idea for integrated treatment of lung cancer. *Semin Cancer Biol*. (2024) 106-107:43–57. doi: 10.1016/j.semcancer.2024.08.006

76. Li M, Yang Y, Xiong L, Jiang P, Wang J, Li C. Metabolism, metabolites, and macrophages in cancer. *J Hematol Oncol*. (2023) 16:80. doi: 10.1186/s13045-023-01478-6

77. Yoshida GJ. Metabolic reprogramming: the emerging concept and associated therapeutic strategies. *J Exp Clin Cancer Res*. (2015) 34:111. doi: 10.1186/s13046-015-0221-y

78. Morigny P, Boucher J, Arner P, Langin D. Lipid and glucose metabolism in white adipocytes: pathways, dysfunction and therapeutics. *Nat Rev Endocrinol*. (2021) 17:276–95. doi: 10.3390/cells9102308

79. You M, Xie Z, Zhang N, Zhang Y, Xiao D, Liu S, et al. Signaling pathways in cancer metabolism: mechanisms and therapeutic targets. *Signal Transduct Target Ther*. (2023) 8:196. doi: 10.1038/s41392-023-01442-3

80. Yang WH, Qiu Y, Stamatatos O, Janowitz T, Lukey MJ. Enhancing the efficacy of glutamine metabolism inhibitors in cancer therapy. *Trends Cancer*. (2021) 7:790–804. doi: 10.1016/j.trecan.2021.04.003

81. Aggarwal C, Thompson JC, Black TA, Katz SI, Fan R, Yee SS, et al. Clinical implications of plasma-based genotyping with the delivery of personalized therapy in metastatic non-small cell lung cancer. *JAMA Oncol*. (2019) 5:173–80. doi: 10.1001/jamaoncol.2018.4305

82. Tong Y, Gao WQ, Liu Y. Metabolic heterogeneity in cancer: An overview and therapeutic implications. *Biochim Biophys Acta Rev Cancer*. (2020) 1874:188421. doi: 10.1016/j.bbcan.2020.188421

83. Lanekoff I, Sharma VV, Marques C. Single-cell metabolomics: where are we and where are we going? *Curr Opin Biotechnol*. (2022) 75:102693. doi: 10.1016/j.copbio.2022.102693

84. Spina E, de Leon J. Metabolic drug interactions with newer antipsychotics: a comparative review. *Basic Clin Pharmacol Toxicol*. (2007) 100:4–22. doi: 10.1111/j.1742-7843.2007.00017.x

85. Sun C, Wang A, Zhou Y, Chen P, Wang X, Huang J, et al. Spatially resolved multi-omics highlights cell-specific metabolic remodeling and interactions in gastric cancer. *Nat Commun*. (2023) 14:2692. doi: 10.1038/s41467-023-38360-5

86. Hu H, Piotrowska Z, Hare PJ, Chen H, Mulvey HE, Mayfield A, et al. Three subtypes of lung cancer fibroblasts define distinct therapeutic paradigms. *Cancer Cell*. (2021) 39:1531–1547.e10. doi: 10.1016/j.ccell.2021.09.003

87. Chaudhri VK, Salzler GG, Dick SA, Buckman MS, Sordella R, Karoly ED, et al. Metabolic alterations in lung cancer-associated fibroblasts correlated with increased glycolytic metabolism of the tumor. *Mol Cancer Res*. (2013) 11:579–92. doi: 10.1158/1541-7786.MCR-12-0437-T

88. Hwang SH, Yang Y, Jung JH, Kim Y. Oleic acid from cancer-associated fibroblast promotes cancer cell stemness by stearoyl-CoA desaturase under glucose-deficient condition. *Cancer Cell Int*. (2022) 22:404. doi: 10.1186/s12935-022-02824-3

89. Yao H, Li Y, Zheng Y, Lin JM. Stability of the arginine-ornithine-citrulline cycle maintained by tumor-stroma interactions in cell coculture hydrogel microspheres. *Anal Chem*. (2023) 95:10999–1006. doi: 10.1021/acs.analchem.3c01134

90. Zhang X, Dong Y, Zhao M, Ding L, Yang X, Jing Y, et al. ITGB2-mediated metabolic switch in CAFs promotes OSCC proliferation by oxidation of NADH in mitochondrial oxidative phosphorylation system. *Theranostics*. (2020) 10:12044–59. doi: 10.7150/thno.47901

91. Bai J, Liu T, Tu B, Yuan M, Shu Z, Fan M, et al. Autophagy loss impedes cancer-associated fibroblast activation via downregulating proline biosynthesis. *Autophagy*. (2023) 19:632–43. doi: 10.1080/15548627.2022.2093026

92. Shi L, Zhu W, Huang Y, Zhuo L, Wang S, Chen S, et al. Cancer-associated fibroblast-derived exosomal microRNA-20a suppresses the PTEN/PI3K-AKT pathway to promote the progression and chemoresistance of non-small cell lung cancer. *Clin Transl Med*. (2022) 12:e989. doi: 10.1002/ctm2.989

93. Cong J, Wang X, Zheng X, Wang D, Fu B, Sun R, et al. Dysfunction of natural killer cells by FBP1-induced inhibition of glycolysis during lung cancer progression. *Cell Metab*. (2018) 28:243–255.e5. doi: 10.1016/j.cmet.2018.06.021

94. La Fleur L, Botling J, He F, Pelicano C, Zhou C, He C, et al. Targeting MARCO and IL37R on immunosuppressive macrophages in lung cancer blocks regulatory T cells and supports cytotoxic lymphocyte function. *Cancer Res*. (2021) 81:956–67. doi: 10.1158/0008-5472.CAN-20-1885

95. Chen Y, Zhou Y, Ren R, Chen Y, Lei J, Li Y. Harnessing lipid metabolism modulation for improved immunotherapy outcomes in lung adenocarcinoma. *J Immunother Cancer*. (2024) 12:e008811. doi: 10.1136/jitc-2024-008811

96. Best SA, Gubser PM, Sethumadhavan S, Kersbergen A, Negrón Abril YL, Goldford J, et al. Glutaminase inhibition impairs CD8 T cell activation in STK11-/Lkb1-deficient lung cancer. *Cell Metab*. (2022) 34:874–887.e6. doi: 10.1016/j.cmet.2022.04.003

97. Hamaidi I, Zhang L, Kim N, Wang MH, Iclozan C, Fang B, et al. Sirt2 inhibition enhances metabolic fitness and effector functions of tumor-reactive T cells. *Cell Metab*. (2020) 32:420–436.e12. doi: 10.1016/j.cmet.2020.07.008

98. Azuma K, Xiang H, Tagami T, Kasajima R, Kato Y, Karakawa S, et al. Clinical significance of plasma-free amino acids and tryptophan metabolites in patients with non-small cell lung cancer receiving PD-1 inhibitor: a pilot cohort study for developing a prognostic multivariate model. *J Immunother Cancer*. (2022) 10:e004420. doi: 10.1136/jitc-2021-004420

99. Abd El-Fattah EE. IDO/kynurenine pathway in cancer: possible therapeutic approaches. *J Transl Med*. (2022) 20:347. doi: 10.1186/s12967-022-03554-w

100. Zhang H, Li S, Wang D, Liu S, Xiao T, Gu W, et al. Metabolic reprogramming and immune evasion: the interplay in the tumor microenvironment. *Biomark Res*. (2024) 12:96. doi: 10.1186/s40364-024-00646-1

101. Zheng Y, Li L, Shen Z, Wang L, Niu X, Wei Y, et al. Mechanisms of neural infiltration-mediated tumor metabolic reprogramming impacting immunotherapy efficacy in non-small cell lung cancer. *J Exp Clin Cancer Res*. (2024) 43:284. doi: 10.1186/s13046-024-03202-9

102. Wang Y, Wang D, Yang L, Zhang Y. Metabolic reprogramming in the immunosuppression of tumor-associated macrophages. *Chin Med J (Engl)*. (2022) 135:2405–16. doi: 10.1097/CM9.0000000000002426

103. Salem A, Asselin MC, Reymen B, Jackson A, Lambin P, West CML, et al. Targeting hypoxia to improve non-small cell lung cancer outcome. *J Natl Cancer Inst*. (2018) 110(1). doi: 10.1093/jnci/djx160

104. Wang D, Zhao C, Xu F, Zhang A, Jin M, Zhang K, et al. Cisplatin-resistant NSCLC cells induced by hypoxia transmit resistance to sensitive cells through exosomal PKM2. *Theranostics*. (2021) 11:2860–75. doi: 10.7150/thno.51797

105. Giatromanolaki A, Koukourakis MI, Pezzella F, Turley H, Sivridis E, Bouros D, et al. Expression of prolyl-hydroxylases PHD-1, 2 and 3 and of the asparagine hydroxylase FIH in non-small cell lung cancer relates to an activated HIF pathway. *Cancer Lett*. (2008) 262:87–93. doi: 10.1016/j.canlet.2007.11.041

106. Nisar H, Labonté FM, Roggan MD, Schmitz C, Chevalier F, Konda B, et al. Hypoxia modulates radiosensitivity and response to different radiation qualities in A549 non-small cell lung cancer (NSCLC) cells. *Int J Mol Sci*. (2024) 25:1010. doi: 10.3390/ijms25021010

107. Chen W, Tang D, Lin J, Huang X, Lin S, Shen G, et al. Exosomal circSHKBP1 participates in non-small cell lung cancer progression through PKM2-mediated glycolysis. *Mol Ther Oncolytics*. (2022) 24:470–85. doi: 10.1016/j.omto.2022.01.012

108. Hua Q, Mi B, Xu F, Wen J, Zhao L, Liu J, et al. Hypoxia-induced lncRNA-AC020978 promotes proliferation and glycolytic metabolism of non-small cell lung cancer by regulating PKM2/HIF-1α axis. *Theranostics*. (2020) 10:4762–78. doi: 10.7150/thno.43839

109. Kokeza J, Strikic A, Ogorevc M, Kelam N, Vukoja M, Dilber I, et al. The effect of GLUT1 and HIF-1α expressions on glucose uptake and patient survival in non-small-cell lung carcinoma. *Int J Mol Sci*. (2023) 24:10575. doi: 10.3390/ijms241310575

110. Miao Y, Wang W, Dong Y, Hu J, Wei K, Yang S, et al. Hypoxia induces tumor cell growth and angiogenesis in non-small cell lung carcinoma via the Akt-PDK1-HIF1α-YKL-40 pathway. *Transl Cancer Res*. (2020) 9:2904–18. doi: 10.21037/tcr.2020.03.80

111. Salaroglio IC, Belisario DC, Akman M, La Vecchia S, Godel M, Anobile DP, et al. Mitochondrial ROS drive resistance to chemotherapy and immune-killing in hypoxic non-small cell lung cancer. *J Exp Clin Cancer Res*. (2022) 41:243. doi: 10.1186/s13046-022-02447-6

112. de Souza LP, Borghi M, Fernie A. Plant single-cell metabolomics—challenges and perspectives. *Int J Mol Sci*. (2020) 21:8987. doi: 10.3390/ijms21238987

113. Planque M, Igelmann S, Ferreira Campos AM, Fendt SM. Spatial metabolomics principles and application to cancer research. *Curr Opin Chem Biol*. (2023) 76:102362. doi: 10.1016/j.cbpa.2023.102362

114. Pang Z, Zhou G, Ewald J, Chang L, Hacariz O, Basu N, et al. Using MetaboAnalyst 5.0 for LC-HRMS spectra processing, multi-omics integration and covariate adjustment of global metabolomics data. *Nat Protoc*. (2022) 17:1735–61. doi: 10.1038/s41596-022-00710-w

115. Baysoy A, Bai Z, Satija R, Fan R. The technological landscape and applications of single-cell multi-omics. *Nat Rev Mol Cell Biol*. (2023) 24:695–713. doi: 10.1038/s41580-023-00615-w

116. Guo Z, Liu Y, Li X, Huang Y, Zhou Z, Yang C. Reprogramming hematopoietic stem cell metabolism in lung cancer: glycolysis, oxidative phosphorylation, and the role of 2-DG. *Biol Direct*. (2024) 19:73. doi: 10.1186/s13062-024-00514-w

117. Saleme B, Gurtu V, Zhang Y, Kinnaird A, Boukouris AE, Gopal K, et al. Tissue-specific regulation of p53 by PKM2 is redox dependent and provides a therapeutic target for anthracycline-induced cardiotoxicity. *Sci Transl Med*. (2019) 11:eaau8866. doi: 10.1126/scitranslmed.aau8866

118. Ying ZH, Li HM, Yu WY, Yu CH. Iridin prevented against lipopolysaccharide-induced inflammatory responses of macrophages via inactivation of PKM2-mediated glycolytic pathways. *J Inflammation Res*. (2021) 14:341–54. doi: 10.2147/JIR.S292244

119. Chen Y, Yan H, Yan L, Wang X, Che X, Hou K, et al. Hypoxia-induced ALDH3A1 promotes the proliferation of non-small-cell lung cancer by regulating energy metabolism reprogramming. *Cell Death Dis*. (2023) 14:617. doi: 10.1038/s41419-023-06142-y

120. Dutta S, Shah RB, Singhal S, Dutta SB, Bansal S, Sinha S, et al. Metformin: a review of potential mechanism and therapeutic utility beyond diabetes. *Drug Des Devel Ther*. (2023) 17:1907–32. doi: 10.2147/DDDT.S409373

121. Kim S, Im JH, Kim WK, Choi YJ, Lee JY, Kim SK, et al. Enhanced sensitivity of non-small cell lung cancer with acquired resistance to epidermal growth factor receptor-tyrosine kinase inhibitors to phenformin: the roles of a metabolic shift to oxidative phosphorylation and redox balance. *Oxid Med Cell Longev*. (2021) 2021:5428364. doi: 10.1155/2021/5428364

122. Sri-Pathmanathan RM, Plumb JA, Fearon KC. Clofazimine alters the energy metabolism and inhibits the growth rate of a human lung-cancer cell line *in vitro* and in *vivo*. *Int J Cancer*. (1994) 56:900–5. doi: 10.1002/ijc.2910560624

123. Ramkumar K, Tanimoto A, Della Corte CM, Stewart CA, Wang Q, Shen L, et al. Targeting BCL2 overcomes resistance and augments response to aurora kinase B inhibition by AZD2811 in small cell lung cancer. *Clin Cancer Res*. (2023) 29:3237–49. doi: 10.1158/1078-0432.CCR-23-0375

124. Falchook G, Infante J, Arkenau HT, Patel MR, Dean E, Borazanci E, et al. First-in-human study of the safety, pharmacokinetics, and pharmacodynamics of first-in-class fatty acid synthase inhibitor TVB-2640 alone and with a taxane in advanced tumors. *EClinicalMedicine*. (2021) 34:100797. doi: 10.1016/j.eclinm.2021.100797

125. Wang J, Lin W, Li R, Cheng H, Sun S, Shao F, et al. The deubiquitinase USP13 maintains cancer cell stemness by promoting FASN stability in small cell lung cancer. *Front Oncol*. (2022) 12:899987. doi: 10.3389/fonc.2022.899987

126. Pisanu ME, Noto A, De Vitis C, Morrone S, Scognamiglio G, Botti G, et al. Blockade of Stearoyl-CoA-desaturase 1 activity reverts resistance to cisplatin in lung cancer stem cells. *Cancer Lett*. (2017) 406:93–104. doi: 10.1016/j.canlet.2017.07.027

127. Hu X, Xiang J, Li Y, Xia Y, Xu S, Gao X, et al. Inhibition of Stearoyl-CoA Desaturase 1 potentiates anti-tumor activity of amodiaquine in non-small cell lung cancer. *Biol Pharm Bull*. (2022) 45:438–45. doi: 10.1248/bpb.b21-00843

128. Boysen G, Jamshidi-Parsian A, Davis MA, Siegel ER, Simecka CM, Kore RA, et al. Glutaminase inhibitor CB-839 increases radiation sensitivity of lung tumor cells and human lung tumor xenografts in mice. *Int J Radiat Biol*. (2019) 95:436–42. doi: 10.1080/09553002.2018.1558299

129. Wang Z, Wei D, Bin E, Li J, Jiang K, Lv T, et al. Enhanced glycolysis-mediated energy production in alveolar stem cells is required for alveolar regeneration. *Cell Stem Cell*. (2023) 30:1028–1042.e7. doi: 10.1016/j.stem.2023.07.007

130. Hou XB, Li TH, Ren ZP, Liu Y. Combination of 2-deoxy d-glucose and metformin for synergistic inhibition of non-small cell lung cancer: A reactive oxygen species and P-p38 mediated mechanism. *BioMed Pharmacother*. (2016) 84:1575–84. doi: 10.1016/j.biopha.2016.10.037

131. Krishnamurthy S, Ng VW, Gao S, Tan MH, Yang YY. Phenformin-loaded polymeric micelles for targeting both cancer cells and cancer stem cells *in vitro* and in *vivo*. *Biomaterials*. (2014) 35:9177–86. doi: 10.1016/j.biomaterials.2014.07.018

132. Berber E, Rouse BT. Controlling herpes simplex virus-induced immunoinflammatory lesions using metabolic therapy: a comparison of 2-deoxy-d-glucose with metformin. *J Virol*. (2022) 96:e0068822. doi: 10.1128/jvi.00688-22

133. Chang L, Fang S, Chen Y, Yang Z, Yuan Y, Zhang J, et al. Inhibition of FASN suppresses the Malignant biological behavior of non-small cell lung cancer cells via deregulating glucose metabolism and AKT/ERK pathway. *Lipids Health Dis*. (2019) 18:118. doi: 10.1186/s12944-019-1058-8

134. Tan YJ, Ali A, Tee SY, Teo JT, Xi Y, Go ML, et al. Galloyl esters of trans-stilbenes are inhibitors of FASN with anticancer activity on non-small cell lung cancer cells. *Eur J Med Chem*. (2019) 182:111597. doi: 10.1016/j.ejmech.2019.111597

135. Zhang J, Song F, Zhao X, Jiang H, Wu X, Wang B, et al. EGFR modulates monounsaturated fatty acid synthesis through phosphorylation of SCD1 in lung cancer. *Mol Cancer*. (2017) 16:127. doi: 10.1186/s12943-017-0704-x

136. Hess D, Chisholm JW, Igal RA. Inhibition of stearoyl-CoA desaturase activity blocks cell cycle progression and induces programmed cell death in lung cancer cells. *PloS One*. (2010) 5:e11394. doi: 10.1371/journal.pone.0011394

137. Kodama M, Oshikawa K, Shimizu H, Yoshioka S, Takahashi M, Izumi Y, et al. A shift in glutamine nitrogen metabolism contributes to the Malignant progression of cancer. *Nat Commun*. (2020) 11:1320. doi: 10.1038/s41467-020-15136-9

138. Riess JW, Frankel P, Shackelford D, Dunphy M, Badawi RD, Nardo L, et al. Phase 1 trial of MLN0128 (Sapanisertib) and CB-839 HCl (Telaglenastat) in patients with advanced NSCLC (NCI 10327): rationale and study design. *Clin Lung Cancer*. (2021) 22:67–70. doi: 10.1016/j.cllc.2020.10.006

139. Momcilovic M, Bailey ST, Lee JT, Fishbein MC, Magyar C, Braas D, et al. Targeted inhibition of EGFR and glutaminase induces metabolic crisis in EGFR mutant lung cancer. *Cell Rep*. (2017) 18:601–10. doi: 10.1016/j.celrep.2016.12.061

140. Wang K, Lu H, Wang X, Liu Q, Hu J, Liu Y, et al. Simultaneous suppression of PKM2 and PHGDH elicits synergistic anti-cancer effect in NSCLC. *Front Pharmacol*. (2023) 14:1200538. doi: 10.3389/fphar.2023.1200538

141. Hamanaka RB, Nigdelioglu R, Meliton AY, Tian Y, Witt LJ, O'Leary E, et al. Inhibition of phosphoglycerate dehydrogenase attenuates bleomycin-induced pulmonary fibrosis. *Am J Respir Cell Mol Biol*. (2018) 58:585–93. doi: 10.1165/rcmb.2017-0186OC

142. Lee HM, Muhammad N, Lieu EL, Cai F, Mu J, Ha YS, et al. Concurrent loss of LKB1 and KEAP1 enhances SHMT-mediated antioxidant defence in KRAS-mutant lung cancer. *Nat Metab*. (2024) 6:1310–28. doi: 10.1038/s42255-024-01066-z

143. Han T, Wang Y, Cheng M, Hu Q, Wan X, Huang M, et al. Phosphorylated SHMT2 regulates oncogenesis through m6A modification in lung adenocarcinoma. *Adv Sci (Weinh)*. (2024) 11:e2307834. doi: 10.1002/advs.202307834

144. Becirovic T, Zhang B, Lindskog C, Norberg E, Vakifahmetoglu-Norberg H, Kaminskyy VO, et al. Deubiquitinase USP9x regulates the proline biosynthesis pathway in non-small cell lung cancer. *Cell Death Discov*. (2024) 10:342. doi: 10.1038/s41420-024-02111-2

145. Yang L, Gilbertsen A, Jacobson B, Kratzke R, Henke CA. Serum splicing factor proline- and glutamine-rich is a diagnostic marker for non-small-cell lung cancer and other solid cancers. *Int J Mol Sci*. (2024) 25:8766. doi: 10.3390/ijms25168766

146. Lu W, Cui J, Wang W, Hu Q, Xue Y, Liu X, et al. PPIA dictates NRF2 stability to promote lung cancer progression. *Nat Commun*. (2024) 15:4703. doi: 10.1038/s41467-024-48364-4

147. Yao CC, Sun RM, Yang Y, Zhou HY, Meng ZW, Chi R, et al. Accumulation of branched-chain amino acids reprograms glucose metabolism in CD8+ T cells with enhanced effector function and anti-tumor response. *Cell Rep*. (2023) 42:112186. doi: 10.1016/j.celrep.2023.112186

148. Li Z, Hao J, Wang T, Guo C, Liu L. Branched-chain amino acids and risk of lung cancer: insights from mendelian randomization and NHANES III. *J Thorac Dis*. (2024) 16:5248–61. doi: 10.21037/jtd-24-420

149. Palanca-Ballester C, Hervas D, Villalba M, Valdes-Sanchez T, Garcia D, Alcoriza-Balaguer MI, et al. Translation of a tissue epigenetic signature to circulating free DNA suggests BCAT1 as a potential noninvasive diagnostic biomarker for lung cancer. *Clin Epigenetics*. (2022) 14:116. doi: 10.1186/s13148-022-01334-3

150. Hu K, Li K, Lv J, Feng J, Chen J, Wu H, et al. Suppression of the SLC7A11/glutathione axis causes synthetic lethality in KRAS-mutant lung adenocarcinoma. *J Clin Invest*. (2020) 130:1752–66. doi: 10.1172/JCI124049

151. Qin L, Cheng X, Wang S, Gong G, Su H, Huang H, et al. Discovery of novel aminobutanoic acid-based ASCT2 inhibitors for the treatment of non-small-cell lung cancer. *J Med Chem*. (2024) 67:988–1007. doi: 10.1021/acs.jmedchem.3c01093

152. Cormerais Y, Massard PA, Vucetic M, Giuliano S, Tambutté E, Durivault J, et al. The glutamine transporter ASCT2 (SLC1A5) promotes tumor growth independently of the amino acid transporter LAT1 (SLC7A5). *J Biol Chem*. (2018) 293:2877–87. doi: 10.1074/jbc.RA117.001342

153. Rajasinghe LD, Hutchings M, Gupta SV. Delta-tocotrienol modulates glutamine dependence by inhibiting ASCT2 and LAT1 transporters in non-small cell lung cancer (NSCLC) cells: a metabolomic approach. *Metabolites*. (2019) 9:50. doi: 10.3390/metabo9030050

154. Hensley CT, Faubert B, Yuan Q, Lev-Cohain N, Jin E, Kim J, et al. Metabolic heterogeneity in human lung tumors. *Cell*. (2016) 164:681–94. doi: 10.1016/j.cell.2015.12.034

155. Aramini B, Masciale V, Samarelli AV, Dubini A, Gaudio M, Stella F, et al. Phenotypic, functional, and metabolic heterogeneity of immune cells infiltrating non-small cell lung cancer. *Front Immunol*. (2022) 13:959114. doi: 10.3389/fimmu.2022.959114

156. Yu T, Liu Z, Tao Q, Xu X, Li X, Li Y, et al. Targeting tumor-intrinsic SLC16A3 to enhance anti-PD-1 efficacy via tumor immune microenvironment reprogramming. *Cancer Lett*. (2024) 589:216824. doi: 10.1016/j.canlet.2024.216824

157. Morrissey SM, Zhang F, Ding C, Montoya-Durango DE, Hu X, Yang C, et al. Tumor-derived exosomes drive immunosuppressive macrophages in a pre-metastatic niche through glycolytic dominant metabolic reprogramming. *Cell Metab*. (2021) 33:2040–2058.e10. doi: 10.1016/j.cmet.2021.09.002

158. Wang W, Huang L, Jin JY, Jolly S, Zang Y, Wu H, et al. IDO immune status after chemoradiation may predict survival in lung cancer patients. *Cancer Res*. (2018) 78:809–16. doi: 10.1158/0008-5472.CAN-17-2995

159. Qin R, Zhao C, Wang CJ, Xu W, Zhao JY, Lin Y, et al. Tryptophan potentiates CD8+ T cells against cancer cells by TRIP12 tryptophanylation and surface PD-1 downregulation. *J Immunother Cancer*. (2021) 9:e002840. doi: 10.1136/jitc-2021-002840

160. Xu S, Xu Y, Solek NC, Chen J, Gong F, Varley AJ, et al. Tumor-tailored ionizable lipid nanoparticles facilitate IL-12 circular RNA delivery for enhanced lung cancer immunotherapy. *Adv Mater*. (2024) 36:e2400307. doi: 10.1002/adma.202400307

161. Hollstein PE, Eichner LJ, Brun SN, Kamireddy A, Svensson RU, Vera LI, et al. The AMPK-related kinases SIK1 and SIK3 mediate key tumor-suppressive effects of LKB1 in NSCLC. *Cancer Discov*. (2019) 9:1606–27. doi: 10.1158/2159-8290.CD-18-1261

162. Mitchell TC, Hamid O, Smith DC, Bauer TM, Wasser JS, Olszanski AJ, et al. Epacadostat plus pembrolizumab in patients with advanced solid tumors: phase I results from a multicenter, open-label phase I/II trial (ECHO-202/KEYNOTE-037). *J Clin Oncol*. (2018) 36:3223–30. doi: 10.1200/JCO.2018.78.9602

163. Matschke J, Larafa S, Jendrossek V. Metabolic reprogramming of antioxidant defense: a precision medicine perspective for radiotherapy of lung cancer? *Biochem Soc Trans*. (2021) 49:1265–77. doi: 10.1042/BST20200866

164. Schuler M, Hense J, Darwiche K, Michels S, Hautzel H, Kobe C, et al. Early metabolic response by PET predicts sensitivity to next-line targeted therapy in EGFR-mutated lung cancer with unknown mechanism of acquired resistance. *J Nucl Med*. (2024) 65:851–5. doi: 10.2967/jnumed.123.266979

165. Ocak S, Sos ML, Thomas RK, Massion PP. High-throughput molecular analysis in lung cancer: insights into biology and potential clinical applications. *Eur Respir J*. (2009) 34:489–506. doi: 10.1183/09031936.00042409

frontiers | Frontiers in Medicine

TYPE Original Research
PUBLISHED 21 May 2025
DOI 10.3389/fmed.2025.1586253

Check for updates

OPEN ACCESS

EDITED BY
Esmaeil Mortaz,
Shahid Beheshti University of Medical Sciences, Iran

REVIEWED BY
Elisa Scalco,
National Research Council (CNR), Italy
Zheng Yuan,
China Academy of Chinese Medical Sciences, China

*CORRESPONDENCE
Hui Wang
✉ wanghuisl@sdfmu.edu.cn

†These authors have contributed equally to this work and share first authorship

RECEIVED 02 March 2025
ACCEPTED 02 May 2025
PUBLISHED 21 May 2025

CITATION
Wang Y, Gao Z, Li M, Feng Z and Wang H (2025) Prognostic effect of CD74 and development of a radiomic model for predicting CD74 expression in non-small cell lung cancer.
Front. Med. 12:1586253.
doi: 10.3389/fmed.2025.1586253

COPYRIGHT
© 2025 Wang, Gao, Li, Feng and Wang. This is an open-access article distributed under the terms of the Creative Commons Attribution License (CC BY). The use, distribution or reproduction in other forums is permitted, provided the original author(s) and the copyright owner(s) are credited and that the original publication in this journal is cited, in accordance with accepted academic practice. No use, distribution or reproduction is permitted which does not comply with these terms.

Prognostic effect of CD74 and development of a radiomic model for predicting CD74 expression in non-small cell lung cancer

Yancheng Wang[1†], Zhen Gao[1†], Meng Li[1,2], Zhen Feng[1,2] and Hui Wang[1,2*]

[1]Department of Thoracic Surgery, Shandong Provincial Hospital Affiliated to Shandong First Medical University, Shandong First Medical University, Jinan, China, [2]Department of Thoracic Surgery, Shandong Provincial Hospital, Shandong University, Jinan, China

Background: The classical prognostic indicators of lung cancer are no longer sufficient for prognostic stratification and individualized treatment of highly heterogeneous non-small cell lung cancer (NSCLC). This study aimed to establish a radiomics model to predict CD74 expression level in NSCLC patients and to explore its role in the tumor immune response and its prognostic value.

Methods: The prediction model was developed based on 122 NSCLC transcriptome samples, including 68 paired enhanced CT and transcriptome samples. Survival analysis, gene set variation analysis, and immune cell infiltration analysis were used to investigate the relationship between CD74 expression and tumor immune response. Logistic regression (LG) and support vector machine (SVM) analysis were used to construct the prediction model. The performance of the model was assessed with respect to its calibration, discrimination, and clinical usefulness.

Results: High CD74 expression is an independent prognostic factor for NSCLC and is positively correlated with antigen presentation and processing gene expression and antitumor immune cell infiltration. The radiomics prediction models for CD74 expression demonstrated good predictive performance. The areas under the receiver operating characteristic curves for the LG and SVM radiomics models were 0.778 and 0.729, respectively, in the training set and 0.772 and 0.701, respectively, in the validation set. The calibration and decision curve analysis curves demonstrated good fit and clinical benefit.

Conclusion: CD74 expression significantly impacts the prognosis of NSCLC patients. The radiomics model based on contrast-enhanced CT exhibits good performance and clinical practicability in predicting CD74 expression.

KEYWORDS

CD74, non-small cell lung cancer, radiomics, machine learning, prediction model

Introduction

Lung cancer ranks first among cancers in terms of mortality and second in terms of overall morbidity (1). Among the various types of lung cancer, non-small cell lung cancer (NSCLC) is the most common (2, 3). Surgical resection is considered the gold standard treatment for early-stage lung cancer; however, the surgical outcome and prognosis for advanced patients are poor (4). Therefore, for advanced lung cancer patients who are not eligible for surgery, it

is essential to predict their prognosis and provide precision treatment for long-term high-quality survival with tumors (5). NSCLC exhibits significant genetic and cellular heterogeneity (6). There is an urgent need for individualized therapy in NSCLC. Traditional diagnostic and prognostic indicators for lung cancer include clinicopathological features, laboratory diagnostic indicators such as carcinoembryonic antigen and carbohydrate antigen 125, and CT imaging methods (7, 8). However, these indicators are no longer sufficient to meet the clinical requirements of precision medicine (2, 9). Therefore, it is necessary to further explore new prognostic indicators to meet the precision treatment needs of NSCLC.

Analysis of gene expression can identify novel markers and targets for patient management and treatment. Several studies have suggested that CD74 may serve as a prognostic factor (10, 11) and therapeutic target (12, 13) for patients with malignant tumors. CD74 encodes class II major histocompatibility complex-associated proteins (13, 14), which are primarily involved in antigen presentation during the immune response (15). Additionally, CD74 can act as a cell surface receptor for macrophage cytokines, mediating the survival and proliferation of macrophages (14). For example, one study demonstrated that CD74 is essential for the distant metastasis of breast cancer, and targeting CD74 therapy may be an effective strategy for breast cancer treatment (16). Furthermore, CD74-ROS1 is the most common form of ROS1 fusion in NSCLC, and CD74-NRG1 gene fusion activates genomic alterations in aggressive mucinous adenocarcinomas, offering potential therapeutic opportunities for lung tumor subtypes that have not yet been effectively treated (17). Currently, the expression level of CD74 can only be detected through peripheral blood cytokine analysis, mRNA or protein level analysis using fresh tissue samples, or paraffin tissue sample analysis, but these methods are expensive and complex, have limited reflection of tumor parenchyma, and are prone to bias.

RNA-seq offers high resolution and low technical variability (18), and demonstrates a high degree of concordance with other gold-standard techniques in transcriptomics, both for absolute and relative gene expression measurements (19). However, its high cost and the invasive nature of sample collection limit its clinical applicability. Immunohistochemistry (IHC), by contrast, is more affordable but suffers from operator variability and antibody bias, leading to inter-laboratory heterogeneity and the lack of quantitative, objective assessments (20). Given these limitations, imaging techniques provide distinct advantages. Previous studies have shown that radiomics can be used to noninvasively predict the pathological type or molecular features of NSCLC by extracting high-throughput features from images for quantitative analysis (21–23). Additionally, it also can effectively identify patients at high risk of disease recurrence and positively improve NSCLC stratification and patient survival through noninvasive prediction of gene expression (18–20). Based on these studies, radiomics may be a powerful tool for facilitating decision making in the individualized management of NSCLC.

In view of the advantages of radiomics, this study used radiomics techniques to predict CD74 mRNA expression in NSCLC tumor tissues and combined them with bioinformatics analysis to explore the molecular mechanism of the tumor immune response related to CD74 expression. This approach provides a convenient and noninvasive new indicator for the stratification and optimal individualized treatment of NSCLC patients.

Abbreviations: NSCLC, non-small cell lung cancer; TCIA, The Cancer Imaging Archive; GEO, Gene Expression Omnibus; LUAD, Lung adenocarcinoma; LUSC, lung squamous cell carcinoma; GSVA, gene set variation analysis; ROI, Region of interest; VOI, volume of interest; ICC, correlation coefficient; RFE, recursive feature elimination; AIC, Akaike information criterion; LR, logistic regression; SVM, support vector machine; ROC, receiver operating characteristic; DCA, decision curve analysis; AUC, area under the curve; FDR, false discovery rate; OS, overall survival; IBSI, Image Biomarker Standardisation Initiative.

Patients and methods

Patients

The flow chart of this study is shown in Figure 1. This workflow is shown in the Graphical Abstract. The NSCLC cohort of this study included medical imaging data from the NSCLC Radiogenomics dataset in The Cancer Imaging Archive (TCIA) Public Access-Cancer Imaging Archive Wiki. The RNA-seq data and clinical follow-up data for the main cohort are from the Gene Expression Omnibus (GEO) database, and the dataset is named GSE103584 (24).[1] The inclusion and exclusion criteria are detailed in Supplementary Table S1. Finally, 122 transcriptome samples with complete clinical information and 68 imaging samples with complete clinical information and transcriptome information were obtained. Lung adenocarcinoma (LUAD) cohort transcriptome data were obtained from the TCGA database.[2] The inclusion and exclusion criteria are detailed in Supplementary Table S2. Finally, 320 transcriptome samples were obtained. All transcriptome data were converted to TPM format, and then log2 conversion was performed.

To determine the optimal cut-off value for CD74 expression, we used the surv_cutpoint function from the R package "survminer," applying the maximally selected rank statistics (also known as the minimum *p*-value method) to automatically identify the expression threshold that most significantly distinguishes survival differences. This method has been used in several high-quality studies because of its sensitivity to survival differences and well-balanced grouping (25–27). This cut-off value was then used to classify patients into high and low CD74 expression groups. Consequently, the cut-off value for CD74 expression in the NSCLC cohort was determined to be 8.7430, and patients were divided into a high expression group and a low expression group accordingly. The clinical baseline characteristics of the NSCLC cohorts are detailed in Table 1. The cut-off value for the CD74 expression level in the LUAD cohort was 9.5861, and the patients were divided into a high expression group and a low expression group. The clinical baseline characteristics are shown in Supplementary Table S3. The cut-off value of the CD74 expression level in the radiomic cohort was 8.7430, and the samples were divided into a high expression group and a low expression group.

1 https://www.ncbi.nlm.nih.gov/geo/query/acc.cgi?acc=GSE103584
2 https://portal.gdc.cancer.gov/

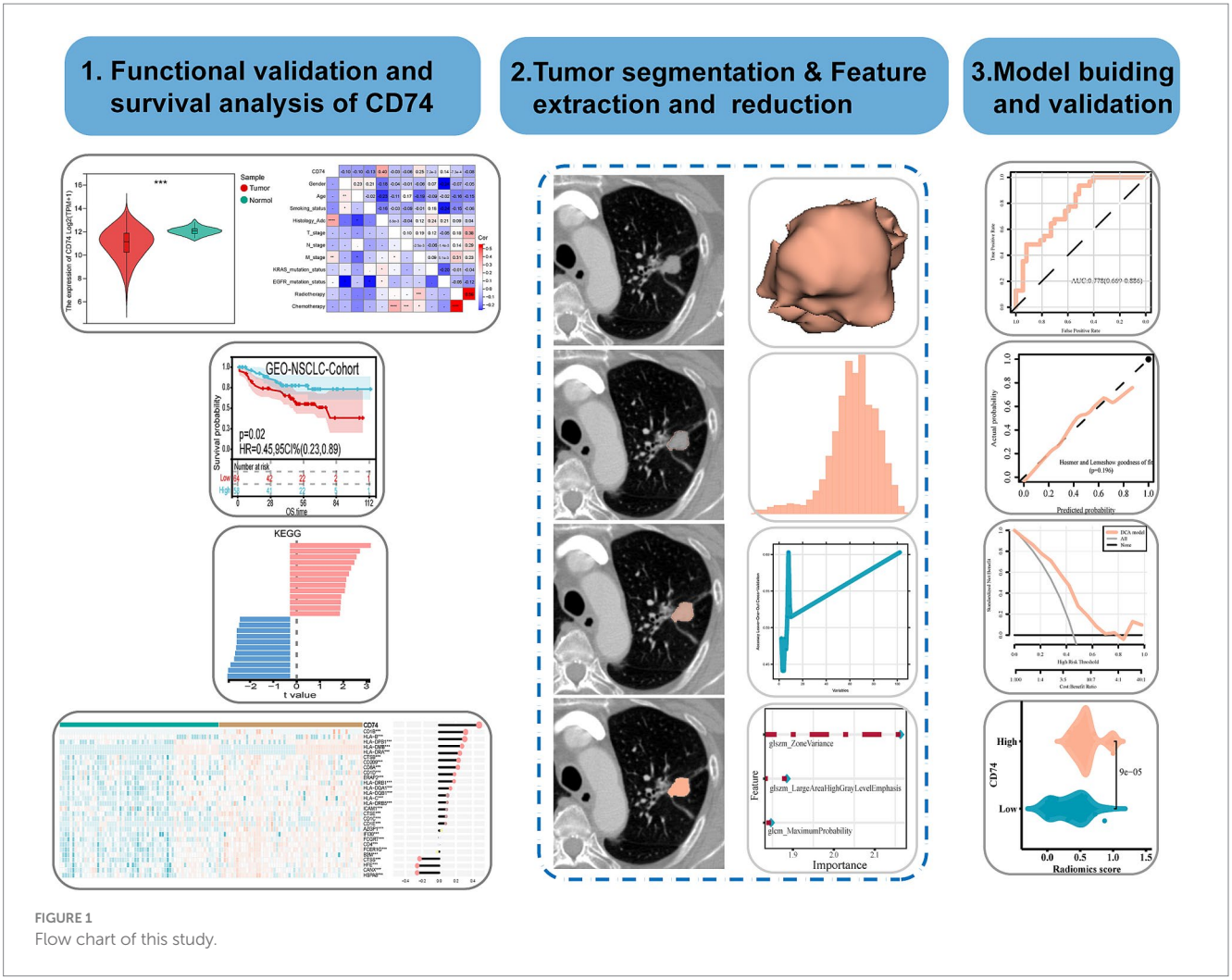

FIGURE 1
Flow chart of this study.

Survival analysis

Univariate Cox regression and multivariate Cox regression survival analyses were performed for each variable. A Kaplan–Meier survival curve was used to show the difference in the survival rates in different groups, and the log-rank test was used to test the significance of differences in the survival rates among groups. Univariate Cox regression was used to analyze the effect of CD74 expression on prognosis in different subgroups of covariates. The interaction between CD74 expression and other covariates was analyzed using the likelihood ratio (OR value) test. Cox regression analysis and survival analysis were performed using the R packages "survival" and "forestplot," and the R package "survminer" was used to summarize and visualize the results.

Gene set variation analysis (GSVA) and correlation analysis between CD74 high and low subgroups

GSVA is mainly used to evaluate the results of gene set enrichment in the transcriptome (28). It is mainly used to transform the expression matrix of genes between different samples into the expression matrix of gene sets between samples to evaluate whether different pathways are enriched in different samples. The enrichment scores of KEGG pathway gene sets and hallmark gene sets[3] in the NSCLC cohort and LUAD cohort samples were calculated by the GSVA algorithm. The R package "limma" was used to analyze the difference in the pathway enrichment score between the high and low CD74 groups, and the different paths were visualized, with $|t| = 1$ as the critical value.

Immune-related analysis associated with CD74 expression

The Wilcoxon rank sum test was used to detect the differential expression of antigen processing and presenting genes between the high and low CD74 groups. Genes with $p < 0.001$ were visualized, and the results are displayed in a heatmap. The gene expression matrix of NSCLC samples and LUAD samples was uploaded to the CIBERSORTx database[4] to calculate the immune cell infiltration of

3 https://www.gsea-msigdb.org/gsea/msigdb/index.jsp
4 https://cibersortx.stanford.edu/

TABLE 1 Demographic and clinicopathological characteristics of patients (NSCLC).

Variables	Total (*n* = 122)	Low (*n* = 64)	High (*n* = 58)	*p*
Gender, *n* (%)				0.741
Female	33 (27)	16 (25)	17 (29)	
Male	89 (73)	48 (75)	41 (71)	
Age, *n* (%)				0.176
≤65	44 (36)	19 (30)	25 (43)	
>65	78 (64)	45 (70)	33 (57)	
Smoking_status, *n* (%)				0.103
Nonsmoker	20 (16)	11 (17)	9 (16)	
Current	24 (20)	17 (27)	7 (12)	
Former	78 (64)	36 (56)	42 (72)	
Histology, *n* (%)				<0.001
Adenocarcinoma	92 (75)	39 (61)	53 (91)	
Squamous cell carcinoma	30 (25)	25 (39)	5 (9)	
T_stage, *n* (%)				0.75
T2/T3/T4	66 (54)	36 (56)	30 (52)	
Tis/T1	56 (46)	28 (44)	28 (48)	
N_stage, *n* (%)				0.863
N0	97 (80)	50 (78)	47 (81)	
N1/N2	25 (20)	14 (22)	11 (19)	
M_stage, *n* (%)				0.022
M0	117 (96)	64 (100)	53 (91)	
M1	5 (4)	0 (0)	5 (9)	
KRAS_mutation_status, *n* (%)				0.145
Mutant	23 (19)	9 (14)	14 (24)	
Unknown	27 (22)	18 (28)	9 (16)	
Wildtype	72 (59)	37 (58)	35 (60)	
EGFR_mutation_status, *n* (%)				0.071
Mutant	18 (15)	8 (12)	10 (17)	
Unknown	28 (23)	20 (31)	8 (14)	
Wildtype	76 (62)	36 (56)	40 (69)	
Radiotherapy, *n* (%)				1
No	108 (89)	57 (89)	51 (88)	
Yes	14 (11)	7 (11)	7 (12)	
Chemotherapy, *n* (%)				0.521
No	86 (70)	43 (67)	43 (74)	
Yes	36 (30)	21 (33)	15 (26)	

each sample (29). The R package "corrplot" was used to analyze the correlation between CD74 expression and the degree of immune cell infiltration.

CT imaging parameters and image processing

CT imaging parameters included a slice thickness ranging from 0.625 to 3 mm (median: 1.5 mm), an X-ray tube current between 124 and 699 mA (mean 220 mA), and a tube voltage ranging from 80 to 140 kVp (mean 120 kVp) (24).

To minimize the variability caused by differences in scanning equipment, imaging protocols, and lesion sizes, a series of standardized preprocessing steps were applied in this study. All CT images were resampled using the 'sitkBSpline' interpolator to achieve an isotropic voxel size of $1 \times 1 \times 1$ mm^3, thereby reducing variability related to scanning parameters and lesion dimensions. Voxel intensity values were discretized using a fixed bin width of 25 HU to reduce image noise and standardize signal intensity, enhancing the stability of radiomic features across different images. Image normalization was performed by scaling signal intensities to a range of 1–500 HU, aiming to minimize intensity variations across images acquired from different machines and further improve data consistency. Additionally, gray-level values were standardized using Z-score normalization to adjust the gray-level distributions across images, reduce inter-patient variability, and enhance the stability of feature computation.

Region of interest (ROI) of image construction and consistency evaluation

3D Slicer software (version 4.10.2) was utilized by an experienced radiologist with over 10 years of expertise in diagnosing chest disease imaging, as well as another radiologist with more than 5 years of experience, to manually outline the entire area of interest to obtain the complete tumor area. In cases where there was disagreement, a consensus was reached through discussion with a more senior imaging physician. The consistency of the image features extracted from the volume of interest (VOI) delineated by the two physicians was assessed using the intraclass correlation coefficient (ICC). To further validate the results, a random sample of 20 cases was chosen using the "random number table method" and assessed by an imaging doctor with more experience.

In this study, radiomics features were extracted using Pyradiomics,[5] including 14 shape features, 18 first-order features, and 75 s-order features, resulting in a total of 107 original radiomics features. The second-order features include GLCM, GLRLM, GLSZM, NGTDM, and GLDM, which are among the most commonly used features in radiomics research. Features with an ICC value of ≥0.75 were selected for the subsequent feature screening process (30–32).

Radiomic feature screening

Prior to model construction, we initially applied the Recursive feature elimination (RFE) method to perform a preliminary screening of the predictors by ranking radiomic features with an ICC ≥ 0.75. RFE iteratively trains the model and eliminates features of lower importance after each iteration until the optimal subset of features is identified (33). Based on the preliminary screening, stepwise regression combined with the Akaike information criterion (AIC) was subsequently employed for secondary feature selection (34). Using AIC to balance model complexity and goodness of fit, a bidirectional stepwise regression approach was applied to further eliminate features that contributed little to the model or showed high multicollinearity. Ultimately, three representative and stable radiomic features were selected for model construction, demonstrating good predictive performance and generalizability in both the training and validation cohorts.

Construction and evaluation of the logistic regression (LR) model and support vector machine (SVM) model

The final radiomic features were fitted using the logistic regression algorithm to establish a binary prediction model for predicting CD74 expression. The logistic regression fitting was performed using the "glm" function from the R package "stats." The radiomics model formula was calculated as the product of the feature and its corresponding coefficient plus the intercept value. Furthermore, the final screening radiomic features were fitted using the SVM algorithm to establish a binary prediction model for predicting CD74 expression. SVM algorithm fitting was performed using the R package "caret."

To evaluate the predictive performance of the LR model and SVM model, we used the receiver operating characteristic (ROC) curve. Additionally, we performed 5-fold internal cross-validation. The fit degree of the prediction model was evaluated using the calibration curve. Moreover, we drew a decision curve analysis (DCA) to assess the clinical benefit of the prediction model.

The LR radiomic model and SVM radiomic model provided the radiomics score for each sample. We employed the Wilcoxon test to assess whether there were differences between the high and low CD74 groups in terms of radiomics score.

Statistical analysis

The statistical analysis for this study was conducted using R 4.1.0. The t test was used for quantitative data that followed a normal distribution, while the Wilcoxon test was utilized for nonnormally distributed data. For the analysis of more than two groups, the Kruskal-Wallis test was employed as a nonparametric test, and ANOVA was used for parametric tests. The "survival" R package was used to analyze the prognostic differences between the two groups, and the significance of the prognostic differences among different groups of samples was assessed using the log-rank test. The pROC package was utilized to generate ROC curves, calculate the area under the curve (AUC), and determine confidence intervals. The DeLong test was used to compare AUC values under the ROC curve. Pearson correlation analysis was used to calculate the correlation between genes, as well as between genes and clinical traits. A p value less than 0.05 was considered statistically significant. For multiple hypothesis testing, the false discovery rate (FDR) was calculated using the Benjamini–Hochberg method (35).

Radiomics workflow quality assessment

To enhance the transparency and methodological rigor of this study, we systematically evaluated the quality of the radiomics workflow based on the Minimum Information for Reporting a Radiomics Study (METRICS) standard proposed by Kocak et al. (36). The total METRICS score was 87.1%. The completed METRICS checklist is provided in Supplementary material 1 to ensure the reproducibility and robustness of the study results and to facilitate the future clinical application of the model.

Results

Differences in expression and clinical characteristics between CD74 expression groups

The expression levels of CD74 in tumor tissues and normal tissues were compared based on the RNA-seq data of lung adenocarcinoma (LUAD) and lung squamous cell carcinoma (LUSC) patients from the TCGA database. As shown in Figure 2A, the expression level of CD74

5 https://pyradiomics.readthedocs.io/en/latest/

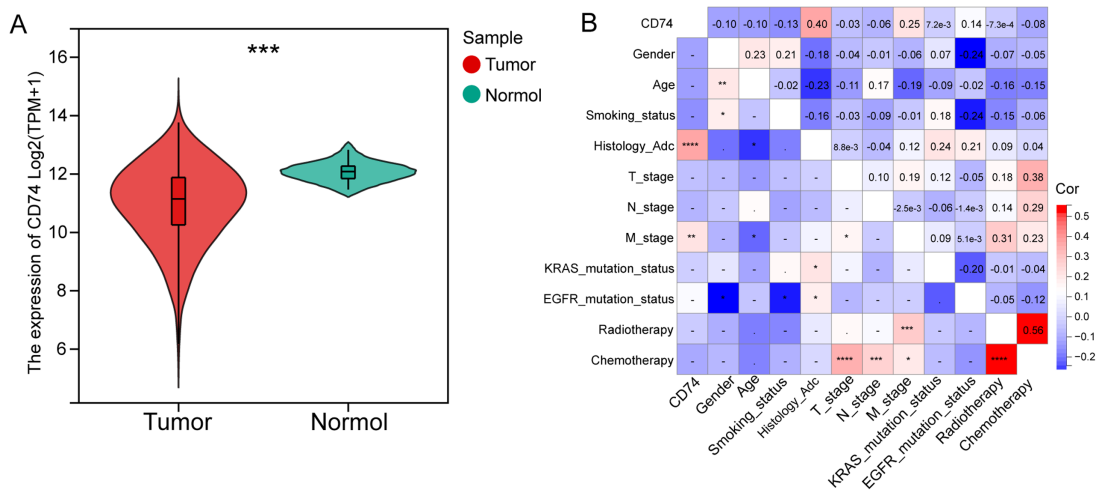

FIGURE 2
Differential expression and clinical correlation analysis of CD74. **(A)** Violin plot of differential analysis of CD74 expression in tumor and normal tissues, as shown in the figure, normal tissues showed significantly higher expression; **(B)** Heatmap of correlation between CD74 and clinical features, red represents positive correlation, blue represents negative correlation, and the higher the degree of color, the more significant the correlation. (Significant symbol: −, $p \geq 0.05$; *, $p < 0.05$; **, $p < 0.01$; ***, $p < 0.001$; ****, $p < 0.0001$).

was found to be lower in tumor tissues than in normal tissues ($p < 0.001$).

The NSCLC cohort consisted of 122 patients, with 58 patients in the CD74 high expression group and 64 patients in the CD74 low expression group. The clinical information of the patients is presented in Table 1. Analysis revealed that only histological subtype showed a statistically significant difference between the high and low expression groups. There were no significant differences observed in age, sex, smoking status, T stage, N stage, M stage, EGFR mutation, KRAS mutation, chemotherapy, or radiotherapy between the two groups. Correlation analysis demonstrated a positive correlation between CD74 expression and histological subtype ($r = 0.4$, $p < 0.0001$) as well as distant metastasis (M stage) ($r = 0.25$, $p < 0.01$), as shown in Figure 2B. Further details on clinical information and clinical correlation analysis in the LUAD cohort can be found in Supplementary Table S3 and Supplementary Figures S1.

Survival analysis between CD74 groups

A total of 122 patients in the NSCLC cohort were included in the survival analysis. The Kaplan–Meier curve showed that high CD74 expression was associated with improved overall survival (OS) ($p = 0.02$) (Figure 3A). Similarly, in the LUAD cohort, the CD74 high expression group had a higher survival rate ($p = 0.006$) (Figure 3B). In the NSCLC cohort, patients with later N stage and M stage had worse OS ($p < 0.005$ and 0.012), and in the LUAD cohort, patients with later T stage and N stage had worse OS ($p < 0.001$) (Supplementary Figures S2a–d). Multivariate Cox regression analysis of variables showed that high CD74 expression was also a protective factor for OS (HR = 0.311, 95% CI 0.129–0.747, $p = 0.009$), which was statistically significant (Figure 3C). Similarly, in the LUAD cohort, both univariate and multivariate COX regression analyses showed that high CD74 expression was a protective factor for OS (HR = 0.595 and 0.638, 95% CI 0.416–0.85 and 0.438–0.931, respectively; $p = 0.004$ and 0.02) (Figure 3D). Therefore, high CD74 expression can be regarded as an independent prognostic factor for NSCLC and LUAD.

The interaction analysis between CD74 and other variables in the NSCLC cohort and LUAD cohort showed that the high expression of CD74 was a protective factor for OS, and there was no statistically significant difference in the interaction test of each variable ($p > 0.05$). It can be assumed that the effect of high CD74 expression on OS is the same across patients with differences in subvariables. For more details, refer to Supplementary Figure S2e.

GSVA of CD74-related genes

The enrichment scores of KEGG pathway gene sets and hallmark gene sets were calculated using GSVA for the expression matrix of the NSCLC cohort and LUAD cohort. Differential analysis of the enrichment score revealed that the CD74 high expression group was significantly enriched in various cancers, such as small lung cancer, non-small cell lung cancer, pancreatic cancer, and others, within the KEGG gene set. Additionally, it was significantly enriched in signaling pathways such as apoptosis, the JAK/STAT pathway, and the ERBB signaling pathway. Please refer to Figure 4A and Supplementary Figure S3a for more details.

In the hallmark gene set, the CD74 high expression group showed significant enrichment in the DNA repair, MYC targets V1, and oxidative phosphorylation signaling pathways. Conversely, the low CD74 group exhibited significant enrichment in the Hedgehog signaling, angiogenesis, and KRAS signaling pathways. Please see Figure 4B and Supplementary Figure S3b for visual representation.

Overall, our analysis indicates that tumor cell behaviors are inhibited in the tumor microenvironment of patients with high CD74 expression, while multiple cancer pathways are activated in tumor cells with low CD74 expression.

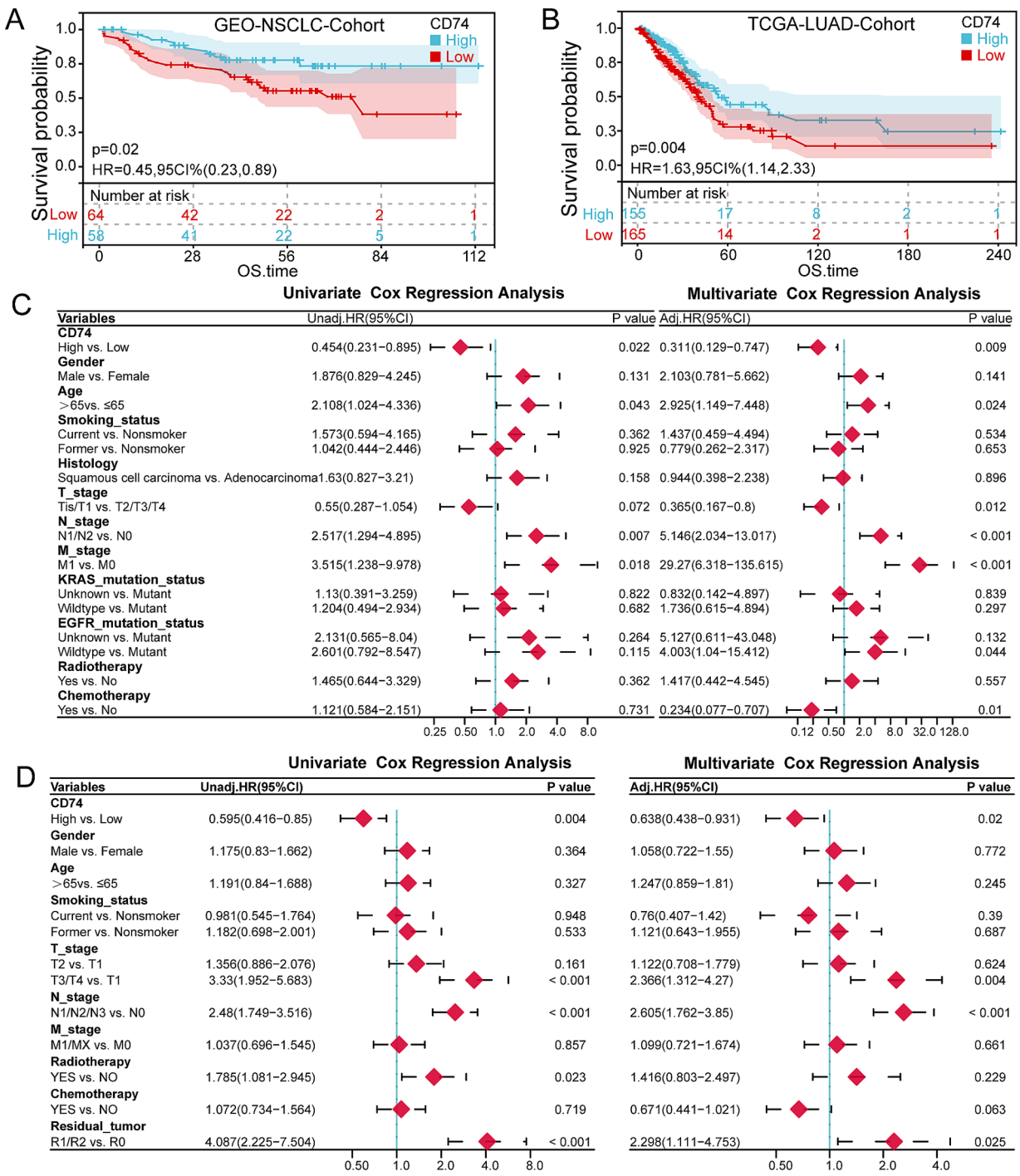

FIGURE 3
Survival analysis. **(A)** KM curve of the relationship between CD74 expression and OS in the NSCLC cohort. **(B)** KM curve of the relationship between CD74 expression and OS in the LUAD cohort. **(C)** Forest plot of univariate and multivariate COX regression analysis of CD74 and clinical characteristics in the NSCLC cohort. **(D)** Forest plot of univariate and multivariate COX regression analysis of CD74 and clinical characteristics in the LUAD cohort.

Analysis of antigen presentation and processing gene differences and immune cell infiltration between CD74 groups

The analysis of antigen processing and presentation gene differences between the CD74 high and low groups revealed that the gene expression levels of CD8A, CD1D, CD1C, and CD4, among others, were significantly increased in the CD74 high expression group. Please refer to Figure 4C and Supplementary Figure S3c for more details.

The expression matrices of the NSCLC cohort and LUAD cohort were uploaded to the CIBERSORTx database to calculate the level of immune cell infiltration for each sample. The correlation analysis between the level of immune cell infiltration

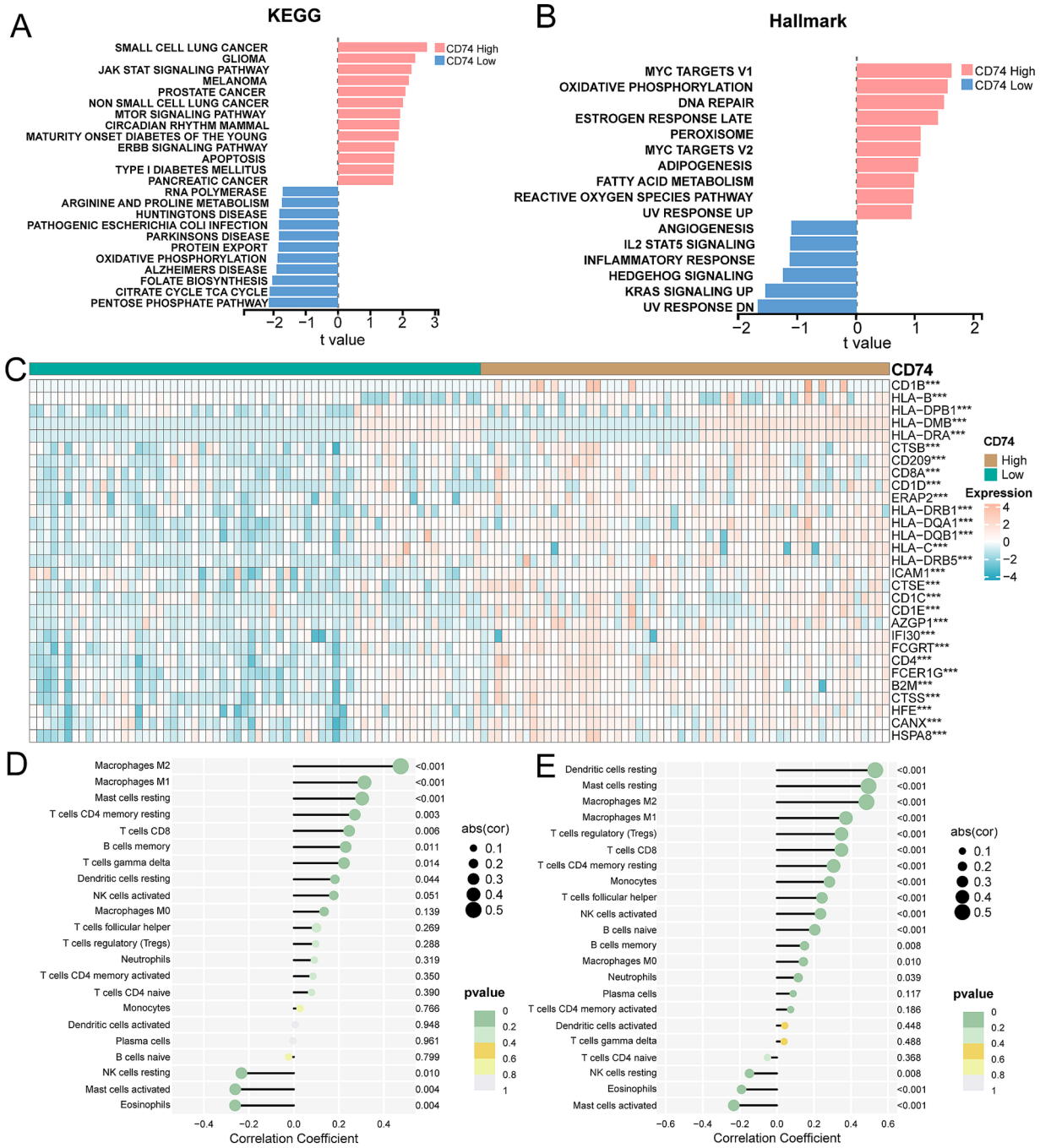

FIGURE 4
Correlation analysis of tumor pathways and immune responses for CD74 expression. **(A)** GSVA showed differential enrichment in KEGG pathway between CD74 high and low expression groups. **(B)** GSVA showed differential enrichment of Hallmarks pathways between CD74 high and low expression groups. **(C)** Heat map of differential expression of antigen processing and presentation genes between CD74 high expression group and CD74 low expression group, (significant symbol: *, $p < 0.05$; **, $p < 0.01$, ***, $p < 0.001$). **(D)** Lollipop plot of correlation between CD74 expression and immune cell infiltration in the NSCLC cohort. **(E)** Lollipop plot of correlation between CD74 expression and immune cell infiltration in the LUAD cohort.

and CD74 expression showed that CD74 was significantly positively correlated with the degree of infiltration of immune cells such as M2 macrophages, M1macrophages, resting dendritic cells, CD8 T cells, and memory B cells. Furthermore, there was a significant negative correlation between CD74 expression and resting NK cell, activated mast cell, and eosinophil infiltration (see Figures 4D,E).

Construction of a radiomics model for predicting CD74 expression

Imaging features were extracted from 68 patients with imaging data in the NSCLC cohort. Finally, 107 radiomics features were obtained, and then the radiomics feature values were standardized. The results of the consistency evaluation showed that the median value of the ICC of

radiomics features was 0.928, and there were 102 radiomics features with ICC values ≥0.75 (95.3% of all features). The features with ICC values ≥0.75 were selected by the REF method, and the top 8 features were obtained. The false positive results were removed by a stepwise regression algorithm, and finally, 3 radiomics features were obtained to construct the prediction model. The three imaging features used to construct the prediction model were glcm maximum probability, glszm large area high gray level emphasis and glszm zone variance (Table 2).

The selected radiomics features were used to construct the LR model and SVM model to predict CD74 gene expression. The importance of radiomics features in the LR model and SVM model is shown in Figures 5A,B, and the specific values are shown in Table 2. The formula of the prediction model is

$$P = 1 / \left(1 + \exp \left(\begin{array}{l} 33.244 * glszm\ ZoneVariance \\ -1.414 * glcm\ MaximumProbability \\ -44.301 * glszm\ Large\ Area\ High\ Gray \\ Level\ Emphasis \end{array} \right) \right).$$

Validation of the radiomics model

The performance of the LR and SVM models was evaluated using ROC curves. As shown in Figure 5C, for the LR model, the training set achieved an AUC of 0.778, with a sensitivity of 0.935 and a specificity of 0.514 at the optimal cut-off point (Table 3). In the validation set, the AUC was 0.772, with a sensitivity of 0.968 and a specificity of 0.459 (Table 3). The calibration curve and the Hosmer-Lemeshow goodness-of-fit test indicated good agreement between the predicted probabilities of high CD74 expression and the actual observations ($p > 0.05$) (Figure 5C). The decision curve analysis (DCA) demonstrated that the model had a high potential for clinical application (Figure 5C). For the SVM model, as shown in Figure 5D, the training set yielded an AUC of 0.729, with a sensitivity of 0.968 and a specificity of 0.486 at the optimal cut-off point (Table 3). In the validation set, the AUC was 0.701, with a sensitivity of 0.903 and a specificity of 0.459 (Table 3). Similarly, the calibration curve and the Hosmer-Lemeshow test showed good consistency between the predicted and actual outcomes ($p > 0.05$) (Figure 5D). The DCA also confirmed the high clinical utility of the SVM model (Figure 5D).

The difference analysis of radiomics scores output by the LR model and SVM model significantly differed in terms of the distribution of radiomics scores between the CD74 high and low groups ($p < 0.05$). As depicted in Figures 5E,F, the CD74 high expression group exhibited higher radiomics scores.

The DeLong test was used to compare the AUC values of the LR model and SVM model before and after cross-validation. The results indicated that the p value was 0.79 before cross-validation and 0.39 after cross-validation. The AUC values of the LR model and SVM model before and after cross-validation were not significantly different, suggesting that each model has good prediction efficiency.

Discussion

The classical prognostic indicators of lung cancer are no longer adequate for prognostic stratification and individualized treatment of highly heterogeneous NSCLC (6). Fortunately, radiomics is currently utilized not only for lung cancer diagnosis, assessing the tumor microenvironment, and predicting survival prognosis but also for identification of gene alterations and even prediction of gene expression (37, 38). Based on this premise, we developed a machine learning-based radiomics model that successfully predicted the expression of CD74 in the tumor microenvironment of NSCLC and established the relationship between enhanced CT radiomics features and tumor prognosis. The radiomics features of the machine learning model included large area high gray level emphasis, maximum probability, and zone variance. The feature scores output by the model can effectively distinguish the level of CD74 expression, providing a new indicator for prognosis stratification and individualized precision treatment of lung cancer patients.

Many studies have confirmed the close relationship between the expression of CD74 and the occurrence and development of tumors. For instance, several studies have found a positive correlation between CD74 and MHC class II molecule expression, leading to a higher overall survival rate in certain tumor patients (39–41). Moreover, other studies have indicated that CD74 promotes tumor proliferation and that its expression is negatively correlated with patient survival (10, 42). However, due to significant biological differences among different malignancies, there may not be a uniform answer regarding the role of CD74 in various tumors. Our analysis of both the NSCLC dataset and LUAD dataset revealed that high expression of CD74 is an independent prognostic factor for improved survival. Additionally, GSVA analysis demonstrated the activation of multiple tumor pathways in the CD74 low expression group. These findings suggest that CD74 can serve as a prognostic biomarker in NSCLC.

CD74 plays an important role in several key processes of the immune response, including antigen processing, endocytic maturation, cell migration and signal transduction (43). One study found that high expression of CD74 enhances the immune function of macrophages and CD8+ T cells in the tumor microenvironment of hepatocellular carcinoma. Additionally, high expression of CD74 is an independent predictor of good prognosis in patients with hepatocellular carcinoma (44). In our study, we observed high expression of antitumor-associated antigen processing and presentation genes in the tumor

TABLE 2 Importance score of radiomics features in the model.

Features	LR-Model importance	SVM-Model importance
Glcm_Maximum Probability	1.847	0.594
Glszm_Large Area High Gray Level Emphasis	1.885	0.611
Glszm_Zone Variance	2.163	0.598

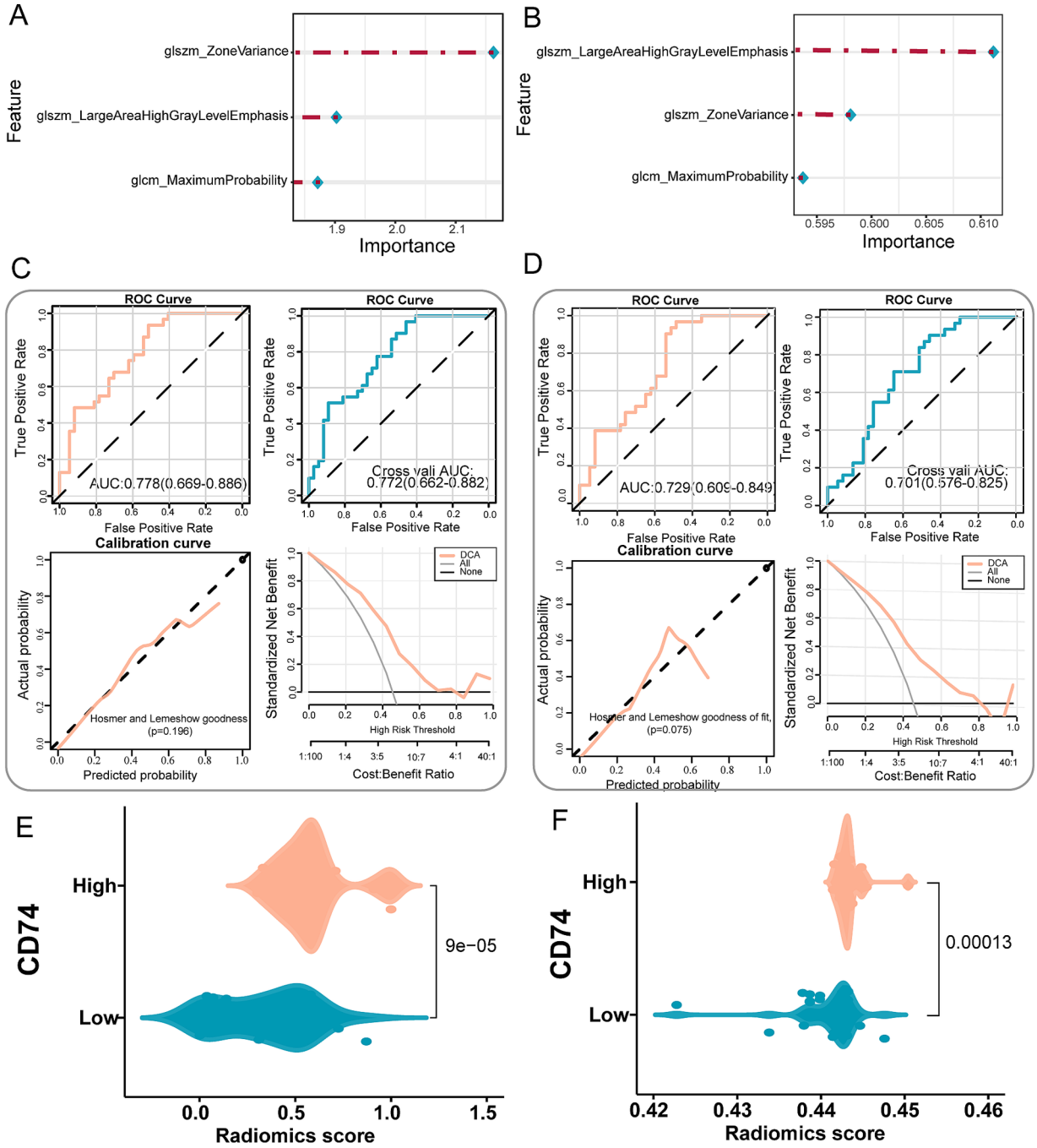

FIGURE 5
Establishment and validation of a radiomics prediction model for CD74 expression. **(A)** Importance of image features in the LR model. **(B)** The importance of image features in the SVM model. **(C)** LR model performance test, top left shows the ROC curve of model evaluation, top right shows the ROC curve of model evaluation after 5-fold cross validation, bottom left shows the Hosmer-Lemeshow goodness of fit test and calibration curve, and bottom right shows the DCA curve of model. **(D)** SVM model performance test, top left shows the ROC curve of model evaluation, top right shows the ROC curve of model evaluation after 5-fold cross validation, bottom left shows the Hosmer-Lemeshow goodness of fit test and calibration curve, and bottom right shows the DCA curve of model. **(E)** Violin plot of radiomics score differences between CD74 high and low groups in the LR model. **(F)** Violin plot of radiomics score differences between CD74 high and low groups in SVM model.

microenvironment of NSCLC patients with high CD74 expression. We also found that CD74 promotes the infiltration of macrophages, memory B cells, and CD8+ T cells in the tumor microenvironment. Macrophages 1 and CD8 + T cells are the main antitumor immune cells in the tumor microenvironment (45, 46). Furthermore, studies have shown that CD74 can be rapidly internalized on tumor cells, making it a determining factor for conjugated chemotherapy or radioisotope carriers. This presents CD74 as a promising target for antibody–drug conjugates (47). A preclinical study demonstrated that the combination of radioisotopes, doxorubicin, amphibian cytosolic ribonuclease

TABLE 3 Performance indicators of the model.

Group	AUC	95%CI	Sensitivity	Specificity	ACC	PPV	NPV	Brier Score
LR-Training set	0.778	0.669–0.886	0.935	0.514	0.706	0.617	0.905	0.19
LR-Validation set	0.772	0.662–0.882	0.968	0.459	0.691	0.6	0.944	0.193
SVM-Training set	0.729	0.609–0.849	0.968	0.486	0.706	0.612	0.947	0.217
SVM-Validation set	0.701	0.576–0.825	0.903	0.459	0.662	0.583	0.85	0.219

ACC, accuracy; PPV, positive predictive value; NPV, negative predictive value.

ranpirnase, and milatuzumab significantly improved the survival of human malignant tumor xenograft mice and was well tolerated (13). Several studies have also suggested that CD74 is a therapeutic target for milatuzumab (12) and a therapeutic tool for vaccine therapy of malignancies (48). Based on the findings of these studies, it can be inferred that overexpression of CD74 may serve as a potential therapeutic modality.

CT imaging is an essential examination for the clinical diagnosis of lung cancer; however, it lacks objectivity and quantification. Radiomics is a high-throughput "imaging sequencing" data technology that can obtain many imaging parameters and dynamically detect and quantitatively reflect tumor characteristics in a noninvasive way (49). For instance, one study utilized paired radiomics data and RNA sequencing data to unveil the biological significance of radiomics phenotypes for glioblastoma prognosis (50). Another study used head and neck enhanced CT radiomics features to predict the expression levels of prognosis-related molecules in head and neck squamous cell carcinoma (38). Some scholars have also compared machine learning models, including logistic regression, random forest, naive Bayes, SVM, AdaBoost, and neural network models, based on MRI texture features to predict occult lymph node metastasis in early tongue squamous cell carcinoma and confirmed that machine learning models can be an effective predictive tool (51).

Due to the exploratory stage of this study, there are still some limitations. First, due to the complexity of valid data collection, this study did not perform external validation on an independent image dataset to provide further confirmation of the reliability of the model. Second, our data were obtained from an open public database, and the CT image quality was not consistent. Third, the data revealed a mismatch, particularly in the proportion of squamous carcinoma and adenocarcinoma. Fourth, the number of samples is relatively small, and there is a lack of multicentre prospective radiomics studies to guide clinical practice. Increasing the number of CT images from multiple institutions in the future will improve the stability and generalizability of the model. Additionally, adopting standardized methods that meet the Image Biomarker Standardisation Initiative (IBSI) criteria may allow the radiomics model to become a clinically meaningful tool.

Conclusion

CD74 expression is identified as an independent prognostic factor that significantly affects the overall survival of patients with NSCLC. The enhanced CT radiomics model demonstrates a favorable level of stability and diagnostic efficiency in predicting CD74 expression. This finding suggests that the radiomics model may have the potential to be utilized as a novel method for individualized precision treatment of NSCLC.

Data availability statement

The original contributions presented in the study are included in the article/Supplementary material, further inquiries can be directed to the corresponding author.

Author contributions

YW: Formal analysis, Investigation, Methodology, Writing – original draft, Writing – review & editing. ZG: Conceptualization, Formal analysis, Investigation, Methodology, Supervision, Writing – original draft, Writing – review & editing. ML: Formal analysis, Writing – original draft, Writing – review & editing. ZF: Formal analysis, Writing – original draft, Writing – review & editing. HW: Conceptualization, Formal analysis, Investigation, Methodology, Supervision, Writing – original draft, Writing – review & editing.

Funding

The author(s) declare that financial support was received for the research and/or publication of this article. Funding support from Natural Science Foundation of Shandong Province (No. ZR2020MH247).

Acknowledgments

We would like to express our gratitude to Dr. Fengying Du for method guidance and professional statistical advice.

Conflict of interest

The authors declare that the research was conducted in the absence of any commercial or financial relationships that could be construed as a potential conflict of interest.

Generative AI statement

The authors declare that no Gen AI was used in the creation of this manuscript.

Publisher's note

All claims expressed in this article are solely those of the authors and do not necessarily represent those of their affiliated organizations, or those of the publisher, the editors and the reviewers. Any product that may be evaluated in this article, or claim that may be made by its manufacturer, is not guaranteed or endorsed by the publisher.

Supplementary material

The Supplementary material for this article can be found online at: https://www.frontiersin.org/articles/10.3389/fmed.2025.1586253/full#supplementary-material

References

1. Sung H, Ferlay J, Siegel RL, Laversanne M, Soerjomataram I, Jemal A, et al. Global cancer statistics 2020: Globocan estimates of incidence and mortality worldwide for 36 cancers in 185 countries. *CA Cancer J Clin*. (2021) 71:209–49. doi: 10.3322/caac.21660

2. Thai AA, Solomon BJ, Sequist LV, Gainor JF, Heist RS. Lung cancer. *Lancet (London, England)*. (2021) 398:535–54. doi: 10.1016/s0140-6736(21)00312-3

3. Yuan Z, Yu X, Wu S, Wu X, Wang Q, Cheng W, et al. Instability mechanism of Osimertinib in plasma and a solving strategy in the pharmacokinetics study. *Front Pharmacol*. (2022) 13:928983. doi: 10.3389/fphar.2022.928983

4. Liu SM, Zheng MM, Pan Y, Liu SY, Li Y, Wu YL. Emerging evidence and treatment paradigm of non-small cell lung cancer. *J Hematol Oncol*. (2023) 16:40. doi: 10.1186/s13045-023-01436-2

5. Wu M, Huang Q, Xie Y, Wu X, Ma H, Zhang Y, et al. Improvement of the anticancer efficacy of Pd-1/Pd-L1 blockade via combination therapy and Pd-L1 regulation. *J Hematol Oncol*. (2022) 15:24. doi: 10.1186/s13045-022-01242-2

6. Chen Z, Fillmore CM, Hammerman PS, Kim CF, Wong KK. Non-small-cell lung cancers: a heterogeneous set of diseases. *Nat Rev Cancer*. (2014) 14:535–46. doi: 10.1038/nrc3775

7. Usuda K, Ishikawa M, Iwai S, Yamagata A, Iijima Y, Motono N, et al. Pulmonary nodule and mass: superiority of Mri of diffusion-weighted imaging and T2-weighted imaging to Fdg-pet/Ct. *Cancers (Basel)*. (2021) 13:5166. doi: 10.3390/cancers13205166

8. Qiu L, Weng G. The diagnostic value of serum Mir-21 in patients with ovarian cancer: a systematic review and meta-analysis. *J Ovarian Res*. (2022) 15:51. doi: 10.1186/s13048-022-00985-3

9. Aberle DR, Adams AM, Berg CD, Black WC, Clapp JD, Fagerstrom RM, et al. Reduced lung-cancer mortality with low-dose computed tomographic screening. *N Engl J Med*. (2011) 365:395–409. doi: 10.1056/NEJMoa1102873

10. Nagata S, Jin YF, Yoshizato K, Tomoeda M, Song M, Iizuka N, et al. Cd74 is a novel prognostic factor for patients with pancreatic cancer receiving multimodal therapy. *Ann Surg Oncol*. (2009) 16:2531–8. doi: 10.1245/s10434-009-0532-3

11. Shachar I, Haran M. The secret second life of an innocent chaperone: the story of Cd74 and B cell/chronic lymphocytic leukemia cell survival. *Leuk Lymphoma*. (2011) 52:1446–54. doi: 10.3109/10428194.2011.565437

12. Berkova Z, Tao RH, Samaniego F. Milatuzumab - a promising new immunotherapeutic agent. *Expert Opin Investig Drugs*. (2010) 19:141–9. doi: 10.1517/13543780903463854

13. Borghese F, Clanchy FI. Cd74: an emerging opportunity as a therapeutic target in cancer and autoimmune disease. *Expert Opin Ther Targets*. (2011) 15:237–51. doi: 10.1517/14728222.2011.550879

14. Calandra T, Roger T. Macrophage migration inhibitory factor: a regulator of innate immunity. *Nat Rev Immunol*. (2003) 3:791–800. doi: 10.1038/nri1200

15. Su H, Na N, Zhang X, Zhao Y. The biological function and significance of Cd74 in immune diseases. *Inflamm Res*. (2017) 66:209–16. doi: 10.1007/s00011-016-0995-1

16. Liu Z, Chu S, Yao S, Li Y, Fan S, Sun X, et al. Cd74 interacts with Cd44 and enhances tumorigenesis and metastasis via Rhoa-mediated Cofilin phosphorylation in human breast cancer cells. *Oncotarget*. (2016) 7:68303–13. doi: 10.18632/oncotarget.11945

17. Fernandez-Cuesta L, Plenker D, Osada H, Sun R, Menon R, Leenders F, et al. Cd74-Nrg1 fusions in lung adenocarcinoma. *Cancer Discov*. (2014) 4:415–22. doi: 10.1158/2159-8290.Cd-13-0633

18. Corchete LA, Rojas EA, Alonso-López D, De Las RJ, Gutiérrez NC, Burguillo FJ. Systematic comparison and assessment of Rna-Seq procedures for gene expression quantitative analysis. *Sci Rep*. (2020) 10:19737. doi: 10.1038/s41598-020-76881-x

19. SEQC/MAQC-III Consortium. A comprehensive assessment of Rna-Seq accuracy, reproducibility and information content by the sequencing quality control consortium. *Nat Biotechnol*. (2014) 32:903–14. doi: 10.1038/nbt.2957

20. Sompuram SR, Vani K, Schaedle AK, Balasubramanian A, Bogen SA. Quantitative assessment of immunohistochemistry laboratory performance by measuring analytic response curves and limits of detection. *Arch Pathol Lab Med*. (2018) 142:851–62. doi: 10.5858/arpa.2017-0330-OA

21. Wang C, Ma J, Shao J, Zhang S, Li J, Yan J, et al. Non-invasive measurement using deep learning algorithm based on multi-source features fusion to predict Pd-L1 expression and survival in Nsclc. *Front Immunol*. (2022) 13:828560. doi: 10.3389/fimmu.2022.828560

22. Wong CW, Chaudhry A. Radiogenomics of lung cancer. *J Thorac Dis*. (2020) 12:5104–9. doi: 10.21037/jtd-2019-pitd-10

23. Rossi G, Barabino E, Fedeli A, Ficarra G, Coco S, Russo A, et al. Radiomic detection of Egfr mutations in Nsclc. *Cancer Res*. (2021) 81:724–31. doi: 10.1158/0008-5472.Can-20-0999

24. Bakr S, Gevaert O, Echegaray S, Ayers K, Zhou M, Shafiq M, et al. A radiogenomic dataset of non-small cell lung cancer. *Sci Data*. (2018) 5:180202. doi: 10.1038/sdata.2018.202

25. Yu Y, Tan Y, Xie C, Hu Q, Ouyang J, Chen Y, et al. Development and validation of a preoperative magnetic resonance imaging radiomics-based signature to predict axillary lymph node metastasis and disease-free survival in patients with early-stage breast cancer. *JAMA Netw Open*. (2020) 3:e2028086. doi: 10.1001/jamanetworkopen.2020.28086

26. Lv L, Xin B, Hao Y, Yang Z, Xu J, Wang L, et al. Radiomic analysis for predicting prognosis of colorectal cancer from preoperative (18)F-Fdg pet/Ct. *J Transl Med*. (2022) 20:66. doi: 10.1186/s12967-022-03262-5

27. Fang Q, Chen H. The significance of M6a Rna methylation regulators in predicting the prognosis and clinical course of Hbv-related hepatocellular carcinoma. *Mol Med*. (2020) 26:60. doi: 10.1186/s10020-020-00185-z

28. Hänzelmann S, Castelo R, Guinney J. Gsva: gene set variation analysis for microarray and Rna-Seq data. *BMC Bioinformatics*. (2013) 14:7. doi: 10.1186/1471-2105-14-7

29. Newman AM, Steen CB, Liu CL, Gentles AJ, Chaudhuri AA, Scherer F, et al. Determining cell type abundance and expression from bulk tissues with digital cytometry. *Nat Biotechnol*. (2019) 37:773–82. doi: 10.1038/s41587-019-0114-2

30. Chiti G, Grazzini G, Flammia F, Matteuzzi B, Tortoli P, Bettarini S, et al. Gastroenteropancreatic neuroendocrine neoplasms (Gep-Nens): a radiomic model to predict tumor grade. *Radiol Med*. (2022) 127:928–38. doi: 10.1007/s11547-022-01529-x

31. Musigmann M, Akkurt BH, Krähling H, Brokinkel B, Henssen D, Sartoretti T, et al. Assessing preoperative risk of Str in skull Meningiomas using Mr Radiomics and machine learning. *Sci Rep*. (2022) 12:14043. doi: 10.1038/s41598-022-18458-4

32. Caruso D, Polici M, Rinzivillo M, Zerunian M, Nacci I, Marasco M, et al. Ct-based radiomics for prediction of therapeutic response to Everolimus in metastatic neuroendocrine tumors. *Radiol Med*. (2022) 127:691–701. doi: 10.1007/s11547-022-01506-4

33. Ding X, Yang F, Ma F. An efficient model selection for linear discriminant function-based recursive feature elimination. *J Biomed Inform*. (2022) 129:104070. doi: 10.1016/j.jbi.2022.104070

34. Dziak JJ, Coffman DL, Lanza ST, Li R, Jermiin LS. Sensitivity and specificity of information criteria. *Brief Bioinform*. (2020) 21:553–65. doi: 10.1093/bib/bbz016

35. Love MI, Huber W, Anders S. Moderated estimation of fold change and dispersion for Rna-Seq data with Deseq2. *Genome Biol*. (2014) 15:550. doi: 10.1186/s13059-014-0550-8

36. Kocak B, Akinci D'Antonoli T, Mercaldo N, Alberich-Bayarri A, Baessler B, Ambrosini I, et al. Methodological Radiomics score (Metrics): a quality scoring tool for radiomics research endorsed by Eusomii. *Insights Imaging*. (2024) 15:8. doi: 10.1186/s13244-023-01572-w

37. Choi Y, Aum J, Lee SH, Kim HK, Kim J, Shin S, et al. Deep learning analysis of Ct images reveals high-grade pathological features to predict survival in lung adenocarcinoma. *Cancers*. (2021) 13:4077. doi: 10.3390/cancers13164077

38. Wang F, Zhang W, Chai Y, Wang H, Liu Z, He Y. Constrast-enhanced computed tomography radiomics predicts Cd27 expression and clinical prognosis in head and neck squamous cell carcinoma. *Front Immunol*. (2022) 13:1015436. doi: 10.3389/fimmu.2022.1015436

39. Zeiner PS, Zinke J, Kowalewski DJ, Bernatz S, Tichy J, Ronellenfitsch MW, et al. Cd74 regulates complexity of tumor cell Hla class ii peptidome in brain metastasis and is a positive prognostic marker for patient survival. *Acta Neuropathol Commun*. (2018) 6:18. doi: 10.1186/s40478-018-0521-5

40. Otterstrom C, Soltermann A, Opitz I, Felley-Bosco E, Weder W, Stahel RA, et al. Cd74: a new prognostic factor for patients with malignant pleural mesothelioma. *Br J Cancer*. (2014) 110:2040–6. doi: 10.1038/bjc.2014.117

41. Wang ZQ, Milne K, Webb JR, Watson PH. Cd74 and intratumoral immune response in breast cancer. *Oncotarget*. (2017) 8:12664–74. doi: 10.18632/oncotarget.8610

42. Tian B, Zhang Y, Li N, Liu X, Dong J. Cd74: a potential novel target for triple-negative breast cancer. *Tumour Biol*. (2012) 33:2273–7. doi: 10.1007/s13277-012-0489-x

43. Schröder B. The multifaceted roles of the invariant chain Cd74--more than just a chaperone. *Biochim Biophys Acta*. (2016) 1863:1269–81. doi: 10.1016/j.bbamcr.2016.03.026

44. Xiao N, Li K, Zhu X, Xu B, Liu X, Lei M, et al. Cd74(+) macrophages are associated with favorable prognosis and immune contexture in hepatocellular carcinoma. *Cancer Immunol Immunother*. (2022) 71:57–69. doi: 10.1007/s00262-021-02962-z

45. Gunassekaran GR, Poongkavithai Vadevoo SM, Baek MC, Lee B. M1 macrophage exosomes engineered to foster M1 polarization and target the Il-4 receptor inhibit tumor growth by reprogramming tumor-associated macrophages into M1-like macrophages. *Biomaterials*. (2021) 278:121137. doi: 10.1016/j.biomaterials.2021.121137

46. Reina-Campos M, Scharping NE, Goldrath AW. Cd8(+) T cell metabolism in infection and cancer. *Nat Rev Immunol*. (2021) 21:718–38. doi: 10.1038/s41577-021-00537-8

47. Govindan SV, Cardillo TM, Sharkey RM, Tat F, Gold DV, Goldenberg DM. Milatuzumab-Sn-38 conjugates for the treatment of Cd74+ cancers. *Mol Cancer Ther*. (2013) 12:968–78. doi: 10.1158/1535-7163.Mct-12-1170

48. Perez SA, Kallinteris NL, Bisias S, Tzonis PK, Georgakopoulou K, Varla-Leftherioti M, et al. Results from a phase I clinical study of the novel ii-key/Her-2/Neu(776-790) hybrid peptide vaccine in patients with prostate cancer. *Clin Cancer Res*. (2010) 16:3495–506. doi: 10.1158/1078-0432.Ccr-10-0085

49. Gao L, Jiang W, Yue Q, Ye R, Li Y, Hong J, et al. Radiomic model to predict the expression of Pd-1 and overall survival of patients with ovarian cancer. *Int Immunopharmacol*. (2022) 113:109335. doi: 10.1016/j.intimp.2022.109335

50. Sun Q, Chen Y, Liang C, Zhao Y, Lv X, Zou Y, et al. Biologic pathways underlying prognostic radiomics phenotypes from paired Mri and Rna sequencing in glioblastoma. *Radiology*. (2021) 301:654–63. doi: 10.1148/radiol.2021203281

51. Yuan Y, Ren J, Tao X. Machine learning-based Mri texture analysis to predict occult lymph node metastasis in early-stage oral tongue squamous cell carcinoma. *Eur Radiol*. (2021) 31:6429–37. doi: 10.1007/s00330-021-07731-1

frontiers | Frontiers in Medicine

TYPE Original Research
PUBLISHED 09 July 2025
DOI 10.3389/fmed.2025.1524176

Check for updates

OPEN ACCESS

EDITED BY
Chao Song,
Harbin Medical University, China

REVIEWED BY
Wencheng Zhang,
Tianjin Medical University Cancer Institute and Hospital, China
Hesong Wang,
Fourth Hospital of Hebei Medical University, China

*CORRESPONDENCE
Hongfu Sun
ice9892@163.com
Wei Huang
alvinbird@163.com

RECEIVED 07 November 2024
ACCEPTED 17 June 2025
PUBLISHED 09 July 2025

CITATION
Wei S, Li Z, Liu T, Sun G, Sun H and Huang W (2025) Immunotherapy in advanced esophageal squamous cell cancer: earlier or later?
Front. Med. 12:1524176.
doi: 10.3389/fmed.2025.1524176

COPYRIGHT
© 2025 Wei, Li, Liu, Sun, Sun and Huang. This is an open-access article distributed under the terms of the Creative Commons Attribution License (CC BY). The use, distribution or reproduction in other forums is permitted, provided the original author(s) and the copyright owner(s) are credited and that the original publication in this journal is cited, in accordance with accepted academic practice. No use, distribution or reproduction is permitted which does not comply with these terms.

Immunotherapy in advanced esophageal squamous cell cancer: earlier or later?

Shuang Wei[1], Zuoji Li[2], Tingting Liu[3], Guizhen Sun[1], Hongfu Sun[4]* and Wei Huang[4]*

[1]Department of Radiation Oncology, Gaomi People's Hospital, Weifang, China, [2]Department of Science and Education, Gaomi People's Hospital, Weifang, China, [3]Department of Nuclear Medicine, Shandong Cancer Hospital and Institute, Shandong First Medical University and Shandong Academy of Medical Sciences, Jinan, China, [4]Department of Radiation Oncology, Shandong Cancer Hospital and Institute, Shandong First Medical University and Shandong Academy of Medical Sciences, Jinan, China

Background and objective: Several large-scale phase III clinical trials have confirmed the survival benefit of immunotherapy in patients with locally advanced or metastatic esophageal cancer (EC). The study aimed to investigate whether early use of immunotherapy can improve long-term survival.

Methods: Patients with locally advanced or metastatic esophageal squamous cell cancer (ESCC) diagnosed from January 2018 to December 2021 were retrospectively analyzed. According to the time of immunotherapy, patients were divided into the early immunotherapy group (EIT group, first-line immunotherapy) and the late immunotherapy group (LIT group, second-line immunotherapy). A 1:1 propensity score matching (PSM) was applied to balance the observable potential confounding factors between the two groups. The primary outcome was overall survival (OS).

Results: A total of 359 patients were enrolled; after propensity score matching, the clinical features were well balanced between the two groups, including 107 patients. The median OS was 15.7 months (95%CI: 12.81–18.59) in the EIT group and 17.7 months (95%CI: 14.89–20.57) in the LIT group, respectively (p = 0.185, HR = 1.25). The PFS1 of patients was 8.7 months (95%CI: 7.53–9.87) and 7.6 months (95%CI: 5.90–9.30), respectively, and the difference was statistically significant (p = 0.032, HR = 0.72). The PFS2 of patients was 12.97 months (95%CI: 11.37–14.58) and 12.93 months (95%CI: 11.65–14.21), respectively, and the difference was statistically significant (p = 0.045, HR = 0.73). Subgroup analysis showed that male patients with middle thoracic EC, younger than 65 years old, with only one site of metastasis, only lymph node progression, no combined radiotherapy after progression, and TP (paclitaxel + platinum) regimen chemotherapy may have greater benefits. The COX multivariate analysis showed that the EIT group and the differentiation degree of the tumor had an impact on OS (*P:* 0.03, 0.04; HR: 0.73, 0.70).

Conclusion: Early immunotherapy can improve PFS without affecting OS for patients with locally advanced or metastatic ESCC.

KEYWORDS

immunotherapy, esophageal squamous cell cancer, overall survival, EIT, LiT

1 Background

Esophageal cancer (EC) is one of the most common malignant tumors in the world, and China is a high-incidence area for EC. The morbidity and mortality ranked sixth and fourth among all malignant tumors, respectively. Multiple phase III clinical studies, such as Keynote-181 (1), Attraction-3 (2), Escort (3), and Rationale302 (4), have suggested that, compared with chemotherapy alone, immunotherapy improved overall survival (OS) (from 6.2 months to 10.9 months) and progression-free survival (PFS) (from 1.6 months to 3.4 months) in the second-line treatment of EC. Following, multiple phase III clinical studies, including Keynote-590 (5), Checkmate-648 (6), Escort-1 (7), Orient-15 (8) and Jupoiter-06 (9) have suggested that, compared with chemotherapy alone, the combination of chemotherapy and immunotherapy improved OS (from 9.8 months to 17.2 months) and PFS (from 5.3 months to 7.3 months) in the first-line treatment of EC. Previous studies have shown that the efficacy of immune checkpoint inhibitors is increased in earlier lines of therapy across multiple tumor types compared with in later lines of therapy (10–14). However, it is rarely reported in the real world whether the first-line application of immunotherapy in locally advanced or metastatic EC can bring longer survival benefits. In this study, we retrospectively analyzed the survival of patients with locally advanced or metastatic esophageal squamous cell cancer (ESCC) treated with immunotherapy as the first-or second-line treatment, exploring the value of early application of immunotherapy. This real-world study focused on EC, which has rarely been reported previously, and conducted a subgroup analysis, indicating the population that can benefit from early immunotherapy, which has more guiding significance for clinical medication.

2 Materials and methods

2.1 Data collection

We retrospectively analyzed patients with locally advanced or metastatic ESCC at Shandong Cancer Hospital from January 2018 to December 2021. The inclusion criteria were as follows: (1) Patients with pathologically confirmed ESCC; (2) Patients initially with unresectable locally advanced or metastatic disease; (3) Patients receiving immunotherapy as first-line or second-line treatment with more than two cycles; (4). Complete imaging data were available for evaluation during treatment or follow-up; (5). Eastern Cooperative Oncology Group (ECOG) score 0–1.

Exclusion criteria: (1) other pathological types of EC, such as adenocarcinoma and small cell carcinoma; (2) Combined with other tumors; (3) Central nervous system metastasis.

According to the time of immunotherapy, patients were divided into the early immunotherapy group (EIT group, first-line immunotherapy) and the late immunotherapy group (LIT group, second-line immunotherapy). The EIT group comprises patients who initially received first-line immunotherapy or progressed to first-line immunotherapy after previous radical treatment. The LIT group was defined as patients who initially received second-line immunotherapy or locally advanced or progressed to second-line immunotherapy after previous treatment. The chemotherapy regimen is paclitaxel or fluorouracil + platinum. The PD-1 inhibitors used among patients included pembrolizumab, toripalimab, sintilimab, envafolimab, and camrelizumab.

2.2 Evaluation and follow-up

The primary end point was OS, defined as the time from diagnosis to death from any cause. The secondary endpoints were PFS1, PFS2, disease control rate, and treatment-related adverse events (TRAEs). PFS1 is the time from diagnosis to disease progression or death from any cause. PFS2 is the time from diagnosis to second disease progression or death from any cause. Disease control rate included complete response, partial response, and stable disease. TRAEs were assessed within 90 days after the last dose of medication and were assessed using the Common Terminology Criteria for Adverse Events (CTCAE) version 5.0. The efficacy was evaluated every two courses during the treatment according to the Response Evaluation Criteria in Solid Tumors (RECIST) version 1.1. After the end of treatment, the patients were followed up every three months for 2 years, and once every six months for 3–5 years. Disease progression was assessed by CT scan according to RECIST 1.1 criteria.

2.3 Statistical analysis

SPSS 26.0 was used for statistical analysis. Clinical characteristics were compared using the Kruskal-Wallis test for continuous data and the chi-square test or Fisher's exact test for categorical data. OS and PFS were estimated using the Kaplan–Meier method and compared by the log-rank test. The propensity score-matched analysis (including age, sex, ECOG score, tumor location, differentiation, metastatic sites, number of organs with metastases, chemotherapy regimens, and immune drugs) was performed using the one-to-one nearest neighbor method (ps 0.1). The COX proportional hazards model was used for multivariate analysis to evaluate the possible factors affecting the OS of patients. Statistical results of $p < 0.05$ were considered statistically significant.

3 Results

3.1 Patients and treatment

A total of 359 patients with ESCC who met the inclusion criteria from January 2018 to December 2021 were included in the analysis. Among them, 122 patients were at the initial stage IV. Twenty-three patients with initially inoperable locally advanced disease were enrolled in the clinical trial and received first-line immunotherapy and chemotherapy. One hundred nineteen patients were in the early stage (stage I + II) and received radical surgery + adjuvant/neoadjuvant therapy. Ninety-five patients with locally advanced disease who were initially inoperable were treated with radical chemoradiotherapy. According to the number of immunotherapy lines, the patients were divided into two groups: EIT group (252 cases) and LIT group (107 cases). The initial stage and treatment of the patients are shown in Figure 1, the basic characteristics of the patients are shown in Table 1, and the disease control rate is shown in Table 2.

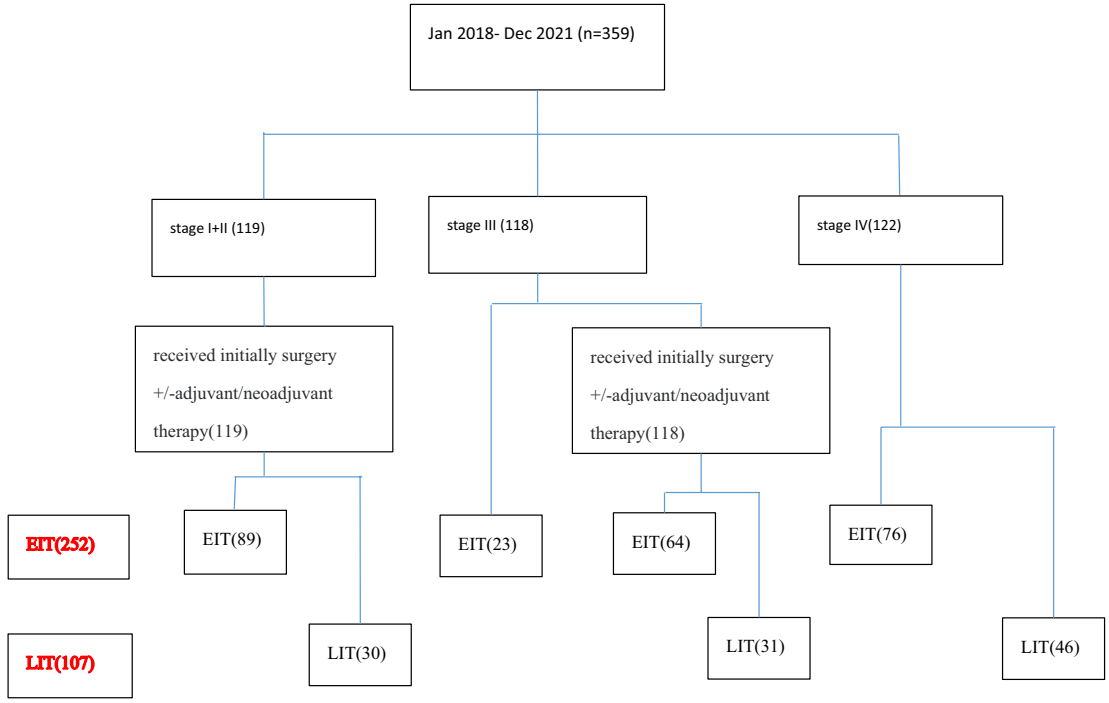

FIGURE 1
The initial stage and treatment of the patients.

The baseline clinical characteristics of all patients were comparable after propensity-score matching. The patient's gender, age, ECOG score, tumor location, degree of differentiation, metastatic site after progression, number of metastatic organs, chemotherapy regimens, different immune drugs used, and whether immunization combined with radiotherapy were analyzed (Table 3). The COX proportional hazard model was used for multivariate analysis to explore the possible factors influencing OS.

3.2 Survival

All patients were followed regularly until November 30, 2022, or death from any cause. The median duration of follow-up was 26.8 months in EIT group and 29.9 months in LIT group. In EIT group, 90 (35.7%) patients did not progress after first-line immunotherapy + chemotherapy; seven patients (4.8%) did not progress after second-line chemotherapy. After the progression of first-line immunotherapy + chemotherapy, 16 patients (6.3%) did not receive second-line chemotherapy. Among them, five patients (2.0%) did not receive second-line treatment due to death, and 11 patients (4.4%) were unable to accept or refused second-line treatment due to poor health. In LIT group, all patients received second-line immunotherapy after progression on first-line therapy, and 16 patients (15%) were still receiving second-line immunotherapy without tumor progression as of the follow-up date. Of the patients who subsequently entered third-line therapy, 15.5% were in the EIT group and 30% were in the LIT group.

After propensity score matching, 107 patients in EIT group were matched to those LIT group; the median OS was 15.7 months (95%CI: 12.81–18.59) in EIT group and 17.7 months (95%CI: 14.89–20.57) in EIT group, respectively, with no statistically significant difference ($p = 0.185$, HR = 1.25) (Figure 2). The median PFS1 of the two groups was 8.7 months (95%CI: 7.53–9.87) in the EIT group and 7.6 months (95%CI: 5.90–9.30) in the LIT group, with a statistically significant difference ($p = 0.032$, HR = 0.72) (Figure 3). The median PFS2 of the two groups was 12.97 months (95%CI: 11.37–14.58) in the EIT group and 12.93 months (95%CI: 11.65–14.21) in the LIT group, with a statistically significant difference ($p = 0.045$, HR = 0.73) (Figure 4).

Subgroup analysis using PFS2 as the end point (Figure 5) showed that in male patients, younger than 65 years of age, with esophageal tumors located in the middle thoracic segment, lymph node metastasis after progression, and one organ metastasis. First-line treatment without combination radiotherapy, and a TP regimen (paclitaxel and platinum) combined with chemotherapy, and the combination of immunotherapy in the first-line treatment may have greater benefits than the second-line combination of immunotherapy. This also provides a reference for our clinical treatment options.

The COX proportional hazard model was established, and multivariate analysis showed (Table 3) that the EIT group ($p = 0.03$, HR = 0.73) and differentiation degree of the tumor affected OS ($p = 0.04$, HR = 0.70). However, gender, age, ECOG score, tumor location, metastatic site, number of metastatic organs, chemotherapy regimen, immune drugs, and whether immunotherapy combined with radiotherapy had no significant effect on OS. Treatment-related adverse effects are shown in Table 4. In this retrospective data, 122 patients with stage IV were selected and divided into two groups, in addition to radiotherapy as part of the initial treatment: 67 patients with radiotherapy and 55 patients without radiotherapy. The median OS was 17.8 months and 15.8 months, respectively ($p = 0.179$).

TABLE 1 Basic characteristics of the patients.

Characteristic	EIT group (*n* = 252) (*n*, %)	LIT group (*n* = 107) (*n*, %)	*p* value	EIT group matched (*n* = 107) (*n*, %)	*P* value (psm)
Age, years Median, range	62 (41–82)	61 (42–84)	0.20	62 (42–84)	0.35
Sex			0.95		00.24
Male	222 (88.1)	94 (87.9)		88 (82.2)	
Female	30 (11.9)	13 (12.1)		19 (17.8)	
ECOG performance status			0.90		0.95
0	124 (49.2)	53 (49.5)		53 (49.5)	
1	128 (50.8)	54 (50.5)		54 (50.5)	
Tumor location			0.23		0.17
Cervical segment	10 (4.0)	2 (1.9)		1 (0.9)	
Upper thoracic segment	34 (13.5)	13 (12.1)		11 (10.3)	
Middle thoracic segment	132 (52.4)	48 (44.9)		64 (59.8)	
Lower thoracic segment	76 (30.2)	44 (41.1)		31 (29)	
Differentiated degree			0.92		0.96
High differentiation	14 (5.6)	8 (7.5)		10 (9.3)	
Middle differentiation	73 (29)	30 (28)		29 (27.1)	
Low differentiation	65 (25.8)	27 (25)		28 (26.2)	
Uncertain	100 (39.7)	42 (39.3)		40 (37.4)	
Site of metastasis			0.19		0.54
Liver	39 (15.5)	10 (9.3)		13 (12.1)	
Lung	44 (17.5)	16 (15)		21 (19.6)	
Bone	16 (6.3)	4 (3.7)		6 (5.6)	
Lymph node	153 (60.7)	77 (72)		67 (62.6)	
Number of organs with metastases			0.22		0.26
1	150 (59.5)	71 (66.4)		63 (58.9)	
≥2	102 (40.5)	36 (33.6)		44 (41.1)	
Chemotherapy			0.005		0.66
PF	76 (30.2)	35 (32.7)		33 (30.8)	
TP	151 (59.9)	60 (56.1)		63 (58.9)	
Uncertain	25 (9.9)	12 (11.2)		11 (10.3)	
Immunotherapy			0.001		0.16
Camrelizumab	121 (48)	71 (66.4)		65 (60.7)	
Pembrolizumab	29 (11.5)	2 (1.9)		5 (4.7)	
Sintilimab	63 (25)	24 (22.4)		23 (21.5)	
Envafolimab	7 (2.8)	1 (0.9)		3 (2.8)	
Toripalimab	13 (5.2)	3 (2.8)		5 (4.7)	

Comparison between the LIT group and the EIT group matched for *P* value.

4 Discussion

Treatment outcomes are poor for patients with advanced disease. The median OS rates are ~10 months and ~6 months for first-line and second-line chemotherapy, respectively, with objective response rates of ~30% and ~10%, respectively (15). With the advent of the immune era, immunotherapy has gradually become the standard treatment for advanced EC. Keynote-181 (1) confirmed the efficacy of pembrolizumab in PD-L1 cps ≥ 10 in patients with locally advanced EC; there was a two-fold improvement in survival at 12 months (43% vs. 20%) compared with chemotherapy alone (fluorouracil combined with platinum). Therefore, in 2019, it became the first immune drug approved for second-line treatment of advanced EC in the United States. Attraction-3 (2) confirmed that at a minimum follow-up time (i.e., time from random assignment of the last patient to data cutoff) of 17.6 months, OS was significantly improved in the

TABLE 2 Short-term efficacy evaluation.

First-line	EIT group (*n* = 252) (immune + chemotherapy)	EIT group (psm, *n* = 107) (immune + chemotherapy)	LIT group (*n* = 107) (chemotherapy)
Complete response	1 (0.4%)	1 (0.9%)	0
Partial response	80 (31.7%)	30 (28.0%)	24 (22.5%)
Stable disease	108 (42.9%)	46 (43%)	53 (50.1%)
Progressive disease	63 (25%)	25 (23.4%)	30 (28%)
Objective response	81 (32.1%)	31 (28.9%)	24 (22.5%)
Disease control	189 (75%)	77 (71.9%)	77 (72.6%)

Second-line	EIT group (*n* = 146) (chemotherapy)	EIT group (psm, *n* = 107) (chemotherapy)	LIT group (*n* = 107) (immunotherapy)
Complete response	0	0	0
Partial response	23 (15.7%)	15 (14.0%)	21 (19.5%)
Stable disease	65 (45%)	50 (46.7%)	39 (36.5%)
Progressive disease	57 (39.3%)	44 (41.1%)	47 (44%)
Objective response rate	23 (15.7%)	15 (14.0%)	21 (19.5%)
Disease control rate	88 (60.7%)	65 (60.7%)	60 (56%)

TABLE 3 Multivariate analysis.

Variables	*p*-value	HR (95%CI)
Sex	0.69	0.91 (0.56–1.46)
Age	0.11	0.78 (0.58–1.05)
ECOG	0.72	0.95 (0.73–1.24)
Location	0.87	0.98 (0.81–1.19)
Differentiation	0.04	0.70 (0.50–0.99)
Site of metastases	0.82	1.01 (0.92–1.11)
Number of organs with metastases	0.07	1.25 (0.98–1.60)
Chemotherapy regimens	0.22	1.11 (0.94–1.31)
Immunotherapy regimens	0.44	1.04 (0.94–1.15)
Immune with or without radiotherapy	0.19	1.20 (0.91–1.58)
EIT group or LIT group	0.03	0.73 (0.55–0.98)

nivolumab group compared with the chemotherapy group (10.9 months vs. 8.4 months, HR = 0.77, $p = 0.019$).

With the overall success of immune drugs in second-line therapy, their use is gradually advancing to first-line therapy. Keynote590 (5) reported that first-line palivizumab + chemotherapy (fluorouracil + platinum-based) vs. first-line chemotherapy in locally advanced or metastatic EC, regardless of the expression status of PD-L1 CPS, showed that the first-line immunized group improved OS (12.4 months vs. 9.8 months; 0.73 [0.62–0.86]; $p < 0.0001$) and progression-free survival (6.3 months vs. 5.8 months; 0.65 [0.55–0.76]; $p < 0.0001$), demonstrating a significant benefit. The escort-1 (7) trial confirmed that first-line immunization + chemotherapy (paclitaxel + cisplatin) was better than chemotherapy alone (paclitaxel + cisplatin) in terms of both OS and progression-free survival in the Chinese population, which were 15.3 vs. 12.0 months, respectively (HR = 0.7) and 6.9 vs. 5.6 months (HR = 0.56). The Orient-15 (8) trial also demonstrated a survival benefit for Sintilimab in first-line chemotherapy (paclitaxel + cisplatin/fluorouracil + cisplatin). Overall survival (median 16.7 vs. 12.5 months, HR = 0.63, 95%CI 0.51–0.78, $p < 0.001$) and progression-free survival (7.2 vs. 5.7 months, HR = 0.56, 95%CI 0.46–0.68, $p < 0.001$).

Our retrospective data show that after PSM, the OS of 15.7 months with first-line immunotherapy + chemotherapy in locally advanced or metastatic ESCC is consistent with the OS reported with camrelizumab (15.3 months) and sintilizumab (16.7 months), which is higher than the OS reported with pembrolizumab. One possible explanation for this discrepancy may be that a smaller proportion of patients in the control arm of the Keynote-590 study had been exposed to second-line immunotherapy. In terms of PFS, our data showed that the median PFS1 of the two groups was 8.7 months and 7.6 months, respectively ($p = 0.032$, HR = 0.72), which was similar to the HR values of the above three reports (0.65, 0.56, 0.56). The median PFS2 of the two groups was 12.97 months in the EIT group and 12.93 months in the LIT group, with a statistically significant difference ($p = 0.045$, HR = 0.73).

Previous reports showed that in non-small cell lung cancer, patients previously treated with fewer lines of therapy (i.e., in the first-line setting) might have less refractory and immunosuppressive tumor microenvironments than patients who have progressed on therapy (16). Pembrolizumab + chemotherapy in the Keynote-189 study reduced the risk of death by 44% in metastatic non-squamous NSCLC (17). Nivolumab as a second-line treatment reduced the risk of death by 27% in metastatic non-squamous NSCLC (18). The keynote-059 (14) trial showed that pembrolizumab monotherapy was effective, safe, and well tolerated in locally advanced gastric or gastroesophageal junction cancer with at least two previous lines of therapy, regardless of PD-L1 expression.

So, whether the early application of immunotherapy is more effective is still controversial. It is also rarely reported whether first-line immunotherapy has a greater survival benefit than second-line

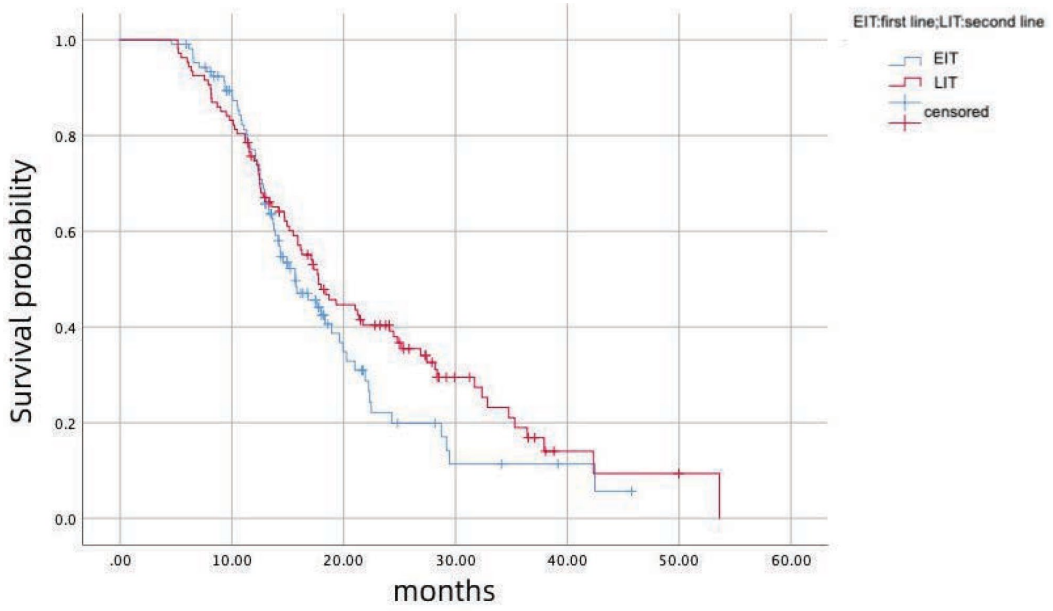

number at risk							
EIT matched	107	86	18	5	2	0	0
LIT	107	88	41	15	2	1	0

FIGURE 2
Overall survival (months).

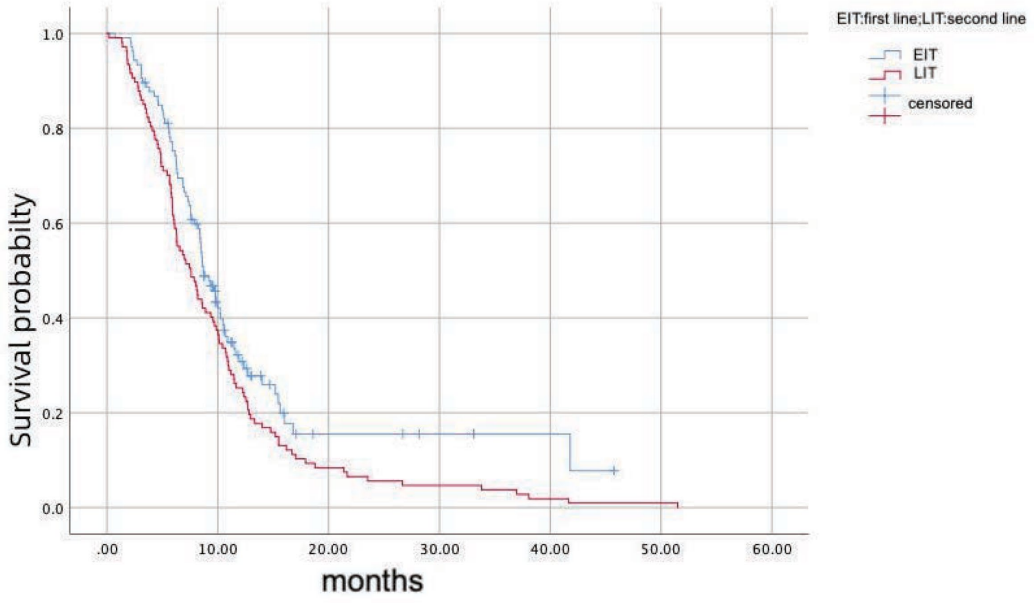

number at risk							
EIT matched	107	35	5	3	1	0	0
LIT	107	39	8	4	1	1	0

FIGURE 3
Progression-free survival 1(months).

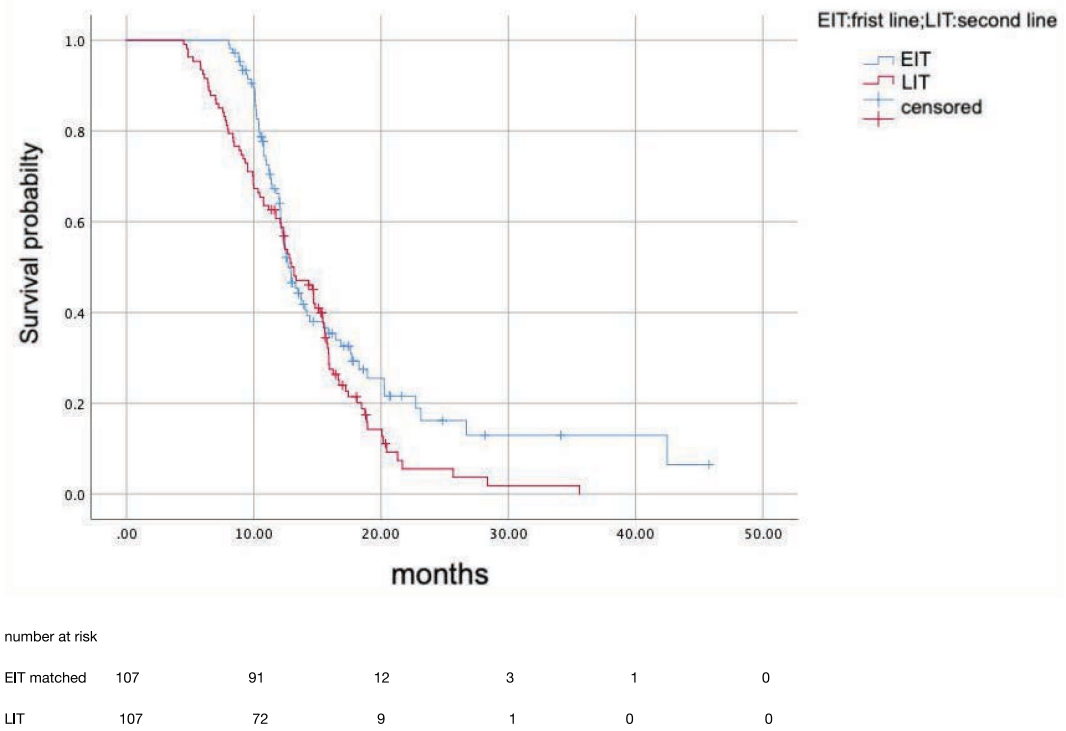

FIGURE 4
Progression-free survival 2(months).

immunotherapy in treating locally advanced or metastatic EC. Our retrospective real-world study showed no significant difference in OS between the use of first-line immunotherapy + chemotherapy and chemotherapy alone in patients with locally advanced or metastatic EC, but a benefit in progression-free survival was observed with the addition of immunotherapy to the first-line regimen.

Our study showed that there was no significant difference in OS between the two groups, which we believe is mainly because twice as many patients in the LIT group compared to the EIT group received third-line therapy by the date of follow-up (15.5% vs. 30%), which resulted in significantly longer OS in the LIT group. However, there were statistically significant differences in PFS1 and PFS2 between the two groups, further indicating the benefit of immune drugs in treatment; the benefit was more significant in the early application.

In EIT groups, our subgroup analysis showed that male patients with middle thoracic EC, younger than 65 years old, with only one site of metastasis, only lymph node progression, no combined radiotherapy after progression, and TP (paclitaxel + platinum) regimen chemotherapy had better progression-free survival. In clinical practice, for young patients with lymph node metastasis or single organ metastasis, or when local radiotherapy cannot be added in time, immunotherapy should be given to patients in a timely manner.

Fluorouracil combined with cisplatin is commonly used in combination chemotherapy in Western countries, while paclitaxel combined with platinum is preferred in China (19, 20). Our retrospective data also showed that more patients chose the paclitaxel + platinum regimen. Previous retrospective reports (21) showed no significant difference in the efficacy of the two regimens in EC. However, our subgroup analysis suggests that the TP (paclitaxel + platinum) regimen is preferred as the chemotherapy regimen when combined with immunotherapy.

Li et al. (22) reported for the first time the difference in survival between first-line immunotherapy + chemotherapy and chemotherapy alone in locally recurrent or advanced metastatic esophageal squamous cell carcinoma. In their retrospective study, there was no significant difference in OS (13.5 vs. 13.1 months, $p = 0.7$) between immunotherapy + chemotherapy and chemotherapy alone, while PFS1 was significantly different (7.1 vs. 4.1 months, $p = 0.001$, HR = 0.53). Our retrospective data showed that the OS of first-line immunotherapy combined with chemotherapy and chemotherapy alone was 15.7 months and 17.7 months, respectively ($p = 0.185$, HR = 1.25). PFS1 was 8.7 months and 7.6 months, respectively ($p = 0.032$, HR = 0.72), consistent with the above conclusions. However, compared with this retrospective study, the number of patients in our article is larger, the follow-up time is longer, and the previous treatment history of the enrolled patients is more detailed, complex, and closer to the actual clinical treatment. Furthermore, we conducted subgroup analyses to inform our practice of which patients would be more inclined to be treated with immunotherapy in the first-line treatment.

4.1 Advantages and defects

4.1.1 Advantages

In this retrospective study, we found that the combination of immune therapy and chemotherapy is more advantageous than chemotherapy alone in the first-line treatment of patients with locally advanced or metastatic EC. Furthermore, our real-world study

Clinical characteristics		EIT arm	LIT arm	*P*	*HR* (95% CI)
gender	male	222/316	94/316	0.029	1.36(1.037−1.788)
	female	30/43	13/43	0.488	1.33(0.593−2.984)
age	<65	61/227	66/227	0.029	1.41(1.036−1.928)
	⩾65	76/132	56/132	0.389	1.22(0.774−1.933)
ECOG	0	124/177	53/177	0.057	1.44(0.990−2.084)
	1	128/182	54/182	0.174	1.28(0.896−1.835)
Tumor location	Cervical and Upper	44/59	15/59	0.216	1.57(0.768−3.229)
	Middle thoracic	132/180	48/180	0.029	1.50(1.041−2.155)
	Lower thoracic	76/120	44/120	0.478	1.17(0.760−1.794)
Differentiated	high and middle	87/125	38/125	0.098	1.44(0.935−2.224)
	low differentiation	65/92	27/92	0.425	1.25(0.726−2.137)
	uncertain	100/142	42/142	0.126	1.37(0.915−2.047)
Site of metastasis	liver	39/49	10/49	0.706	0.86(0.386−1.904)
	lung	44/60	16/60	0.409	1.32(0.681−2.565)
	bone	16/20	4/20	0.095	0.33(0.092−1.209)
	lymph node	153/230	77/230	0.002	1.65(1.205−2.267)
Number of organs	1	150/221	71/221	0.007	1.59(1.138−2.216)
with metastases	⩾2	102/138	36/138	0.458	1.17(0.772−1.774)
With radiotherapy	yes	107/17	64/171	0.737	1.07(0.710−1.621)
	no	124/188	84/188	0.015	1.52(1.086−2.135)
Chemotherapy	PF	76/111	35/111	0.308	1.25(0.816−1.901)
	TP	151/211	60/211	0.034	1.42(1.026−1.973)

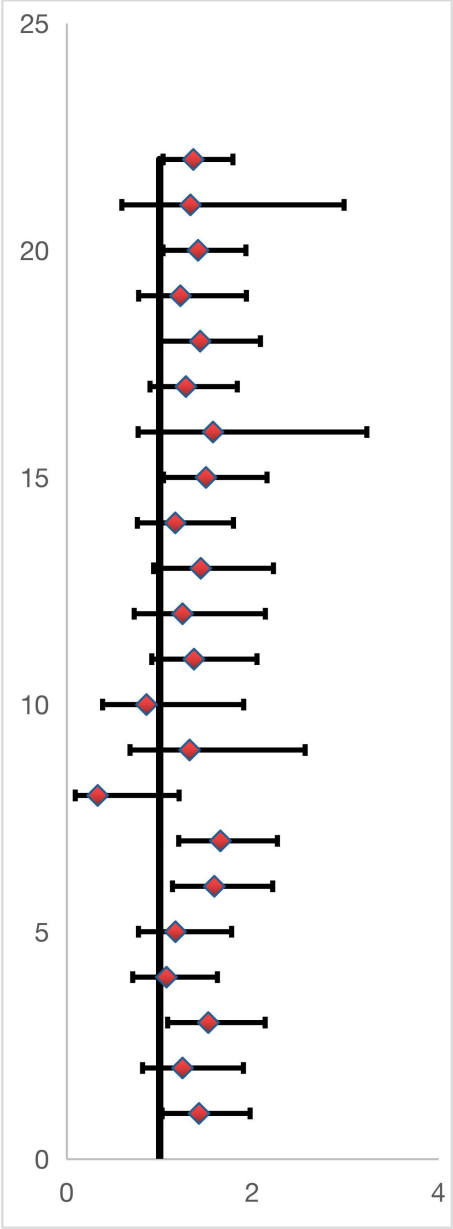

FIGURE 5
Subgroup analysis.

included a larger number of cases and was closer to the actual clinical treatment situation than the study by Li et al. (22). The results of subgroup analysis also hold certain guiding value for our clinical practice.

4.1.2 Defects

This article is a single-center, retrospective study, and the data may have a certain loss bias. The short follow-up time and some patients still in treatment may have a certain impact on the calculation of survival time. In this retrospective study, PD-L1 expression status was unknown in most patients, and the effect of PD-L1 expression level on survival could not be assessed. Our study included only esophageal squamous-cell carcinoma and not adenocarcinoma, which has a very low incidence, and therefore has no significant value in guiding the clinical management of esophageal adenocarcinoma.

5 Conclusion

For patients with locally advanced and metastatic EC, early application of immunotherapy has a progression-free survival benefit. In clinical practice, patients with middle thoracic EC, younger than 65 years old, with only one site of metastasis, only lymph node progression, no combined radiotherapy after progression, and TP (paclitaxel + platinum) regimen chemotherapy are inclined to be treated with immunotherapy in the first-line treatment.

TABLE 4 Adverse events related to treatment.

Adverse events	No. (%) of patients					
	EIT group (n = 252)		EIT group (psm, n = 107)		LIT group (n = 107)	
	Any grade	≥ Grade 3	Any grade	≥ Grade 3	Any grade	≥ Grade 3
Treatment-related adverse events	249 (98.9)	152 (60.4)	104 (97.2)	64 (59.8)	104 (97.0)	67 (62.5)
Anemia	193 (75)	42 (16.5)	78 (72.9)	16 (15)	79 (74.2)	13 (12.5)
White blood cell counts decreased	157 (77.8)	63 (25)	82 (76.6)	25 (23.4)	75 (70.3)	27 (25.6)
Neutrophil count decreased	167 (66.5)	79 (31.2)	73 (68.2)	35 (32.7)	80 (63.5)	48 (45.4)
Nausea	132 (52.4)	4 (1.5)	54 (50.4)	2 (1.9)	55 (51.3)	2 (1.7)
Asthenia	122 (48.5)	6 (2.2)	48 (44.9)	2 (1.9)	46 (43.4)	3 (2.5)
Decreased appetite	107 (42.5)	1 (0.5)	46 (43)	1 (0.9)	47 (44.1)	2 (1.5)
Vomiting	89 (35.5)	6 (2.4)	33 (30.8)	2 (1.9)	34 (31.7)	2 (2.0)
Platelet count decreased	64 (25.5)	5 (2.0)	25 (23.4)	2 (1.9)	25 (23.6)	2 (2.0)
Weight decreased	60 (23.8)	2 (0.7)	24 (22.4)	3 (2.8)	23 (21.6)	2 (2.0)
Aspartate aminotransferase increased	30 (12.1)	3 (1.0)	10 (9.3)	1 (0.9)	11 (10)	1 (1.0)
Immune-related adverse events	252 (84.6)		34 (31.8)		98 (33.0)	
Reactive capillary endothelial proliferation	121 (48)		48 (44.9)		71 (66.4)	
Hypothyroidism	31 (12.3)		9 (8.4)		7 (6.5)	
Hyperthyroidism	6 (2.4)		2 (1.9)		1 (1.0)	
Rash	16 (6.4)		6 (5.6)		2 (2.0)	
Pneumonitis	16 (6.5)		5 (4.7)		2 (2.0)	

Data availability statement

The raw data supporting the conclusions of this article will be made available by the authors, without undue reservation.

Ethics statement

The studies involving humans were approved by Medical Ethics Committee of Gaomi People's Hospital. The studies were conducted in accordance with the local legislation and institutional requirements. The ethics committee/institutional review board waived the requirement of written informed consent for participation from the participants or the participants' legal guardians/next of kin because n this study, the results of hematological examination of patients were retrospectively studied, and the diagnosis and treatment process of patients were not interfered.

Author contributions

SW: Writing – original draft, Writing – review & editing. ZL: Data curation, Writing – original draft. TL: Data curation, Writing – original draft. GS: Data curation, Writing – original draft. HS: Methodology, Supervision, Validation, Writing – review & editing. WH: Supervision, Validation, Writing – review & editing.

Funding

The author(s) declare that no financial support was received for the research and/or publication of this article.

Conflict of interest

The authors declare that the research was conducted in the absence of any commercial or financial relationships that could be construed as a potential conflict of interest.

Generative AI statement

The author(s) declare that no Gen AI was used in the creation of this manuscript.

Publisher's note

All claims expressed in this article are solely those of the authors and do not necessarily represent those of their affiliated organizations, or those of the publisher, the editors and the reviewers. Any product that may be evaluated in this article, or claim that may be made by its manufacturer, is not guaranteed or endorsed by the publisher.

References

1. Kojima T, Shah MA, Muro K, Francois E, Adenis A, Hsu CH, et al. KEYNOTE-181 investigators. Randomized phase III KEYNOTE-181 study of Pembrolizumab versus chemotherapy in advanced esophageal Cancer. *J Clin Oncol*. (2020) 38:4138–48. doi: 10.1200/JCO.20.01888

2. Kato K, Cho BC, Takahashi M, Okada M, Lin CY, Chin K, et al. Nivolumab versus chemotherapy in patients with advanced oesophageal squamous cell carcinoma refractory or intolerant to previous chemotherapy (ATTRACTION-3): a multicentre, randomised, open-label, phase 3 trial. *Lancet Oncol*. (2019) 20:1506–17. doi: 10.1016/S1470-2045(19)30626-6

3. Huang J, Xu J, Chen Y, Zhuang W, Zhang Y, Chen Z, et al. Camrelizumab versus investigator's choice of chemotherapy as second-line therapy for advanced or metastatic oesophageal squamous cell carcinoma (ESCORT): a multicentre, randomised, open-label, phase 3 study. *Lancet Oncol*. (2020) 21:832–42. doi: 10.1016/S1470-2045(20)30110-8

4. Shen L, Kato K, Kim KB, Ajani JA, Zhao K, He ZY. RATIONALE 302: randomized, phase 3 study of tislelizumab versus chemoth erapy as second-line treatment for advanced unresectable/metast atic esophageal squamous cell carcinoma. *J Clin Oncol*. (2021) 39:4012. doi: 10.1200/JCO.2021.39.15_suppl.4012

5. Sun JM, Shen L, Shah MA, Enzinger P, Adenis A, Doi T, et al. Pembrolizumab plus chemotherapy versus chemotherapy alone for first-line treatment of advanced oesophageal cancer (KEYNOTE-590): a randomised, placebo-controlled, phase 3 study. *Lancet*. (2021) 398:759–71. doi: 10.1016/S0140-6736(21)01234-4

6. Doki Y, Ajani JA, Kato K, Xu J, Wyrwicz L, Motoyama S, et al. Nivolumab combination therapy in advanced esophageal squamous-cell carcinoma. *N Engl J Med*. (2022) 386:449–62. doi: 10.1056/NEJMoa2111380

7. Luo H, Lu J, Bai Y, Mao T, Wang J, Fan Q, et al. ESCORT-1st investigators. Effect of Camrelizumab vs placebo added to chemotherapy on survival and progression-free survival in patients with advanced or metastatic esophageal squamous cell carcinoma: the ESCORT-1st randomized clinical trial. *JAMA*. (2021) 326:916–25. doi: 10.1001/jama.2021.12836

8. Lu Z, Wang J, Shu Y, Liu L, Kong L, Yang L, et al. Sintilimab versus placebo in combination with chemotherapy as first line treatment for locally advanced or metastatic oesophageal squamous cell carcinoma (ORIENT-15): multicentre, randomised, double blind, phase 3 trial. *BMJ*. (2022) 377:e068714. doi: 10.1136/bmj-2021-068714

9. Wang ZX, Cui C, Yao J, Zhang Y, Li M, Feng J, et al. Toripalimab plus chemotherapy in treatment-naïve, advanced esophageal squamous cell carcinoma (JUPITER-06): a multi-center phase 3 trial. *Cancer Cell*. (2022) 40:277–288.e3. doi: 10.1016/j.ccell.2022.02.007

10. Herbst RS, Baas P, Kim DW, Felip E, Pérez-Gracia JL, Han JY, et al. Pembrolizumab versus docetaxel for previously treated, PD-L1-positive, advanced non-small-cell lung cancer (KEYNOTE-010): a randomised controlled trial. *Lancet*. (2016) 387:1540–50. doi: 10.1016/S0140-6736(15)01281-7

11. Reck M, Rodriguez-Abreu D, Robinson AG, Hui R, Csoszi T, Fulop A. Pembrolizumab versus chemotherapy for PD-L1-positive non-small-cell lung cancer. *N Engl J Med*. (2016) 375:1823–33. doi: 10.1056/NEJMoa1606774

12. Ribas A, Puzanov I, Dummer R, Schadendorf D, Hamid O, Robert C, et al. Pembrolizumab versus investigator-choice chemotherapy for ipilimumab-refractory 28 melanoma (KEYNOTE-002): a randomised, controlled, phase 2 trial. *Lancet Oncol*. (2015) 16:908–18. doi: 10.1016/S1470-2045(15)00083-2

13. Bang Y-J, Kang Y-K, Catenacci DV, Muro K, Fuchs CS, Geva R, et al. Pembrolizumab alone or in combination with chemotherapy as first-line therapy for patients 29 with advanced gastric or gastroesophageal junction adenocarcinoma: results from the phase II nonrandomized KEYNOTE-059 study. *Gastric Cancer*. (2019) 22:828–37. doi: 10.1007/s10120-018-00909-5

14. Fuchs CS, Doi T, Jang RW, Muro K, Satoh T, Machado M, et al. Safety and efficacy of pembrolizumab monotherapy in patients with previously treated advanced gastric and gastroesophageal junction cancer: phase 2 clinical KEYNOTE-059 trial. *JAMA Oncol*. (2018) 4:e180013. doi: 10.1001/jamaoncol.2018.0013

15. Ku GY. Systemic therapy for esophageal cancer: chemotherapy. *Chin Clin Oncol*. (2017) 6:49. doi: 10.21037/cco.2017.07.06

16. Pacheco JM, Camidge DR, Doebele RC, Schenk E. A changing of the guard: immune checkpoint inhibitors with and without chemotherapy as first line treatment for metastatic non-small cell lung cancer. *Front Oncol*. (2019) 9:195. doi: 10.3389/fonc.2019.00195

17. Gadgeel S, Rodríguez-Abreu D, Speranza G, Esteban E, Felip E, Dómine M, et al. Updated analysis from KEYNOTE-189: Pembrolizumab or placebo plus pemetrexed and platinum for previously untreated metastatic nonsquamous non-small-cell lung cancer. *J Clin Oncol*. (2020) 38:1505–17. doi: 10.1200/JCO.19.03136

18. Borghaei H, Paz-Ares L, Horn L, Spigel DR, Steins M, Ready NE, et al. Nivolumab versus docetaxel in advanced nonsquamous non-small-cell lung cancer. *N Engl J Med*. (2015) 373:1627–39. doi: 10.1056/NEJMoa1507643

19. Petrasch S, Welt A, Reinacher A, Graeven U, König M, Schmiegel W. Chemotherapy with cisplatin and paclitaxel in patients with locally advanced, recurrent or metastatic oesophageal cancer. *Br J Cancer*. (1998) 78:511–4. doi: 10.1038/bjc.1998.524

20. Zhang X, Shen L, Li J, Li Y, Li J, Jin M. A phase II trial of paclitaxel and cisplatin in patients with advanced squamous-cell carcinoma of the esophagus. *Am J Clin Oncol*. (2008) 31:29–33. doi: 10.1097/COC.0b013e3181131ca9

21. Jiang C, Liao FX, Rong YM, Yang Q, Yin CX, He WZ, et al. Efficacy of taxane-based regimens in a first-line setting for recurrent and/or metastatic Chinese patients with esophageal cancer. *Asian Pac J Cancer Prev*. (2014) 15:5493–8. doi: 10.7314/APJCP.2014.15.13.5493

22. Li X-Y, Huang L-S, Cai H-Q. First-line or second-line PD-1 inhibition in advanced oesophageal squamous cell carcinoma: a prospective, multicentre, registry study. *J Clin Pharm Ther*. (2021) 1–6.

Frontiers in Immunology

Explores novel approaches and diagnoses to treat immune disorders.

The official journal of the International Union of Immunological Societies (IUIS) and the most cited in its field, leading the way for research across basic, translational and clinical immunology.

Discover the latest Research Topics

See more →

Frontiers

Avenue du Tribunal-Fédéral 34
1005 Lausanne, Switzerland
frontiersin.org

Contact us

+41 (0)21 510 17 00
frontiersin.org/about/contact